COMBINATION OF METFORMIN AND VALPROIC ACID FOR PROSTATE CANCER TREATMENT

by

Ngoc Khac Linh Tran, M.D., M.Sc.(Med.)

Thesis
Submitted to Flinders University
for the degree of

Doctor of Philosophy

Flinders Centre for Innovation in Cancer
College of Medicine and Public Health
22nd January 2018

Contents

FIGURES

TABLES

DECLARATION

I certify that this thesis does not incorporate without acknowledgment any material previously submitted for a degree or diploma in any university, and that to the best of my knowledge and belief it does not contain any material previously published or written by another person except where due reference is made in the text.

Ngoc Khac Linh Tran

ACKNOWLEDGEMENTS

First and foremost, I would like to thank Professor Pamela Sykes for giving me a chance to undertake a PhD in her laboratory. Pam has taken warm care not only in my scientific professional development, but also in my personal life, especially when we are living far away from our hometown. Pam has encouraged and provided an excellent support to my PhD candidature from getting a scholarship, a very first step, to submitting the thesis and my continuing professional development. I also appreciate Adrian for supporting me and getting me involved in social life. Without Pam and Adrian's help and support, I would not have gotten nearly this far.

Special thanks to my co-supervisors, Dr Michael Michael and Dr Karen Lower for your support, guidance and friendship during my time here. I would like to pay my great acknowledgement to Associate Professor Bryone Kuss for giving me an opportunity for a research assistant position, which greatly supported our lifestyle as students.

My sincere thanks also go to Dr. Ganessan Kichenadasse for working together to get the concept of drug combination. I would like to acknowledge the research team of Associate Professor Lisa Butler, Dr Margaret Centenera, and Swati Irani at the South Australian Health and Medical Research Institute for their collaboration in conducting the explant prostate tumour experiments.

Various groups and services within Flinders University and Medical Centre have also assisted me, for which I am very grateful. Special thanks to the Animal House Facility Staff who supported me in monitoring the mice. I greatly appreciate Dr. Tina Lavranos and Donna Beaumount for their training and

advice on nude mice handling. Thanks to Dr. Lewis Vaughan for his useful and quick support during my animal work.

My work could not be done without the generous support donated by both past and present members of the Sykes' lab. Acknowledgement, particularly to Dr Katherine Morel and Dr Mark Lawrence for showing me the various techniques needed for my project. Special thanks to Dr Rebecca Ormsby who spent many hours giving advice on my thesis. In particular, I wish to directly acknowledge Monica Dreimanis for her side-by-side cell culture training which enabled my confidence in cell culture.

Furthermore, I would not have been able to undertake my PhD if it were not for the support provided by my Australian Awards Scholarship. I acknowledge the funding sources which supported this work, including grants from the Flinders Faculty of Health Sciences, Flinders Foundation, and Flinders Centre for Innovation in Cancer.

I would like to thank my family and friends for their patience and support over the years. In particular, I would like to thank my mum, my dad, my beautiful wife Cuc, and dearest son Bach for their support. Thank you for all your love and belief in me.

ABBREVIATIONS

ACN	: Acetonitrile
ADT	: Androgen deprivation therapy
AMP	: Adenosine monophosphate
AMPK	: AMP-activated protein kinase
AR	: Androgen receptor
Bax	: Bcl-2 associated X protein
Bcl-2	: B cell lymphoma 2
bp	: Base pair (s)
cdk2 pTyr15	: Cyclin dependent kinase 2 (phosphorylated at Tyrosine 15)
C-V- α	: ATP synthase subunit alpha
CRPC	: Castration-resistant prostate cancer
dsRNAs	: Double strand RNAs
DUCaP	: Dura Mater Cancer of the Prostate
EF2K	: Elongation factor 2 kinase
EGF	: Epidermal growth factor
ERG	: Erythroblastosis t26-related gene – ETS-related gene
ERK	: Extracellular signal-regulated kinases
ETS	: Erythroblast transformation specific
GFP	: Green fluorescent protein
HAT	: Histone acetyltransferase
HDAC	: Histone deacetylase
HDACi	: Histone deacetylase inhibitor
H&E stain	: Haematoxylin and eosin stain
HR	: Hazard ratio
IFN	: Interferon-α
kD	: Kilodalton

LB	: Lysogeny broth
LNCaP	: Lymph Node Metastasis Cancer of the Prostate
MET	: Metformin
mTOR	: Mammalian target of rapamycin
p53	: Tumour protein p53
PARP	: Poly ADP ribose polymerase
PC-3	: Prostate Cancer 3
PCa	: Prostate cancer
PDH-E1-α	: Pyruvate dehydrogenase E1- α subunit
PSA	: Prostate-specific antigen
PTEN	: Phosphatase and tensin homolog
RNAse	: Ribonuclease
siRNA	: Small interference RNA
TMPRSS2	: Trans-membrane protease, serine 2
TP53	: Tumour protein 53 gene
UPLC-MS	: Ultra-performance liquid chromatography – mass spectrometry
VCaP	: Vertebral Cancer of the Prostate
VPA	: Valproic acid
v/v	: Volume / volume
w/v	: Weight / volume

STANDARD INTERNATIONAL UNITS OF MEASUREMENT

^{o}C	degree Celsius
g	gram (s)
h	hour (s)
d	day(s)
min	minute(s)
s	second (s)
L	litre (s)
M	molar
A	ampere
V	volt

Indicators of magnitude

k	kilo ($x10^{3}$)
m	milli ($x10^{-3}$)
µ	micro ($x10^{-6}$)
n	nano ($x10^{-9}$)

SUMMARY

Prostate cancer (PCa) is the most common cancer in developed countries. Despite aggressive local treatments such as radical prostatectomy and high-dose radiotherapy, 20-30% of men will relapse after 5-10 years. Androgen deprivation therapy and chemotherapy are used for the treatment of metastatic disease, but castration-resistant prostate cancer (CRPC) invariably emerges resulting in fatal outcomes. There is no durably effective targeted therapy for this stage of the disease. At present, FDA-approved treatments for CRPC consist of abiraterone acetate, enzalutamide, docetaxel, cabazitaxel, radium 223 and Sipuleucel-T, each of which only extend survival by a mean of 3-6 months. So, new treatment options are urgently required.

Metformin (MET; N', N-dimethylbiguanide) is widely used in diabetic patients as first-line therapy for control of blood glucose. Recent studies show pleiotropic beneficial effects of MET including in cancer prevention. The antiepileptic drug, valproic acid (VPA) is a broad-range histone deacetylase inhibitor (HDACi) targeting HDAC class I (Ia, Ib) and class II (IIa) enzymes, and has been shown to have potential as an anti-cancer therapeutic. MET and VPA, when used alone, have shown varying anti-cancer effects in PCa. However, high doses are required which results in unacceptable toxicity. The mechanisms of both drugs have been widely studied.

Repurposing of commonly used drugs is an attractive approach for rapid development of new systemic cancer therapy options. Both MET and VPA have limitations when used alone as anti-cancer agents, however combinatorial therapy of MET and VPA could potentially be more effective than

monotherapy as: (1) MET and VPA induce cell cycle arrest, and antiproliferative and proapoptotic effects via different biological pathways; (2) Lower doses of VPA and MET in combination could reduce the toxicity observed with higher doses of the single drugs; (3) Translation into the clinic would be rapid as MET and VPA are currently widely used drugs for non-cancer purposes.

Here the potential of combining MET and VPA (MET+VPA) was investigated in order to determine if the combination could be used to enhance anti-tumour responses in PCa. In this thesis, the findings demonstrated that MET+VPA induced a synergistic anti-proliferative effect *in vitro* (human PCa cell lines LNCaP and PC-3), inhibited proliferation *in vivo* (nude mouse xenografts bearing LNCaP and PC-3 cells) compared to either drug alone, and reduced proliferation *ex vivo* (human prostate tumour explants) compared to vehicle treatment. MET+VPA induced synergistic apoptosis in LNCaP cells but not PC-3 cells. Increased apoptosis was also observed in human prostate tumour explants. MET+VPA induced an increase in cytochrome c release from the mitochondria to the cytoplasm in LNCaP, but not PC-3 cells, suggesting the involvement of intrinsic apoptosis in the response to the drug combination in LNCaP. The drugs did not have the same effect on normal PrEC cells. Additionally, MET+VPA, at the doses used here, did not cause weight change or tissue toxicity (liver and kidney) in nude mice.

Knock-down of p53 in LNCaP ($p53^+$) reduced the MET+VPA-induced synergistic apoptotic response, and p53 plasmid transfection into PC3 ($p53^-$) increased apoptosis, indicating a role for p53 in the response to MET+VPA. The p53-dependent response to MET+VPA may be explained by dual action

of MET-induced p53 phosphorylation (Ser15) and VPA-induced acetylation (Lys373-382), which activates p53 and induces intrinsic apoptosis. Androgen receptor (AR) inhibition in LNCaP, an androgen-sensitive cell line, reduced the synergistic apoptosis response to MET+VPA, while having no effect in PC-3, an androgen-resistant cell line. The highest induced synergistic apoptotic effect observed was in the presence of both functional p53 and AR suggesting that MET+VPA is acting through these pathways and could be particularly effective in tumours with functional p53 and AR signalling which have critical roles in prostate carcinogenesis. However, in terms of anti-proliferative effects, MET+VPA consistently reduced proliferation in both LNCaP and PC-3, in cell culture and as nude mouse xenografts, indicating that MET+VPA can provide an anti-cancer effect regardless of p53 and AR status.

The demonstration of efficacy of MET+VPA in *vitro*, *in vivo*, and *ex vivo* supports translation of the drug combination into clinical trials as a novel systemic therapy for PCa. The results of this thesis have formed the basis for a Phase I clinical trial (ACTRN 12616001021460) investigating MET+VPA as a neoadjuvant therapy which is currently underway.

PUBLICATIONS AND PRESENTATIONS ARISING DURING CANDIDATURE

Publications

Linh N.K. Tran, Ganessan Kichenadasse, Lisa M. Butler, Margaret M. Centenera, Katherine L. Morel, Rebecca J. Ormsby, Michael Z. Michael, Karen M. Lower, Pamela J. Sykes. The combination of metformin and valproic acid induces synergistic apoptosis in the presence of p53 and androgen signaling in prostate cancer. Molecular Cancer Therapeutics, vol. 16, no. 12, pp. 2689-700, 2017 (ISSN 1535-7163).

Published abstracts

Linh N.K. Tran, Kichenadasse G, Butler LM, Centenera MM, Ormsby RJ, Morel, KL and Sykes PJ. Combination of metformin and valproic acid for prostate cancer: a rapid approach from bench to clinical trial. 2017 Annual Meeting of the American Urological Association (AUA 2017). The Journal of Urology, Vol. 197, No. 4S, e1108, May 15, 2017.

Linh N.K. Tran, Kichenadasse G, Morel, KL and Sykes PJ. The combination of metformin and valproic acid causes synergistic apoptosis of prostate cancer cells via p53 activation and the intrinsic pathway. AACR 108th Annual Meeting 2017, April 1-5, Washington, D.C., USA. Cancer Research *(in press).*

Linh N.K. Tran, Kichenadasse G, Butler LM, Centenera MM, Ormsby RJ, Morel, KL and Sykes PJ. Combination of metformin and valproic acid in personalized prostate cancer treatment: the role of p53 and androgen receptor signaling. AACR 107th Annual Meeting 2016, April 16-20, New Orleans, Louisiana, USA. Cancer Research 76: Issue 14 Supplement, pp LB-233, 2016. DOI: 10.1158/1538-7445.AM2016-LB-233.

Oral presentations

Linh N.K. Tran, Ganessan Kichenadasse, Lisa M. Butler, Maggie M. Centenera, Rebecca J. Ormsby, Katherine L. Morel, Pamela J. Sykes. Repurposing metformin and valproic acid in prostate cancer treatment. 2016 Australian Society of Medical Research (ASMR) South Australian Scientific Meeting, Adelaide, Australia, 8 June 2016.

Poster presentations

Linh N.K. Tran, Ganessan Kichenadasse, Rebecca J. Ormsby, Katherine L. Morel, Pamela J. Sykes. The role of p53 and androgen receptor in the synergistic apoptosis response to metformin and valproic acid in prostate cancer. Cell Signaling in Cancer Biology and Therapy, 7th Barossa Meeting, Tanunda, Australia, 18 - 21 Nov 2015.

Linh N.K. Tran, Ganessan Kichenadasse, Rebecca J. Ormsby, Katherine L. Morel, Pamela J. Sykes. Combination of metformin and valproic acid in the treatment of prostate cancer. Cancer Clinical Research Day, Flinders Centre for Innovation in Cancer, Adelaide, Australia, 23 Oct 2015.

Linh N.K. Tran, Ganessan Kichenadasse, Rebecca J. Ormsby, Katherine L. Morel, Pamela J. Sykes. Role of ERG over-expression in response to metformin and valproic acid in prostate cancer. Australian Society for Medical Research SA Annual Scientific Meeting, Adelaide, Australia, 4 June 2014.

1. INTRODUCTION

Prostate cancer (PCa) is the most common cancer among males in Western countries and the risk of PCa is associated with increased age (Grönberg 2003; Torre et al. 2015). Current PCa therapies such as surgery or radiotherapy for local stage PCa and androgen deprivation therapy (ADT) for advanced PCa have associated serious adverse side-effects. Long-term ADT can eventually result in castration-resistant prostate cancer (CRPC), a lethal stage of disease. Current CRPC therapies only extend the overall survival by 3-6 months, therefore new treatment, especially personalised therapy, is urgently needed in order to slow PCa progression and/or prolong the survival of CRPC patients. The potential of metformin, a hypoglycaemic agent, and valproic acid, an anti-epileptic drug, in cancer prevention and treatment has been widely reported with various effects and limitations. This chapter introduces the current evidence on PCa epidemiology, and clinical and laboratory findings regarding the potential to repurpose metformin and valproic acid in combination as an anti-cancer therapy.

1.1. The prostate and prostate cancer (PCa)

1.1.1. Anatomy and histology of the normal prostate

The human prostate is an exocrine gland of the male reproductive organs. It lies in the pelvic floor inferior to the bladder base, pubis symphysis anteriorly, rectum posteriorly, and urogenital diaphragm superiorly. The supporting ligaments anchoring the prostate to the pelvic floor include the puboprostatic ligament and the pubococcycal portion of the levator ani (Lowsley 1912). The average weight of a normal adult prostate is 18-20 grams and its size is 2.5 –

3 cm in length, 3 cm in width and 2 cm in depth. (McDougal et al. 2011; Smith 2007)

The prostate is classified into different zones depending on the pathological or clinical purpose. The most common classification divides the prostate into 5 zones including: (1) the peripheral zone which comprises around 70% of the PCa region, (2) the central zone which is important for tubular and sperm drainage, (3) the transitional zone which is responsible for prostatic hyperplasia, (4) the anterior segment containing the fibromuscular stroma, and (5) the pre-prostatic sphincter located at the apex of the prostate (McNeal 1981) (Figure 1-1). From the clinical perspective, Lowsley (2007) identifies 5 prostatic lobes including the anterior, posterior, median, right and left lateral lobes. This classification provides better access to prostatic orientation and location (Smith 2007).

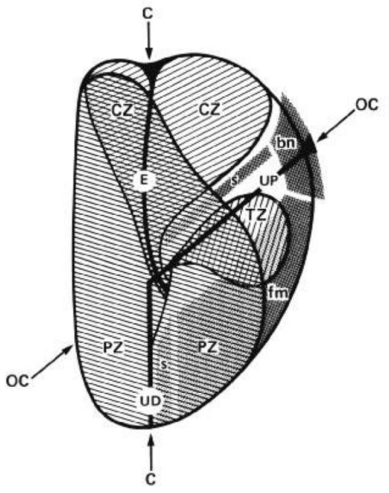

Figure 1-1. Zonal anatomy of the prostate

The anatomical relationship of anterior fibromuscular stroma (fm), central zone (CZ), peripheral zone (PZ), pre-prostatic sphincter (s), transitional zone (TZ), distal prostatic urethral segment (UD), proximal urethral segment (UP), ejaculatory duct (E), bladder neck (bn), and distal striated sphincter (s) is described in the sagittal plan of the distal urethral (taken from McNeal (1988)).

1.1.2. Epidemiology of PCa

PCa is the most common cancer diagnosed in Australian males with 18,560 cases in 2012 (AIHW & AACR 2012) and is also the most common cancer in males in the Western world (Grönberg 2003; Torre et al. 2015) with a lifetime risk of PCa of 16.8% and a death rate of 2.6% in the United States (AIHW & AACR 2012; Smith 2007). In Australia, approximately 3,235 deaths were due to PCa in 2012, the second most frequent cause of cancer death (AIHW & AACR 2012; Smith 2007). The incidence and death rates vary around the world with a higher incidence in s North America, Scandinavia and Australia compared to Asian countries such as China and Japan (Ferlay et al. 2010). Autopsy studies have shown that the natural incidence of PCa increases with age; 30% of males aged 40, 50% of males aged 60, and 75% of males aged 85 years or older (Grönberg 2003; Sakr et al. 1993).

Due to the development of diagnostic and screening tests, new cases are now detected at an earlier stage. The median age of diagnosis has decreased in recent years with 68% of cases being diagnosed at age 65 in 2011 (Kohler et al. 2011). Furthermore, there has been an increase in the percentage of PCa identified at the local regional stage and a decrease in metastatic disease since the application of the prostate specific antigen (PSA) test (McDougal et al. 2011). The 5-year survival rate of PCa is relatively high at around 90% in the United States, Canada, and Australia, while some other countries such Poland, Algeria and Denmark have a lower survival rate at approximately 40% (Ferlay et al. 2010) which may be due to late diagnosis of disease.

1.1.3. Pathology of PCa

The normal prostate consists of 70% glandular element and 30% fibromuscular stroma. More specifically, the prostatic urethra is surrounded by prostatic stroma. Prostatic stroma consists of connective tissues, elastic tissue, smooth muscle tissue fibre, and epithelial glands containing the majority of the excretory ducts (Gonzalgo et al. 2003) (Figure 1-2).

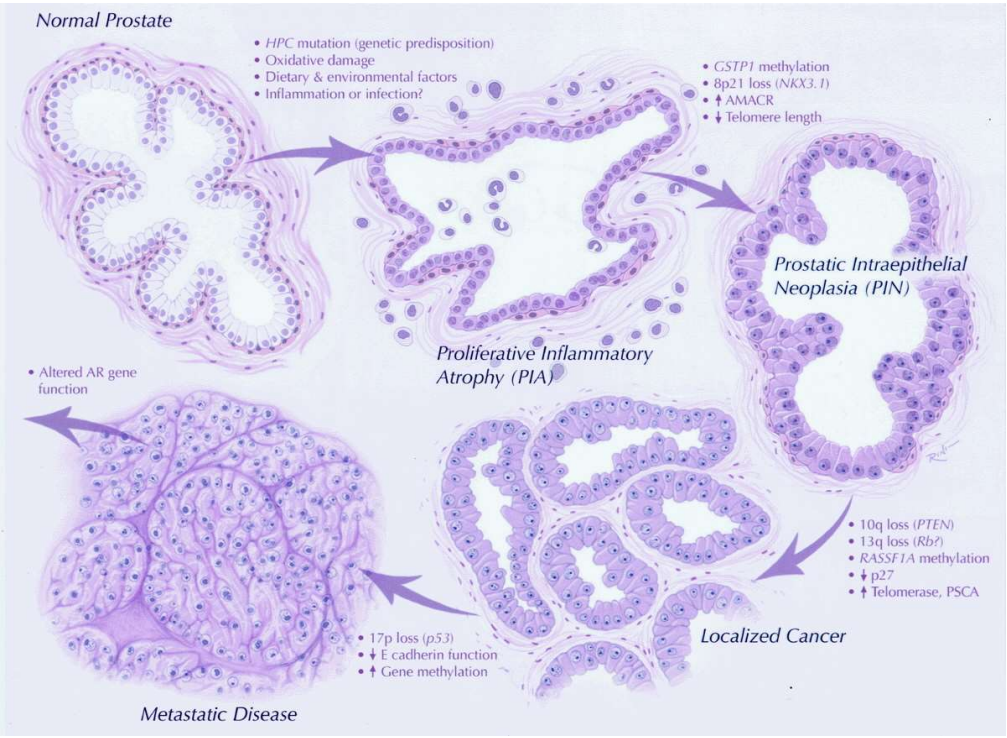

Figure 1-2. PCa progression from the normal prostate gland.

The normal prostate gland is composed of two layers: outer and inner epithelium. The fibromuscular stroma is normally distributed between the glands. Different mutations and damage can cause a change in the gland structure to proliferative inflammatory atrophy (PIA) and prostatic intraepithelial neoplasia (PIN) (reversible pre-cancer lesions), and then to localised cancer and metastasis (taken from Gonzalgo et al. (2003)).

Malignant transformation of the prostate evolves from prostatic intraepithelial neoplasia (PIN), a reversible pre-cancer lesion, to adenocarcinoma (Gonzalgo et al. 2003) (Figure 1-2). The most popular pathological classification for PCa, the Gleason grading system which investigates the pathological patterns of the glandular element in the prostate and plays a crucial role in PCa diagnosis, treatment, and prognosis (Figure 1-3). Highly malignant and poorly differentiated PCa have higher Gleason scores and are associated with poor prognosis.

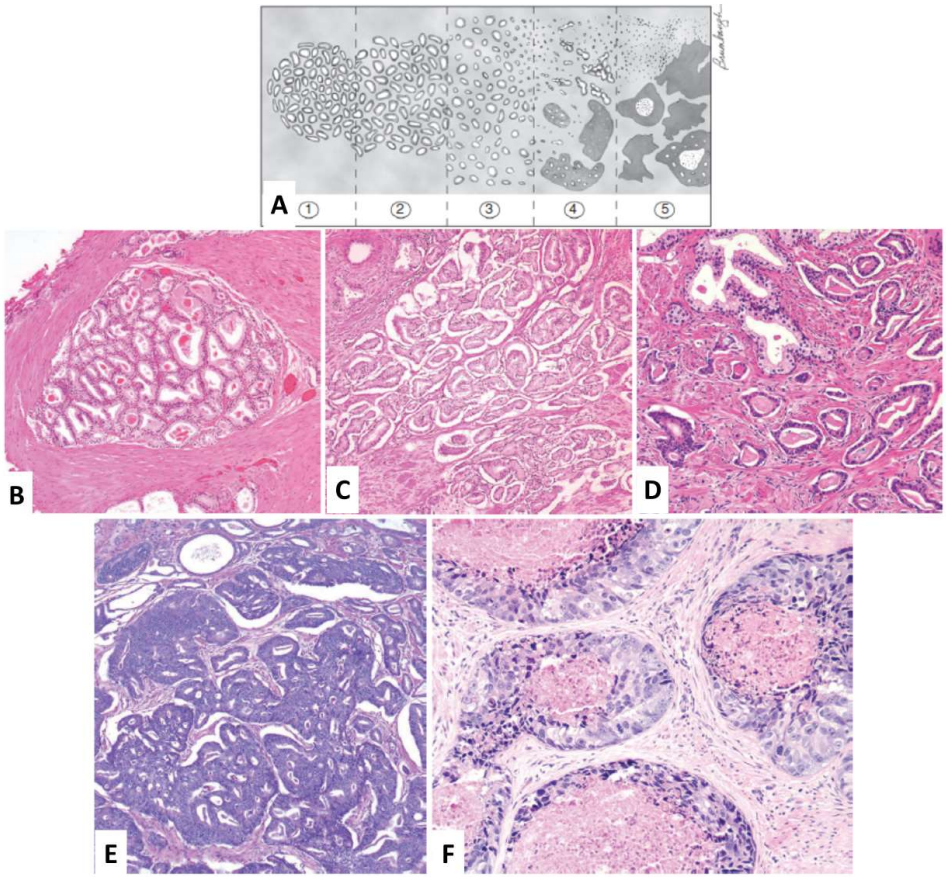

Figure 1-3. The Gleason grading system.

A, *Progression of 5 stages of the Gleason grading system.* ***B,*** *Gleason 1 has well-circumscribed nodule of glands.* ***C,*** *Gleason 2 has nodules with more loosely arranged glands.* ***D,*** *Gleason 3 has small glands and infiltrative pattern.* ***E,*** *Gleason 4 has irregular glands.* ***F,*** *Gleason 5 has solid cell nests of the tumour and central comedonecrosis (taken from McDougal et al. (2011)).*

1.1.4. Population screening for PCa

The role of mass screening for PCa is contentious. In a prostate, lung, colorectal, and ovarian (PLCO) cancer study, performed in 76,693 men aged 55 to 74 years, in ten U.S centres with 7 years follow-up, PCa screening was associated with no significant difference in the incidence of death compared with the non-screened group (Andriole et al. 2009). This study, however, has been criticised due to the short follow-up time and inconsistencies in the control group. On the other hand, the European Randomized Study of Screening for PCa (ERSPC) study, which had a larger sample size and longer surveillance time compared to the PLCO study, indicated that screening can reduce the mortality by up to 20% compared to the control group. Despite this, the cost-effectiveness of screening should be taken into consideration as 1410 individuals needed to be screened and 48 cases needed to be treated to save one death from PCa (Schröder et al. 2009). Therefore selective screening programs should be carefully considered based on the specific cost-effective analysis of the population (Vu Le et al. 2010).

1.1.5. Diagnosis and treatment of PCa

The diagnosis and stage evaluation of PCa depend on clinical examination including serum concentration of prostate specific antigen (PSA), digital rectal examination (DRE), Gleason score evaluation, and transrectal ultrasound biopsy (TRUS). These findings are integrated into the D'Amico classification to stratify PCa into low, intermediate, and high risk of invasion (D'Amico et al. 2003; Heidenreich et al. 2014a).

Based on the stage and aggressiveness of the disease, different modalities of treatment can be applied. Local disease can be treated by active surveillance,

radical prostatectomy, and/or radiation therapy (external beam radiation or low dose rate brachytherapy). Low volume and highly differentiated cancer can be followed up individually by active surveillance. Advanced or relapsing disease are treated either with hormonal therapy or chemotherapy (Heidenreich et al. 2014a; 2014b). There is a large proportion of castration-resistant PCa (CRPC) following hormonal therapy which remains a challenge in PCa treatment. At present, FDA-approved treatments for CRPC consist of mitoxantrone, abiraterone acetate, Enzalutamide, docetaxel and Sipuleucel-T (Robinson et al. 2015). There is no durably effective targeted therapy for this stage of the disease.

1.1.6. PCa prognosis

Bill-Axelson et al. (2005) demonstrated in a study of patients with localised PCa, that the survival rate in patients without intervention is 85.6%, and for radical prostatectomy is 91.4% after 8.2 years follow-up, with the mortality rate at lower than 10% after 10 years follow-up. Patients diagnosed with high risk (PSA>10 ng/mL, Gleason score 8-10, >T2c) and locally advanced PCa have a higher risk of biochemical failure (rising PSA), distant metastasis, and death from PCa and benefit most from radical treatment compared to low and intermediate risk (Wilt et al. 2012). Without the radical treatments (such as radical prostatectomy or radiation therapy), the 10-year and 15-year PCa mortality rate of high risk localised PCa have been reported to be 28.8% and 35.5%, respectively (Engel et al. 2010; Ghavamian et al. 1999; Rider et al. 2013).

After radical treatments such as prostatectomy and high dose radiotherapy, 20-30% of men will relapse after 5-10 years and require additional treatments

such as ADT and chemotherapy (Heidenreich et al. 2011). While reducing circulating hormone levels by ADT is an effective short-term treatment for metastatic disease, these therapies inevitably fail with the emergence of castration-resistant cancer cells resulting in the lethal form of PCa.

PCa patients with lymph node positive metastatic disease have a lower cancer-specific survival rate at 5-, 10-, and 15- years follow-up ranging from 84-95%, 51-86%, and 45%, respectively after surgery compared to lymph node negative patients (Briganti et al. 2009). The overall survival of patients with metastatic PCa, especially CRPC is relatively short ranging from 12-18 months. FDA-approved chemotherapies for CRPC only extend survival by a mean of 3-6 months (Beer et al. 2014; Kantoff et al. 2010; Ryan et al. 2015; Tannock et al. 2004). The results of the Systemic Therapy in Advancing or Metastatic Prostate cancer: Evaluation of Drug Efficacy (STAMPEDE) trial found that median overall survival of patients with newly diagnosed locally advanced and metastatic PCa undergoing hormonotherapy was 71 months. The median overall survival was significantly extended to 81 months ($p=0.006$, HR=0.78, CI 0.66-0.93) when Docetaxel was combined with hormonotherapy (James et al. 2016). These results supported the Chemohormonal Therapy versus Androgen Ablation Randomized Trial for Extensive Disease in Prostate Cancer (CHAARTED) trial which found that the combination of Docetaxel and hormonal therapy extended the median overall survival by 13.6 months compared to hormonotherapy alone (57.6 months versus 44.4 months, $p<0.001$, HR 0.61, CI 0.47-0.8) (Sweeney et al. 2015).

1.1.7. Important molecular markers in PCa diagnosis and treatment

The androgen receptor (AR) is a transcription factor. The full length of AR protein (919 kD) contains 3 main domains including the N-terminal domain (NTD), the DNA binding domain (DND), and the ligand binding domain (LBD) (Tan et al. 2015) (**Error! Reference source not found.**). AR is localised in the cell cytoplasm and translocates to the nucleus upon activation via the binding of testosterone or dihydrotestosterone (DHT) to the LBD. This results in the release of heat shock proteins (HSPs), induction of N- and C- terminus interactions, and conjugation with the transporter importin-α (Bardin et al. 1983). AR plays a role in the development of primary and secondary male characteristics (Frank 2003). AR gene mutation predisposes to the risk of PCa (Gottlieb et al. 1998; Hsing et al. 2000). AR mutations occur in approximately 8% of local stage (Marcelli et al. 2000) and in 62% of advanced stage of disease (Robinson et al. 2015). PCa progression is highly dependent on AR activity, therefore ADT is an important therapeutic target for PCa treatment (Heinlein et al. 2004; Huggins et al. 1941). CRPC progresses from long-term ADT (Harris et al. 2009), which possibly results from **(1)** enhanced AR sensitivity to androgen, **(2)** AR mutations in the ligand binding site, **(3)** AR activation not related to the ligand binding site, and **(4)** AR-independent proliferation (Feldman et al. 2001).

Mutations in *TP53*, androgen receptor (AR), and phosphatase and tensin homolog (*PTEN)*, as well as *ETS* gene fusions are the four most common changes observed in metastatic CRPC at a frequency of 53.3%, 67.2%, 40.7%, and 56.7%, respectively (Robinson et al. 2015).

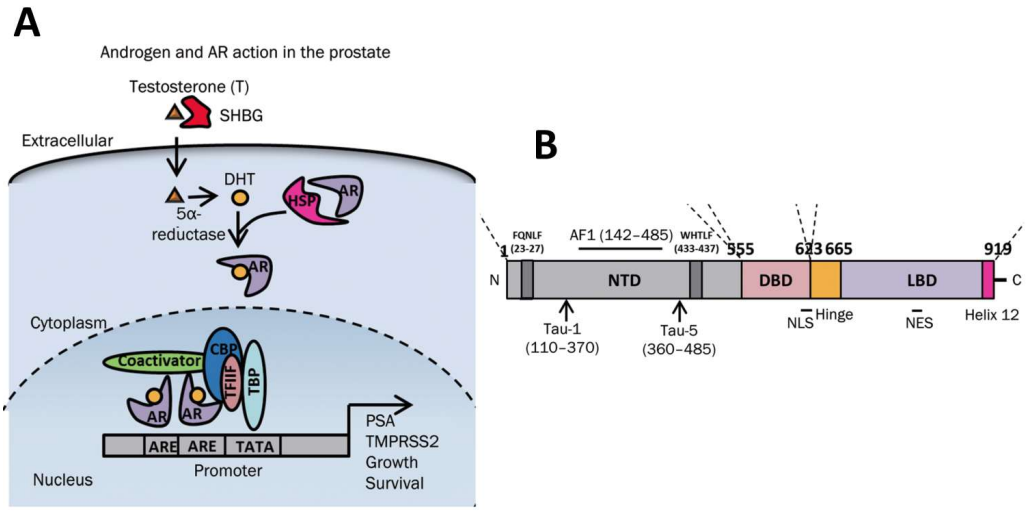

Figure 1-4. AR structure and mechanism of action of androgen signalling pathway

A, *AR normally conjugates with heat shock protein (HSP) in the deactivated-form. The binding of testosterone/DHT to AR releases HSP, and AR is transported from the cytoplasm to the cell nucleus and binds to the promoter region of target genes (PSA, TMRPSS2, etc.).* ***B,*** *Normal AR contains eight exons and codes for 919 amino acids. The three main functional domains consist of the N-terminal domain (NTD), the DNA binding domain (DND), and the ligand binding domain (LBD) (adapted from Tan et al. (2015)).*

p53 is an important tumour-suppressor protein which has a short half-life (5-20 mins), is tightly regulated, and controls cell metabolism and signalling. When activated, p53 initiates cellular responses via transcriptional activation of genes involved in cell cycle arrest, DNA repair, and/or apoptosis (Lane et al. 1990; Levine 1997). *TP53* is one of the most commonly mutated genes in human cancer and is usually associated with cancer progression and/or poor prognosis (Blondal et al. 1994; Whibley et al. 2009). In PCa, the mutation rate of TP53 in local stage ranges from 0-30% (Ecke et al. 2007), and increases up

to 53.3% in advanced stage (Robinson et al. 2015). The most common mutation site is in exon 7-8, resulting in overexpression of mutated p53 and is associated with increased tumour aggressiveness (Ecke et al. 2010; Kuczyk et al. 1998).

PTEN protein, encoded by the PTEN gene, is a tumour suppressor protein that regulates the Akt/PKB signalling pathway. Mutations in PTEN were first found in many cancer cell lines such as glioblastoma (13/42 cell lines), breast cancer (4/65 cell lines), and PCa (4/4 cell lines) (Li, J et al. 1997). Mutations in the PTEN gene cause PTEN protein loss in from 30% to 80% in primary PCa and 50% in bone metastases (Attard et al. 2009; Li, J et al. 1997; Tomlins, Scott A. et al. 2005). The loss of PTEN expression is associated with aggressiveness of disease (McMenamin et al. 1999).

The understanding of the pathogenesis of PCa due to chromosomal translocations has improved significantly in recent years. The fusion between the ETS gene family including *ERG* (50% of cases), *ETV1* (10% of cases), *ETV4* (<1% of cases), *ETV5* (<10% of cases) and *ELK4* (1% of cases) and other genes are the most frequent types of translocation (Hermans et al. 2008; Kumar-Sinha et al. 2008; Pflueger et al. 2009; Rickman et al. 2009). Among these possibilities, the fusion between TMPRSS2 and the ETS family, especially ERG, is the most frequent and plays an important role in malignant transformation as it can affect cell proliferation, differentiation, migration, invasion, and angiogenesis (Tomlins, Scott A et al. 2008). The TMPRSS2-ERG fusion results in overexpression of the ERG protein (486 amino acids, 7 isoforms, half-life from 2 to 21 h (Murakami et al. 1993), a transcriptional regulator which can bind directly to DNA, proteins and its isoforms (Figure 1-5).

The biological effects of ERG include cell proliferation, cell differentiation, multicellular organismal development, protein phosphorylation, regulation of RNA polymerase II promoter, and signal transduction (Universal Protein Resource (UniProt) 2013). The biological function of ERG overexpression is still unknown, however, studies have found a role for this protein in some epithelial cancers such as PCa and pancreatic cancer (Hooper et al. 2001; Ryu et al. 2002). ERG is considered an oncogenic transcription factor which contains the ETS domain which can be either a DNA binding site or a protein-protein interaction site (John et al. 2012). These changes in cellular activities can lead to malignant transformation (Attard et al. 2009; Murakami et al. 1993; Reddy et al. 1987). Tomlins et al. Tomlins, Scott A et al. (2008) showed that, although the TMPRSS-ERG gene fusion alone was insufficient for malignant transformation, it could at least enhance cell proliferation rate and invasiveness. The co-expression of multiple variant ERG transcripts can increase cell proliferation compared to single ERG expression (Wang, J et al. 2008). The *TMPRSS2-ERG* fusion is considered a poor prognostic indicator for PCa and is associated with a decrease in cancer-free survival rate, high Gleason score and more aggressive disease (Tomlins, Scott A et al. 2008).

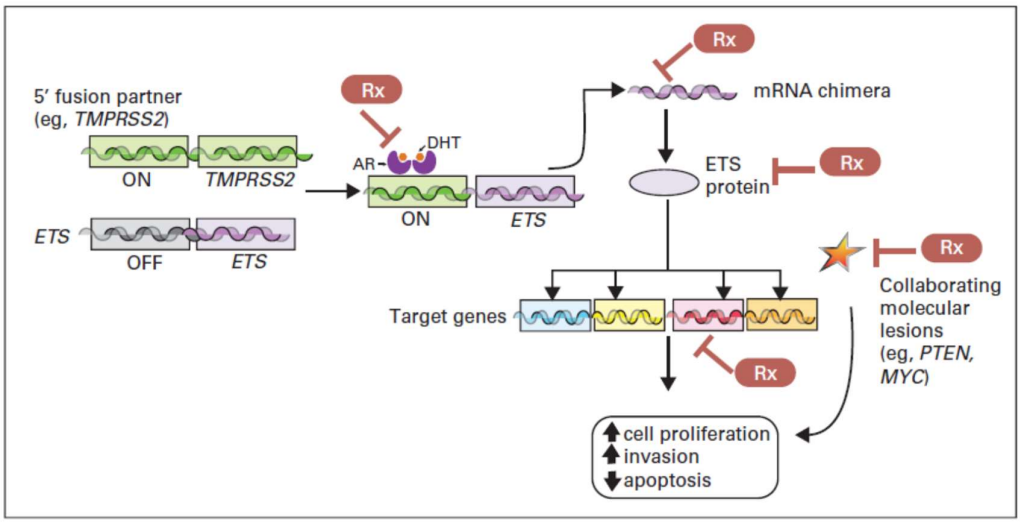

Figure 1-5. Gene fusion between *TMPRSSS* and *ETS* genes in PCa

The "on" switch in TMPRSS2 gene fuses with the ETS gene which is normally "off" causing the overexpression of ETS protein. The activation of AR also targets the TMPRSS2 gene and increases the expression of ETS protein. The effects of ETS protein overexpression includes an increase in cell proliferation, invasion and a decrease in apoptosis. (adapted from Rubin et al. (2011)).

1.1.8. Interactions between common molecular markers of PCa

It has been shown that CBP/p300, a type of histone acetyltransferase (HAT), acetylates p53 (Lys 375/382) and enhances its transcriptional activities (Bode et al. 2004). The TMPRSS2-ERG gene fusions may interfere with the acetylation of p53 protein as the result of the binding of overexpressed ERG to CBP/p300, inhibiting its activity. Fortson et al. (2011) demonstrated that high dose valproic acid (10 mM), a histone deacetylase inhibitor, can reduce the expression of overexpressed ERG in the VCaP cell line in the first 12 h, then indirectly recover the function of CBP/p300 protein which is important for the acetylation of p53 protein. However, there was no investigation to determine if the recovered p53 protein was functional or not as p53 protein is mutated in VCaP, an ERG (+) PCa cell line, and is considered to be non-functional. AR

has been shown to upregulate *TMPRSS2-ERG* transcripts and cause ERG overexpression in VCaP cells (Cai et al. 2010) (Figure 1-6).

The *PTEN gene,* located on chromosome 10 (10q23), is considered a tumour suppressor gene through its phosphatase protein which regulates the cell cycle process and controls the rate of proliferation. The loss of the regulation of *PTEN* in PCa leads to un-controlled cell proliferation and differentiation. Additionally, the combination of PTEN loss and a TMPRSS2-ERG gene fusion can increase the aggressiveness of disease resulting in a worse prognosis (Carver et al. 2009; Reid et al. 2010) (Figure 1-6).

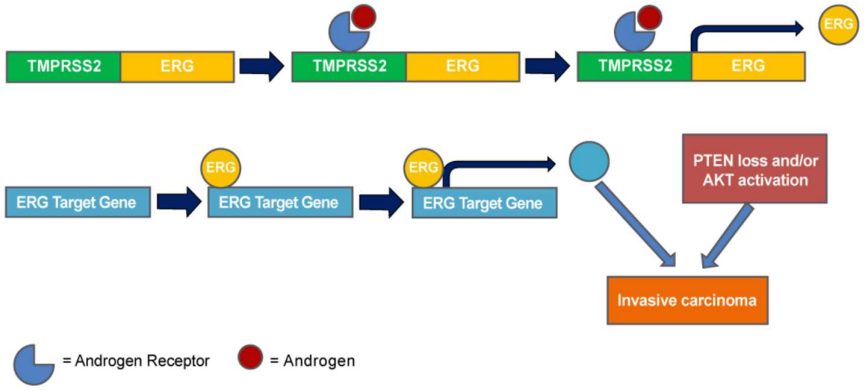

Figure 1-6. The TMPRSS2-ERG gene fusion and its relation to androgen in PCa development.

Activated AR binds to the TMPRSS2 gene, then increasing the activity of the TMPRSS2-ERG fusion gene resulting in further expression of ERG protein. The association of PTEN loss and/or AKT activation with ERG overexpression results in an increase in the invasiveness of the cancer (taken from John et al. (2012)).

1.2. Metformin and PCa

1.2.1. Metformin

Metformin (MET) is derived from biguanide and is widely used in diabetic patients as first-line therapy for control of blood glucose. MET can reduce blood glucose levels by decreasing glycogenesis in the liver and increasing

glucose uptake in tissues. The latter effect is achieved via the activation of Glucose Transporters 1 and 4 in several tissues such as liver, adipose tissue, skeletal and heart muscle (Kozka et al. 1995; Shaw et al. 2005). This drug is of specific benefit to the diabetic patient due to its low incidence of reversibly adverse consequences such as severe hypoglycaemia and lactic acidosis (<1/1000).

When using MET as a hypoglycaemic agent in type 2 diabetes, epidemiological studies show pleiotropic beneficial effects of MET including reduction of plasma lipid levels and in cancer prevention (Zhou et al. 2001). In a retrospective cohort study, Currie et al. (2009) recognized that the application of MET can reduce the incidence of some cancers such as colon, pancreatic, and PCa in diabetes patients treated with glucose-lowering therapies (oral agents and insulin). A Finnish study found that long-term use of MET in diabetes patients can reduce the incidence of PCa by 37% at 7 years follow-up (Murtola et al. 2008). A case-control study in Caucasians in 2009 demonstrated a correlation between MET and PCa with 44% risk reduction in PCa in the MET group (adjusted OR = 0.56) (Wright et al. 2009). However, the epidemiological findings are not consistent. No relationship between MET and breast cancer or PCa was observed by Currie et al. (2009) which may be due to only a sub-set of patients responding to this drug. Other limitations of these observational studies such as retrospective data collection and risk of selection bias may explain the differential findings (Lilienfeld 1983).

MET reduces the progression of PCa in some clinical studies. The first retrospective clinical study indicates, among localised PCa patients that underwent external beam radiation therapy in the United States, that MET use

has been associated with an increase in prostate-specific antigen-recurrent-free-survival, distant metastasis-free survival, and overall survival, a decrease in prostate cancer-specific mortality, and reduction in the development of CRPC (Spratt et al. 2013). Furthermore, a clinical phase II – single arm trial has demonstrated the effectiveness of MET in increasing the prolongation of PSA doubling time. This study, however, lacked an appropriate control arm. Therefore, further clinical investigations are needed to fully elucidate the benefit of MET for PCa treatment (Rothermundt et al. 2014).

1.2.2. Potential molecular mechanisms of MET in PCa prevention and treatment

1.2.2.1. *Direct and indirect pathways of molecular action of MET*

MET is transported into the cell through organic cation transfer protein (OCT) which is highly expressed in liver (OCT1) (Wang, D-S et al. 2002), kidney (OCT2), and prostate (Joerger et al. 2015). The anti-cancer mechanism of MET has been attributed to the inhibition of mammalian target of rapamycin (mTOR) activity via both direct (Ben-Sahra et al. 2008) and indirect pathways (through adenosine monophosphate protein kinase (AMPK) activation) (Bolster et al. 2002; Long et al. 2006). In the indirect pathway, MET interacts with the serine-threonine kinase LBK1, a tumour suppressor protein, resulting in the phosphorylation of AMPK (Shaw et al. 2005). MET can inhibit mitochondrial complex 1 (Doran et al. 2000), inducing a change in ATP/AMP ratio which also activates AMPK. This AMPK activation confers 2 main effects: **(1)** Inhibition of the mTOR which leads to cell cycle arrest and decreased protein synthesis (Bolster et al. 2002; Hardie 2003; Long et al. 2006); **(2)** Activation of the *p53* gene, a tumour suppressor gene, which can affect cell

metabolism and drive the cell towards autophagy (Feng et al. 2010) (Figure 1-7). Birsoy et al. (2014) found that cell lines with mitochondrial DNA mutations and defective oxidative phosphorylation (OXPHOS) are more susceptible to MET and low glucose level.

In the direct pathway, MET can be independent of the AMPK pathway and directly inhibit the activity of mTOR (Figure 1-7). Ben-Sahra et al. (2008) blocked the function of AMPK by knocking down two catalytic units of AMPK, α1 and α2, and found that MET can inhibit cell proliferation in LNCaP and DUCaP cell lines regardless of the AMPK function. The authors also concluded that some cell lines, including PCa cell lines, potentially have an alternative pathway such as REDD1 to inhibit mTOR activities (Ben-Sahra et al. 2011). Honjo et al. (2014) found that MET targeted the component of mTOR, hence reducing mTOR activity and sensitised to chemotherapy (5-FU) in oesophageal cancer cell lines (FL-1, BE3, SKGT-4, OE33, JHESO, and OACP). Additionally, MET has been shown to inhibit mitochondrial complex 1 causing a decrease in protein synthesis and cell proliferation in both normal and cancer cells (Zhou et al. 2001).

1.2.2.2. *MET and glucose metabolism in cancer cells:*

MET can interfere with energy metabolism in PCa cells by inhibiting the activities of Mitochondrial Complex 1, thereby reducing the conversion of glucose to α-ketoglutarate in the tricarboxylic acid (TCA) cycle that could subsequently increase glutamine metabolism (Figure 1-8) (Fendt et al. 2013).

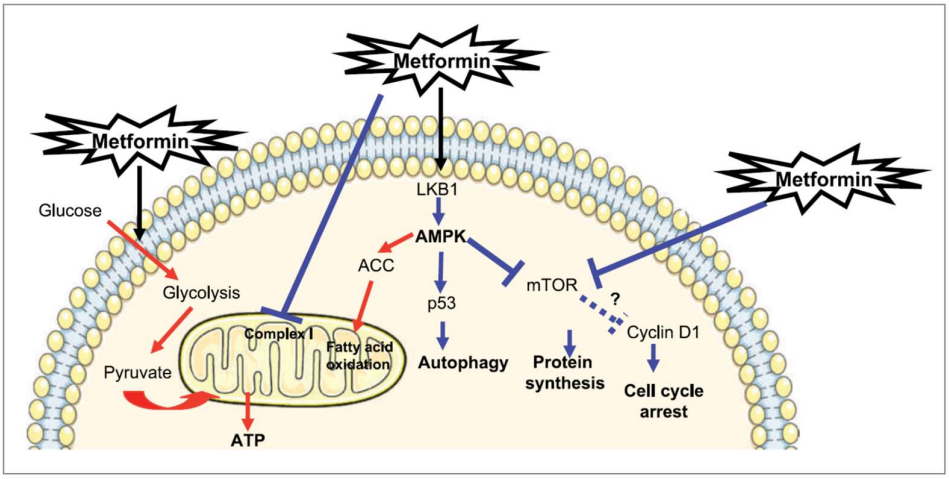

Figure 1-7. Potential mechanism of MET on cell proliferation and metabolism

MET reduces blood glucose level via increasing glucose uptake. MET can also indirectly activate AMPK via mitochondrial complex 1 inhibition, which then inhibits mTOR activities, or directly inhibits mTOR. AMPK activation can also activate p53 protein (Adapted from Ben-Sahra et al. (2010)).

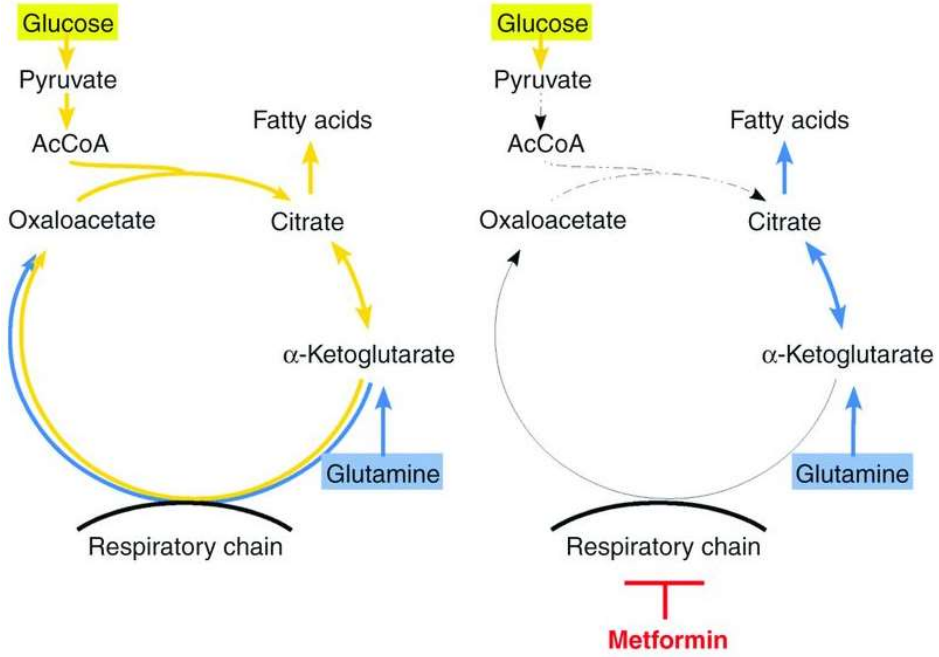

Figure 1-8. Potential molecular mechanism of MET action on glucose metabolism in PCa cells.

The respiratory chain in mitochondria with and without MET. MET inhibits mitochondrial complex 1, which reduces the conversion of glucose to α-ketoglutarate in PCa cells. The conversion of glutamine to α-ketoglutarate is subsequently increased to compensate the reduction in α-ketoglutarate (adapted from Fendt et al. (2013)).

1.2.3. Molecular targets of MET in PCa

MET demonstrates consistent anti-proliferative effects in most cell lines with a dose ranging from 1 to 30 mM. MET at even lower doses (0.1-0.3 mM) can kill cancer stem cells which are chemo-resistant (Hirsch et al. 2009). *In vitro* and xenograft studies indicate that MET causes cell cycle arrest in G0/G1 or S phase. This effect is achieved through reduction of Cyclin D1 and increase in $p27^{Kip}$ and $p21^{Cip}$ (Ben-Sahra et al. 2008). Zhuang et al. (2008) observed a pro-apoptotic effect due to MET in pancreatic and breast cancer cell lines. Interestingly, normal epithelial cell lines respond to a lesser extent to MET compared to cancer cell lines. This suggests that MET has greater specificity for cancer cells (Ben-Sahra et al. 2008).

Although MET, through AMPK activation, enhances p53 expression causing changes in cell metabolism (Bensaad et al. 2007; Feng et al. 2010; Okoshi et al. 2008), current evidence supports that MET has an anti-cancer effect regardless of p53 status. However, cells with functional *p53* demonstrate a greater response to MET compared with *p53* (-) cells (Ben-Sahra, Laurent, et al. 2010; Gotlieb et al. 2008; Zakikhani et al. 2006).

MET has been shown to downregulate AR, repress cell viability, and increase apoptosis by targeting the AR signalling pathway in PCa cell lines (LNCaP and CWR22Rv1) (Wang, Y et al. 2015). PTEN appears not to play a major role in the effect of MET on the AMPK pathway in PCa (Feng et al. 2007).

1.3. Valproic acid and PCa

1.3.1. Valproic acid

Valproic acid (VPA) (2-propylvaleric acid, 2- propylpentanoic acid or n-dipropylacetic acid) is a short-chain fatty acid derived from valeric acid (*Valeriana Officinalis*). This drug was first synthesised in 1882 by B.S Burton (Burton 1882) (Figure 1-9).

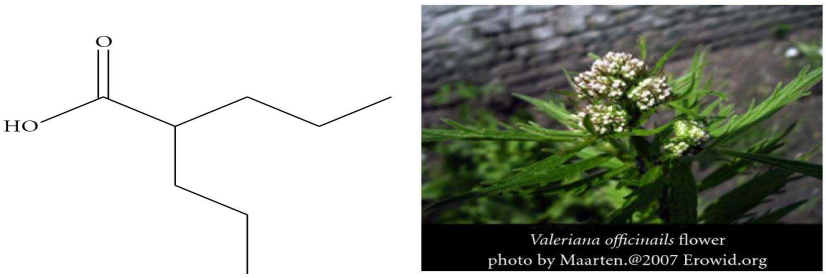

Figure 1-9. The molecular structure of VPA.

The molecular formula of VPA is $C_8H_{12}O_2$ (left). VPA was first synthesised from the valeriana officinails flower (right) in 1882 by B.S Burton (Images adapted from erowid.org, accessed in June 2015).

The first description of its anti-convulsive effect was studied in rodents and reported in 1962 (Meunier et al. 1962). Since then, VPA has been shown to inhibit the activity of the neurotransmitter gamma-aminobutyric acid (GABA) and has widely been prescribed as an anti-epileptic drug in humans (Mesdjian et al. 1982). Besides the principal application in epilepsy, VPA is used clinically to treat other neurogenic related diseases such as bipolar disorder, clinical depression (Calabrese et al. 1989), absence seizure (Coppola et al. 2004; Erenberg et al. 1982), tonic-clonic seizure (Dean et al. 1988), complex partial seizure, juvenile myoclonic epilepsy (Calleja et al. 2001), migraine headaches, schizophrenia, and seizure in Lennox Gastaut syndrome (Friis 1998). Possible

serious side effects of VPA include teratogenic effects, and physical and cognitive alteration (Hardy et al. 2001). The majority of side effects range from mild to transient levels which are acceptable in most cases.

1.3.2. Potential molecular mechanism of VPA in PCa prevention and treatment

VPA is a broad-range histone deacetylase inhibitor (HDACi) targeting HDAC class I (Ia, Ib) and class II (IIa) enzymes, and has been shown to have potential in anti-cancer therapy (Bradbury et al. 2005; Ververis et al. 2011). VPA prevents the transformation of chromatin from an open or transcriptionally active form to a closed or transcriptionally inactive form, resulting in enhanced expression of numerous genes and activates several molecular pathways (Figure 1-10). VPA has been shown to be responsible for a 20% overall change in the transcriptome in a tissue-dependent manner (Chateauvieux et al. 2010), having a marked effect on cellular activities which are important in cancer growth including apoptosis, cell cycle regulation, DNA repair, and cell differentiation (Chen, Y et al. 2009; Martirosyan et al. 2006; Rosato et al. 2003; Savickiene et al. 2006).

Besides the effect on histone acetylation status, VPA can maintain the acetylation of non-histone proteins such as Ku70 (Cohen et al. 2004) and p53 (Condorelli et al. 2008), therefore further extending the time of protein activation. (Duenas-Gonzalez et al. 2008; Göttlicher et al. 2001; Gurvich et al. 2004). VPA has been considered an epigenetic drug as it can cause DNA demethylation and enable genes to be more transcriptionally active (Bhattacharya et al. 1999; Bradbury et al. 2005; Cervoni et al. 2002). VPA has not been shown to directly up-regulate the activities of DNA demethylase,

however, the exact mechanism is still unknown. Marchion et al. (2005) found that VPA reduces the expression of some proteins which are mandatory for protein maintenance such as SMCs1-6, DNMT1, and HP1. Additionally, VPA can induce the mono, di-, tri-methylation of Histone 3, especially at lysine 9 which further opens the chromatin and increases the transcriptional activities of the genome (Cervoni et al. 2001; Harikrishnan et al. 2008; Nightingale et al. 2007).

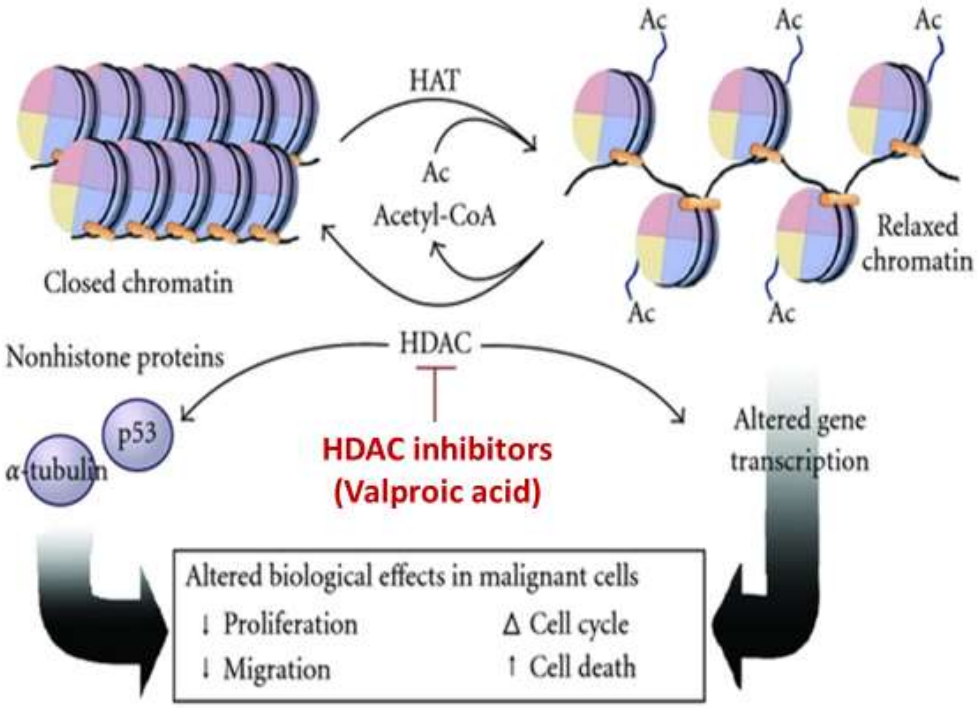

Figure 1-10. The regulation of histone acetylation through the opposite action of histone acetyl-transferases and histone deacetylases.

Histone acetyltransferases (HATs) add acetyl-CoA to histones and transform closed chromatin to relaxed chromatin, which subsequently alters gene transcription. Histone deacetylases (HDACs) convert closed chromatin back to the relaxed form. HDACs also affect non-histone proteins including p53 and α-tubulin. VPA is an HDAC inhibitor (HDACi). (Adapted from Rodd et al. (2012))

1.3.3. Molecular targets of VPA in PCa

VPA can affect cell death and growth. *In vitro* studies have demonstrated that VPA causes apoptosis in the LNCaP cell line in both an androgen-dependent and androgen-independent manner (Thelen et al. 2004). Furthermore, Shabbeer et al. (2007) found that VPA exerts an anti-proliferative effect in PC-3 and DU145 cell lines. *In vivo* studies demonstrated inhibition of tumour growth in xenograft models under VPA treatment (Thelen et al. 2004; Xia et al. 2006). Similarly, in a study in nude mice bearing PC-3 and DU145 tumours, VPA can delay tumour growth, increase cell death, cause senescence, and confer anti-angiogenic effects. VPA can also induce cell cycle arrest *in vitro* at G1 in DU-145 cells, while at G2/M in PC-3 (Shabbeer et al. 2007), and up-regulate estrogen receptor and down-regulate the anti-apoptotic gene BCL-2 in breast cancer cells (Graziani et al. 2003; Iacopino et al. 2008; Takai et al. 2004).

The study by Chen et al. (2011) showed that VPA stabilised the acetylation status of p53, therefore causing an increase in its proapoptotic function via mitochondrial membrane interaction. This effect of VPA on p53 was found in both wildtype and mutated p53 in prostate and colon cancer cell lines (LNCaP, DU, and HCT 116) and to be independent of other mechanisms of activation of p53.

VPA has also been shown to increase cell death in most PCa cell lines, with a greater effect in PCa cell lines overexpressing ERG such as DUCaP and VCaP (Xia et al. 2006). Fortson et al. (2011) found that ERG can deregulate the acetylation–deacetylation cycle by binding and inhibiting HATs in combination with the higher expression of HDACs. VPA, as an HDACi, can suppress the function of ERG in the HAT pathways by inhibiting HDAC activity and

repressing the expression of ERG. Not only ERG (+) but also ERG (-) PCa cell lines may respond to the addition of VPA.

Although the effect of VPA on AR in PCa is not clearly understood, PCa relies on AR activity and VPA can down-regulate AR activity by interfering with acetylation status of AR in PCa cells (Gaughan et al. 2002).

1.4. Combination of MET and VPA for PCa treatment

1.4.1. Combination of non-cancer drugs for cancer treatment

Repurposing currently used drugs for cancer treatment offer an attractive approach to cancer patients with numerous benefits including **(1)** well-established toxicity profiles with greater potential for long-term therapy; **(2)** they can allow for rapid translation into clinical trials and the clinic; **(3)** they are generally inexpensive as most repurposed drugs are generic products. Shah et al. (2016) identified six non-cancer drugs including mitoxantrone hydrochloride, simvastatin, fluvastatin, and vandetanib that could inhibit the invasion and migration of the PCa cell line (PC-3).

The combination of drugs for cancer therapy has been widely investigated and implemented. The rationale for combination therapy includes **(1)** cancer initiation is associated with at least 12 different types of biological mechanisms which involve multiple events including gene mutation, amplification, deletion, and single nucleotide polymorphisms that accumulate over several years (Vogelstein et al. 2013), **(2)** the intra-tumour and tumour micro-environments are complex and heterogeneous (Gerlinger et al. 2012), **(3)** a large number of DNA alterations (Dienstmann et al. 2015) are involved in cancer resistance

after chemotherapy. Therefore, combinational therapy targeting multiple neoplastic pathways is more likely to be effective than monotherapy (Figure 1-11). One example is the combination of ADT and chemotherapy (Docetaxel) in advanced PCa treatment (Gravis et al. 2013).

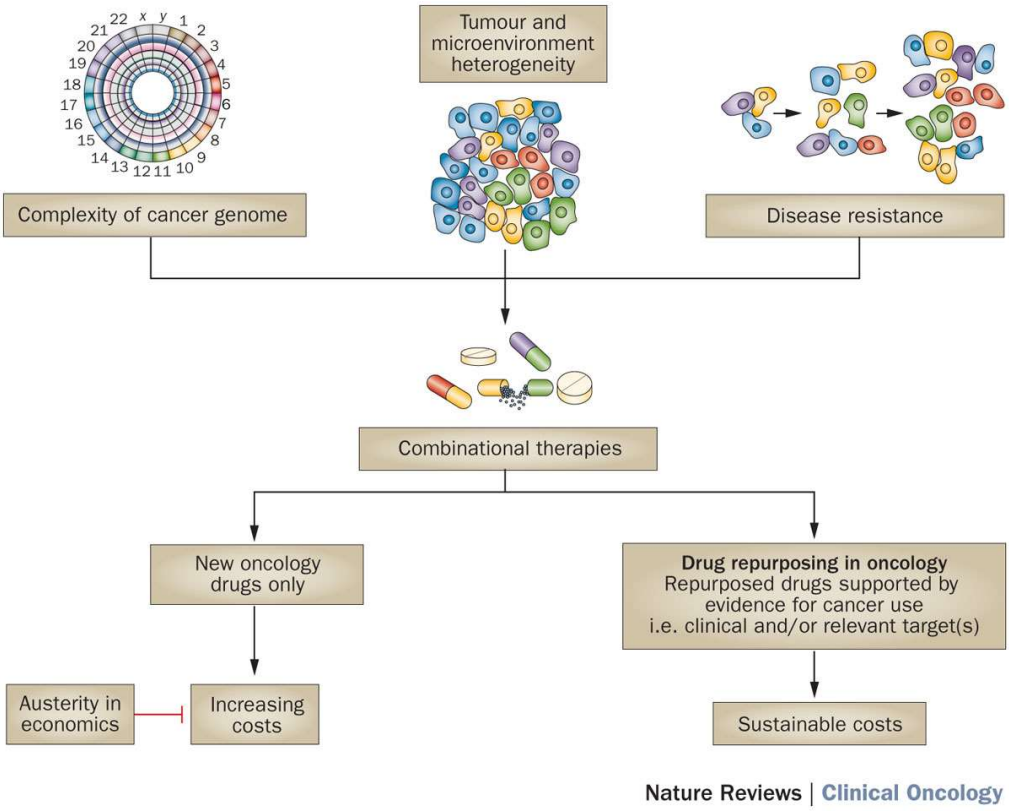

Figure 1-11. The algorithm of combinational therapy and drug repurposing in cancer

The complexity of the cancer genome, tumour and microenvironment heterogeneity, and cancer resistance after chemotherapy make combinatorial therapy preferable. The discovery of new oncology drugs is expensive and takes a very long time to be translated into the clinic. Therefore repurposing non-cancer drugs with anti-cancer activities could be cheaper and more rapidly translated into the clinic (taken from Bertolini et al. (2015)).

The advantages of combinational therapy include **(1)** decreasing the dose and therefore reducing the toxic adverse side-effects of a particular single therapy; **(2)** targeting different mechanistic pathways for multiple downstream molecular targets, which might result in greater response and less refractory

or resistant disease; **(3)** possible compensation of the side effects of a single drug.

The progression of PCa from local stage to CRPC involves multiple mechanisms including clonal selection, mutation or increased level of co-activator causing the activation of AR and upregulation of anti-apoptosis (So et al. 2005). The combination of current non-cancer drugs for PCa therapy could target multiple pathways to provide an efficient PCa treatment.

1.4.2. Limitations of MET or VPA monotherapy

MET and VPA have been investigated individually *in vitro,* and in pre-clinical studies *in vivo* as anti-PCa drugs with some success (Chen, Y et al. 2009; Martirosyan et al. 2006; Rosato et al. 2003; Savickiene et al. 2006; Zhou et al. 2001), however epidemiological studies and clinical trials have indicated limitations of MET and VPA as monotherapies. Although MET prolonged prostate-specific antigen (PSA) doubling time in progressive metastatic CRPC in a phase II clinical trial (Rothermundt et al. 2014), the study was limited by the lack of a control arm, the use of a high dose of MET (1000 mg x 2 per day), low response rate, and short treatment period (12 weeks). In a case-control study, MET did not reduce the incidence of PCa in patients treated with MET for diabetes type II (Azoulay et al. 2011). This evidence suggests that MET alone is not effective in all subsets of PCa patients. The fact that most epidemiological studies are investigated retrospectively, using different treatment regimens with multiple risk factors involved, added to the molecular heterogeneity of PCa, might contribute to the different findings. A recent investigation into the transportation of MET into cancer cells showed that the different responses depend on the level of organic cation transfer protein

(OCT) in the cell membrane. Subsequently, MET was found to be highly transported into liver cells, which express a high level of OCT1 (Wang, D-S et al. 2002), and kidney cells, which express a high level of OCT2 (Kimura et al. 2005). Prostatic cells also express OCT, and one clinical trial has shown that CRPC patients that are carriers of the OCT1 C-allele are associated with more disease progression with no MET-related toxicity compared to the carriers of at least one wild-type A-allele (Joerger et al. 2015). Thus, differences in the level of OCT expression and/or activity might be the cause of the different responses to MET in the different studies. Furthermore, the doses of MET needed to induce anti-cancer effects might be far higher than the therapeutic doses used clinically for treating diabetes. The *in vitro* doses of MET that induce anti-cancer effects range from 1 mM to 10 mM (Ben-Sahra et al. 2011; Fendt et al. 2013), which is far higher than the human therapeutic dose currently used in the clinical setting and is also much higher than the toxic threshold of 0.31 mM (Dowling et al. 2012; Vecchio et al. 2014). This suggests that as a monotherapy MET could not be used at the dose required to be effective without causing toxicity and therefore using a lower dose of MET in combinational therapy could produce less toxicity.

Similarly for VPA, a phase II clinical trial of 10 CRPC patients found that, although PSA levels in blood declined, no effect of VPA on disease progression was detected (Sharma, S et al. 2008). This was attributed to the failure to achieve the optimal pharmacological level due to VPA toxicity, suggesting that VPA alone as an anti-cancer agent may not be feasible.

1.4.3. Combinational therapy using MET for PCa treatment

Combinational therapy of MET on cell metabolism

Cancer cell energy metabolism which depends primarily on glycolysis rather than oxidative phosphorylation (Warburg Effect) is a target of combinational therapy involving MET (Warburg 1956). Ben-Sahra et al. (2010) demonstrated *in vitro* that the combination of MET and 2-deoxyglucose (2DG), a hexokinase inhibitor, induced additive p53 dependent apoptosis via the AMPK pathway in PCa cells (LNCaP) compared to using MET and 2DG alone. However, in an epidemiological study, the combination of MET and Sulfonylurea, another oral anti-hyperglycaemic medication, did not change the risk of PCa (Hazard ration (HR) 1.18, 95% CI 0.89–1.57) (Currie et al. 2009). Other combinational therapies using MET with different drug targets could be more promising. Diabetic patients often have lipoprotein abnormalities and require lipid-lowering statins, which are the hydroxymethylglutaryl-CoA (HMG-CoA) reductase inhibitors. When statins were combined with MET, a decrease in PCa risk was observed in retrospective studies (HR = 0.069, 95% CI 0.50-0.92) (Chen-Pin et al. 2014; Lehman et al. 2012). Additionally, the use of statins with MET in diabetic patients who had undergone radical prostatectomy synergistically reduced the biochemical failure in a retrospective study (Danzig et al. 2015). The mechanism of action of statins in combination with MET was related to the reduction of AMPKα1/α2 inhibitory proteins such as phospho-Akt (Ser473, Thr308, Ser485, Ser491) and also the induction of Ripk1 and Ripk3 dependent necrosis in PCa cells (C4-2B) (Babcook, Shukla, et al. 2014). Pennanen et al. (2016) found similar results where statins combined with MET

increased autophagy and necrosis in PCa cells (LNCaP) without significant harmful effects on normal prostatic epithelial cells (RWPE-1).

Combinational therapy of MET on androgen signaling inhibition

The androgen signaling pathway is crucial in PCa progression and ADT is the first line therapy for advanced PCa, however, long-term ADT comes with serious side effects including cardiovascular disease, obesity, anaemia, and osteoporosis. Eventually, most patients on ADT progress and develop CRPC, a lethal stage of the disease. The combination of MET and ADT has been investigated using epidemiology, *in vitro*, and *in vivo* studies, however the findings are controversial. Colquhoun et al. (2012) demonstrated that the combination of bicalutamide, an AR blocker, and MET reduced colony survival in AR^+ (LNCaP and PC-3AR), AR^- (PC-3) cells, and nude mouse xenografts (LNCaP) via activation of pAMPK, but was more pronounced in AR^+ cells. Investigation of AR expression showed that MET reduced the level of AR mRNA, therefore, further reducing the expression of AR in combination with Bicalutamide (Wang, Y et al. 2015). However, epidemiological findings have not supported the *in vitro* and *in vivo* results where the combination of MET and 5α-reductase inhibitor (Finasteride) increased PCa risk (HR = 1.42, $p < 0.001$) (Chen-Pin et al. 2014). The new generation of AR blockers such as enzalutamide and abiraterone acetate potentially provide an area of interest for future combination therapy with MET.

Combinational therapy of MET and mTOR inhibitors

One of the anti-cancer mechanisms of MET acts via the inhibition of mTOR activity. Combining MET and Rapamycin, an mTOR inhibitor, increased the

expression of pAMPK, therefore decreasing the expression of pmTOR^{Ser2448}, pP70S6K^{Thr389}, and pS6 Ribo$^{Ser240/244}$ (Saha et al. 2015). In the same study, the expression of inflammation and angiogenesis markers (CCL5, IL1α, IL1β, IL6, IL23, TNF- α, CXCL12, HIF1- α, VEGFA, VEGFB) was significantly reduced *in vitro* and *in vivo*. Another combination, MET with Vitamin D3, was recently found to inhibit mTOR activity (Al-Hendy et al. 2016), resulting in an additive reduction in the expression of mTOR in PCa cells (DU145) (Li, HX et al. 2015).

In general, most of the studies using combination therapies with MET have been epidemiological, *in vitro*, and pre-clinical animal studies. More clinical trials are needed to translate these findings into clinical practice. The main findings from the literature on combination therapy with MET for PCa are summarized in Table 1-1.

Table 1-1. Summary of combinational therapies using MET for PCa treatment

MET in combination with:	Study design	Main findings	References
Sulfonylurea (SUL)	Retrospective cohort study in diabetic patients diagnosed with PCa (n = 62,809).	MET+SUL reduced the PCa risk in diabetic patients (HR = 1.18, 95% CI 0.89-1.57).	Currie et al. (2009)
2-deoxyglucose (2DG)	*In vitro* study in PCa cell line (LNCaP)	MET+2DG induced p53 dependent apoptosis via AMPK pathway. Autophagy induced by 2DG was switched to apoptosis in response to MET+2DG	Ben-Sahra et al. (2010)
Lifestyle intervention (low glycaemic index diet and exercise)	Prospective, randomised pilot study in PCa patients treated with ADT (n = 40).	Lifestyle intervention + MET reduced the complication of ADT.	Nobes et al. (2012)
Dendrimer-vehiculised siRNA to block the MAPK signaling pathway	*In vitro* study in PCa cell lines (LNCaP and PC-3)	siRNA knock down of MAPK pathway enhanced anti-tumour effect of MET.	Monteagudo et al. (2012)
Statins (STA)	Retrospective cohort study (n = 5,042).	MET+STA reduced the risk of PCa (HR = 0.69, 95% CI 0.50-0.92).	Lehman et al. (2012)

MET in combination with:	Study design	Main findings	References
Bicalutamide (BIL)	*In vitro* study in PCa cell lines (LNCaP, PC-3, PCAR2, and DU145) and *in vivo* study in nude mice bearing LNCaP xenograft.	MET+BIL induced a direct anti-proliferative effect via activation of pAMPK in AR^+ cells (LNCaP and PC-3AR), but no reduction in mTOR expression. MET+BIL increased cell death via increased level of apoptosis in AR^- cells.	Colquhoun et al. (2012)
Finasteride (FIN) and/or statins (STA)	Cohort study (Retrospective) in type 2 diabetes mellitus patients (n = 71,999).	MET alone reduced PCa risk (HR = 0.89, p = 0.02). MET+STA further reduced PCa risk (HR = 0.72, p < 0.001). MET+FIN increased PCa risk (HR = 1.42, p < 0.001).	Chen-Pin et al. (2014)
Simvastatin (SIM)	*In vitro* study in osseous metastatic CRPC cell lines (C4-2B3/B4/B5 and PC-3 D12) and *in vivo* study in C4-2B4 orthotopic male NCr-*nu/nu* mice	MET+SIM decreased the expression of Phos-Akt Ser-473, Thr-308, reducing the inhibition of Pho-Ser-485/491 on AMPKα1/ α2, increased Thr-172 phosphorylation, and activated AMPKα kinase. MET+SIM induced Ripk1 and Ripk3 dependent necrosis in C4-2B cells.	Babcook, Shukla, et al. (2014)
Zyflamend (ZYF) (herbal extracts)	Case series in CRPC patients (n = 4) (one patient had ZYF+MET)	ZYF+MET reduced the PSA level in chemo-resistance CRPC patient.	Bilen et al. (2015)

MET in combination with:	Study design	Main findings	References
Statins (STA)	Retrospective study in type 2 diabetes mellitus patients that underwent radical prostatectomy (n = 777).	MET+STA synergistically reduced risk of biochemical recurrence (HR = 0.2, p = 0.037).	Danzig et al. (2015)
Vitamin D3 (Vit D3)	*In vitro* study in PCa cell line (DU145)	MET+Vit D3 further increased the expression of AMPK and further inhibited the expression of mTOR.	Li, HX et al. (2015)
Rapamycin (RAPA)	*In vitro* study PCa cell lines (HMVP2, LNCaP) and *in vivo* in HiMyc mice.	MET+RAPA further increased the expression of pAMPK, decreased further the expression of $pmTOR^{Ser2448}$, $pP70S6K^{Thr389}$, and pS6 $Ribo^{Ser240/244}$. MET+RAPA further reduced the expression of inflammation and angiogenesis markers (CCL5, IL1α, IL1β, IL6, IL23, TNF- α, CXCL12, HIF1- α, VEGFA, and VEGFB).	Saha et al. (2015)
Bicalutamide (BIL)	*In vitro* study in PCa cell lines (LNCaP and CWR22Rv1).	MET reduced the level of AR mRNA and BIL inhibited activation of AR. MET+BIL induced an additive decrease in proliferation and increase in apoptosis.	Wang, Y et al. (2015)

MET in combination with:	Study design	Main findings	References
p53 stabilisers (SIRT1 [Tneovin-1 inhibitor] and BI2536 [Polo-like kinase 1 inhibitor])	*In vitro* study in PCa cell lines (C4-2 and LNCaP).	MET+SIRT1/BI2536 potentiated the oxidative phosphorylation inhibition of MET. Synergistic apoptosis achieved through regulation of energy metabolism in CRPC.	Chen, L et al. (2016)
Statins (STA)	*In vitro* study in PCa cell line (LNCaP) and normal cells (RWPE-1).	MET+STA synergistically decreased ATP levels in cytosol and induced necrosis and autophagy in LNCaP cells. The synergistic effect was not observed in RWPE-1.	Pennanen et al. (2016)
Multiple myeloma SET domain (MMSET) siRNA-mediated knockdown	*In vitro* study in PCa cell lines (DU145 and 22Rv1) and normal cells (RWPE-1).	PCa cells overexpress MMSET. MET+MMSET siRNA showed a further reduction in cellular migration and invasion.	White-Al Habeeb et al. (2016)
GLI-Antagonist 61 (GANT61) – a Hedgehog signaling inhibitor ± X-radiation	*In vitro* and *in vivo* studies in PCa cell lines (PC-3, DU145, and 22Rv1).	MET+GANT61 reduced further the cell growth *in vitro* and enhanced radiation response of 22Rv1 cells. *In vivo* study did not observe the same effect as *in vitro*.	Gonnissen et al. (2017)

MET in combination with:	Study design	Main findings	References
Docetaxel (DTX)	Retrospective cohort study in diabetic and non-diabetic patients diagnosed with CRPC (n = 2,832)	MET+DTX did not improve PCa specific survival (HR = 0.96, p = 0.66) or overall survival (HR = 9.94, p = 0.39).	Mayer et al. (2017)

1.4.4. Combinational therapy using VPA for PCa treatment

Combinational therapy of VPA and pro-apoptotic agents

In order to enhance the apoptotic effect of VPA, Ouyang et al. (2011) investigated the combination of VPA and Gossypol (GOS), a natural mimetic of BH3 domains. GOS normally binds to the Bcl-2 family and inhibits the effects of Bad, Bax and Bim (anti-apoptotic proteins) and enhances the expression of pro-apoptotic proteins. This study found that VPA+GOS downregulated DNA repair proteins, causing more DNA fragmentation and cell death. In addition, GOS-induced-mitochondrial stress, glycolysis- and hypoxia-associated proteins was further increased in response to VPA+GOS.

Combination therapy of VPA and protein kinase inhibitors

VPA can alter not only the acetylation status of histone proteins, but also transcriptional factors such as kinase proteins. The combination of VPA with different types of protein kinase inhibitors has been widely investigated in the literature and some promising results have been reported. Polo-like kinase 1 inhibitors (Plk1) BI 2536 and BI 6727, which inhibit serine-threonine kinase, when combined with VPA showed a synergistic reduction in the clonogenic survival of PCa cells (PC-3, DU145, LNCaP) via down-regulating Plk1 expression (Wissing et al. 2013). It is known that the Aurora kinases A (involved in centrosome maturation, cell cycle progression, and spindle assembly) and B (involved in cell cycle G2/M and the final step of cytokinesis) are overexpressed in tumour cells. Combination of Pan-aurora kinase inhibitor (AMG 900) and VPA increased multipolar spindle formation and polyploidy as compared to single agents in PCa cell lines (PC-3, DU145, LNCaP) and DU-145 xenografts in NOD/SCID mice (Paller et al. 2014). Another study by Qian

et al. (2004) found that the combination of VPA and VEGF receptor tyrosine kinase inhibitor (PTK787/ZK222584), a common target of cancer treatment, further inhibited PCa in the PC-3 cell line and PC-3 xenografts via both cell cycle arrest (p21 inhibition) and angiogenesis inhibition (VEGF pathway block). The safety of this combination was investigated in a phase I clinical trial using a combination of Bevacizumab, an anti-VEGF monoclonal antibody, and it was found that this combination was feasible in advanced cancer (Wheler et al. 2014). However, the combination of VPA and a multiple receptor tyrosine kinase inhibitor (AEE788) in different PCa cell lines (PC-3, DU145, and LNCaP) did not induce an additive anti-tumour effect (Wedel, Hudak, Seibel, Juengel, Oppermann, et al. 2011). These findings suggest that the anti-cancer response of VPA in combination with protein kinase inhibitors requires further investigation.

Other VPA combination therapies

HDAC3 regulates the activity of peroxisome proliferator-activated receptor γ (PPARγ), an E-Cadherin regulator. In PCa, the total level of PPARγ is overexpressed and largely in the inactivated form. The combination of VPA and Pioglitazone, a PPARγ agonist, induced increased expression of E-Cadherin, therefore reducing the invasiveness of PCa cell lines (LNCaP, DU145, PC-3) and PC-3 xenografts in mice (Annicotte et al. 2006).

The combination of Trichostatin-A, an HDACi of class I and II, and VPA has been useful in PCa with ERG overexpression, a poor prognostic factor in PCa. Fortson et al. (2011) showed that, ERG overexpression in PCa cells (VCaP) inhibited HATs and increased HDAC inhibition, and the addition of Trichostatin-A and VPA counteracted this action via repressing ERG

expression, releasing the inhibitory effect of ERG on CBP/p300, and restoring p53 activation (Fortson et al. 2011). However, given the context of HDACi-related toxicity, the combination of two similar HDACi could potentially cause more adverse effects in normal cells.

The very early results of a phase I clinical trial using VPA and *all-trans* retinoic acid IV (ATRA-IV) in advanced PCa showed a positive response in PCa patients. However, this study had a very small sample size (n = 2) and needs further investigation before a conclusion can be made (David et al. 2010). The main findings from the literature on combination therapy with VPA for PCa are summarized in Table 1-2.

Table 1-2. Summary of combinational therapies using VPA for PCa treatment

VPA in combination with:	Study design	Main findings	References
Pioglitazone (peroxisome proliferator-activated receptor γ [PPARγ] agonist)	*In vitro* study in PCa cell lines (LNCaP, DU145, PC-3) and *in vivo* study in male *Rj:NMRI-nu* and *CD17-SCID/bg* mice bearing PC-3 xenografts (luminescent).	VPA+Pioglitazone further inhibited HDAC3, therefore activating PPARγ and inducing greater expression of E-Cadherin.	Annicotte et al. (2006)
All-trans retinoic acid IV (ATRA-IV)	Phase I clinical trial in patients with solid cancer (n = 9 with two cases of PCa).	The best response was in one patient who had PCa (in advanced stage)	David et al. (2010)
1,25-dihydroxyvitamin D3 (Vit D3 1,25) and X-radiation	*In vitro* study in PCa cell line (DU145).	VPA+Vit D3 1,25 further increased DNA double strand breaks in response to radiation.	Gavrilov et al. (2010)
Gossypol (GOS) (natural mimetics of BH3 domains)	*In vitro* study in PCa cell lines (DU145).	VPA+GOS downregulated DNA repair proteins and anti-apoptotic proteins (Bax, Bad and Bim), inducing more DNA fragmentation and cell death. VPA+GOS further increased GOS-induced mitochondrial stress and upregulated glycolysis- and hypoxia-associated proteins.	Ouyang et al. (2011)

VPA in combination with:	**Study design**	**Main findings**	**References**
Multiple receptor tyrosine kinase inhibitor (AEE788)	*In vitro* study in PCa cell lines (PC-3, DU145, and LNCaP).	VPA and ARR788, by itself, impaired the expression of proteins involved in cell cycle (cyclin B, cdk1, cyclin E, p21, cdk2, D1, and p27). VPA+AEE788 did not induce an additive anti-tumour effect.	Wedel, Hudak, Seibel, Juengel, Oppermann, et al. (2011)
mTOR inhibitor (RAD001)	*In vitro* study in PCa cell lines (PC-3, DU145, and LNCaP).	VPA targeted cdk1, cdk2, p21, and EGFr-ERK-Akt signalling. RAD001 targeted Akt-p70S6k phosphorylation (integrin-related signalling), VPA+RAD001 induced additive inhibition on migratory and invasive behaviour and prevented a negative feedback loop.	Wedel, Hudak, Seibel, Juengel, Tsaur, et al. (2011)
Multiple receptor tyrosine kinase inhibitor (AEE788) and mTOR inhibitor (RAD001)	*In vitro* study in PCa cell lines (PC-3, DU145, and LNCaP).	VPA+AEE788+RAD001 induced a stronger reduction of cdk1, cdk2, cdk4, and cyclin B, altered the expression integrin α and β subtypes, and decreased the expression of EGFr (PC-3, LNCaP), pEGFr (DU145), pERK, and pp70S6k.	Wedel, Hudak, Seibel, Makarevic, Juengel, Tsaur, Waaga-Gasser, et al. (2011)

VPA in combination with:	**Study design**	**Main findings**	**References**
Dihydrotestosterol (DHT)	*In vitro* in PCa cell lines (LNCaP, C-81, C4-2, and MDA PCa2b-AI).	Pre-treatment with VPA enhanced the androgen responsiveness in response to DHT in androgen-sensitive cell lines.	Chou, Y-W et al. (2011)
Trichostatin-A (TSA)	*In vitro* study in PCa cell line (VCaP).	VPA+TSA repressed TMRPSS2-ERG expression, releasing the inhibitory effect of ERG on CBP/p300 which restores p53 activation.	Fortson et al. (2011)
Interferon-α (IFN-α)	*In vitro* study in PCa cell lines (PC-3, DU145, and LNCaP) and *in vivo* study in xenograft in NOD/SCID mice bearing CWR-22 PSA-positive PCa cells.	VPA+IFN-α further increased Histone H3 acetylation, integrin α1 and β1, therefore reducing migration and differentiation.	Hudak et al. (2012)
Polo-like kinase 1 inhibitors (Plk1) BI2536 and BI6727.	*In vitro* study in PCa cell lines (PC-3, DU145, and LNCaP) and normal prostate epithelial cells (PrEC) and human prostate fibroblasts.	VPA+BI2536/BI6727 down-regulated Plk1 expression and synergistically reduced clonogenic survival (more prominent in BI 2536).	Wissing et al. (2013)

VPA in combination with:	**Study design**	**Main findings**	**References**
Pan-aurora kinase inhibitor (AMG900)	*In vitro* study in PCa cell lines (PC-3, DU145, LNCaP) and *in vivo study* in NOD/SCIDs mice bearing DU-145 xenografts.	VPA+AMG900 further inhibited aurora kinase expression, additively decreasing proliferation and survival of PCa cells. VPA+AMG 900 also increased multipolar spindle and polyploidy compared to single agents.	Paller et al. (2014)
Anti-VEGF monoclonal antibody (Bevacizumab (BEV))	Phase I clinical trial in metastatic PCa (n = 57).	VPA (5.3 mg/kg) + BEV (11 mg/kg) was safe in advanced PCa patients.	Wheler et al. (2014)

1.4.5. Combination of MET and VPA for PCa treatment

MET and VPA have been trialled individually as anti-cancer drugs with varying success. The combination of MET and VPA for prostate cancer treatment has several potential advantages. MET and VPA are widely used drugs for non-cancer purposes and their pharmacokinetics and toxicity have been well-studied. MET and VPA have been demonstrated to induce cell death i*n vitro* and in *in vivo* animal studies by different molecular pathways. The study of Wedel et al. (2011), which demonstrated that the combination of an mTOR inhibitor (RAD001) with VPA in PCa cell lines induced an additional anti-cancer effect (Wedel, Hudak, Seibel, Juengel, Tsaur, et al. 2011), also supports the opportunity to combine MET, an mTOR inhibitor, and VPA, a HDACi, in prostate management.

Additionally, combinatorial therapy of MET and VPA could potentially be more effective than monotherapy as: **(1)** MET and VPA induce cell cycle arrest, and their antiproliferative and proapoptotic effects occur via different mechanisms; **(2)** Lower doses of VPA and MET in combination could reduce the toxicity observed with higher doses of the single drugs; **(3)** Translation into the clinic would be rapid as MET and VPA are currently widely used drugs for non-cancer purposes.

The combination of MET and VPA for PCa treatment has not been studied thoroughly in the literature. There has been one report published during the course of this PhD project using MET and VPA in combination in clear cell renal cell carcinoma cell lines (786-0 and Caki-2) where synergistic antiproliferative and proapoptotic effects were observed, however normal cells

were not studied, and the rationale for the drug combination was not based on detailed mechanism (Zhang et al. 2015).

It is hypothesised here that the combination MET and VPA induces a synergistic anti-cancer effect in PCa, while inducing minimal effect on normal cells and tissues, and the anti-cancer response will be dependent on the expression of common molecular markers of PCa such as p53 and AR.

1.5. Aims of this thesis

The overall aim of this thesis was to determine if the combination of MET and VPA (MET+VPA) was more effective as an anti-cancer therapy compared to either drug alone. This was explored:

1. *in vitro* in PCa cell lines with different p53 and AR status (LNCaP and PC-3) and primary prostate epithelial cells (PrEC).
2. *in vivo* in nude mouse xenografts bearing LNCaP and PC-3.
3. *ex vivo* in human PCa tumour explants.

2. MATERIALS AND METHODS

2.1. In vitro experiments

2.1.1. Cell lines

Human PCa cell lines, LNCaP (clone FGC) (CRL-1730), and PC-3 (CRL-1435) were newly obtained from the American Type Culture Collection (ATCC®, USA). LNCaP cells are derived from a left supraclavicular prostatic lymph node metastasis of a 50-year-old PCa patient (Horoszewicz et al. 1983). LNCaP has normal AR expression (AR^+), is androgen sensitive, with normal p53 protein expression ($p53^+$) (Horoszewicz et al. 1983), no ERG overexpression (ERG^-), and no PTEN expression ($PTEN^-$) (Van Bokhoven et al. 2003). PC-3 is derived from a human prostatic adenocarcinoma metastasis to the bone (Kaighn et al. 1979). PC-3 is a poorly-differentiated adenocarcinoma and has the characteristics of small cell carcinoma of PCa (Tai et al. 2011), is AR^-, androgen insensitive (Tai et al. 2011), $p53^-$ (Van Bokhoven et al. 2003), ERG^-, and $PTEN^-$ (Sobel, R. E. et al. 2005). The normal, non-immortalized human prostate epithelial cell line (PrEC, CC2555) was purchased from Lonza (USA). It was derived from the prostate of a 14-year-old. PrEC harbours normal p53 and is $PTEN^+$, however AR and PSA expression are not detected in this cell line (Sobel, Richard E et al. 2006). The expression of p53, PTEN, ERG, and AR (via PSA expression) in these cell lines is summarised in Table 2-1.

Table 2-1. Molecular characteristics of LNCaP, PC-3, and PrEC cells

	Androgen sensitive	AR	ERG	p53	PTEN
LNCaP	Yes [a]	Yes [a]	No [e]	Yes [c]	*No* [e]
PC-3	No [b]	No [b]	No [e]	No [c]	No [e]
PrEC	No [d]	No [d]	No [e]	Yes [f]	Yes [g]

[a] Horoszewicz et al. (1983), [b] Kaighn et al. (1979), [c] Carroll et al. (1993), [d] Sobel, Richard E et al. (2006), [e] Tomlins, Scott A et al. (2008), [f] Aimola et al. (2012), [g] John et al. (2012)

2.1.2. Cell culture conditions

All cell lines were maintained in a humidified incubator at 37°C under 5% CO_2 and cells were passaged for a maximum of 4 months. PC-3 and LNCaP cells were grown in RPMI 1640 (Roswell Park Memorial Institute) medium (ThermoFisher, #11875) supplemented with 100 Units/mL Penicillin / 100 µg/mL Streptomycin (ThermoFisher, #15070063) and 5% Foetal Bovine Serum (FBS Lot No 1111A) from Bovogen (AU).

PrEC were grown in Prostate Epithelial Cell Medium BulletKit® (Lonza, CC3166) containing Prostate Epithelial Cell Basal Medium and the following growth supplements for each 500 mL of medium: 2 mL bovine pituitary extract; 0.5 mL hydrocortisone; 5 mL human epidermal growth factor; 0.5 mL epinephrine; 0.5 mL transferrin; 0.5 mL insulin; 0.5 mL retinoic acid; 0.5 mL triiodothyronine; 0.5 mL gentamicin-amphotericin B (GA-1000).

2.1.3. Cell passaging

All cells were grown in T-75 flasks (ThermoFisher, NUN156499) in a total volume of 15 mL and passaged twice weekly. When cells reached 90% confluence, they were washed with sterile filtered (0.22 µm) PBS, incubated with 1 mL 0.05% Trypsin/0.48 mM EDTA (ThermoFisher, #15400054) for 3-5 mins until the cells were completely detached from the culture vessel. A volume of culture medium (9 mL) was added back into the flasks. The cells were resuspended into a sterile tube, centrifuged at 160 x *g*, and transferred to a new flask at an appropriate dilution (LNCaP 1:5, PC-3 1:20).

PrEC were allowed to grow until 60-80% confluence and then harvested using ReagentPack™ (Lonza, CC5034) as per instructions from Lonza. The cells were washed with HEPES Buffered Saline Solution (HEPES-BSS), then covered with 2 mL of Trypsin/EDTA solution and incubated for 2-6 mins until all cells were detached. Trypsin Neutralizing Solution was added to neutralise the Trypsin. The cell solution was centrifuged at 160 x *g* for 5 mins, then resuspended in a new flask at 10,000 cells/cm^2.

2.1.4. Mycoplasma testing

Cell lines were checked regularly for *Mycoplasma* contamination and only *Mycoplasma* negative cells were used in experiments. DNA extraction from cells was performed using Alkali Lysis buffer. One mL of Sodium Chloride (0.9%) was added to 200 µL of cell suspension, then the cells were centrifuged at 4700 x *g* for 5 mins and the supernatant was discarded. The pellets were resuspended in 90 µL 0.05 M NaOH and then heated at 98^{o}C for 10 mins to lyse the cells. After cooling down to room temperature, 10 µL of 1 M Tris pH 7.5 was added to each tube to neutralise the solution. PCR primers, GPO-1

and MGSO, were used to amplify a 715 bp region of *Mycoplasma* species (four humans and five mouse species) (Van Kuppeveld et al. 1992). HRAG-1-F and HRAG-1-R primers were used to amplify a 522 bp region of the *Rag1* gene as a DNA amplification positive control (Hayakawa et al. 1996). PCR reactions were performed in 10X *Taq* DNA polymerase PCR Buffer (ThermoFisher, #18067-017). Each PCR sample contained 0.2 µL of platinum *Taq* DNA polymerase (ThermoFisher, #10966018), 0.5 µL of 10 mM dNTP mix (ThermoFisher, #18427088), 2.5 µL of PCR Buffer, 50 ng of HRAG-1-F and HRAG-1-R, 50 ng of GPO-1 and MGSO, and 2.5 µL of 10X *Taq* DNA polymerase PCR Buffer. The PCR cycle conditions were 95^{o}C for 5 mins to activate the Platinum *Taq* DNA polymerase, then 50 cycles of 94^{o}C for 30 seconds, 53^{o}C for 1 min, and a final extension of 5 mins at 72^{o}C. The PCR controls included DNA extracted from *Mycoplasma* positive cells (positive control), negative (negative control) cells, and no DNA template water (water used in dilution).

2.1.5. Treatment with MET and VPA

Metformin (PHR1084-500MG) and valproic acid (P4543-10G) were purchased from Sigma (U.S.) and stocks (100 mM) were made in distilled water and sterilised using a 0.22 µm filter.

The adherent prostate cell lines in T75 culture flasks were washed briefly with filtered sterile PBS and incubated with 1 mL Trypsin-EDTA until cells were detached. The cells were resuspended in 9 mL of cell culture medium and transferred to a 10 mL sterile tube. Fifty µL of cell suspension was taken for a haemocytometer count before centrifuging the cells at 160 x *g* for 5 mins. After centrifugation, the medium was removed and the cell pellet was resuspended

in 5 mL fresh medium. Cells were seeded at a predetermined number into a 96-well plate in a volume of 100 µL, then allowed to grow 24-48 h before treating with MET and/or VPA. MET and VPA stocks were diluted to a desired final concentration (1 mM and 2.5 mM, respectively) in the medium before adding to the culture vessel to a final volume of 200 µL.

2.1.6. Treatment with Enzalutamide

Enzalutamide (S1250) was purchased from Selleck Chemicals (U.S.), sterilised using a 0.22 µm filter and stored as a 5 mM stock in Dimethyl Sulfoxide (DMSO) (Sigma). Enzalutamide binds to AR and blocks the AR activation in LNCaP, a hormone sensitive cell line (Guerrero et al. 2013). For validation of AR inhibition efficiency of Enzalutamide, LNCaP cells were grown in 6-well plates and treated with Enzalutamide for 24 h, 72 h or 96 h, proteins were extracted and the expression of prostate-specific antigen (PSA) was measured using western blot (see Section 2.1.11.1). LNCaP cells were grown in 96-well culture plates and treated with 1 µM Enzalutamide for 24 h before treating with the vehicle, MET alone, VPA alone, or MET+VPA at 1 mM and 2.5 mM for 72 h. Cell apoptosis was investigated using the CellPlayer™ 96-well Kinetic Caspase 3/7 Apoptosis Assay Kit (Millennium Science, #4440) (Section 2.1.7).

2.1.7. Detection of proliferation and apoptosis using the Incucyte® FLR imaging system

Cell proliferation was measured using an Incucyte® FLR imaging system (Essen BioScience) which analysed the occupied area (% confluence) using live cell time-lapse imaging. PCa cell lines were seeded at 7000 cells/well (LNCaP) or 5000 cells/well (PC-3) in 96-well culture plates (#163320, Nunc) in

100 µL/well RPMI 1640 with 5% FBS and allowed to grow overnight at 37°C. The next day, fresh medium containing vehicle, MET alone, VPA alone, or MET+VPA (1 mM or 2.5 mM of each drug) was added. The percentage of cell confluence was monitored automatically every 2 h for 3 days after treatment using the Incucyte® FLR – phase contrast mode.

The CellPlayer™ 96-well Kinetic Caspase 3/7 Apoptosis Assay Kit (#4440, Millennium Science) was used to measure apoptosis automatically in live cells every 2 h for 3 days. The Incucyte™ Caspase-3/7 Reagent is coupled to NucView™488, a DNA intercalating dye, via the activated caspase-3/7 recognition motif (DEVD). Upon entering the cell, the fluorescent dye is released following cleavage with activated caspase 3/7 in cells resulting in green fluorescent staining of nuclear DNA (wavelength 488 nm) (Figure 2-1).

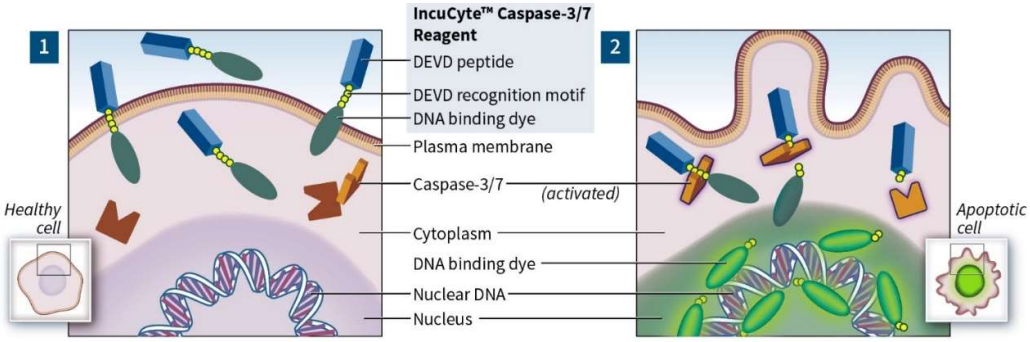

Figure 2-1. CellPlayer™ 96-well Kinetic Caspase 3/7 Apoptosis Assay Kit overview schematic.
(1) *No fluorescence in the presence of healthy cells. The Caspase-3/7 Reagent freely crosses the cell membrane and is non-fluorescent.* ***(2)*** *Activated caspase-3/7 cleaves the Caspase-3/7 Reagent at the DEVD recognition motif, releasing a fluorescent dye which binds to nuclear DNA (adapted from www.essenbioscience.com, accessed in Oct 2016).*

At the end of day 3, the DNA Vybrant® DyeCycle™ Stain (ThermoFisher, V35004) was added at 1 µM per well and incubated for 1 h before scanning with the Incucyte® fluorescence mode. The automated Incucyte® FLR object counting algorithm was used to count the number of positive staining cells. The percentage of apoptosis was calculated by dividing the number of caspase 3/7 positive objects by the total number of DNA containing objects:

$$\% \text{ apoptosis} = \frac{No.\,Caspase\ 3/7\ positive\ objects}{Total\ No.of\ DNA\ containing\ objects}$$

2.1.8. Knock down of mRNA using RNA interference

siRNA p53 and siRNA control were purchased from SignalSilence® (#6231). siRNA was transfected into the LNCaP cell line using Lipofectamine® 2000 (ThermoFisher, #11668019) according to the manufacturer's instructions. LNCaP cells were seeded at 7000 cells/well and grown for 24 h in antibiotic-free medium until reaching 40-60% confluence. siRNA p53 and siRNA controls were prepared by diluting in OptiMEM® I Reduced Serum medium (ThemoFisher, #31985088). Lipofectamine™ 2000 was added to OptiMEM® I Reduced Serum medium, then incubated for 5 mins at room temperature before mixing with diluted siRNA oligomers. The solution was mixed gently and incubated for 20 mins at room temperature before adding to cells. The final concentration of siRNA, when added to the cells, was 25 nM and the volume of Lipofectamine™ 2000 was 0.5 µL for each well.

The transfection efficiency was validated by western blot using the Chemidoc™ MP system (Biorad). The detailed protocol for western blot analysis is described in Section 2.1.11. Primary p53 antibody (SC-126, Santa Cruz Biotechnology) binding was detected by horseradish peroxidase (HRP)

secondary antibody using Clarity™ Western enhanced chemiluminescence (ECL) blotting substrate. β-actin primary antibody (Abcam, ab8227) binding was detected by Alexa Fluor® 488 conjugated goat anti-rabbit IgG secondary antibody (ThermoFisher, A-11008) or by HRP-conjugated secondary antibody using Clarity™ Western ECL blotting substrate. The percentage of reduction in p53 expression was calculated using a ChemiDoc™ MP system (Bio-Rad) and normalised to both β-actin and total protein.

2.1.9. Ectopic expression of TP53 gene using plasmid DNA transfection

2.1.9.1. *Plasmid purification and plasmid extraction*

Green fluorescence protein (GFP)-integrated p53 plasmid (Boyd et al. 2000) was purchased from Addgene ((#12091) (full sequence of GFP-integrated p53 is described in Appendix B). The plasmid was transfected into *E.coli DH5-α* bacteria using Lipofectamine 3000® (ThermoFisher), then streaked onto an lysogeny broth (LB) agar plate containing 50 µg/mL kanamycin and incubated overnight at 37°C. Single colonies were transferred to a tube containing 20 mL of liquid LB with 50 µg/mL kanamycin and incubated at 37°C for 12-18 h in a shaking incubator. Bacterial stocks were prepared by adding 500 µL of overnight culture to 500 µL of 50% glycerol in cryovials, which were subsequently stored at -80°C.

For plasmid extraction, a single transfected colony was transferred into liquid LB, and allowed to grow overnight at 37°C in a shaking incubator. A Qiagen® Plasmid *Plus* Midi Kit (#12943, Qiagen®) was used to extract the plasmid from the bacteria. The culture was harvested by centrifugation at 6000 x *g* for 15 mins at 4°C. The supernatant was aspirated and the bacterial pellet resuspended in 2 mL of Buffer P1, followed by 2 mL of Buffer P2 and gently

mixed until the lysate appeared viscous. The lysate was incubated at room temperature for 3 mins, after which 2 mL of Buffer S3 was added. The lysate was then transferred to a QIAfilter Cartridge and incubated at room temperature for 10 mins. The cell lysate in the QIAfilter Cartridge was filtered into the tube, then 2 mL of Buffer BB was added to the lysate. The solution was transferred to a QIAGEN Plasmid *Plus* spin column and filtered until the liquid had been drawn through all columns. The residual wash buffer was removed by centrifuging at 10,000 x *g* for 1 min. Plasmid DNA was eluted by adding 200 µL Buffer EB to the centre of the QIAGEN Plasmid *Plus* spin column and centrifuging at 10,000 x *g* for 1 min. The p53 plasmid quantification was performed using a NanoDrop™ 8000 (ThermoFisher) Spectrophotometer at 260 nm before storing at -20°C.

2.1.9.2. *Plasmid transfection control*

The plasmid transfection control used was the GFP-only plasmid which was made from the GFP- p53 plasmid. In short, to remove the p53 region of the GPR-integrated p53 plasmid, 10 units of digestion enzymes BamHI (New England Biolabs, R3136) and BglII (New England Biolabs, R0144S) were added to 1 µg of plasmid DNA with an appropriate amount of NEBuffer 3.1 (New England Biolabs, B7203S). The solution was incubated at 37°C for 4 h. The digestion efficiency was verified by running 0.2 µg of digest on a 1% agarose gel at 110 V in TAE buffer, and the band containing GFP-only and backbone plasmid (at 4683 kb) was removed from the gel using a scalpel. The plasmid DNA in gel was purified using an Ultraclean 15 DNA Purification Kit (Qiagen, 12100-300), then religated using T4 DNA ligase (Promega, M180A) before transforming into the DH5-α competent bacteria. A single colony was

selected for plasmid extraction. The control plasmid was verified by gel electrophoresis and for the expression of GFP (see Section 3.3.3).

2.1.9.3. *Plasmid transfection*

PC-3 (p53^{null}) cells were grown in CellCarrier™ 96-microplates and allowed to reach 60-70% confluence before transfecting with 0.1 µg GFP-p53 (Boyd et al. 2000) or GFP-only plasmid using Lipofectamine 3000® (ThermoFisher), according to the manufacturer's instructions. Cell nuclei were then stained with *1,5-bis[[2-(di-methylamino)ethyl]amino]-4, 8-dihydroxyanthracene-9, 10-dione* (DRAQ5™) (Abcam, ab108410) at 12 h, 48 h or 96 h after transfection. Cells expressing p53/GFP were detected using green fluorescence (excitation band 460-490 nm and emission band 500-550 nm) on an Operetta® High Content Imaging System (PerkinElmer) and the total cell number was visualised using far-red fluorescence DRAQ5™ stain (excitation band 620-640 nm and emission band 650-760 nm). Transfection efficiency was calculated by dividing the number of positive GFP cells by the number of total cells stained with DRAQ5™ using Harmony® High Content Imaging and Analysis Software (PerkinElmer).

2.1.10. Apoptosis using the Operetta® High Content Imaging System

Cells that were transfected with p53 plasmid were treated with vehicle, MET, VPA or MET+VPA (1 mM or 2.5 mM) 12 h after transfection, and cultured for 3 days. Cells were first fixed with 4% formaldehyde and permeabilised with 0.5% Triton-X in phosphate-buffered saline (PBS), and then incubated with 3% Bovine Serum Albumin (Sigma) in PBS for 1 h at room temperature. Cleaved-caspase 3 (CC-3) was labelled using anti-active caspase-3 primary antibody (Abcam, b32042) and visualised with an Alexa Fluor 555 IgG (H+L) secondary

antibody (ThermoFisher, A21428). Cell nuclei were stained with DRAQ5™. The Operetta® and Harmony® Imaging systems were used to capture and analyse the images of cell cultures. Fluorescence intensity of CC-3 was obtained using the Operetta® (excitation band 520-560 nm and emission band 560-630 nm). The emission and excitation bands of GFP and DRAQ5™ were the same as described above. Apoptosis was scored using mean fluorescent intensity of CC-3 in the nucleus. The cell apoptosis assay was optimised using PC-3 cells treated with 1 μM Paclitaxel (Abcam, ab120143) for 72 h in both the Operetta® High Content Imaging System (PerkinElmer) and the Incucyte® FLR imaging system (Essen BioScience) (Figure 2-2). The measurement of the fold-induction of apoptosis by Paclitaxel was similar with both imaging systems. Cell death was also investigated using the Nuclear Fragmentation Index (NFI) which is the coefficient of variation of fluorescence intensity of the nuclear stain (standard deviation/mean).

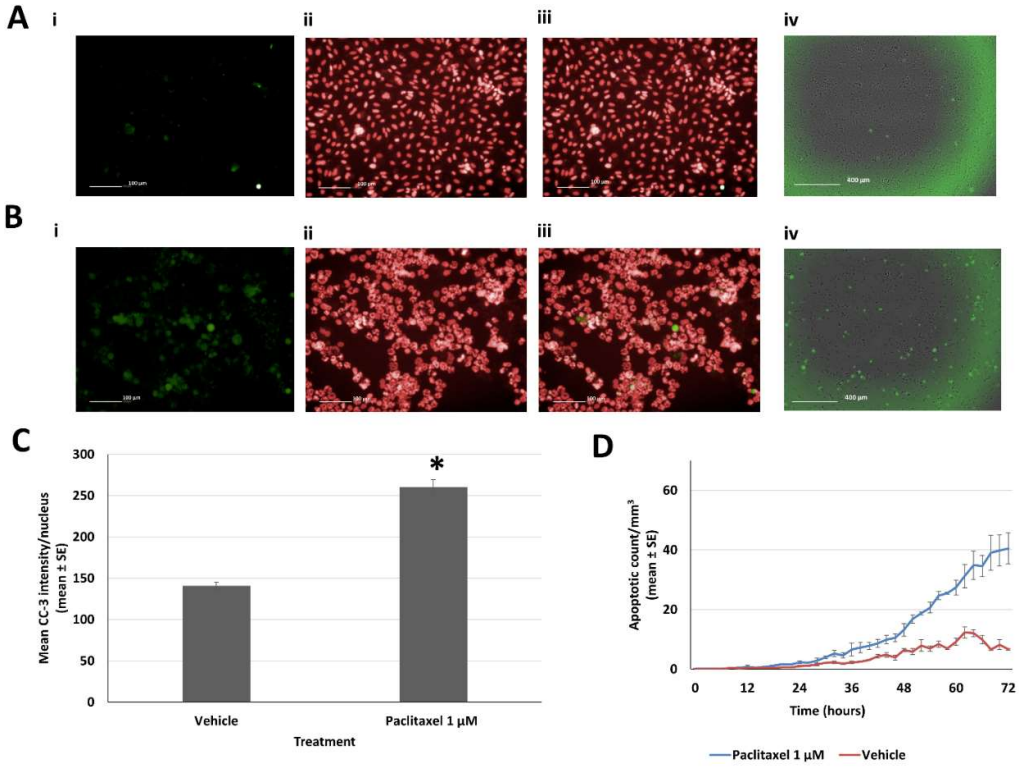

Figure 2-2. Comparison of the Incucyte® FLR imaging system (Essen BioScience) and Operetta® High Content Imaging System for detection of apoptosis in PC-3 cells induced by Paclitaxel.
*Paclitaxel was used to induce apoptosis in PC-3 cells as a positive control. The mean fluorescence intensity of CC-3 in the nucleus of PC-3 cells using Operetta® and Harmony® analysis was calculated and compared with the percentage of apoptosis using the Incucyte® fluorescence mode and the CellPlayer™ 96-well Kinetic Caspase 3/7 Apoptosis Assay Kit. PC-3 cells were grown in 96 well plates and exposed to vehicle **(A)** or 1 µM Paclitaxel **(B)** for 72 h. 20X images taken from the Operetta® High Content Imaging System detecting: **(Ai, Bi)** CC-3 stained with Alexa 488® dye, **(Aii, Bii)** the cell nucleus and cytosol stained with DRAQ5™, **(Aiii, Biii)** Combined images of CC-3 and nucleus stain, **(Aiv, Biv)** 20 X images of the Incucyte® fluorescence mode using the CellPlayer™ 96-well Kinetic Caspase 3/7 Apoptosis Assay Kit. **(C)** Mean fluorescence intensity of nuclear CC-3 using the Operetta® and Harmony® analysis. **(D)** Apoptotic count over 72h using Incucyte® analysis (3≤n≤4). * $p < 0.05$ in comparison with vehicle (3≤n≤4).*

2.1.11. Western blot analysis

2.1.11.1. *Total protein extraction*

Radioimmunoprecipitation assay buffer (RIPA buffer) was purchased from ThermoFisher (#89900) and protease inhibitor cocktail tablet (Roche, #04693116001) was added to RIPA buffer to inhibit the proteases (serine, cysteine, metalloprotease and calpains). For total protein extraction, the culture medium from adherent cells was removed and cells were washed twice with cold PBS. One mL of cold RIPA buffer was added to the cells for each 75 cm^2 flask (from 5 x 10^6 to 10 x 10^6 cells). The cell lysate was gathered to one side using a cell scraper (on ice), collected and homogenised through a 21-gauge needle attached to a 2-mL syringe. The cell lysate was centrifuged at 14,000 x *g* (4^{o}C) for 15 mins to pellet the cell debris. The supernatant containing soluble proteins was carefully transferred to a tube on ice and stored at -20^{o}C.

2.1.11.2. *Fractional protein extraction*

Proteins from mitochondrial and cytoplasmic cell fractions were extracted using a Cell Fractionation Kit (Abcam, Ab109719). The extraction buffers A, B, and C were prepared as per the manufacturer's instructions (with protease inhibitor). Adherent cells were collected using Trypsin-EDTA 0.25% (1X) and centrifuged at 300 *x* g for 5 mins at room temperature. Cell pellets were resuspended in 5 mL of 1X buffer A and cells were then centrifuged at 300 x *g* at room temperature. Fifty µL of the suspension was used for cell counting. The supernatant was removed and the cell pellet was resuspended in 1X buffer A at 6.6 x 10^6 cell/mL. Buffer B was added to the lysate at a ratio of 1:1, mixed by pipetting and incubated for 7 mins on a rotator at room temperature. The

lysate was centrifuged at 5000 x *g* for 1 min at 4°C. The supernatant was collected into a new set of tubes and the pellet was saved on ice. The supernatant was centrifuged again at 10,000 x *g* for 1 min at 4°C and the remaining supernatant contained the cytosolic fraction (*C*). The mitochondrial fraction (*M*) obtained from the cell pellets was combined in 5 mL buffer A, and then the same volume of Buffer C was added and mixed by pipetting. The sample was incubated for 10 mins on a rotator at room temperature before centrifuging at 5000 x g for 1 min at 4°C. All supernatants were transferred to a new set of tubes and cell pellets were kept on ice. The supernatant was centrifuged again at 10,000 x *g* for 1 min and the remaining supernatant constituted the mitochondrial fraction (*M*).

Western blots were used to confirm the purity of cytoplasmic and mitochondrial fractions by measuring the presence of β-actin (Abcam, Ab8227), pyruvate dehydrogenase subunit E1-α (PDH-E1-α), and ATP synthase subunit-α protein (CVα), and to detect the release of cytochrome c from mitochondria to the cytoplasm (Abcam, Ab110415). Total protein expression in the stain-free gel (Bio-Rad, #4568124) was used as the loading control (Colella et al. 2012; Eaton et al. 2013). The level of cytochrome c expression was determined using a ChemiDoc™ MP system (Bio-Rad) and normalised to total protein expression. The distribution of cytochrome c in the cytoplasm and mitochondria was calculated by dividing the expression of cytochrome c in the cytoplasm or mitochondria by the total expression of cytochrome c in the cytoplasmic and mitochondrial fractions. The formula for calculating the percentage of distribution of cytochrome c is outlined below:

$$\text{Cyt c } C\ (\%) = \frac{\text{Cyt c } C}{(\text{Cyt c } C + \text{Cyt c } M)} \text{ x } 100$$

Where

Cyt c *C* = cytochrome c in the cytoplasm

Cyt c *M* = cytochrome c in mitochondria

The proportion of cytochrome c released from the mitochondria to the cytoplasm was calculated as follows:

$$\text{Cyt c } C \text{ Released } (\%) = \text{ Cyt c } C \text{ Treated } (\%) - \text{ Cyt c } C \text{ UnTreated } (\%)$$

2.1.11.3. *Determination of protein concentration*

The EZQ® protein quantitation kit (Molecular Probes, R33200) was used to quantify protein concentration. Briefly, ovalbumin was prepared from the stock concentration at 2 mg/mL and diluted to 1 mg/mL, 0.5 mg/mL, 0.2 mg/mL, 0.1 mg/mL, 0.05 mg/mL, 0.02 mg/mL. One µL of each standard, sample and blank were pipetted onto the assay paper (in the EZQ kit) in triplicate. The assay paper was allowed to dry, then incubated in 40 mL of methanol while stirring for 5 mins. The methanol was removed and the paper dried on low heat using an Easy Breeze Gel Dryer (company). EZQ Protein Quantification Reagent (35 mL) was then added, incubated for 30 mins, the reagent was removed and 40 mL of EZQ destain was added and incubated for 2 mins. This step was repeated twice for a total of 3 rinses. The wet assay paper was scanned in a ChemiDoc MP system using an excitation/emission setting of 485/590 nm. Carestream Molecular Imaging (Carestream Health Inc.) was used to create a protein standard curve. The concentration of the experimental samples was determined from the standard curve.

2.1.11.4. *Gel Electrophoresis of protein lysates*

Mini-PROTEAN® TGX™ (Tris-Glycine eXtended shelf life) stain-free pre-cast gels (Bio-Rad, #4568124) were used to separate proteins via gel electrophoresis as per the manufacturer's instruction. The gels contain trihalo compounds that react with tryptophan residues in the proteins enabling rapid fluorescent detection of whole protein bands on gels and polyvinylidene difluoride (PVDF) blots.

In brief, Mini-PROTEAN® TGX™ Stain-Free gels were placed into the Mini-PROTEAN® Tetra Vertical Electrophoresis Chamber (Bio-Rad, #1658004). Tris/SDS/Glycine running buffer was added to the chamber. Ten to twenty µg of protein sample diluted with 2X or 4X sample buffer was loaded into each well of the gel (Appendix A). Precision Plus Protein™ Unstained Protein Standards (Bio-Rad, #161-0363) were used as molecular weight markers on western blots. The samples were run at 110V for 40 mins. After running and prior to transfer, the trihalo compound in gels was activated using UV light in the ChemiDoc™ MP Imaging System (Bio-Rad, #1708280).

2.1.11.5. *Semi-dry transfer of protein*

Immun-Blot® Polyvinylidene difluoride (PVDF) membrane (Bio-Rad, #162-0260) and semi-dry transfer were used to transfer proteins from gels to the PDVF membrane. After gel electrophoresis, the gel and the blotting papers (ion reservoir stack) were equilibrated in 1X transfer buffer (Appendix A) for 10 mins. The PDVF membrane was activated in methanol, then equilibrated in transfer buffer. The blotting sandwich was assembled on the cassette of the Trans-Blot® Turbo™ Transfer Starter System (Bio-Rad, #1704155). A roller

was used to remove any air bubbles. Proteins were transferred at 1.3 A / 25 V for 7 mins.

2.1.11.6. *Detection of proteins*

Antibody detection of proteins

The PVDF membrane was rinsed in PBS, then, depending on the antibody being used, was blocked in either PBS-T or TBS-T (Appendix A) containing 5% skim milk powder at room temperature for 1 h in a shaking incubator. After blocking, the blot was incubated in primary antibody diluted in 5 mL PBS-T or TBS-T containing 1% skim milk at 4^{o}C overnight with gentle rocking. The concentration of primary antibodies used is listed in Table 2.2. The following day, the blot was washed in PBS-T or TBS-T at room temperature three times for 10 mins with gentle rocking. The blots were then incubated with the secondary antibody diluted in 1% skim milk in PBST or TBST for 1 h at room temperature with gentle agitation. The choice of secondary antibody was dependent on the type of primary antibody and the detection system used (chemiluminescent or fluorescent detection). The secondary antibodies are shown in Table 2-2. After secondary antibody incubation, the blot was rinsed three times in PBS-T or TBS-T for 10 mins. Chemiluminescent blots (Horseradish peroxidase (HRP)-conjugated secondary antibody) were incubated in 2 mL of enhanced chemiluminescence (ECL) reagent (1705061, Bio-Rad) for 3 mins before imaging using the chemiluminescent mode of the ChemiDoc^{TM} MP Imaging System. Fluorescent blots (Alexa 488 secondary antibody) were imaged using the fluorescent mode of the same imaging system.

Table 2-2. Primary and secondary antibodies

Primary antibody	Molecular weight (kD)	Secondary antibody	Detection system
Rabbit anti-cleaved PARP (Ab32561)	85	HRP-Donkey anti-rabbit (Jackson 715-035-152)	Chemiluminescence
Mouse anti-p53 (SC-126)	53	HRP-Donkey anti-mouse (Jackson 715-035-150)	Chemiluminescence
Mouse anti-PSA (10679-1-AP)	29	HRP-Donkey anti-mouse (Jackson 715-035-150)	Chemiluminescence
Rabbit anti-p53 pSer46 (Ab76242)	53	HRP-Donkey anti-rabbit (Jackson 715-035-152)	Chemiluminescence
Mouse anti-cytochrome c (ab13575)	15	HRP-Donkey anti-mouse (Jackson 715-035-150)	Chemiluminescence
Mouse anti-PDH-E1-α (ab110330)	43	HRP-Donkey anti-mouse (Jackson 715-035-150)	Chemiluminescence
Mouse anti-C-V-α (ab14748)	53	HRP-Donkey anti-mouse (Jackson 715-035-150)	Chemiluminescence
Rabbit anti-Cdk2 pTyr15 (ab32147)	34	HRP-Donkey anti-rabbit (Jackson 715-035-152)	Chemiluminescence
Rabbit anti-Histone H3 pSer10 (ab47297)	15	HRP-Donkey anti-rabbit (Jackson 715-035-152)	Chemiluminescence
Rabbit Anti-β-actin (Ab8227)	42	HRP-Donkey anti-rabbit (Jackson 715-035-152) Alexa 488 Goat anti-rabbit (A-11008)	Chemiluminescence Fluorescence (Alexa 488)

Quantitation of protein bands

Image Lab 5.1 software (Bio-Rad) was used to analyse the images taken by the ChemiDoc™ MP Imaging System. Total protein expression in stain-free gels and/or β-actin expression were used as the loading controls for protein expression (Colella et al. 2012; Eaton et al. 2013). In brief, for total protein normalisation, the relative amount of protein in each lane was measured, then the expression level of the target protein in each lane was normalised to the total protein using the Images Lab 5.1 automated total protein normalisation function. For β-actin loading control, the relative amount of β-actin protein and the target protein was measured in each lane. The expression level of the target protein in each lane was then normalised to the relative expression of β-actin expression.

2.2. In vivo experiments

2.2.1. Mice

Male 5-week old nude mice (*BALB/c-Foxn1^{nu}*/Arc) were purchased from the Animal Resource Centre, Perth, Australia. This project was approved by the Flinders University Animal Welfare Committee (AWC Approval #893/15). Mice were housed in the Flinders University School of Medicine Animal Facility according to the standard operating procedures for the Facility. Nude mice are athymic animals and are very sensitive to infection, therefore they were maintained in sterile cages with micro-isolators, on a 12-h light/dark cycle, and at 23^{o}C. Quality control for viral, parasitic and bacterial contamination was ensured following the guidelines of the Animal House Facility. The mice were

fed with autoclaved Gordon's premium rat & mouse pellets (Gordon's Specialty Stockfeeds P/L, New South Wales, Australia) (Table 2-3) and autoclaved tap water.

Table 2-3. Ingredient and nutritional information of Gordon's premium rat & mouse pellets used in the Flinders University Animal Facility.

Nutritional analysis	Speciality feed: irradiated rat and mouse cubes
Min. crude protein	23%
Min. crude fat	6%
Min. crude fibre	5%
Digestible Energy	12.0 millijoule/kg
Ingredients	Wheat, sorghum, pollard, bran, soybean meal, sunflower meal, meat meal (derived from beef/mutton), fishmeal, blood meal, Lucerne meal, vegetable oil, salt, lysine, vitamins A, B1, B2, B6, B12, C, D3, E, K, niacin, calcium, pantothenate, biotin, folic acid, choline chloride, manganous oxide, zinc oxide, cobalt proteinate, potassium iodide, copper sulphate, iron sulphate, sodium molybdate, endox.

Sample size and power calculations were adapted from Rosner (2015).The key outcome measure of interest is the change in tumour volume between control and treatment groups. Using data from Ben-Sahra et al. (2008), who studied the effect of MET in drinking water on LNCaP xenograft tumour growth in nude mice, the mean tumour volume (cm^3) in the vehicle treated group at day 41 after treatment was reported as 0.6 ± 0.17 (mean ± SE). The estimated standard deviation of the mean (SD) of the vehicle treatment group was 0.45 (SEM = SD/√n, n = 7). An effect size of 33% was chosen for the current study. Using this data in power calculations, a sample size of 6 animals per treatment group would be required to have a power level (1-β) at 0.8 and a statistical significance level of 0.05. The tumour take-rate of LNCaP was estimated to be 70%, and therefore 10 animals per treatment group were used to ensure that at least 6-7 animals per treatment group had tumours that would take.

2.2.2. Experimental design for investigating the response of nude mouse xenografts to MET and VPA

The aim of this study was to determine the effect of MET and VPA in combination on prostate tumour growth in nude mouse xenografts. The overall experimental design is shown in Figure 2-3 for LNCaP and PC-3 cells. Briefly, male nude (nu/nu) mice were obtained at five weeks of age and allowed to acclimatise in the animal facility for one week. The mice were injected with the appropriate number of LNCaP or PC-3 cells determined in pilot studies (Section 4.1) and the tumours allowed to grow to a volume of 100 mm^3. The mice were then randomised into 4 different groups (n = 10 / group), which received one of the following in normal drinking water for a total period of 8 weeks: **(1)** Drinking water; **(2)** 200 µg/mL MET; **(3)** 4 mg/mL VPA; **(4)** 200 µg/mL

MET + 4 mg/mL VPA. Mouse weight was recorded 3 times a week. Tumour size was measured using digital callipers and tumour volume was calculated using the formula:

$$V\ (mm^3) = a^2\ (mm) \times b\ (mm) \times (\pi/6)$$

Where

V: volume (mm^3)

a: smaller diameter of the tumour (mm)

b: larger diameter of the tumour (mm)

$\pi = 3.1416$

Mice were monitored for body weight, faeces consistency, dehydration, movement, breathing, faeces, and tumour volume during this time. When the tumours reached a volume of 2000 mm^3, peripheral blood was collected from the submandibular vein to assess plasma levels of MET and VPA, after which the mice were euthanised and the tumours were harvested.

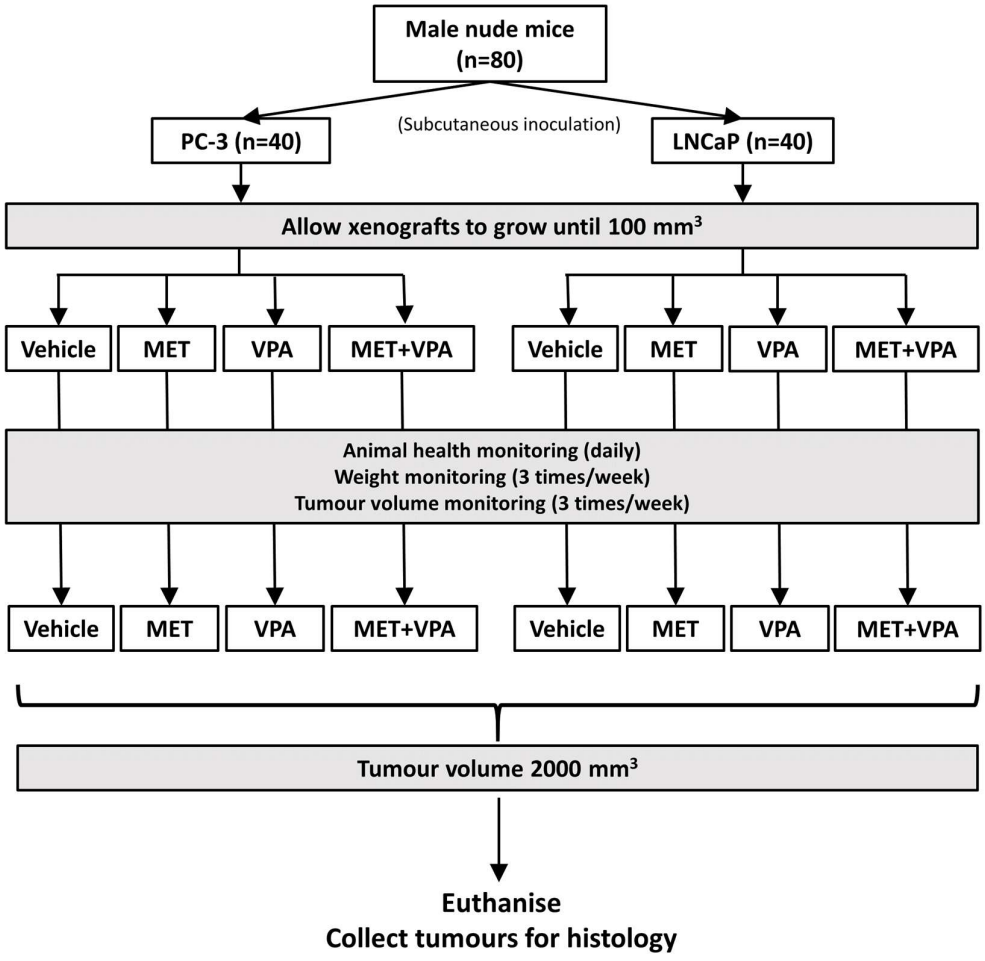

Figure 2-3. Flowchart outlining xenograft study using LNCaP and PC-3 cells.

Six-week-old mice were inoculated in the right flank with LNCaP cells or PC-3 cells suspended in Matrigel®. The xenograft tumour was allowed to grow to 100 mm^3 before allocating mice into one of four treatment groups: 1) drinking water, 2) 200 µg/mL MET in drinking water, 3) 4 mg/mL (4% w/v) VPA in drinking water, 4) 200 µg/mL MET + 4 mg/mL (4% w/v) VPA in drinking water. Animal heath was monitored daily, body weight and tumour volume were monitored three times a week. Mice were euthanised when tumours reached a volume of 2000 mm^3 and the tumours were collected for histology.

2.2.3. Dose and administration of MET and VPA

MET and VPA were added to the drinking water and changed every 3.5 days. The interval of water change was based on the half-life of MET and VPA in water (Sharma, VK et al. 2010) and the previous literature (Xia et al. 2006). MET stock was prepared at 15 mg/mL in a total volume of 2 mL, filtered sterilised (0.22 µm) and then diluted in 148 mL water in the drinking bottle to give a final concentration of 200 µg/mL. For VPA preparation, 40 mL stock of VPA at 15 mg/mL (0.22 µm filtered sterile) was added to 110 mL drinking water to give a final concentration of 4%. For MET+VPA administration, 2 mL of MET stock and 40 mL of VPA stock were added to 108 mL drinking water. The vehicle control was 150 mL of water. The dose of MET alone or VPA alone was chosen from previous studies (Ben-Sahra et al, 2008; Xia et al, 2006).

2.2.4. Matrigel injection of PC-3 and LNCaP into nude mice

Corning® Matrigel® Matrix was purchased from In Vitro Technologies (FAL354230). The process of subcutaneous injection was adapted from Dr Tina Lavranos (Bionomics, South Australia). In brief, Matrigel was thawed in a 4^{o}C cold room overnight prior to inoculation. Cells were allowed to grow until reaching 70-80% confluence on the day of inoculation. The medium was removed and cells were washed briefly with PBS, then centrifuged at 300 x *g*. Cell pellets were resuspended in PBS and the same volume of cold (4^{o}C) Matrigel was added to the cell suspension to achieve the required number of cells in a total volume of 100 µL (50 µL cells/PBS + 50 µL Matrigel). Cell suspensions were kept on ice until inoculation into mice. The cells were injected subcutaneously into the right hind flank using a 26-gauge needle in a position where the mouse would be unable to scratch or bite the injection site.

2.2.5. Monitoring tumour growth

All animals were checked for general health on a daily basis. Mouse weight and tumour size were measured 3 times per week throughout the study. Tumour volume was calculated outlined in Section 2.2.2. The animals were humanely euthanised by CO_2 inhalation if the tumour burden volume reached 2000 mm^3. All remaining mice were euthanised 90 days after drug treatment started. The tumours were collected and processed for histochemical analysis. Gross necropsy of the animals was performed to ensure that there were no confounding health effects in the animals.

2.2.6. Plasma collection and mouse tissue isolation

Mouse tissue including xenograft tumours (half of the tumour), testis, kidney, liver, spleen, pancreas, heart, lung, and colon were surgically dissected after CO_2 euthanisation, fixed in formalin, and embedded in paraffin for histological analysis. The other half of the xenograft tumours were embedded in cryoprotectant agent (OCT compound, Tissue-Tek) and stored at -80^oC until subsequent tissue sectioning.

For peripheral blood collection from the submandibular vein, mice were restrained by hand and a small puncture was made to the position of the submandibular vein with a Goldenrod lancet using the standard procedure adapted from the Animal Facility, Flinders University. Following blood collection (approx. 50-100 µL) in an EDTA-capillary blood collection tube (Sarstedt, microvette®, #16.444), plasma was isolated from total blood by centrifuging at 1000 *x* g for 10 mins at 4^oC, which was then stored at -20^oC for subsequent analysis.

2.2.7. Analysis of MET and VPA plasma concentration using mass spectrometry

Ultra-performance liquid chromatography – mass spectrometry (UPLC-MS) was used to determine the concentration of MET and VPA in plasma. The protocol was performed by David Elliot (Department of Clinical Pharmacology, Flinders Medical Centre and Flinders University) and adapted for mice.

In brief, for MET detection, the calibration curve was prepared using spiked plasma at 0.5, 2 and 4 mg/L MET and normal plasma as the negative control. Fifteen µL of 1 mg/L d6-MET solution was added to a 1.5 mL microfuge tube followed by 10 µL of a plasma calibrator, quality control or patient sample, and then mixed for 1 min at 400 rpm (Mixmate®, Eppendorf). The samples were added to 75 µL of 0.1% formic acid in acetonitrile and mixed for 3 mins, then centrifuged at 18,000 x *g* for 3 mins. Ten µL of the supernatant was transferred to a glass vial insert containing 100 µL of 0.1% formic acid in acetonitrile and mixed thoroughly. For UPLC-MS, 2 µL of the sample for analysis was injected onto a Phenomenex Kinetex HILIC column (2.1 x 100 mm, 2.6 µm) and analysed in an Acquity™ Ultra Performance LC (Waters). The system was set with 17.5% mobile phase A (10 mM ammonium formate,10% acetonitrile (ACN), 0.1% formic acid in water), 82.5 % mobile phase B (0.1% formic acid in ACN) at a flow rate of 0.4 mL/min.

For VPA detection, 20 µL of sample or calibrator plasma was mixed with 500 µL 0.1% (v/v) aqueous formic acid and then loaded onto a pre-conditioned (1 mL methanol followed by 1 mL 0.1% (v/v) aqueous formic acid), 30 mg Waters Oasis HLB solid phase extraction cartridge under gravity. The cartridge was then washed with 1 mL water after which VPA was eluted with 500 µL 4:1

ACN-water solution. Five μL of eluate was injected for UPLC-MS analysis. Calibrators were prepared by spiking plasma with VPA at 1, 2 and 5 mg/L and normal plasma was used as the negative control. UPLC-MS analysis was performed on an Acquity™ Ultra Performance LC system (Waters) coupled to a Premier qToF mass spectrometer (Waters). Chromatographic separation was achieved on an Aquity BEH C18 column (2.1 x 100 mm, 1.7 μm, Waters) using a gradient mobile phase consisting of acetonitrile (A) and 10% acetonitrile in water (B) at a flow rate of 0.3 mL/min. The mobile phase composition was as follows: a linear change from 30% A at 0 min to 80% A at 4 min then held at 80% A for 3.5 min before returning to 30% A with re-equilibration for 3 minutes before injection of the following sample. The retention time for VPA was 2.6 min. The mass spectrometer was operated in negative ionisation mode with a capillary voltage, 2.6 kV, source temperature 100ºC, desolvation temperature 300ºC, sample cone voltage 26 V and collision energy 6 V. VPA was detected in MSMS mode by pseudo MRM at the parent ion mass $[M-H]^-$ = 143.1 Da. Concentrations of VPA in mouse plasma were calculated by reference to a standard curve constructed from a plot of peak area vs VPA concentration for the spiked plasma calibrators.

2.2.8. Preparation of formalin-fixed paraffin-embedded tissue sections and haematoxylin – eosin staining

Tissues were fixed in 10% formalin (Sigma, #HT501128,) overnight, and then processed in an STP 120 Spin Tissue Processor (ThermoFisher , #813150). The processed tissues were embedded in paraffin (Paraplast®, Surgipath®) using a Histostar™ Embedding Workstation (ThemoFisher, #A81000001).

For haematoxylin – eosin (H&E) staining, paraffin embedded tissues were cut into 5 µm sections using a Microtome (Leica). The sections were mounted on APES (3-aminopropyltriethoxysilane) coated slides (Appendix A). The remaining paraffin was removed by placing the slides in an oven at 70^{o}C for 20 mins, then washing slides twice with Histochoice® Clearing Agent (Sigma, #H2779) for 2 mins with shaking. The sections were rehydrated by washing twice each in 100%, 95%, 70% and 50% ethanol for one min per wash with shaking, followed by a final wash in tap water. The slides were quickly dipped in acid ethanol and ammonia water (Appendix A) before staining with Eosin (Sigma, #HT110116) for 2 mins followed by haematoxylin stain (Fronine, #II500JJ,) for 2 mins. The slides were rehydrated serially in tap water, ethanol, and Histochoice® Clearing Agent, allowed to dry, and then mounted with Leica CV Mount (Leica Microsystems).

2.2.9. Evaluating kidney and liver toxicity using histological score of H&E stained sections

In order to investigate the toxicity of the kidney, the histological score adapted from Chen, S-m et al. (2002) was used to evaluate the glomerular changes (hypercellularity, hypertrophy, cellular crescent formation, thrombotic changes, fibrinoid material deposition), tubular dilation, necrosis, and inflammation. For investigating the toxicity of the liver, the histological score adapted from Mendler et al. (2005) was used to evaluate the portal fibrosis, lobular inflammation or necrosis, Mallory bodies, hepatocyte ballooning, peri-sinusoidal fibrosis, and fatty change. The detailed histological scores are described in Appendix C.

2.3. Explant culture of human prostate tumours

2.3.1. Prostate tumour collection and tissue culture

Human ethics approval was obtained from the University of Adelaide Human Ethics Committee and the Southern Adelaide Clinical Human Research Ethics Committee (#H-2012-016). Fresh PCa specimens were obtained with written informed consent from men undergoing robotic radical prostatectomy at St Andrew's Hospital, Adelaide, through the Australian Prostate Cancer BioResource. The prostatectomy specimens were sent for routine diagnostic pathology examination. Prior to fixing and paraffin embedding, small 6 mm cores of fresh tissue from regions of the prostatectomy specimen that exhibited gross tumour morphology were taken by a pathologist and made available for explant culture studies. Following explant culture, H&E staining for histological evaluation was performed on tissue from each treatment group, for every patient. A single 6 mm core of tissue was dissected into 1 mm^3 pieces and cultured in triplicate on a pre-soaked gelatine sponge (Johnson and Johnson) in 24-well plates containing 500 µL RPMI 1640 with 10% FBS, antibiotic/antimycotic solution (Sigma), 0.01 mg/mL hydrocortisone, 0.01 mg/mL insulin (Sigma) (Centenera et al. 2012). Tissues were treated by adding vehicle or MET (2.5 mM or 5 mM) or VPA (2.5 mM or 5 mM) to the culture medium. Tissues were cultured at 37°C for 48 h and then formalin-fixed and paraffin embedded before being analysed by immunohistochemistry for the proliferative marker Ki67 and apoptosis marker cleaved caspase-3 (CC-3).

2.3.2. Preparation of tissue sections and immunohistochemistry

Preparation of tissue sections and immunohistochemistry staining were performed by S. Irani (South Australia Health and Medical Research Institute) and all analysis was performed by the Ph.D candidate (Linh N.K. Tran). In short, paraffin-embedded explant tissue sections (2 μm) on SuperFrost-plus slides were de-paraffinized, rehydrated and blocked for endogenous peroxidase before being subjected to heat-induced epitope retrieval. Sections were blocked in 5% goat serum and incubated with Ki67 (#M7240, Dako) (1:200), CC3 (Abcam) (1:1000), or AR (1:1000) (SC-816, Santacruz) primary antibodies followed by the appropriate secondary antibody (1:400), then developed using 3-3'-diaminobenzidine chromogen (DAB) and counterstained with hematoxylin. Positive and negative controls were included in all runs. Images were captured with a Nanozoomer scanner (Hamamatsu). The proportion of Ki67 positive cells was calculated using the ImmunoRatio plugin in ImageJ (Tuominen et al. 2010). The proportion of CC-3 positive cells was counted using the Cell Counter plugin in ImageJ.

2.4. Statistical analysis

Triplicate to quadruplicate samples were used in each *in vitro* experiment and experiments were repeated 2-3 times. Data are presented as the mean ± SEM. The difference in the mean at single time points was calculated using an independent Student t-test or ANOVA test and for multiple time points was calculated using repeated measures ANOVA (RM-ANOVA) in IBM SPSS 23.0. Differences were considered to be statistically significant when $p < 0.05$.

Differences in tumour volumes *in vivo* were analysed using an ANOVA where data was normally distributed and displayed homogeneity of variance and a two-sided Kruskal-Wallis test was used where these assumptions were not met.

In order to validate the synergistic action of MET and VPA in combination, the drug combination index (CI) was calculated using at least 5 data points based on the Chou-Talalay method and Compusyn software (Chou, T-C 2010; Chou, T-C et al. 1984). According to this method, a CI less than 1 indicates a synergistic effect of the combination, while a CI = 1 indicates an additive effect, and the combinatorial effect is antagonistic if the CI is more than 1 (Chou, T-C 2010).

3. EFFECT OF MET+VPA ON PCA CELL LINES AND NORMAL EPITHELIAL CELLS *IN VITRO*

3.1. Proliferation

Proliferation of normal and PCa cell lines in response to MET and/or VPA was examined. Cells were grown in 96-well culture plates and proliferation was investigated over 72h after MET/VPA treatment using the Incucyte® FLR – phase contrast mode as described in Section 2.1.7. Serial doses from 0.16 mM to 20 mM (two-fold increments) of MET and VPA, both alone and in combination, were added to the cells to generate a dose-response curve.

Treatment with 2.5 mM MET or 2.5 mM VPA alone reduced proliferation of LNCaP ($p = 0.018$ and 0.0001, respectively) and PC-3 ($p = 0.047$ and 0.003, respectively) PCa cell lines over 72 h of treatment (Figure 3-1A and Figure 3-1B), but not proliferation of the normal PrEC cell line ($p = 0.687$ and 0.077, respectively) (Figure 3-1C) compared to vehicle (RM-ANOVA). MET+VPA significantly reduced proliferation of LNCaP and PC-3 cells ($p < 0.001$) compared to vehicle, MET alone, and VPA alone, but not in PrEC cells ($p = 0.54$). The CI for combination treatment with MET+VPA indicated a synergistic decrease in both LNCaP (CI=0.42) and PC-3 cells (CI=0.51) at 72 h, and an antagonistic effect in PrEC cells (CI=1.35) (Figure 3-1D).

Dose-response curves for proliferation at 72 h were performed in the presence of MET, VPA and MET+VPA. The IC_{50} of MET alone, VPA alone, and MET+VPA was 2.9 mM, 2.7 mM, and 0.5 mM respectively in LNCaP cells (Figure 3-1E), 16.5 mM, 6.5 mM, and 2.9 mM respectively in PC-3 cells (Figure 3-1F), and 3.4 mM, 2.4 mM, and 2.8 mM respectively in PrEC cells (Figure 3-1G).

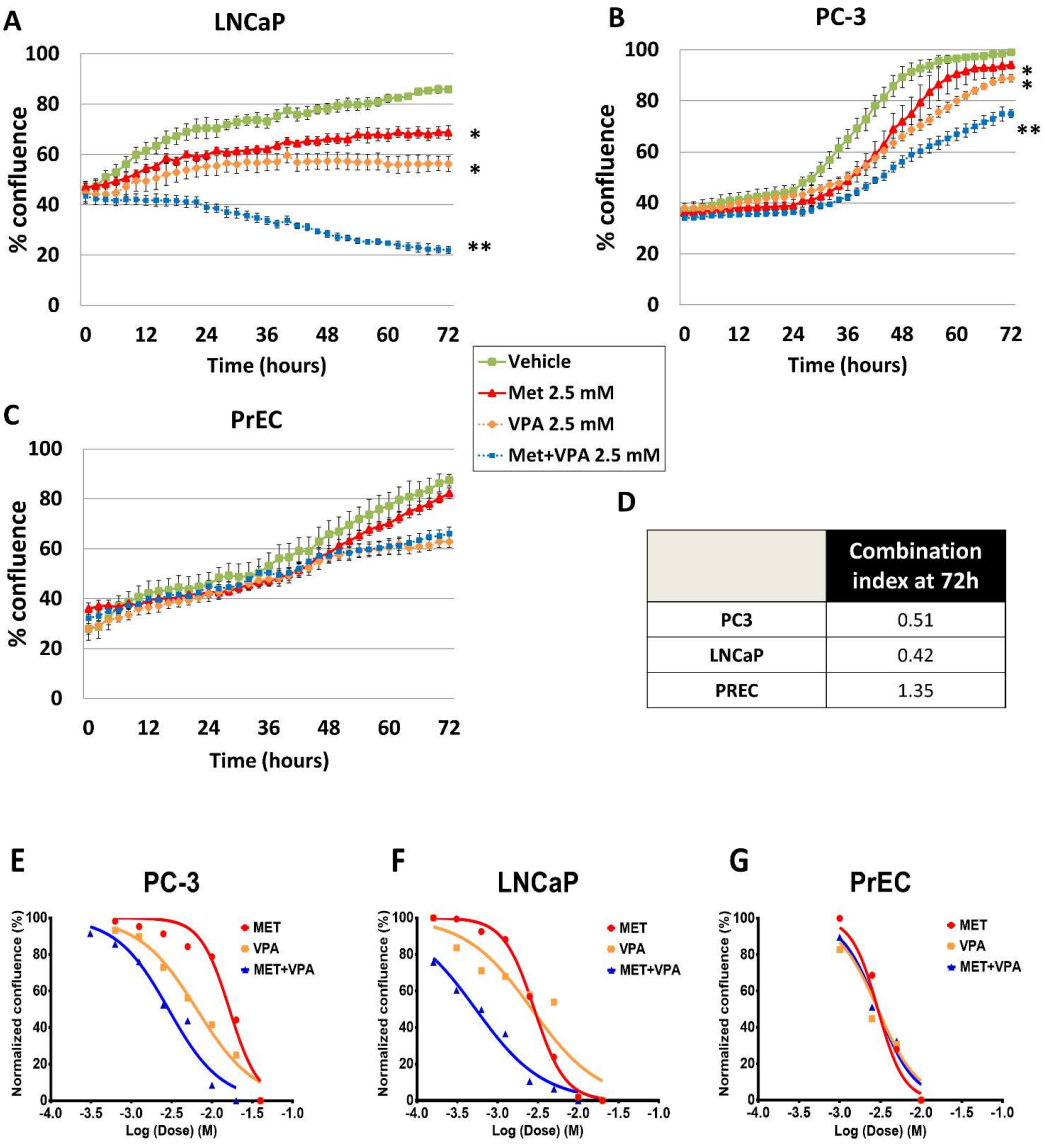

	Combination index at 72h
PC3	0.51
LNCaP	0.42
PREC	1.35

Figure 3-1. Proliferation of PCa cell lines (LNCaP and PC-3) and normal prostate epithelial cells (PrEC) in response to MET and VPA.
*MET and VPA in combination synergistically reduces proliferation of PCa cell lines, but not of normal prostatic epithelial cells. **A,** LNCaP, **B,** PC-3, and **C,** PrEC were grown in 96 well plates and treated for 72 h with vehicle control, 2.5 mM MET alone, 2.5 mM VPA alone or 2.5 mM MET+VPA. Cell proliferation was monitored by measuring % confluence (mean ± SE) using Incucyte real-time imaging. **D,** Combination index (CI) of anti-proliferative effect of MET and VPA at 72 h using Chou-Talalay method (CompuSyn) based on at least 2 different doses. Dose-response curves for proliferation at 72 h of PC-3 **(E)**, LNCaP **(F)**, and PrEC **(G)** cells. $p < 0.05$ in comparison with (*) vehicle ($3 \leq n \leq 4$) and (**) vehicle, MET alone, and VPA alone ($3 \leq n \leq 4$).*

The IC_{50} for MET+VPA was significantly reduced compared to using MET and VPA alone in LNCaP (5.8 and 5.4-fold decrease respectively; $p < 0.001$) and PC-3 cells (5.6 and 2.2-fold decrease respectively; $p < 0.001$), but not in PrEC cells ($p > 0.05$).

3.2. Apoptosis

In order to investigate the role of apoptosis in the anti-proliferative effect of MET+VPA, cell apoptosis was analysed by calculating the proportion of cleaved caspase 3/7 positive cells exposed to MET and VPA alone and in combination. MET and VPA doses at 1 mM and 2.5 mM were chosen based on the closest value of IC_{50} of proliferation (see Section 3.1) of LNCaP and PC-3 cells. Each cell line demonstrated different baseline levels of apoptosis, with PrEC (10-15%) and PC-3 (5-10%) being higher than LNCaP (2-4%) (Figure 3-2A, B, C). In comparison with vehicle control, LNCaP was the only cell line to exhibit a significant increase in apoptosis when treated with either drug alone or in combination at 1 mM doses. At 2.5 mM MET+VPA, LNCaP exhibited significantly higher apoptosis in comparison with MET alone (470% increase, $p < 0.001$), VPA alone (260% increase, $p < 0.001$), or vehicle control (1,010% increase, $p < 0.001$) (Figure 3-2A). In PrEC and PC-3 cells, the addition of 2.5 mM MET alone and 2.5 mM VPA alone induced significantly more apoptosis compared to vehicle treatment. Although MET+VPA at 2.5 mM induced significantly higher frequency of apoptosis ($p = 0.007$ and 0.011, respectively) in comparison with the vehicle, there was no significant difference compared with MET alone or VPA alone ($p > 0.05$) (Figure 3-2B, C).

The CI of apoptosis at 72 h indicated that the apoptotic increase was strongly synergistic (CI = 0.03) in LNCaP, whereas the apoptotic response was antagonistic in PrEC and PC-3 cells (CI = 1.46 and 2.62, respectively) (Figure 3-2D).

The release of cytochrome c from the mitochondria to the cytoplasm, which is a key initiating event in the apoptotic process, was analysed in LNCaP and PC-3 cells following MET and VPA treatment by semi-quantitative western blot. The percentage of cytochrome c in the cytoplasm was significantly increased up to 12-fold ($p < 0.05$) in LNCaP, but not in PC-3 cells, in response to 2.5 mM MET+VPA compared to vehicle, 2.5 mM MET alone, and 2.5 mM VPA alone (Figure 3-2E, F).

3.3. Role of p53 in the synergistic apoptotic response to MET+VPA

Previous findings found that MET+VPA induced a synergistic apoptosis (intrinsic pathway) in LNCaP, but not in PC3. p53 plays a major role in the pro-apoptotic response in normal and cancer cell lines and is also one of the major molecular differences between LNCaP and PC-3. While LNCaP expresses wildtype p53, p53 synthesis in PC-3 is impaired causing no p53-expression. Here, p53 was targeted to elucidate the response to MET+VPA in the presence and absence of p53.

3.3.1. Knock-down of p53 in LNCaP cells by siRNA

In order to knock down p53 expression in LNCaP cells, p53 siRNA or control siRNA was transfected into LNCaP cells using Lipofectamine™ 2000. Transfection efficiency was validated at 6 h, 24 h, and 72 h after transfection by western blot. Positive and negative controls for p53 protein expression were

protein lysates from PrEC ($p53^{+}$) and PC-3 cells ($p53^{null}$), respectively (Figure 3-3A). At 6 h after siRNA p53 transfection, the expression of p53 was significantly reduced by approximately 66% (Figure 3-3B). The expression of p53 was reduced by a total of 74% and 83% at 24 h and 72 h after transfection, respectively (Figure 3-3B).

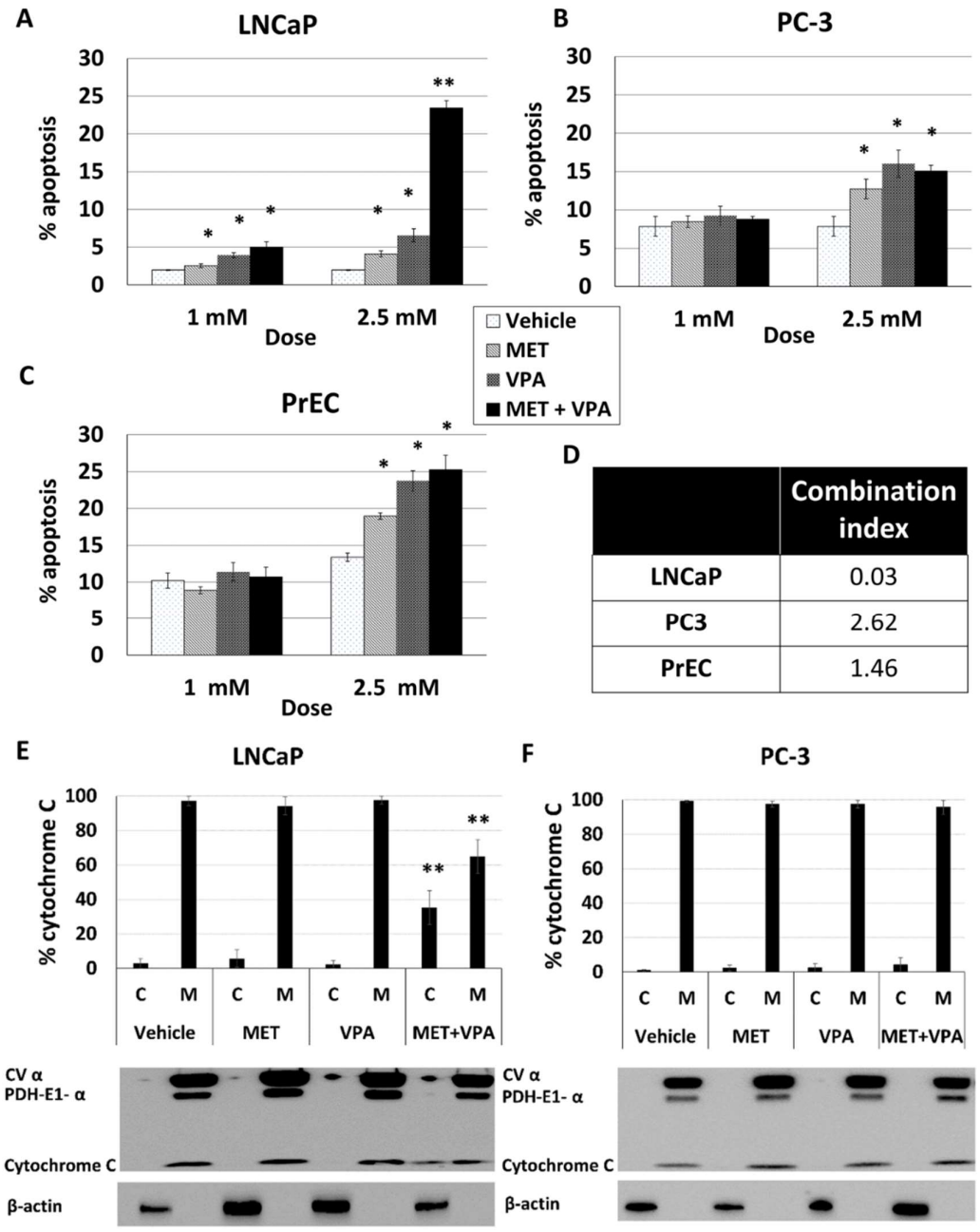

	Combination index
LNCaP	0.03
PC3	2.62
PrEC	1.46

Figure 3-2. Apoptosis of PCa cells (LNCaP and PC-3) and normal prostate epithelial cells (PrEC) in response to MET and VPA.

MET and VPA in combination induces synergistic apoptosis in LNCaP but not in PC-3 or PrEC cell lines. Cells were treated with MET and VPA at 1 mM or 2.5 mM, either alone or in combination. The percentage of apoptosis (mean ± SE) per total cells was measured 72 h after treatment. ***A,*** *LNCaP cells.* ***B,*** *PC-3 cells.* ***C,*** *PrEC cells.* ***D,*** *Combination index (CI) of the percentage of apoptosis at 72 h using Chou-Talalay method based on at least 2 different doses (CompuSyn). Percentage of cytochrome c (mean ± SE) in* ***(E)*** *LNCaP and* ***(F)*** *PC-3 in the cytoplasm (C) and mitochondria (M) in response to vehicle, 2.5 mM MET, 2.5 mM VPA, and 2.5 mM MET+VPA determined by semi-quantitative western blot. Pyruvate dehydrogenase subunit E1-α (PDH-E1-α) and ATP synthase subunit-α protein (CV α) are mitochondrial markers. β-actin is a cytoplasmic marker. $p < 0.05$ in comparison with (*) vehicle control and (**) vehicle control, MET alone, and VPA alone, ($3 \leq n \leq 4$).*

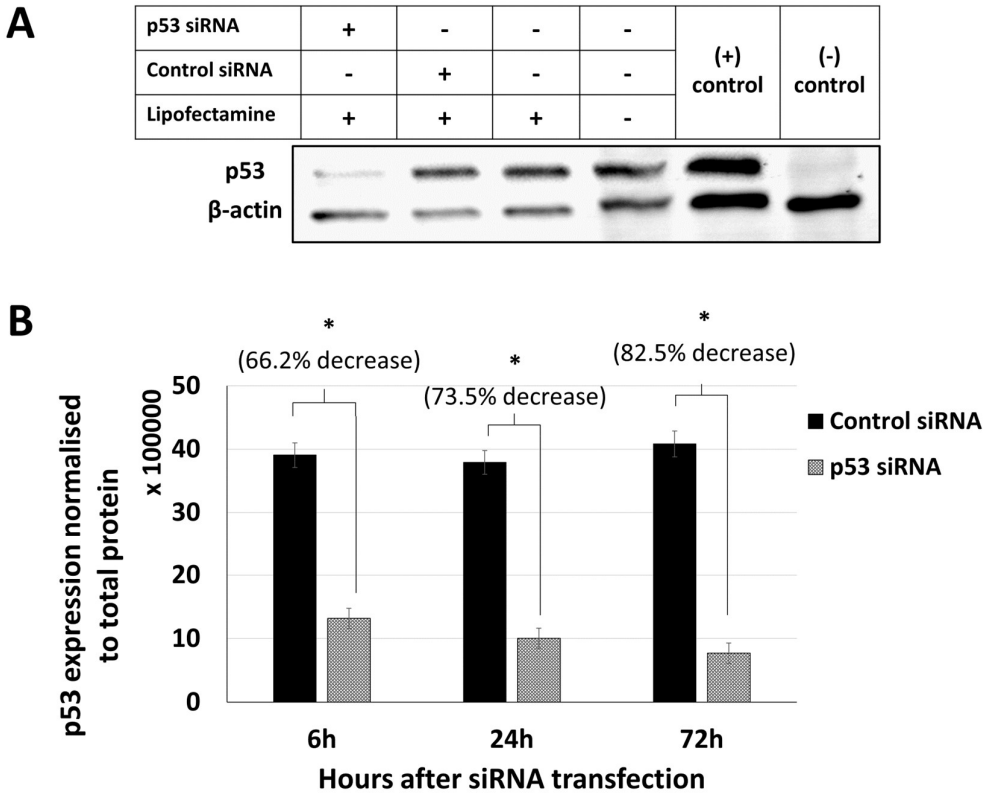

Figure 3-3. p53 knock-down in LNCaP cells using siRNA.

A, *Western blot showing the expression of p53 and β-actin with and without p53 siRNA. The relative expression of p53 to total protein was quantified by signal intensity on a* ChemiDoc™ MP Imaging System***. B,*** *There was approximately a 66%, 74%, and 83% decrease in p53 expression in the presence of p53 siRNA at 6 h, 24 h, and 72 h, respectively, compared to control siRNA. * $p < 0.05$ in comparison with control siRNA ($3 \leq n \leq 4$).*

3.3.2. Apoptotic response of LNCaP cells to MET+VPA in the presence of p53 siRNA

LNCaP cells ($p53^+$) were transfected with p53 siRNA and then treated with MET and/or VPA at 1 mM or 2.5 mM at 6 h after transfection. Knock-down of p53 was associated with a significant reduction in apoptosis in response to MET+VPA at both 1 mM (47% decrease, $p < 0.001$) and 2.5 mM (58% decrease, $p = 0.001$) (Figure 3-4), indicating that the apoptotic effect due to the combination of these drugs occurs in a p53-dependent manner.

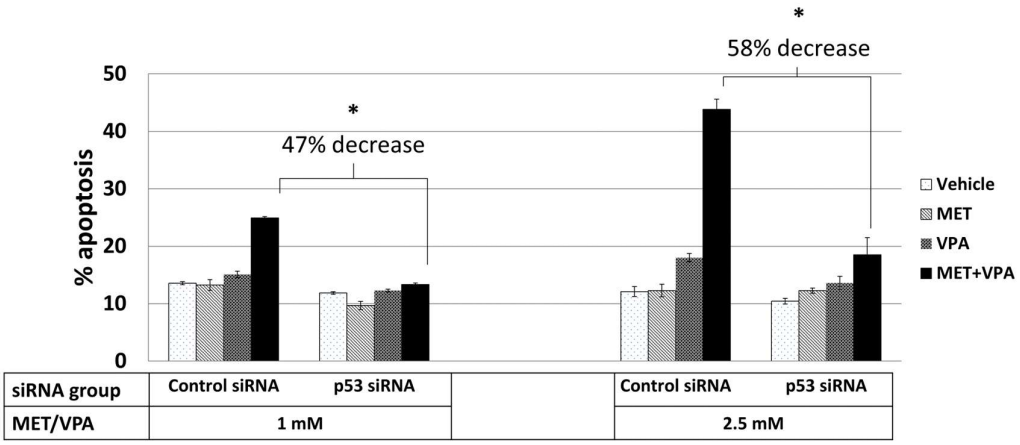

Figure 3-4. Apoptotic response of LNCaP cells to MET and VPA in the presence of p53 siRNA.

*p53 siRNA and control siRNA were transfected into LNCaP cells. Transfected cells were treated with MET and/or VPA at 1 mM and 2.5 mM for 72 h. The percentage of apoptosis (mean ± SE) in LNCaP cells with control siRNA or p53 siRNA was investigated. *, $p < 0.05$ in comparison with the same dose of MET+VPA in siRNA groups ($3 \leq n \leq 4$).*

3.3.3. GFP-p53 plasmid transfection and construction of GFP-only plasmid for transfection control

In order to express p53 protein in PC-3 cells ($p53^-$), GFP-p53 or GFP-only plasmid was transfected into PC-3 cells using Lipofectamine™ 3000. A GFP-only version of the GFP-p53 plasmid, required as a control, was not commercially available, therefore a GFP-only plasmid was constructed by

removing the p53 region from the GFP-p53 integrated plasmid using digestion enzymes BamHI and BglII (BioLab) followed by religation. The chosen enzymes, BamHI and BglII, were based on the sequence of the GFP-p53 plasmid (Appendix B). Digestion of the GFP-p53 plasmid with either BamHI or BglII enzyme produced a single band of the correct molecular size (5,895 bp), and when digested with both BamHI+BglII produced two bands of the expected size (backbone + GFP at 4,683 bp and p53 at 1,212 bp) (Figure 3-5A). The GFP + backbone only (GFP-only) plasmid was extracted from the gel, religated, and then transformed into competent bacteria *DH5-α E.coli*. Single colonies were selected for plasmid extraction. Digestion of plasmids (from two different single colonies) with enzyme NotI produced the correct molecular weight of GFP-only plasmid (4683bp) (Figure 3-5B).

GFP-only plasmid was transfected into PC-3 cells ($p53^{null}$) to ensure that GFP could still be expressed. In brief, PC-3 cells were seeded at 10,000 cells/well in a 96 well-plate and allowed to grow for 24 h before transfecting with GFP-p53 plasmid or GFP-only plasmid using Lipofectamine 3000. Incucyte™ FLR fluorescence mode was used to investigate the expression of GFP in the transfected cells. Both GFP-p53 plasmid and GFP-only plasmid expressed GFP when transfected into PC-3 cells (Figure 3-6).

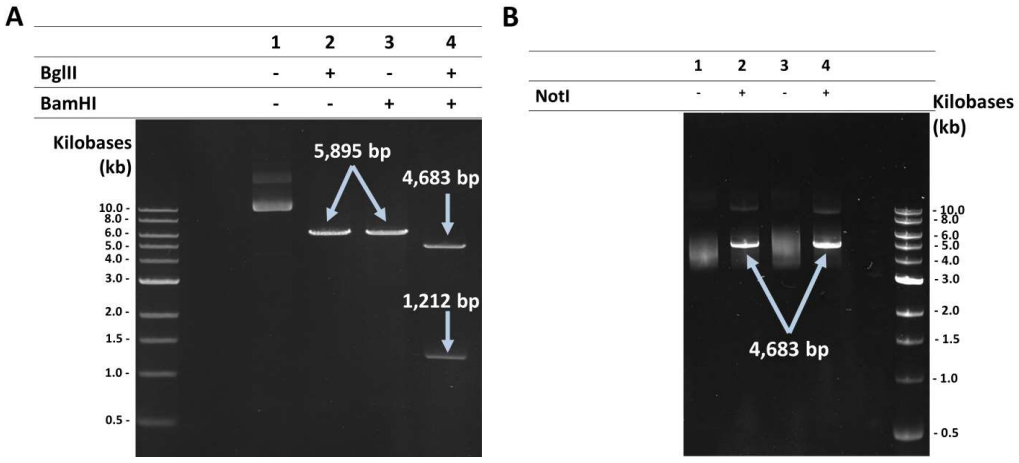

Figure 3-5. Removal of p53 from the GFP-p53 plasmid.

Electrophoresis of GFP-p53 plasmid and GFP-only plasmid before and after digesting with BglII, BamHI, and NotI. ***A,*** *Double digestion of GFP-p53 plasmid using BglII and BamHI enzyme. Lane 1: undigested GFP-p53. Lane 2: GFP-p53 digested with BglII. Lane 3: GFP-p53 digested with BamHI. Lane 4: GFP-p53 digested with BglII and BamHI. The predicted size of the GFP-p53 plasmid is 5895 bp, the GFP-only plasmid (GFP + backbone) is 4,683 bp, and p53 is 1,212 bp.* ***B,*** *GFP-only plasmid extracted from two different single colonies 1 and 2 were digested using NotI. Lane 1: undigested GFP-only plasmid (extracted from colony 1). Lane 2: GFP-only plasmid (extracted from colony 1) digested with NotI. Lane 3: undigested GFP-only plasmid (extracted from colony 2). Lane 4: GFP-only plasmid (extracted from colony 2) digested with NotI. Molecular marker: 1 kb DNA ladder (BioLabs, #N3232S) was used for molecular marker.*

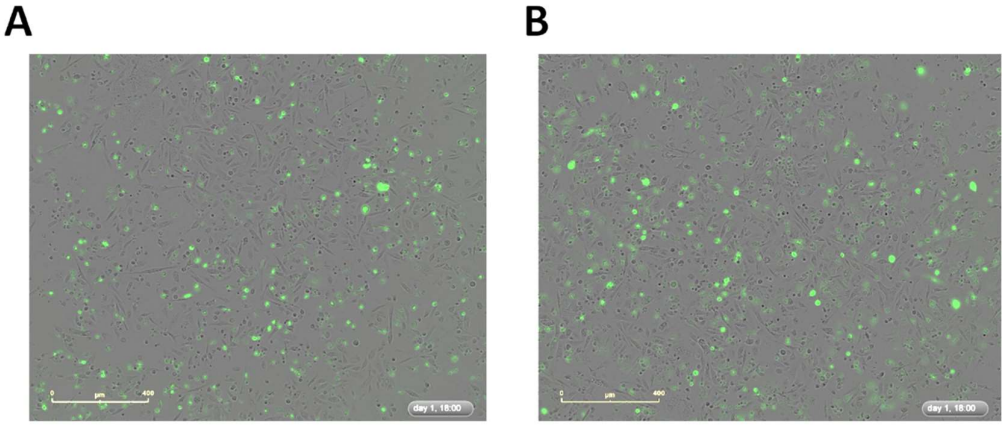

Figure 3-6. Validating the GFP expression of GFP-p53 plasmid and GFP-only plasmid using Incucyte® fluorescence mode.

A, *Day 2 after transfection of GFP-p53 into PC-3 cells.* ***B,*** *Day 2 after transfection of GFP-only plasmid into PC-3 cells.*

In order to determine transfection efficiency, PC-3 cells were grown in CellCarrier™ 96-microplates before transfecting with GFP-p53 or GFP-only plasmid. Cell nuclei were stained with DRAQ5™ and the Operetta® and Harmony® Imaging systems were used to capture and analyse the proportion of GFP positive cells in the total number of cells (Figure 3-7C). Plasmid DNA (0.1 μg) diluted into 0.15 μL Lipofectamine 3000 with 0.2 μL P3000 reagent resulted in approximately 50% transfection efficiency at 12 h, 60 h, and 84 h after transfection for both plasmids. MET/VPA treatment was started 12 h after plasmid DNA transfection and apoptosis was investigated at 72 h after commencement of treatment. The proliferation (% confluence) of cells transfected with GFP-p53 plasmid increased from 40% to 80% at 96 h after transfection compared to 45% to 100% at 96 h for the GFP-only plasmid. The transfection efficiency was approximately 50% at 12 h, 60 h, and 84 h after transfection (Figure 3-7A, B).

3.3.4. Induced expression of p53 in PC-3 cells stimulates apoptosis in response to MET+VPA

GFP-p53- or GFP-only-transfected PC-3 ($p53^{null}$) cells were treated with MET and/or VPA 12 h after transfection and apoptosis was evaluated by measuring nuclear CC-3 intensity 72 h after treatment using the Operetta® High-Content Imaging System (Figure 3-8A). In the GFP-only transfected PC-3 cells, there was no difference in apoptosis in the presence of MET+VPA compared to MET and VPA alone (Figure 3-8B). In p53 transfected PC-3 cells, MET+VPA induced a significant increase in apoptosis compared to MET+VPA in the control transfected cells (GFP-only plasmid transfection) (13.2% increase, $p = 0.009$ at 1 mM and 24.5% increase, $p = 0.002$ at 2.5 mM). Ectopic

expression of p53 in PC-3 cells resulted in significantly higher apoptotic rate in response to MET+VPA than in either MET alone (10.3% increase, $p = 0.009$ at 1 mM and 18.9% increase, $p < 0.001$ at 2.5 mM) or VPA alone (6.9% increase, $p = 0.046$ at 1 mM and 14.1% increase, $p = 0.002$ at 2.5 mM) (Figure 3-8B and C). Furthermore, the combination index of apoptosis of 0.07 in GFP-p53 transfected cells and >10 in GFP-only transfected cells indicated that, in the presence of p53, MET+VPA induced synergistic apoptosis, whereas this response was antagonistic in the absence of p53.

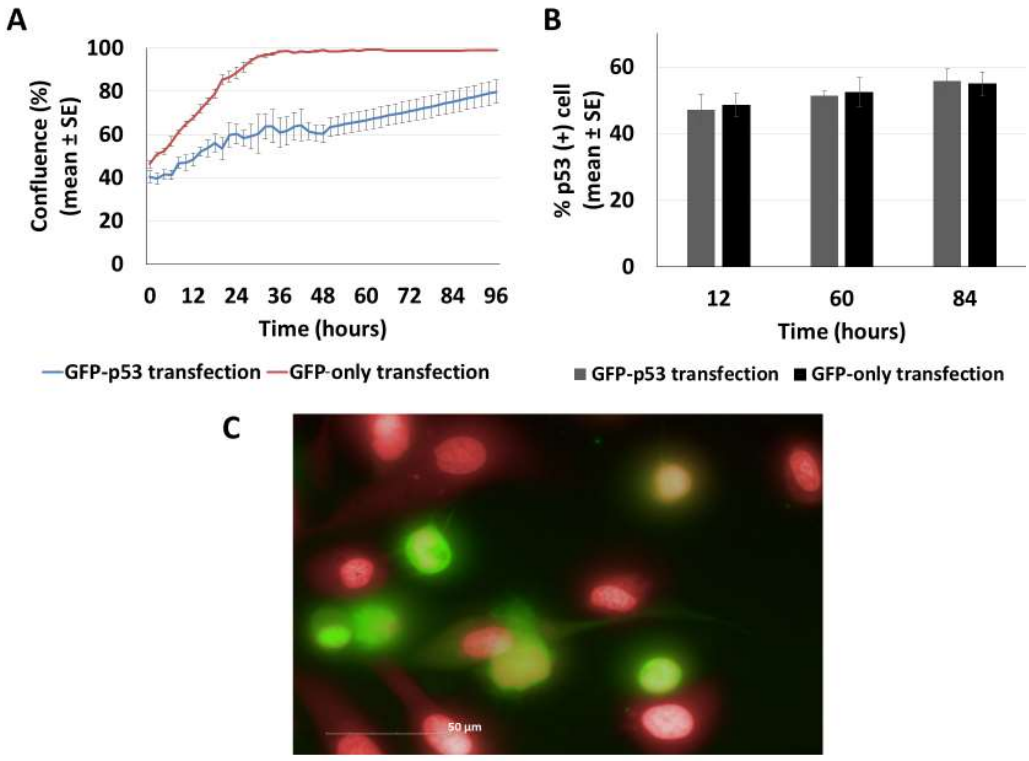

Figure 3-7. Efficiency of GFP-p53 and GFP-only plasmid transfection in PC-3 cells

A, *Proliferation of PC-3 cells transfected with either GFP-p53 or GFP-only plasmid for 96 h.* ***B,*** *Percentage of GFP (+) cells at 12 h, 60 h and 84 h after transfection with GFP-p53 or GFP-only plasmid.* ***C.*** *40X image of GFP-p53 plasmid transfection using an Operetta® High Content Imaging System. The cell nucleus and cytosol were stained using DRAQ5™ (red). Transfected cells were detected using GFP (green).*

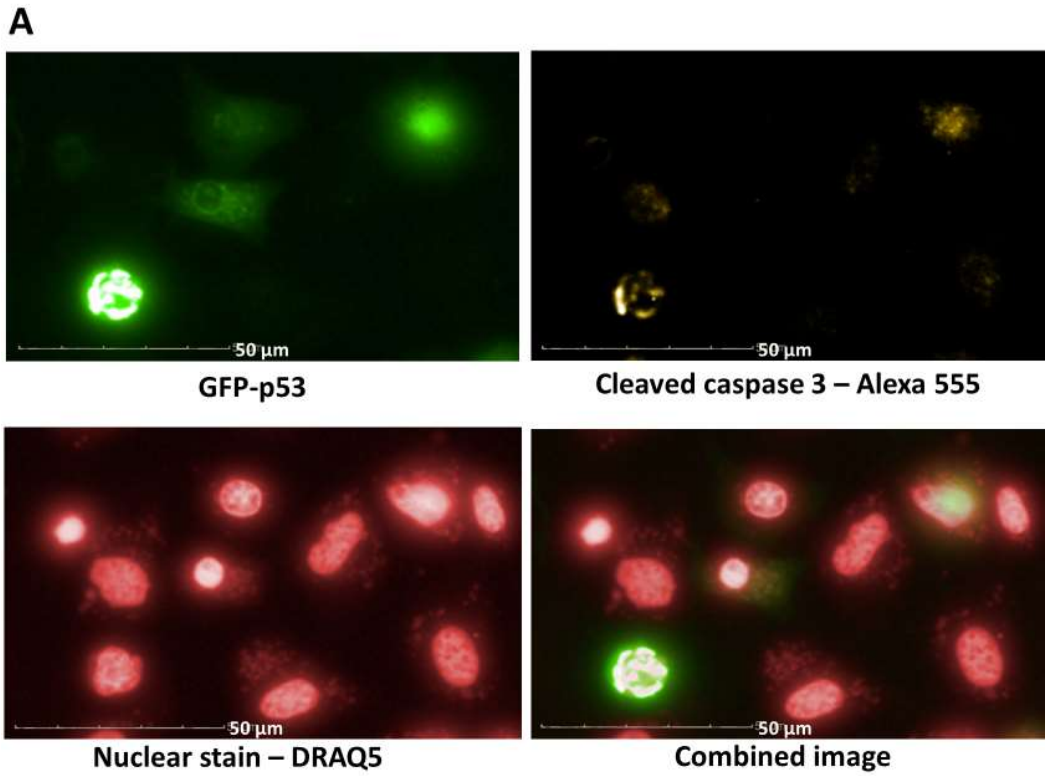

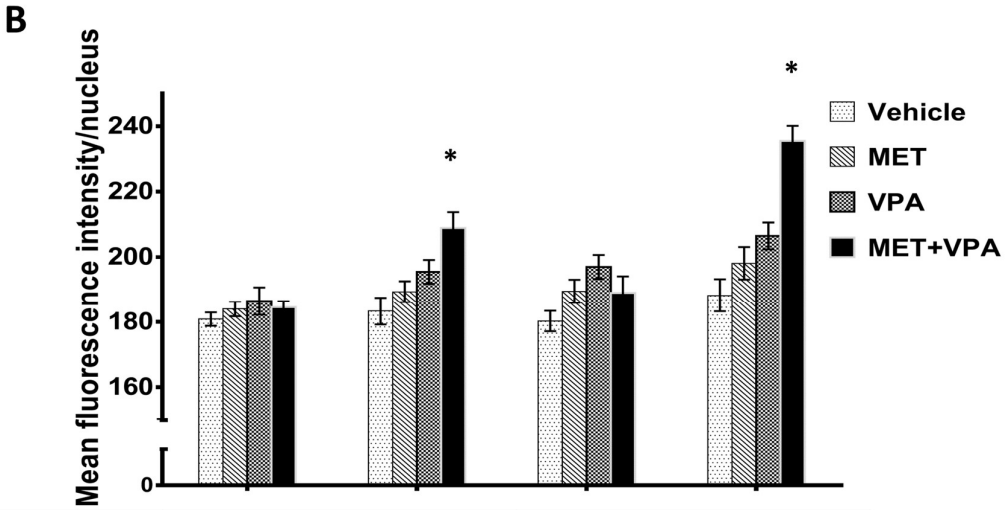

Plasmid transfection	GFP-only	GFP-p53	GFP-only	GFP-p53
Doses of MET/VPA	1 mM		2.5 mM	

C

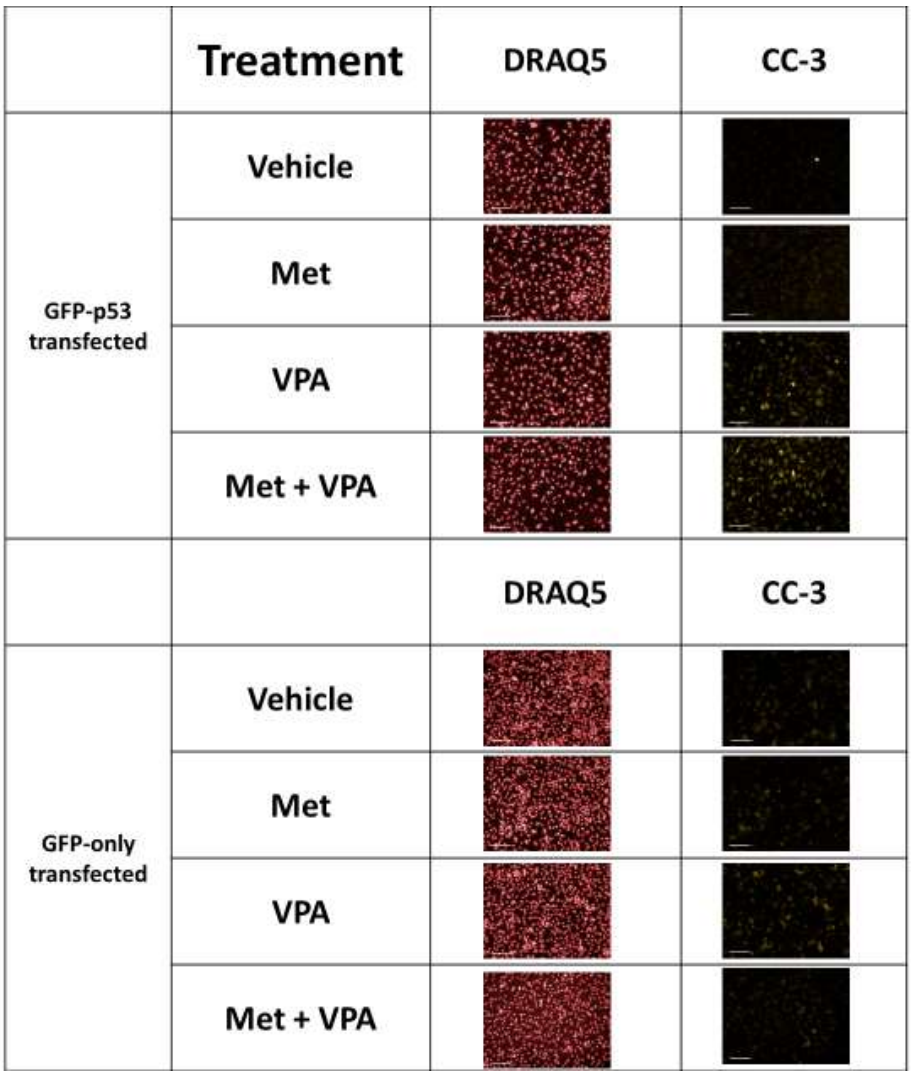

Figure 3-8. Apoptosis of PC-3 cells with and without ectopically expressed p53 in response to MET and VPA

Ectopic expression of p53 in PC-3 ($p53^{null}$) cells induces apoptosis in response to MET and VPA combination treatment. PC-3 cells were grown in 96 well-plates, transfected with GFP-p53 plasmid or GFP-only plasmid and treated with MET and/or VPA at 1 mM or 2.5 mM for 72 h. Apoptosis was evaluated by mean fluorescence intensity of nuclear CC-3. ***A****, 40X images were taken using an Operetta® High Content Imaging System. The cell nucleus and cytosol were stained using DRAQ5™, CC-3 was detected using Alexa 555® dye and p53-transfected cells were detected using green fluorescence protein (GFP).* ***B,*** *Mean fluorescence intensity of nuclear CC-3 (mean ± SE) in GFP-p53 and GFP only transfected PC-3 cells. * $p < 0.05$ in comparison with vehicle, MET alone, and VPA alone ($3 \leq n \leq 4$).* ***C,*** *20X images using Operetta® High Content Imaging System (scale bar = 50 µm) of PC-3 cells transfected with GFP-p53 or GFP-only plasmid and treated with vehicle, MET, VPA, and MET+VPA (2.5 mM) for 72 h.*

In addition, the role of p53 in response to MET+VPA was investigated using the nuclear fragmentation index (NFI). A higher NFI means greater cell death. Figure 3-9Ai shows the normal value of NFI of 0.2518 in PC-3 cells without intervention. Paclitaxel induces apoptosis and cell death in PC-3 and was used as the positive control. As expected, NFI in PC-3 cells treated with 1 μM Paclitaxel NFI increased to 0.3340 as shown in Figure 3-9Aii. In response to MET and VPA with p53 plasmid transfection, MET+VPA induced more cell death compared to MET alone (3.6% increase, $p = 0.003$ at 1 mM and 8.1% increase, $p = 0.007$ at 2.5 mM) and VPA alone (3.4% increase, $p = 0.003$ at 1 mM and 8.4% increase, $p = 0.004$ at 2.5 mM). In the presence of p53, MET+VPA induced a significantly higher NFI in comparison with MET+VPA in the control transfected cells (7.3% increase, $p = 0.005$ at 1 mM and 9.6% increase, $p = 0.006$ at 2.5 mM) (Figure 3-9B).

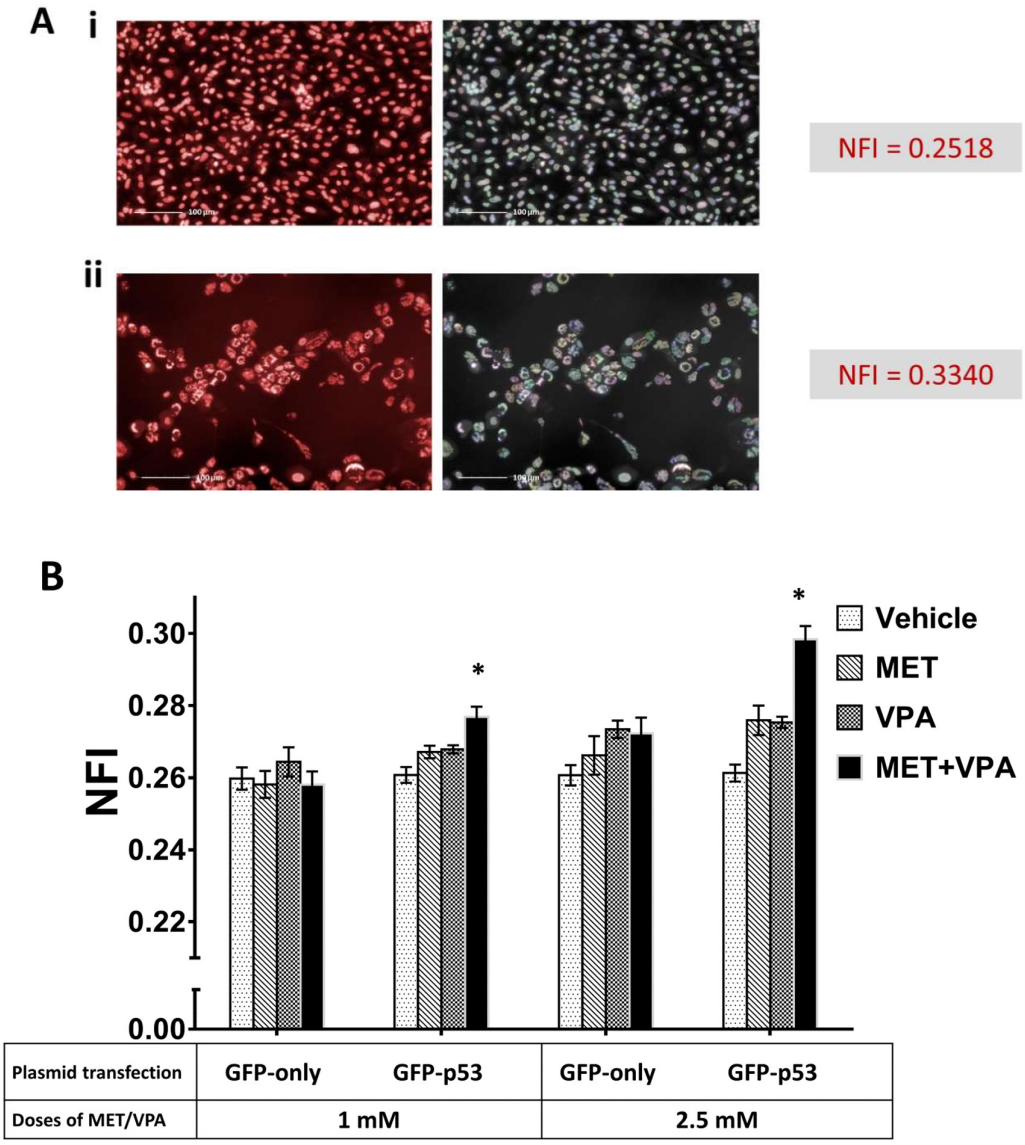

Figure 3-9. Nuclear fragmentation index of PC-3 cells in the presence and absence of ectopically expressed p53 in response to MET and VPA.

*Cell death in PC-3 cells was investigated using Nuclear Fragmentation Index (NFI) which is defined as the coefficient of variation of nuclear stain fluorescence intensity (standard deviation/mean). PC-3 cells were grown in 96 well plates and treated for 72 h. Cells were stained with DRAQ5™. **A,** The NFI assay was validated in PC-3 cells treated with Paclitaxel. 20X images were taken using an Operetta® High Content Imaging System of PC-3 cells treated with (**Ai**) vehicle and (**Aii**) 1 μM Paclitaxel. Cell nuclei were stained with DRAQ5™ (left images) and the NFI was calculated using Harmony® analysis. **B,** NFI (mean ± SE) of PC-3 cells treated with vehicle, MET, VPA, or MET+VPA (1 mM or 2.5 mM) for 72h in the presence or absence of ectopically expressed p53. * $p < 0.05$ in comparison with the vehicle, MET alone, and VPA alone ($3 \leq n \leq 4$).*

3.4. The role of the androgen signalling pathway in response to MET+VPA

In order to determine if the androgen-signalling pathway plays a role in the apoptotic response to MET+VPA, the androgen receptor (AR) antagonist Enzalutamide (1 μM) was used in the AR-positive PCa cell line LNCaP (AR sensitive). As expected, treatment of LNCaP cells with Enzalutamide inhibited PSA expression at 24 h, 72 h and 96 h (Figure 3-10A) and also induced a significant dose-dependent increase in apoptosis (Figure 3-10B) (53.7% increase at 1 μM and 90% increase at 2 μM, $p < 0.05$). In the absence of Enzalutamide, MET+VPA induced a synergistic increase in apoptosis response compared to MET alone, VPA alone and vehicle treatment at both 1 mM and 2.5 mM. In the presence of Enzalutamide, the apoptotic response to 2.5 mM MET+VPA was significantly reduced (28.5% decrease, $p = 0.029$) compared to MET+VPA treated cells in the absence of Enzalutamide (Figure 3-10C).

When PC-3, an AR^- cell line (androgen insensitive), was treated with MET+VPA, no significant change in the apoptotic response of PC-3 cells was observed in the presence or absence of Enzalutamide (Figure 3-11).

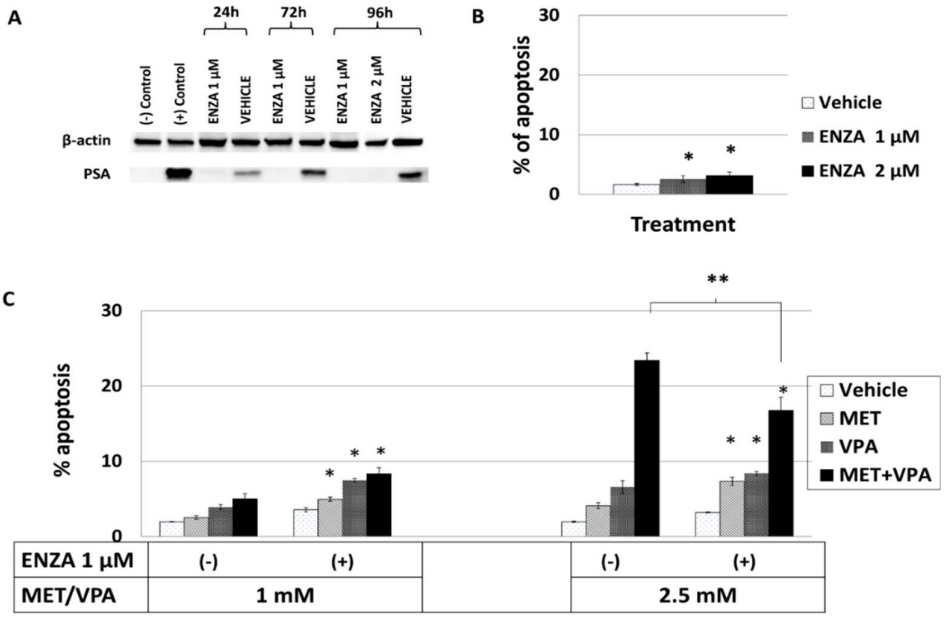

Figure 3-10. AR inhibition reduces the synergistic apoptosis induced by MET+VPA in LNCaP cells.

LNCaP cells were exposed to 1 µM Enzalutamide (ENZA) for 24 h before treating with MET and/or VPA at 1 mM or 2.5 mM. The percentage of apoptosis was measured at 96 h. ***A****, Enzalutamide (1 µM) inhibited PSA expression in LNCaP at 24 h, 72 h and 96 h. (-) control: PC-3 cells, (+) control: LNCaP cells. Vehicle: 0.001% DMSO.* ***B,*** *Percentage apoptosis (mean ± SE) with doses of ENZA at 1 µM and 2 µM at 96 h. * $p < 0.05$ in comparison with vehicle.* ***C****, Percentage apoptosis (mean ± SE) in LNCaP cells with and without ENZA in response to MET and/or VPA alone at 1 mM or 2.5 mM. * $p < 0.05$ in comparison with vehicle and with the same dose of MET alone and VPA alone in the presence and absence of ENZA. ** $p < 0.05$ in comparison with the same dose of MET+VPA in the presence and absence of ENZA ($3 \leq n \leq 4$).*

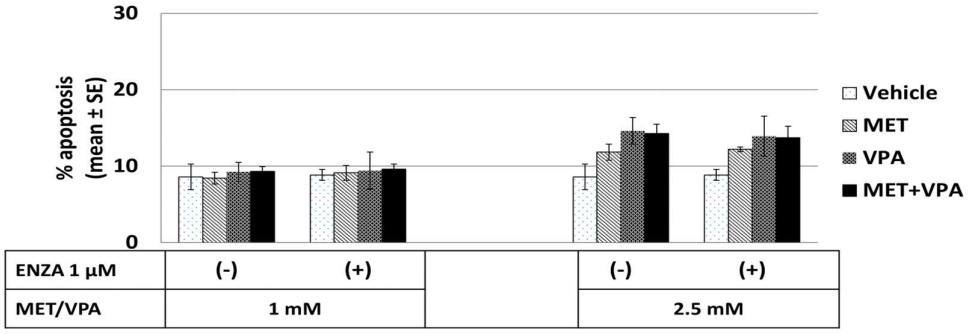

Figure 3-11. Apoptosis in PC-3 cells in response to MET and VPA in the presence and absence of Enzalutamide.

The percentage of apoptosis was measured at 96 h. Enzalutamide (ENZA) did not significantly alter apoptosis in PC-3 cells in response to MET+VPA ($p > 0.05$) in comparison with vehicle and with the same dose of MET alone and VPA alone in the presence and absence of ENZA ($3 \leq n \leq 4$).

3.5. Discussion

The aim here was to study the potential of MET+VPA as a cancer therapy based on the hypothesis that their different mechanisms of action would combine to give a synergistic anti-cancer effect.

Although VPA shows promise as an anti-cancer monotherapy, the doses tested so far in humans have demonstrated unacceptable toxicity, therefore a lower drug concentration of VPA could be achievable if additive or synergistic anti-cancer effects were obtained in combination with another drug, such as MET. Monotherapy doses of MET or VPA ranging from 1 mM to 10 mM have been used in previous *in vitro* studies (Ben-Sahra et al. 2011; Fendt et al. 2013) with up to 40 mM in the one study where MET and VPA were combined (Zhang et al. 2015). Here, proliferation and apoptosis were investigated in two PCa cell lines and in normal prostate epithelial cells in response to MET and VPA, either alone, or in combination at doses of 1 mM and 2.5 mM. Doses of VPA examined here are lower than the toxic threshold level of VPA in human plasma at 3.1 mM (Spiller et al. 2000). Previously published *in vitro* and *in vivo* studies have used MET doses higher than the toxic threshold in human plasma (0.31 mM) (Dowling et al. 2012; Vecchio et al. 2014). Here, doses of MET were in the low range of previous *in vitro* studies.

The combination of MET and VPA synergistically inhibited cell proliferation in two PCa cell lines (PC-3 and LNCaP) derived from metastases of PCa patients (Horoszewicz et al. 1983; Kaighn et al. 1979), while being antagonistic in normal prostatic epithelial cells (PrEC). MET+VPA significantly lowered the IC_{50} for proliferation compared to MET or VPA alone in both LNCaP and PC-3, but not in PrEC cells, suggesting that the concentration of MET and VPA could

be reduced in combination treatment for PCa, potentially reducing the toxicity caused by higher doses of MET and/or VPA. This differential antiproliferative response in cancer and normal cells may be explained by the selective inhibition of MET on glucose metabolism in cancer cells, which is more effective than in normal epithelial cells (Tsai et al. 2015). Cancer cells, in general, have a higher rate of glycolysis even under aerobic conditions and are less adaptive to glucose starvation compared to normal cells (Menendez et al. 2012; Warburg 1956). Furthermore, Zhuang et al. (2014) demonstrated that lower glucose concentration in the culture medium preferentially sensitised breast and ovarian cancer cell lines to MET compared to normal cells. VPA, a histone deacetylation inhibitor that causes DNA double strand breaks (DSBs), may also contribute to the observed differential anti-proliferative response between cancer and normal cells, as it preferentially affects cancer cells due to their reduced ability to repair DNA DSBs compared to normal cells (Lee et al. 2010).

Although MET+VPA synergistically inhibited proliferation of both LNCaP and PC-3 cells, a synergistic effect for apoptosis was only observed in LNCaP cells. In the one previous report using MET+VPA in combination, Zhang et al. (2015) observed a similar synergistic decrease in proliferation and increase in apoptosis in two renal carcinoma cell lines (786-0 and Caki-2) compared to the single drug alone.

The reason for a differential response to MET+VPA treatment between LNCaP and PC-3 cells is unclear but is likely to be due to the underlying genetic differences between these cell lines. LNCaP cells have intact p53 and AR signalling, while PC-3 cells do not express p53 (due to a premature stop

codon) or AR (Carroll et al. 1993; Horoszewicz et al. 1983; Kaighn et al. 1979). Both LNCaP and PC-3 cells have mutations in *PTEN* and neither express *ERG* translocation. Therefore, p53 and AR are potential candidates for mediating the synergistic apoptotic response observed in LNCaP cells in response to MET+VPA treatment. In support of this hypothesis, when p53 was substantially depleted in LNCaP cells, the synergistic apoptotic response was reduced by approximately 50%. Likewise, a synergistic apoptotic response to MET+VPA was observed in PC-3 cells that expressed ectopic p53. Taken together, these results suggest that p53 is required for the apoptotic response of the PCa cell lines to the combination of MET and VPA. Prior evidence supports this finding, as MET has been shown to inhibit cell growth and induce cell apoptosis to a greater extent in p53 (+) PCa cells compared with p53 (-) cells (Ben-Sahra, Laurent, et al. 2010; Gotlieb et al. 2008; Zakikhani et al. 2006). It has been shown that MET targets PCa cell metabolism by inhibiting mitochondrial respiration and glycolysis (Fendt et al. 2013). The inhibition of mitochondrial complex 1 alters the AMP/ATP ratio, which in turn activates AMPK, resulting in phosphorylation of p53 at Ser15 and leading to p53-dependent cell death (Bensaad et al. 2007; Feng et al. 2010; Jones et al. 2005; Okoshi et al. 2008). In a study similar to the present one, Ben-Sahra et al. (2010) found that ectopic expression of p53 in PC-3 cells significantly enhanced AMPK activity in response to MET and 2-deoxyglucose in combination. In addition, VPA has also been shown to cause acetylation of p53 at lysine residues 373 and 382, resulting in its activation (Condorelli et al. 2008). Therefore, the combination of MET and VPA may result in increased p53 protein activation, driving p53-dependent cell death via intrinsic or extrinsic pathways. Here, a significant increase in cytochrome c released from the mitochondria to the cytoplasm in

LNCaP ($p53^+$) cells was demonstrated, indicating that intrinsic apoptosis was induced in response to MET+VPA but not to either drug when administered alone. Although the proliferation in these cell lines in the presence and absence of p53 was not investigated, MET+VPA may further inhibit cell proliferation as p53 plays a crucial role in cell cycle control (Lane et al. 1990; Levine 1997). The two renal cancer cell lines that responded (cell cycle arrest and pro-apoptosis) to MET and VPA combination treatment in the study by Zhang et al. (2015) also expressed wild-type p53 (Stickle et al. 2005; Warburton et al. 2005). Current findings suggest that combining MET and VPA may provide a useful anticancer therapeutic option in a variety of cancer types, particularly those expressing p53.

The androgen signalling pathway plays a vital role in PCa development in which the mutation rate of AR increases from a low frequency in localised PCa to a higher frequency in CRPC (Marcelli et al. 2000). Previous reports showed that the second generation AR antagonist Enzalutamide increased apoptosis in a dose-dependent manner in androgen-sensitive LNCaP cells (Li, Y et al. 2013; Tran et al. 2009). The same response was observed in this present study. Apoptosis was also increased by Enzalutamide in the presence of MET alone. There is no clear evidence indicating a direct interference of Enzalutamide on glucose metabolism. Previous studies found that the androgen signalling pathway stimulates aerobic glycolysis (Christofk et al. 2008; Vander Heiden et al. 2009) and anabolism in PCa cells (Massie et al. 2011). Consequently, blocking the AR signalling pathway by Enzalutamide may impair the effectiveness of aerobic glucose metabolism in PCa cells, causing them to be more susceptible to MET as the result of altering the

cellular ATP/AMP ratio as well as preventing glucose recruitment into oxidative phosphorylation processes. MET has also been shown to inhibit mTOR which can further impede cell anabolism in the absence of the AR signalling pathway (Xu, Y et al. 2006).

Using VPA in the presence of Enzalutamide induced more apoptosis than VPA alone in this present study. Gaughan et al. (2002) showed that direct or indirect acetylation (through Tip60) of AR increases AR transcriptional activity, and histone deacetylase 1 (HDAC1) down-regulates AR activity. In this manner, the HDACi activity of VPA enhances the transcriptional activity of AR (Xia et al. 2006), which may recover androgen responsiveness in CRPC (Iacopino et al. 2008).

In response to MET and VPA combination treatment, although there was no significant difference in the apoptosis frequency in LNCaP cells at the lower dose of 1 mM, the apoptotic response was significantly reduced in the presence of Enzalutamide at the higher dose of 2.5 mM compared to the absence of Enzalutamide, suggesting that the AR signalling pathway is important in the synergistic apoptosis response. As expected, there was no significant effect of Enzalutamide in the presence of MET+VPA on the apoptotic response of PC-3 cells which have no AR expression. PrEC cells also do not exhibit AR expression (Sobel, Richard E et al. 2006), which may contribute to the lack of a significant inhibitory response in response to MET+VPA in the present study. Although an interaction between p53 and AR in PCa is not well defined, the AR cofactor WDR777 may interact with p53 to form the p53-WDR77-AR complex and enhance the activity of AR (Kumari et al. 2016). However, it is not clear if MET+VPA has an effect on the p53-

WDR77-AR complex in PCa cells. Further investigation is needed to explore the interaction between AR and p53 in response to MET+VPA.

Recent next-generation sequencing efforts have revealed that the most frequent aberrations in CRPC include mutations in p53 (53.3%), AR (62.7%) and PTEN (40.7%), as well as ETS gene fusions (56.7%) (Robinson et al. 2015). Confirming that MET+VPA combination therapy is indeed p53-dependent and AR-dependent could provide a basis for individualised patient therapy in future clinical trials. The observation here that MET+VPA reduced cell proliferation in PC-3 cells which has no p53 or AR expression, suggests that MET+VPA can reduce cancer proliferation but not apoptosis independently of p53 and AR expression. Therefore, MET+VPA could still, potentially, provide a useful therapy in an advanced stage of PCa where multiple mutations have occurred.

4. EFFECT OF MET+VPA ON HUMAN TUMOUR XENOGRAFTS IN NUDE MICE AND *EX VIVO* HUMAN PROSTATE TUMOUR EXPLANTS

In order to confirm the *in vitro* findings described in Chapter 3 and provide safety evidence for clinical use of MET+VPA *in vivo*, LNCaP and PC-3 xenograft experiments in nude mice and *ex vivo* human prostate tumour explant studies were performed.

4.1. *In vivo* growth kinetics of LNCaP and PC-3 and determination of the optimal number of cells required for inoculation in nude mouse xenografts

An initial pilot study was conducted in order to determine the growth rates of LNCaP and PC-3 prostate tumour cell lines as xenografts in male nude mice. This experiment aimed to provide data on; 1) the variation in tumour volume in the animals; 2) the number of animals forming a tumour from the injected cells (take-rate); and 3) whether tumours formed would continue to grow or regress in the absence of treatment. In brief, twenty 5-week-old male nude mice (*BALB/c-Fox1^{nu}/Arc*) were allowed to acclimatise at the Flinders University School of Medicine Animal Facility for 1 week. The mice were randomised into 4 groups (n = 5) and injected in the left hind limb with either LNCaP or PC-3 cells suspended in Matrigel®. Two different starting cell numbers (1 x 10^6 and 3 x 10^6 cells/mouse) were inoculated for each cell line. The xenograft tumours were allowed to grow until reaching a maximum volume of 2000 mm^3, at which stage the mice were euthanised and the tumours dissected for histochemical analysis. The experimental plan is outlined in Figure 4-1.

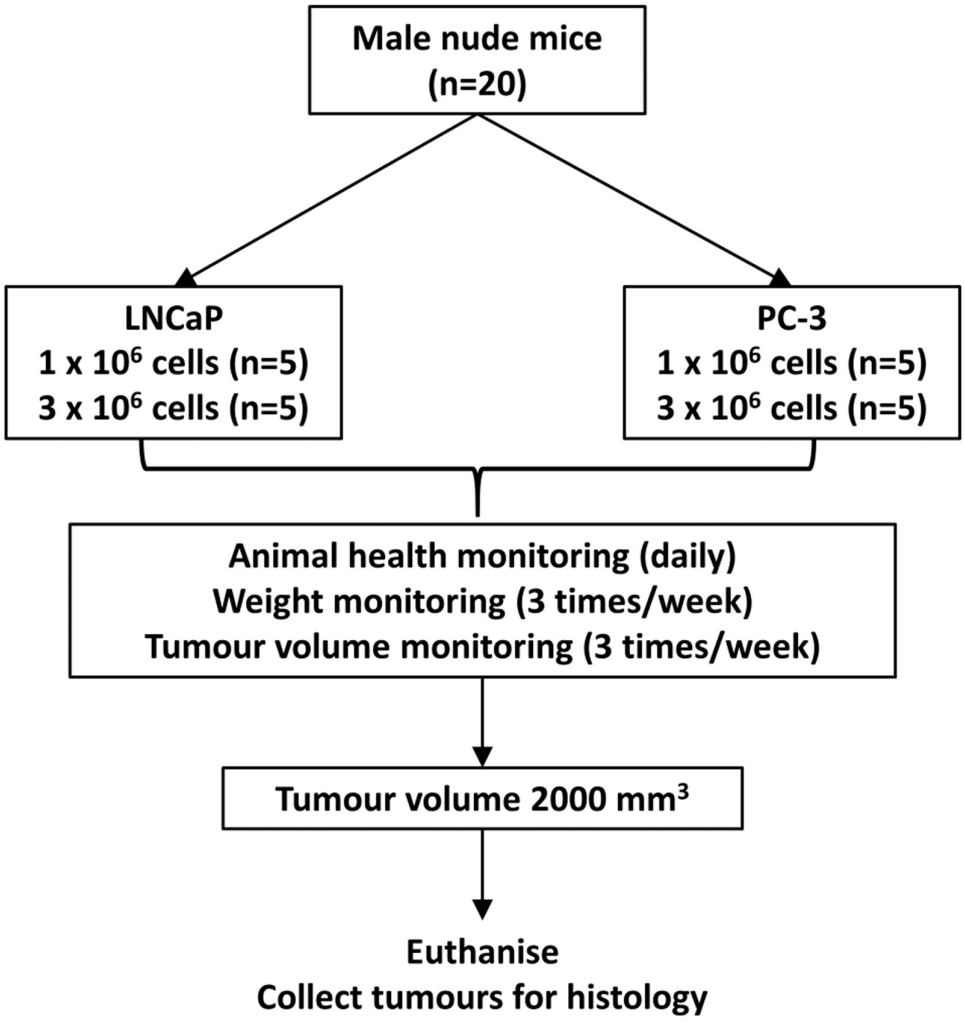

Figure 4-1. Xenograft tumour growth kinetic studies.

The mice were injected in the left hind limb with the cell lines (LNCaP and PC-3) in Matrigel®. Two different starting cell numbers of 1 x 10^6 and 3 x 10^6 were used for each cell line. The xenograft tumours were allowed to grow until reaching a maximum volume of 2000 mm^3 at which point the mice were euthanised.

In PC-3 xenografts, all of the mice developed tumours (100% take-rate) after inoculating with either 1 x 10^6 or 3 x 10^6 cells/mouse. There was no significant difference in palpable detection time between the two starting cell numbers which occurred approximately 7 days after inoculation. Inoculation with 1 x 10^6 and 3 x 10^6 cells/mouse induced a tumour volume of 2000 mm^3 at 53.6 $\pm$ 1.75 days and 59.4 $\pm$ 3.9 days (Mean $\pm$ SE), respectively, and the difference was not significant between the two groups ($p = 0.101$). However, inoculation of 1 x 10^6 cells produced less variation in time to achieve the volume of 2000 mm^3 (from day 49 to day 59 after inoculation) compared to 3 x 10^6 cells inoculation (from day 49 to day 70 after inoculation) (Figure 4-2A and B). As the inoculation of 1 x 10^6 PC-3 cells/mouse provided a more consistent growth rate between animals, this number was chosen for the PC-3 cell line for subsequent experiments (Figure 4-2A). Macroscopic findings showed the tumours to be yellowish, well circumscribed and solid (Figure 4-2C).

Where mice were inoculated with the LNCaP cell line, none of the mice inoculated with 1 x 10^6 cells developed a tumour (Figure 4-3A), whereas a 100% take-rate (5/5) was observed in the mice with 3 x 10^6 cells (Figure 4-3B). Formed tumours were first detected 31 days after inoculation and reached the maximum tumour volume of 2000 mm^3 at day 92.2 $\pm$ 9.4 (mean $\pm$ SE) (Figure 4-3B). The starting cell number of 3 x 10^6 was chosen for the LNCaP cell line in subsequent experiments. Macroscopic findings showed the tumours to be dark red and well circumscribed (Figure 4-3C). No tumour regression was observed in PC-3 and LNCaP xenografts in this study.

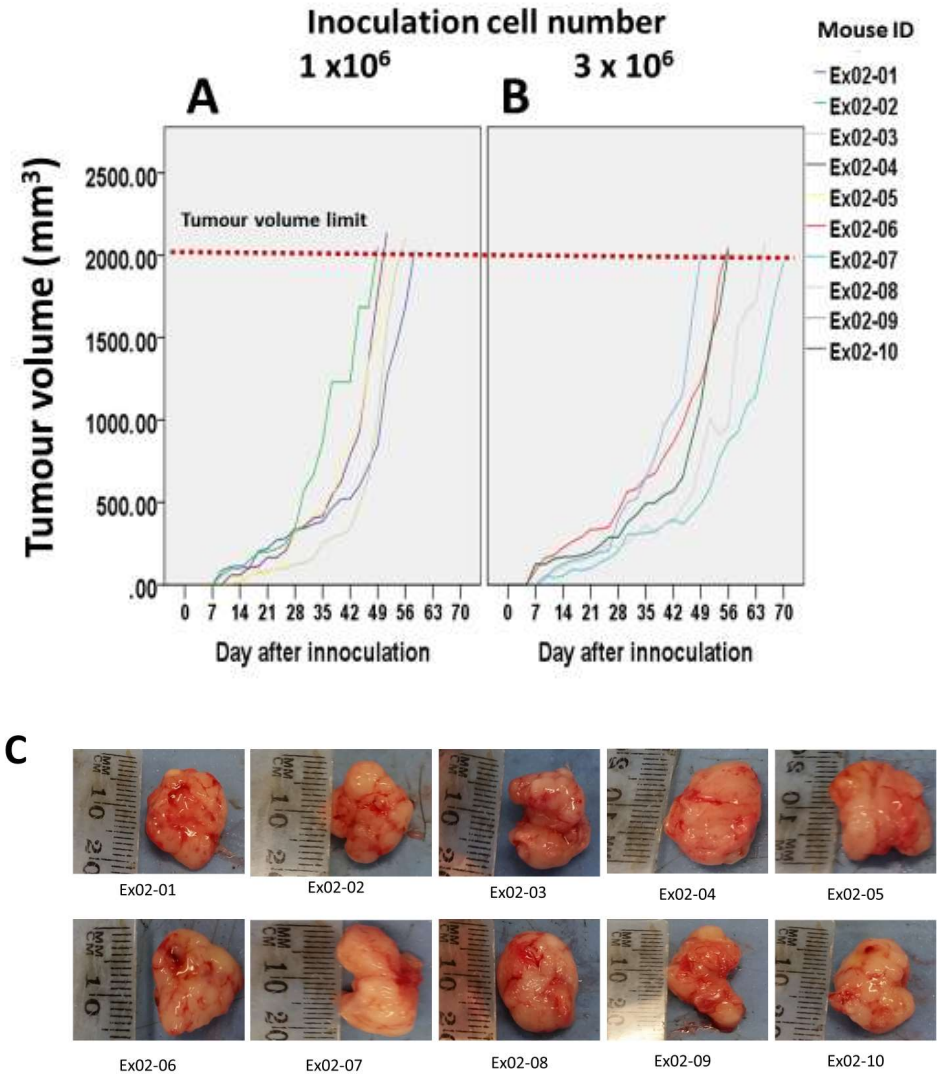

Figure 4-2. Tumour growth of PC-3 xenografts.

*Male nude mice at 6 weeks of age were inoculated subcutaneously with **(A)** 1 x 10^6 or **(B)** 3 x 10^6 PC-3 cells per mouse (n = 5). The mice were euthanised when the tumour volume reached 2000 mm^3. Xenograft tumours were removed and imaged. **C,** Images showing size and physical appearance of LNCaP xenografts. From mouse ID Ex02-01 to Ex02-05: 1 x 10^6 cells inoculation per mouse, from mouse ID Ex02-06 to Ex02-10: 3 x 10^6 cells inoculation per mouse.*

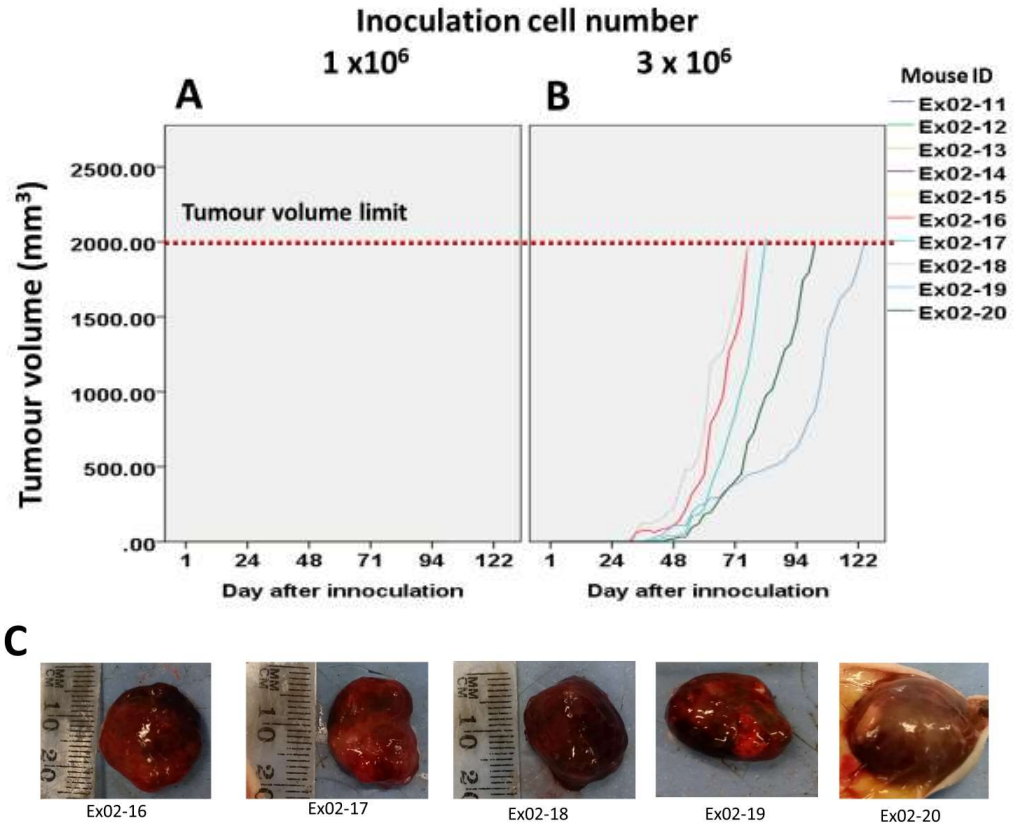

Figure 4-3. Tumour growth of LNCaP xenografts.
Male nude mice at 6 weeks of age were inoculated subcutaneously with ***(A)*** *1 x 10^6 or* ***(B)*** *3 x 10^6 LNCaP cells per mouse (n = 5). The mice were euthanised when the tumour volume reached 2000 mm^3. Xenograft tumours were removed and imaged****. C,*** *Images showing size and physical appearance of LNCaP xenografts. From mouse ID Ex02-16 to Ex02-20: 3 x 10^6 cells inoculation per mouse.*

4.2. Blood plasma concentration in mice treated with MET and VPA in drinking water

This pilot study aimed to determine the plasma concentration of MET/VPA treated-mice over 8 weeks of treatment. 200 µg/mL MET and/or 4% VPA were diluted in drinking water and the plasma was collected from mice before, 4 weeks, and 8 weeks after treatment. The plasma concentration of MET and VPA in mice was measured using UPLC-MS. MET alone in drinking water induced a plasma concentration from 0.3 to 1.0 µmol/L and from 0.3 to 1.1 µmol/L in the presence of VPA ($p > 0.05$) (Figure 4-4A). VPA alone in drinking water induced a plasma level from 4.8 – 10.9 µM which was significantly lower than in the presence of MET (11.7 – 127.7 µM) at 8 weeks after treatment ($p < 0.05$) (Figure 4-4B).

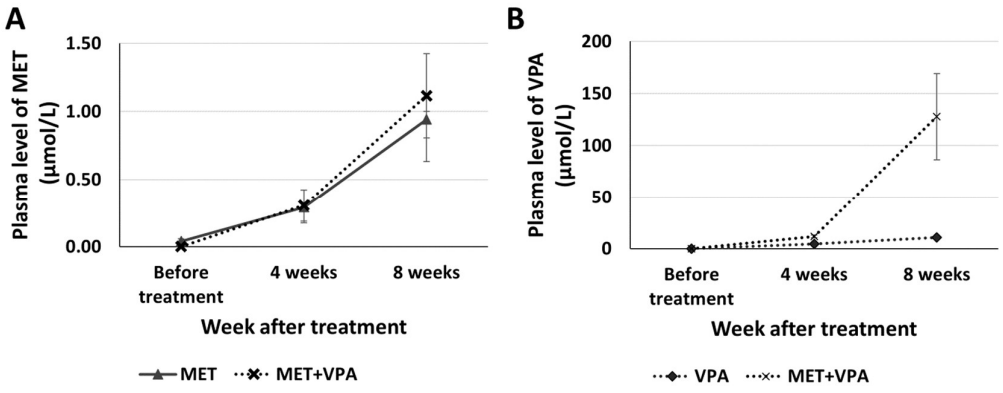

Figure 4-4. Plasma concentration of MET alone, VPA alone, and in combination.

Plasma concentrations (Mean ± SE) of MET and VPA were measured before, 4 weeks, and 8 weeks after treatment using UPLC-MS. ***A,*** *Plasma concentration of MET alone and in the presence of VPA.* ***B,*** *Plasma concentration of VPA alone and in the presence of MET.*

4.3. Weight change, liver and kidney toxicity in nude mice treated with MET and VPA

There are no reports of adverse health effects from chronic administration of 200 µg/mL MET alone and 4% VPA alone in nude mice. A pilot study was conducted to investigate health effects on nude mice in response to either vehicle, 200 µg/mL MET alone, 4% VPA alone, or 200 µg/mL MET + 4% VPA treatment (n = 3 in each group). There was no significant difference in mouse weight observed between the vehicle, MET alone, VPA alone, and MET+VPA treatment groups throughout the experiment (Figure 4-5A). Histological scoring of the kidney (Figure 4-5B) and liver (Figure 4-5C) showed no or minimal damage (score = 0) to the kidney or liver.

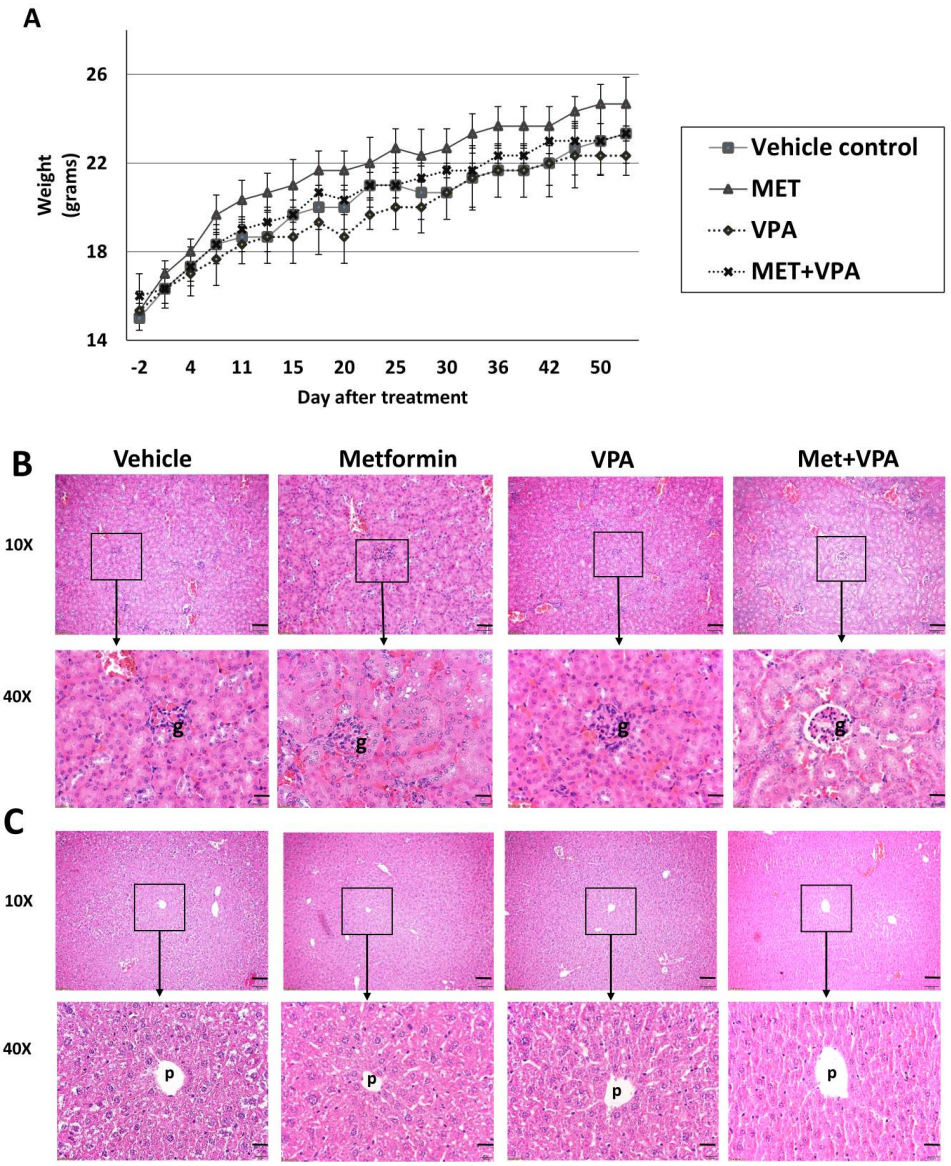

Figure 4-5. The weight of nude mice (A) and histology of kidney (B) and liver (C) in response to 8 weeks of MET and VPA treatment.

Six-week-old nude mice were treated with either vehicle control, 200 µg/mL MET alone, 4% VPA alone, or 200 µg/mL MET + 4% VPA for 8 weeks. ***A,*** *The weight of nude mice (mean ± SE) during MET and VPA treatment (n = 3). There was no significant difference in weight between groups over eight weeks of treatment (p > 0.05). Representative histological images (H&E) at 10X and 40X magnification of the kidney* ***(B)*** *and liver* ***(C)*** *after 8 weeks of treatment. The histological scoring of the kidney* ***(B)*** *shows no glomerular* ***(g)*** *change, thrombosis, tubular dilation, necrosis, or inflammation (score 0). The histological scoring of the liver* ***(C)*** *showed no fibrosis in the portal* ***(p)*** *region, lobular inflammation or necrosis, Mallory bodies, hepatocyte ballooning, peri-sinusoidal fibrosis, or fatty change (score 0). Scale bar represents 1 mm for 10X images, and 20 µm for 40X images.*

4.4. Effect of MET+VPA on tumour growth of PC-3 and LNCaP xenografts

In order to investigate the tumour growth of PC-3 and LNCaP xenografts in response to MET and VPA, 6-week-old male mice were inoculated with LNCaP (n = 40) or PC-3 (n = 40), then randomly assigned into vehicle (water), MET, VPA, or MET+VPA treatment groups (n = 10 / treatment group / cell line). Once the xenograft tumour reached 100 mm^3, mice were treated with either vehicle control, 200 µg/mL MET alone, 4% VPA alone, or 200 µg/mL MET + 4% VPA for a maximum of 12 weeks. The tumour take-rate in this study was 87.5% (35/40) for LNCaP and 90% (36/40) for PC-3 cells. No tumour regression was observed in the study. In the PC-3 xenograft group, two mice were euthanized at day 2 and 3 of treatment due to lesions sustained from fighting, and one mouse was euthanized at day 14 due to chylothorax. One mouse with a LNCaP xenograft was euthanised at day 32 due to the tumour affecting mouse movement, and one mouse with a PC-3 xenograft was euthanised due to tumour ulceration at day 58. The experimental design and final animal number analysed are summarised in Figure 4-6. Tumour volumes were compared after treatment, using the cut-off time of when the first xenograft tumour reached 2000 mm^3, which was 28 days for PC-3 and 21 days for LNCaP xenografts.

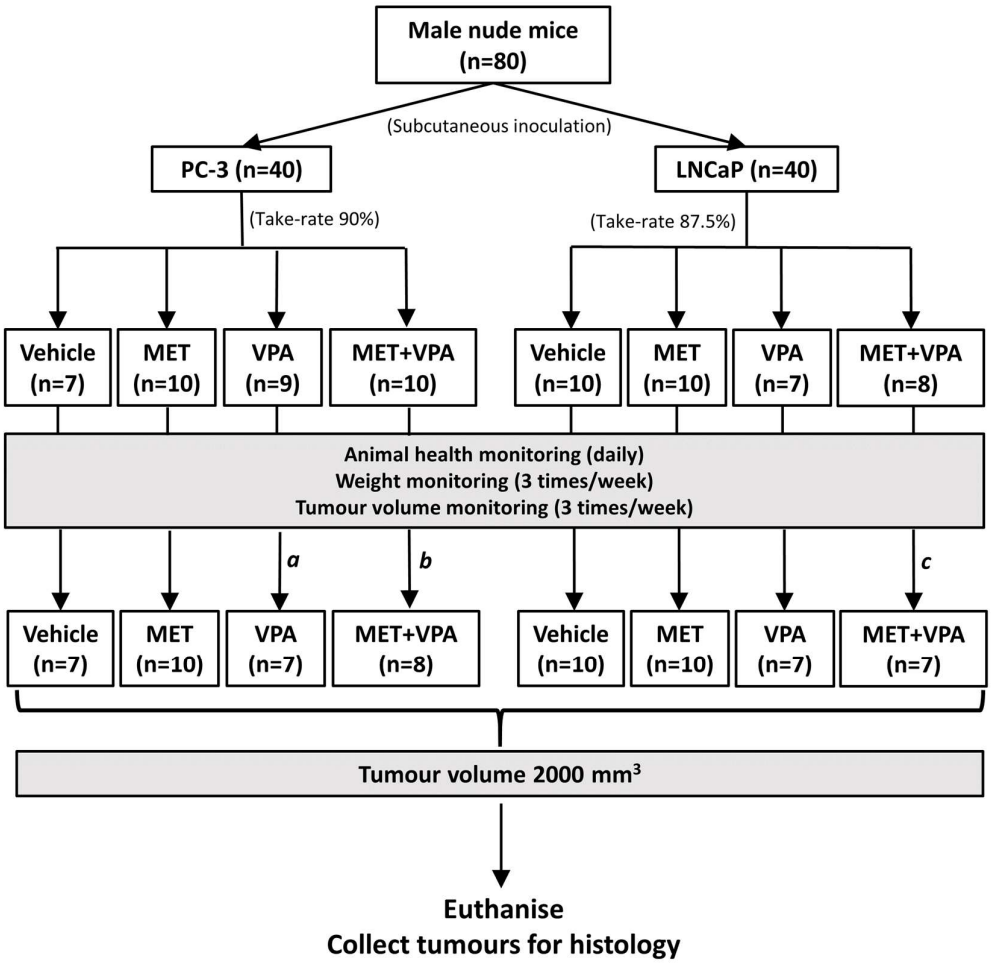

Figure 4-6. Summary of study design of MET+VPA treatment in PC-3 and LNCaP xenografts.

6-week-old nude mice (n = 80) were randomly assigned into two groups and inoculated with either LNCaP (n = 40) or PC-3 (n = 40) cells. Mice were randomly assigned into 4 groups (n = 10 / group). Once the xenograft tumour reached 100 mm^3, mice were treated with either vehicle control, 200 µg/mL MET alone, 4% VPA alone, or 200 µg/mL MET + 4% VPA for a maximum of 12 weeks. The xenograft tumours were allowed to grow until reaching a maximum volume of 2000 mm^3. [a] two mice were excluded from the study, one due to fighting lesions on day 3 after treatment and the other due to chylothorax on day 14 after treatment. [b] one mouse was excluded from the study due to fighting lesions on day 2 after treatment and one mouse was censored on day 58 after treatment due to tumour ulceration. [c] one mouse was censored on day 32 after treatment due to tumour affecting mouse movement.

In the PC-3 xenograft group, there was no significant difference in tumour volume in the mice treated with MET alone, VPA alone, or vehicle treatment ($p > 0.05$). The combination of MET+VPA significantly inhibited the volume of the PC-3 tumour xenograft compared to vehicle treatment (86.7 % decrease, $p = 0.001$), MET alone (63.9% decrease, $p = 0.005$), and VPA alone (59.7% decrease, $p = 0.04$) (Figure 4-7A) at day 28 of treatment.

In the LNCaP xenograft group, the addition of MET inhibited tumour growth compared to vehicle treatment (40.1% decrease, $p <0.001$), as did VPA (42.2% decrease, $p < 0.001$) (Figure 4-7B). MET+VPA induced a significant inhibition in tumour growth compared to vehicle treatment (77% decrease, $p < 0.001$), MET alone (61.6% decrease, $p < 0.001$), and VPA alone (60.2% decrease, $p < 0.001$) at day 21 of treatment.

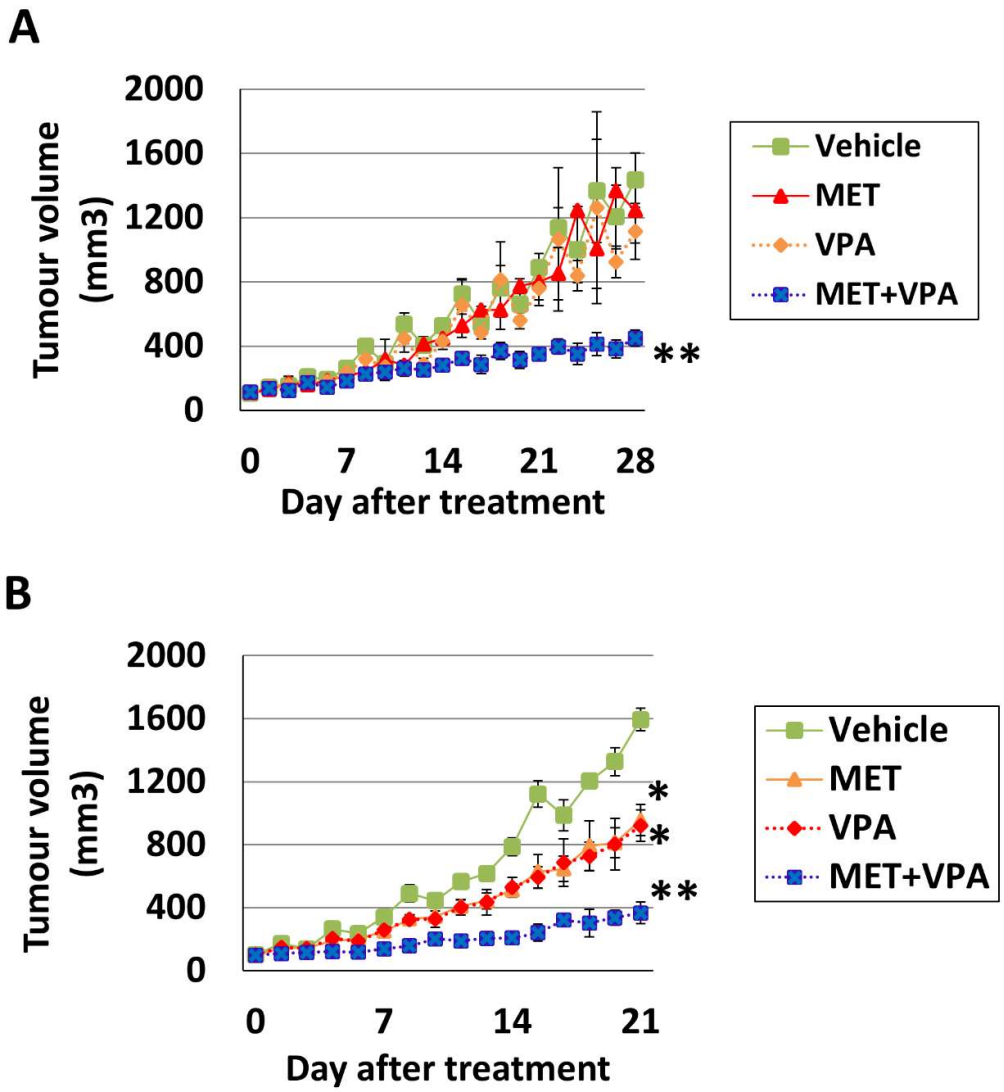

Figure 4-7. Tumour volume in PC-3 and LNCaP xenografts in response to MET and/or VPA treatment.

Nude mice at 6 weeks of age were inoculated subcutaneously with PC-3 ***(A)*** *or LNCaP* ***(B)*** *cells. The xenograft tumours were allowed to grow to 100 mm^3 before treating with either vehicle control, 200 µg/mL MET alone, 4% VPA alone, or 200 µg/mL MET + 4% VPA. Tumour volumes (mean ± SE) were measured three times/week. Treatment was continued until the first tumour to reach 2000 mm^3 in any one xenograft group was detected. This was determined to be 28 days and 21 days for the PC-3 and LNCaP xenograft groups respectively. * $p < 0.05$ in comparison with the vehicle, MET alone, and VPA alone. ** $p < 0.05$ in comparison with the vehicle, MET alone, VPA alone, and MET+VPA.*

4.5. Time-to-maximum tumour volume in LNCaP and PC-3 xenografts treated with MET and VPA

The mice were humanely euthanised when the tumour volume reached 2000 mm^3 or 90 days after treatment, whichever came first. Cumulative survival using Kaplan-Meier analysis showed that MET+VPA significantly extended the time-to-maximum tumour volume in PC-3 compared to vehicle treatment (92.2% increase, $p < 0.001$), MET alone (60.5% increase, $p = 0.002$), and VPA alone (43.7% increase, $p = 0.01$). Treatment of nude mice bearing PC-3 xenografts with VPA alone also induced a significant longer time-to-maximum tumour volume compared to vehicle treatment (32.8% increase, $p = 0.006$), whereas the difference was not significant in MET alone compared to vehicle treatment ($p = 0.08$) (Figure 4-8A).

In the LNCaP xenograft group, the time-to-maximum tumour volume in response to MET+VPA was significantly longer than MET alone (44.2% increase, $p = 0.002$), VPA alone (43.9 % increase, $p = 0.001$), and vehicle treatment (120%, $p < 0.001$). Treatment with MET alone and VPA alone significantly extended the time-to-tumour volume of 2000 mm^3 compared to vehicle treatment (52.4% increase, $p < 0.001$ and 52.8% increase, $p < 0.001$, respectively) (Figure 4-8B).

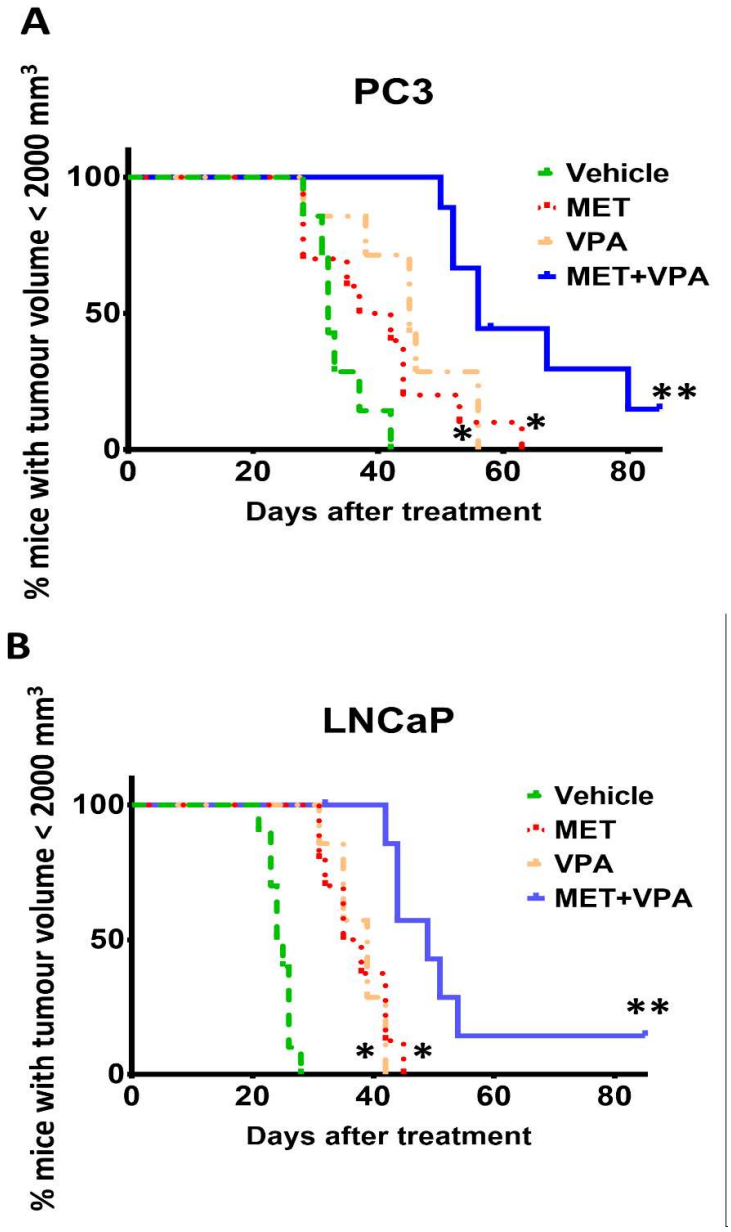

Figure 4-8: Kaplan-Meier analysis of percentage of animals reaching a tumour volume of 2000 mm^3 over the period of treatment with MET and VPA.

*Mice bearing tumour PC-3 or LNCaP xenografts were treated with either vehicle control, 200 µg/mL MET alone, 4% VPA alone, or 200 µg/mL MET + 4% VPA for a maximum of 90 days. The mice were humanely euthanised when the tumour volume reached 2000 mm^3 or at the end of the experiment. * $p < 0.05$ in Kaplan-Meier analysis compared to vehicle treatment. ** $p < 0.05$ in Kaplan-Meier analysis compared to vehicle treatment, MET alone, and VPA alone ($7 \leq n \leq 10$).*

4.6. Clinical and pathological features of patient-derived prostate tumour explants

In order to further confirm the effect of MET+VPA in a preclinical model, the response to MET+VPA was investigated in human prostate tumour explants derived from PCa patients who underwent surgery (radical prostatectomy). Eight human prostate tumour explants were available for this study. The age of the patients was 64.6 ± 2.2 years (mean ± SE) and the PSA level was 9.1 ± 2.8 ng/mL (mean ± SE). The clinico-pathological features of the PCa patients who had undergone radical prostatectomy are given in Table 4-1. The pathological stage ranged from pT2C to pT3A. Most of the patients (7/8) had Gleason score of 7 and one patient had the Gleason score of 9. All prostate tumour explants expressed normal AR immunohistochemistry.

Table 4-1. Clinico-pathological features of PCa patient tumour explants

Patient No.	Patient age (years)	PSA (ng/mL)	Gleason score [a]	Pathological stage [a]	AR status
1	67.2	14.1	3+4=7	pT3a	+
2	58.9	8.3	3+4=7	pT3a	+
3	57.4	7.8	3+4=7	pT3a	+
4	69	8.3	4+3=7	pT3a	+
5	71.5	10.4	4+3=7	pT3a	+
6	66.5	5.7	3+4=7	pT2c	+
7	70.6	6.5	3+4=7	pT2c	+
8	55.8	12	5+4=9	pT3b	+

[a] All tumours are adenocarcinoma of acinar type. Pathological stage as per AJCC TNM 7th Edition (Edge et al. 2010).

4.7. Proliferation and apoptosis of human prostate tumour explants in response to MET+VPA.

The prostate tumour explants were cultured in 24 well-plates and exposed to vehicle or MET+VPA at doses of either 2.5 mM or 5 mM for 48 h. The individual patient responses are shown for proliferation (% Ki67 positive) (Figure 4-9A i) and apoptosis (% CC3 positive) (Figure 4-9B i) 48 h after treatment. Compared to vehicle control, 2.5 mM MET+VPA significantly decreased the proportion of Ki-67 positive cells (90% decrease, $p < 0.001$) (Figure 4-9A ii, iii, and iv) and increased the percentage of positive CC-3 cells (300% increase, $p < 0.001$) (Figure 4-9B ii, iii, and iv). When the MET+VPA dose was increased to 5 mM, the inhibitory effect on proliferation was not significantly changed compared to 2.5 mM MET+VPA. The apoptosis response however was further increased in the 5 mM group compared to vehicle control (600% increase, $p < 0.001$) and to 2.5 mM MET+VPA (200% increase, $p < 0.05$) (Figure 4-9A ii and B ii).

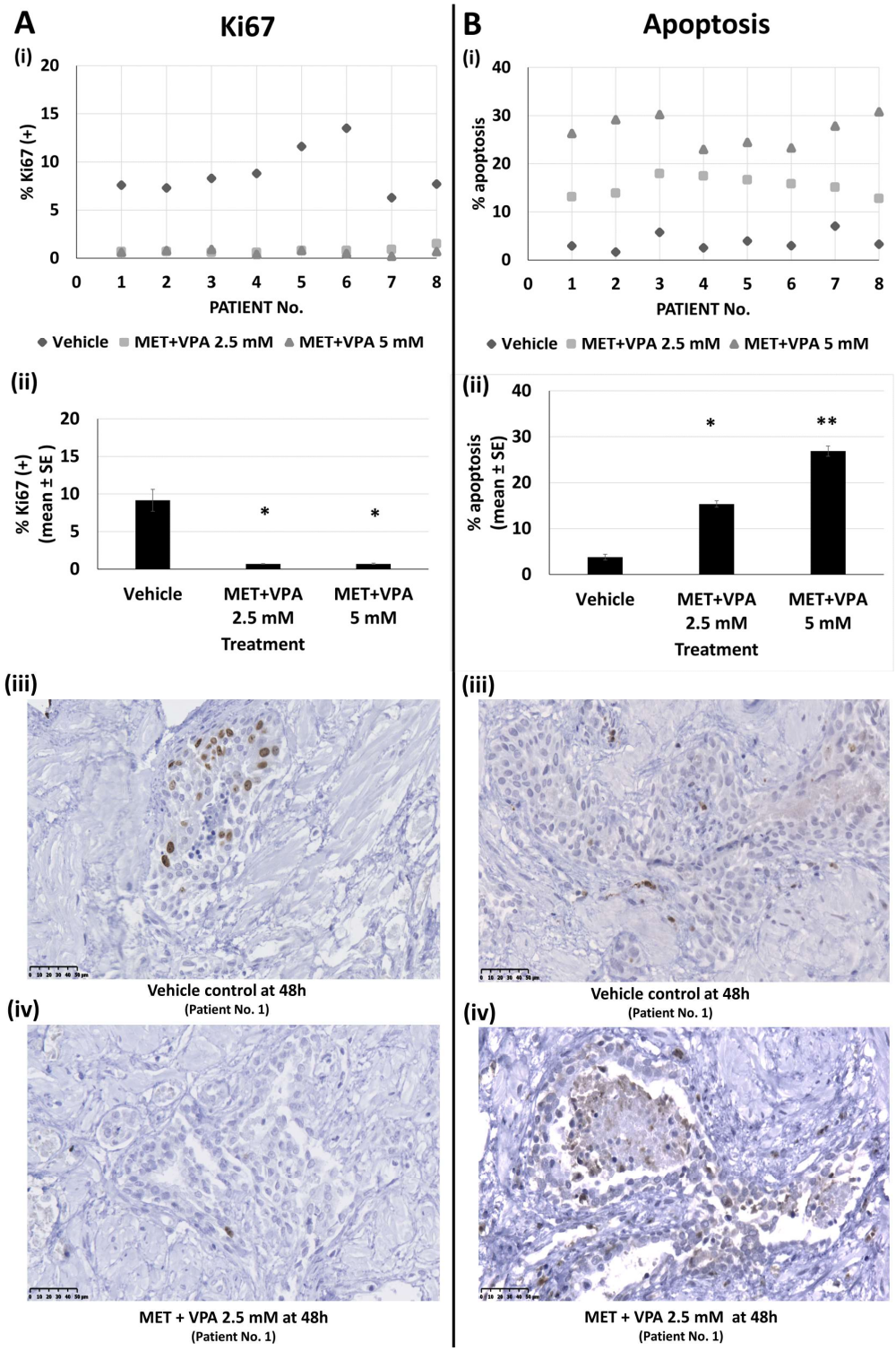
A
Ki67
(i)
% Ki67 (+)
PATIENT No.
Vehicle
MET+VPA 2.5 mM
MET+VPA 5 mM
(ii)
% Ki67 (+) (mean ± SE)
Vehicle
MET+VPA 2.5 mM
MET+VPA 5 mM
Treatment
(iii)
Vehicle control at 48h
(Patient No. 1)
(iv)
MET + VPA 2.5 mM at 48h
(Patient No. 1)
B
Apoptosis
(i)
% apoptosis
PATIENT No.
Vehicle
MET+VPA 2.5 mM
MET+VPA 5 mM
(ii)
% apoptosis (mean ± SE)
Vehicle
MET+VPA 2.5 mM
MET+VPA 5 mM
Treatment
(iii)
Vehicle control at 48h
(Patient No. 1)
(iv)
MET + VPA 2.5 mM at 48h
(Patient No. 1)

Figure 4-9: **MET+VPA reduced cell proliferation and increased apoptosis in patient-derived human prostatic *ex vivo* tumour explants.**

Tissues were treated with 2.5 mM or 5 mM MET+VPA for 48 h, and then were fixed in formalin and paraffin embedded. Ki67 and CC-3 immunochemistry staining were performed. ***A, (i)*** *Percentage of Ki67 positive cells in individual patient explants (n = 8),* ***(ii)*** *Percentage (mean ± SE) of Ki67 positive cells in all patient explants, and representative Ki67 stained sections (scale bar = 50 µm) in patient No.1 of* ***(iii)*** *vehicle treated and* ***(iv)*** *MET+VPA (2.5 mM) treated explants at 48 h.* ***B, (i)*** *Percentage of CC3 positive cells in individual patient explants (n = 8),* ***(ii)*** *Percentage (mean ± SE) of CC3 positive cells in all patient explants, and representative CC3 stained sections in patient No.1 of* ***(iii)*** *vehicle treated and* ***(iv)*** *MET+VPA (2.5 mM) treated explants at 48 h. * $p < 0.05$ in comparison with the vehicle. ** $p < 0.05$ in comparison with MET+VPA (2.5 mM) and vehicle (n = 8).*

4.8. Discussion

The *in vitro* findings presented in Chapter 3 demonstrated that the combination of MET and VPA-induced a synergistic anti-proliferative response in PCa cell lines (LNCaP and PC-3), and a synergistic apoptotic response in LNCaP only, with no significant effects in normal prostatic epithelial cells (PrEC). The presence of p53 and the androgen signalling pathway were shown to play an important role in the synergistic apoptosis of PCa cell lines in response to MET+VPA. Here, in this pre-clinical study, the effect of MET and VPA in PCa xenografts in nude mice was investigated to support the *in vitro* findings and provide safety evidence for clinical use. This xenograft experiment used 200 µg/mL of MET and 4% of VPA diluted in drinking water which is equivalent to the human doses of 2.0 - 4.1 mg/kg/day for MET (Reagan-Shaw et al. 2008) and 40.6 – 79.4 mg/kg/day for VPA. These doses were in the therapeutic range for non-cancer purposes in humans which have been shown to induce minimal adverse effects (Burke et al. 1985).

The growth rate of human carcinoma cell lines in nude mice is low, with a general take-rate of 12% for PCa cell lines (Fogh et al. 1982), with a higher tumorigenicity of PC-3 at 30% and only 5% for LNCaP (Untae Kim 2011) cells. Matrigel™, an extracellular matrix derived from the extract of basement membrane proteins of Engelbreth-Holm-Swarm (EHS) mouse sarcoma cells (Kleinman et al. 2005), was used to enhance the tumorigenicity of LNCaP and PC-3 cells in the present study. The tumour take-rate in this study was 87.5 % for LNCaP and 90% for PC-3 xenografts with no tumour regression observed. These results are higher than reported by Davoodpour et al. (2007) where the

take-rate of PC-3 xenografts was 60%, and is comparable to that of Gustavsson et al. (2010) who found the take-rate of LNCaP xenografts to be approximately 90% in the presence of Matrigel. Only one abdominal lymph node metastasis was found in a mouse with a PC-3 xenograft (n = 36) in the vehicle treatment group (day 33 after treatment), and no metastasis of LNCaP xenografts (n = 35) was observed. This finding agrees with the literature, where the metastatic rate of PCa xenografts is relatively low at less than 1.7% (Sharkey et al. 1979). The subcutaneous injection of PCa cells causes less metastasis than other routes of inoculation such as intravenous, orthotopic, or intraosseous injection. The study of Cifuentes et al. (2015) found no metastasis in immunocompromised mice (SCID) after subcutaneous injection of PC-3 cells, whereas lung metastasis was observed in all mice with anterior prostate injection of PC-3 cells (Pettaway et al. 1996; Wu, TT et al. 1998). Orthotopic injection of LNCaP into nude mice induced para-aortic lymph node metastases in 12 out of 43 mice over a period of 100 days (Pettaway et al. 1996). This current study used subcutaneous injection of PC-3 and LNCaP cells and found a low metastatic rate at 2.7% (1/36) in PC-3 xenografts and no metastasis in LNCaP xenografts which is similar to the findings from the literature.

The dose of 200 µg/mL of MET diluted in drinking water used in the xenograft studies induced a plasma level of MET from 0.3 to 1.1 µmol/L. The plasma level of MET in mice has not been fully investigated in the literature. Studies by Iliopoulos et al. (2011) and Ben-Sahra et al. (2008) used the same dose of 200 µg/mL MET used here, but the plasma concentration of MET was not reported. Another study by Gou et al. (2013) used the same human equivalent

doses (by normalization to surface area) in mice (100-200 mg/kg/day in mice is equivalent to 8.1-16.3 mg/kg/day in human (Reagan-Shaw et al. 2008)) and found the plasma concentration to be approximately 20 µmol/L which falls within the human therapeutic level (7.7 – 30.8 µmol/L) in diabetic patients (FDA 2015), however the method of MET measurement was not described. The dose of MET in the current study (25-50 mg/kg/day in mice is equivalent to 2 – 4.1 mg/kg/day) which is lower than human therapeutic doses (8.3 – 16.6 mg/kg/day) (FDA 2015) which could explain the lower plasma concentration observed in the mice used here (0.4-1.1 µmol/L) compared to humans.

The VPA dose of 0.4% in drinking water, which is similar to the human therapeutic dose, induced a mouse plasma level of 3.8 – 9.0 µM in response to VPA treatment alone and 9.7 – 106.4 µM in response to MET+VPA. In general, the plasma levels reported in the study presented here are lower than reported in the literature. The study of Shabbeer et al. (2007) used an immunoassay (valproic acid II assay in Roche/Hitachi 917 System) to measure the concentration of VPA in mouse plasma and found that 0.4% VPA in drinking water induced a plasma level of approximately 100 µM , while Xia et al. (2006), using the same dose of VPA in mice, found variable plasma levels of 20.8 – 485.4 µM (3-70 mg/L). In humans, the therapeutic dose of VPA at 10-20 mg/kg/day induced plasma concentrations ranging from 50-100 µg/mL (350 to 700 µmol/L) (Schobben et al. 1980; Turnbull et al. 1983). The error bars were large in this study as the number of animals was small. Also, in some animals the volume of plasma was sometimes insufficient for MET and VPA quantification using mass spectrometry, and therefore some time-points had only data from 2 samples. These issues, along with the variation in the last

drink time for animals might have contributed to the large error bars and difference in VPA plasma level. Also the different technique (UPLC-MS) used here might explain the different findings compared to the literature. Mice administered MET+VPA in this study had lower plasma levels of these drugs compared to those in humans, which suggests the potential to lower the doses of MET and VPA in combinational therapy while still maintaining efficacy.

There is prior literature where mice have been administered chronic dosing of the drug MET alone, or the drug VPA alone in drinking water for the purpose of xenograft experiments with no negative health-related issues reported in the mice (Ben-Sahra et al. 2008; Xia et al. 2006), however there are no reports regarding potential tissue toxicity in mice in response to the combination of MET and VPA. There are a small proportion of patients that receive both MET and VPA for diabetes and epilepsy management without remarkable adverse events (eHealthMe 2016). The mice in this study showed no weight change during the 8 weeks of receiving either 200 µg/mL MET, 0.4% VPA or both drugs in drinking water. Gross necropsy indicated no tissue toxicity and histopathological analysis on kidney and liver (major metabolic sites of MET and VPA, respectively) showed no or limited damage. Although the metabolism of the drugs in mouse and human can be different, these results suggest that MET and VPA, at the doses reported here, can be combined as a long-term therapy for cancer treatment with minimal side effects.

After confirming that there was no negative health effect of administration of MET and VPA in combination, and determining the rate of tumour growth, xenografted mice were treated with MET and VPA, either alone or in

combination, to determine if the drug combination reduces tumour growth. There was no significant difference in tumour growth of PC-3 xenografts in response to MET alone or VPA alone compared to vehicle treatment over the first 4 weeks of treatment. This finding differs from the report of Shabbeer et al. (2007) where the administration of 0.4% VPA in drinking water for 4 weeks significantly reduced the PC-3 xenograft tumour volume by 57% compared to vehicle treatment ($p = 0.05$, $n = 8$). Although the anti-tumour effect of VPA alone was not observed here in the short-term, long-term administration of VPA did delay tumour progression by 32.8%. Importantly, the combination of MET and VPA, compared to MET alone, VPA alone and vehicle treatment, inhibited tumour growth of PC-3 xenografts by 59 – 86% in both the first 4 weeks of treatment and extended the time-to-maximum tumour volume of 2000 mm^3 by 43 - 92% with long term treatment. PC-3 has the characteristics of a small cell neuroendocrine carcinoma, is highly aggressive, and hormone refractory. Thus, the response of PC-3 xenografts to MET+VPA in this study suggests this combination of drug may be an effective therapy for CRPC.

The anti-tumour growth effect of MET or VPA alone in LNCaP xenografts was more prominent than in PC-3. Both MET alone and VPA alone reduced the tumour volume by approximately 40% in the first 4 weeks after treatment and prolonged the time-to-maximum tumour volume by approximately 44% compared to vehicle treatment. MET or VPA in drinking water in nude mice bearing LNCaP xenografts reduced the tumour volume growth after 3-4 weeks of treatment (55% and 40% reduction, respectively) (Ben-Sahra et al. 2008; Xia et al. 2006). Combining MET and VPA here induced a greater reduction of initial tumour growth of 60-77% in the short-term and extended the time-to-

maximum tumour-volume by 42-120% with long-term treatment, indicating the potential effectiveness of MET+VPA combinational therapy over monotherapies. It is possible that the increased blood present in the LNCaP xenografts may have better access of the drugs to the tumours than in PC-3 xenografts which may have also contributed to the greater efficacy of the drug combination.

The efficacy of combining MET and VPA to inhibit proliferation and increase apoptosis in PCa was further confirmed in clinical specimens using human prostate tumour explants. This pre-clinical model maintains the native tumour microenvironment including cancer cells, surrounding stroma (fibroblasts, macrophages, lymphocytes, vessels, and extracellular matrix components), thereby facilitating the integration of stromal-epithelial signalling in PCa (Centenera et al. 2012; Centenera et al. 2013). In this study, all PCa tissues were collected from PCa patients undergoing radical prostatectomy and cancer morphology was confirmed by a pathologist. Most of the tissues were graded as local or locally advanced PCa (pT2c-3b, Gleason 7-9). The expression of normal AR was positive in all samples using immunohistochemistry. Although the expression of p53 was not analysed in these tissues, almost all PCa patients with localised disease express both AR and p53 (Bookstein et al. 1993; Feldman et al. 2001; Taplin et al. 1995). MET+VPA reduced proliferation and increased apoptosis in all eight prostatic explants which is consistent with the *in vitro* and xenograft results presented above, and suggests that MET+VPA is likely to show some efficacy as a systemic therapy in patients with local or locally advanced PCa.

LNCaP cells have normal p53 expression and are androgen receptor (AR) sensitive as is the case in the majority of localised PCa, while PC-3 cells have no p53 expression and are AR-independent, similar to that observed in CRPC, which suggests that these cell lines represent PCa disease at different stages. The *in vivo* findings of this study that MET+VPA resulted in a greater reduction in tumour growth in both initial and long-term treatment of MET+VPA compared to MET alone, VPA alone and vehicle treatment, was accompanied by no or minimal toxicity to normal tissues. These findings were further confirmed in human prostate tumour explants where MET+VPA inhibited cell proliferation and promoted apoptosis. These results together suggest that MET+VPA could be a safe and useful systemic therapy at different stages of PCa.

5. GENERAL DISCUSSION AND CONCLUSIONS

Both MET and VPA have been shown to individually have anti-cancer effects. The aim of this project was to investigate whether MET and VPA cause an additive or synergistic effect, when used in combination. The role of p53 and AR in the MET+VPA-mediated anti-cancer effect were also investigated *in vitro*. The current study demonstrated that MET+VPA showed significant efficacy in PCa cell lines (LNCaP and PC-3), human prostate tumour explants, and nude mouse xenografts bearing LNCaP and PC-3 cells, while inducing minimal effects in normal prostate cells and tissues (PrEC cells and kidney and liver of nude mice). The synergistic anti-cancer effect was highest in the presence of functional p53 and AR, suggesting that the drug combination is acting via pathways involving these proteins and could be particularly effective against tumours with functional p53 and AR. These important findings and proposed mechanism are discussed below.

5.1. MET+VPA induces intrinsic apoptosis via p53 activation

In this thesis it was demonstrated that, in tumour explants derived from patients with localised PCa, MET+VPA induced a significant increase in apoptosis compared to the vehicle control. Although the expression of functional p53 was not confirmed in these tissues, almost all PCa patients with localised disease have been shown to express normal p53 (Bookstein et al. 1993; Feldman et al. 2001; Taplin et al. 1995). *In vitro* investigations showed that MET+VPA induced synergistic apoptosis in the PCa cell line LNCaP ($p53^+$), but not in PC-3 ($p53^-$). Furthermore, MET+VPA caused further release of cytochrome c from the mitochondria to the cytosol in LNCaP cells, indicating that MET+VPA could

target mitochondrial activity either directly or indirectly, causing intrinsic apoptosis. MET can bind directly to Mitochondrial Complex 1, interfering with mitochondrial activities in PCa cells (Fendt et al. 2013). Chen, H et al. (2012) found that VPA reduces the expression of nuclear enzyme ten-eleven translocation methylcytosine dioxygenase 1 (TET1) which consequently decreases the 5-hydroxymethylcytosine content of mitochondrial DNA, therefore interfering with mitochondrial activity. The combination of MET and VPA, via different mitochondrial targets, could further inhibit mitochondrial activity and cause intrinsic apoptosis in PCa cells. Further investigation on mitochondrial respiration such as mitochondrial membrane potential change (electron transport chain) and mitochondrial respiration profiles (basal respiration, maximal respiration, and spare respiration capacity) could provide a better understanding about the mitochondrial metabolic changes in response to MET+VPA.

Knock-down of p53 in LNCaP cells ($p53^+$, AR^+) reduced the synergistic apoptotic response, while ectopic expression of p53 in PC-3 cells ($p53^-$, AR^-) increased apoptosis in response to MET+VPA, which suggests that p53 plays a role in the MET+VPA-induced apoptosis. There is a body of evidence supporting the regulatory role of p53 in response to MET and VPA, both alone and in combination, for PCa treatment. *In vitro* studies demonstrated that PCa cells that are *p53* (+) have a greater response to MET compared to *p53* (-) (Ben-Sahra, Laurent, et al. 2010; Gotlieb et al. 2008; Zakikhani et al. 2006). More specifically, through AMPK activation, MET enhances p53 expression, which induces p53-related cellular metabolism changes such as energy metabolism, mitochondrial respiration and antioxidant activities (Bensaad et

al. 2007; Feng et al. 2010; Okoshi et al. 2008). The correlation between the response of MET and p53 was strengthened when the combination of MET and SIRT1/BI2536 (Tneovin-1 inhibitor), a p53 stabilizer, further inhibited oxidative phosphorylation of MET and induced a synergistic apoptosis via the regulation of energy metabolism in CRPC (Chen, L et al. 2016). On the other hand, VPA was found to increase the DNA binding of p53 and enhance the transcriptional activity of p53 on the p21 promoter (Bode et al. 2004; Gu et al. 1997). Furthermore, VPA can rescue the inhibited-CBP/p300, a p53-acetylation factor, in ERG(+) cells by reversing the inhibitory effect of ERG on CBP/p300 in PCa cells, thus maintaining p53 acetylation status (Fortson et al. 2011). These studies provide a rationale for MET+VPA induced intrinsic apoptosis via p53 regulation for PCa treatment. Based on the current literature and the results presented in this thesis, a proposed mechanism for the role of p53 in the apoptotic response to MET+VPA is presented in Figure 5-1. Extra experiments would be required to support such as model including investigation of extrinsic apoptosis in response to MET+VPA, given that extrinsic apoptosis is triggered by p53 activation (Bennett et al. 1998; Liu et al. 1998), and VPA can increase the release of extrinsic apoptosis components (FAS and FASL) (Bouzar et al. 2009). Dual activation of p53 (phosphorylation of Ser 15 and acetylation of lysine 373-382) in response to MET+VPA requires validation using 2D western blot and/or mass spectrometry.

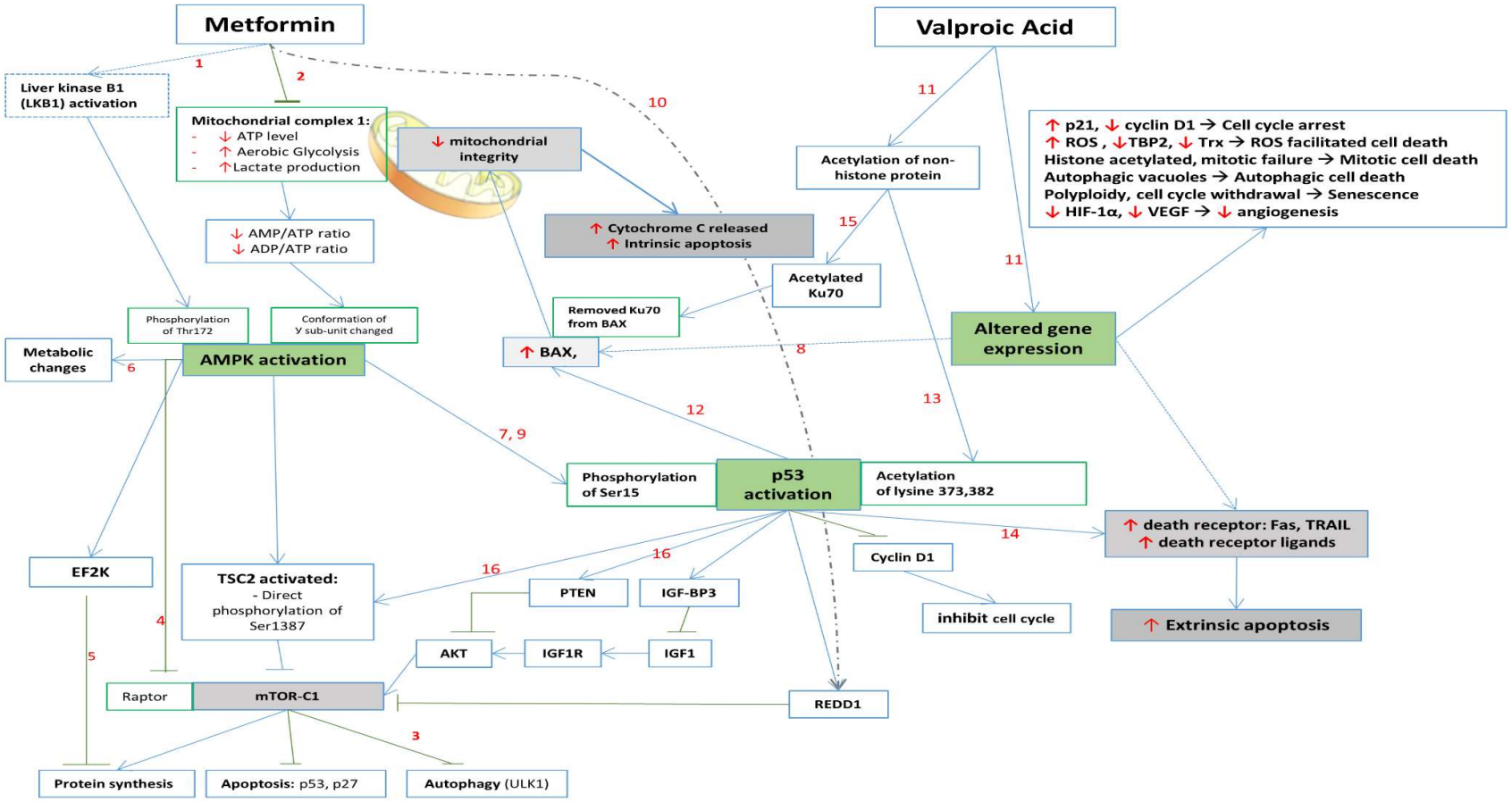
Metformin
Valproic Acid
Liver kinase B1 (LKB1) activation
Mitochondrial complex 1:
- ↓ ATP level
- ↑ Aerobic Glycolysis
- ↑Lactate production
↓ mitochondrial integrity
↓ AMP/ATP ratio
↓ ADP/ATP ratio
↑ Cytochrome C released
↑ Intrinsic apoptosis
Acetylation of non-histone protein
↑ p21, ↓ cyclin D1 → Cell cycle arrest
↑ ROS , ↓TBP2, ↓ Trx → ROS facilitated cell death
Histone acetylated, mitotic failure → Mitotic cell death
Autophagic vacuoles → Autophagic cell death
Polyploidy, cell cycle withdrawal → Senescence
↓ HIF-1α, ↓ VEGF → ↓ angiogenesis
Acetylated Ku70
Removed Ku70 from BAX
Phosphorylation of Thr172
Conformation of γ sub-unit changed
Metabolic changes
AMPK activation
↑ BAX,
Altered gene expression
Phosphorylation of Ser15
p53 activation
Acetylation of lysine 373,382
↑ death receptor: Fas, TRAIL
↑ death receptor ligands
Cyclin D1
inhibit cell cycle
↑ Extrinsic apoptosis
EF2K
TSC2 activated:
- Direct phosphorylation of Ser1387
PTEN
IGF-BP3
AKT
IGF1R
IGF1
Raptor
mTOR-C1
REDD1
Protein synthesis
Apoptosis: p53, p27
Autophagy (ULK1)
1
2
3
4
5
6
7, 9
8
10
11
12
13
14
15
16

Figure 5-1. Proposed mechanism of MET+VPA induction of intrinsic apoptosis via p53 activation and mitochondrial inhibition.

MET can inhibit the activity of mitochondrial complex 1 which alters the AMP/ATP ratio. This change can activate AMPK which phosphorylates p53 at Ser15 and leads to p53-dependent cell death. As a non-specific HDACi, VPA causes protein acetylation, including at lysine residues 373 and 382 of p53. By combining MET and VPA, increased p53 protein activation can occur through phosphorylation of p53 at different sites driving p53-dependent cell apoptosis via the intrinsic pathway, as evidenced by release of cytochrome c into the cytoplasm. MET+VPA induces intrinsic apoptosis via p53 activation and mitochondrial inhibition. The numbers in the figure correspond to the following literature: ***1.*** *Xie et al. (2008);* ***2.*** *Shaw et al. (2005), Wheaton et al. (2014).* ***3.*** *Shi et al. (2012);* ***4.*** *Gwinn et al. (2008);* ***5 and 6.*** *Hardie et al. (2003);* ***7.*** *Cerezo et al. (2013);* ***8.*** *Ko et al. (1996);* ***9.*** *Jones et al. (2006);* ***10.*** *Ben Sahra et al. (2011);* ***11.*** *Xu et al. (2007);* ***12.*** *Chipuk et al. (2004)****; 13.*** *Condorelli et al. (2008);* ***14.*** *Bennett et al. (1998), Waring et al. (1999), Muller et al. (1998), Owen et al. (1995), Nagata et al. (1995);* ***15.*** *Minucci et al. (2006).* ***16.*** *Feng et al. (2007). →: activation pathway; ⊥: inhibition pathway.*

5.2. Intact AR signalling is required for synergistic apoptosis in response to MET+VPA

ADT can delay the progression of hormone-sensitive PCa at the advanced stage. The present study demonstrated that MET+VPA reduced proliferation and increased apoptosis in patient-derived tumour explants which had normal AR expression. In the present *in vitro* study, MET, when used alone, was found to enhance Enzalutamide-induced apoptosis (Enzalutamide is a second-generation AR antagonist) in androgen-sensitive LNCaP cells. This finding agrees with the reports of Li, Y et al. (2013) and Tran et al. (2009). Blocking the AR signalling pathway impairs the effectiveness of aerobic glucose metabolism in PCa cells, causing them to be more susceptible to MET as the result of interrupting the ATP/AMP ratio as well as preventing glucose recruitment into oxidative phosphorylation processes. MET has also been shown to inhibit mTOR which can further inhibit cell anabolism in the absence of the AR signalling pathway (Xu, Y et al. 2006). VPA, combined with Enzalutamide, also induced more apoptosis than VPA alone. VPA conducts the acetylation of AR directly or indirectly through Tip60, therefore maintaining AR transcriptional activity (Gaughan et al. 2002). Also Xia et al. (2006) found that VPA can recover androgen responsiveness in CRPC, therefore increasing the apoptotic response to Enzalutamide.

However, the present findings demonstrated that the addition of Enzalutamide in LNCaP cells reduced apoptosis in response to 2.5 mM MET+VPA, suggesting that the AR signalling pathway may be important in the synergistic apoptosis response to MET+VPA. There was no significant change at 1 mM MET+VPA. It is possible that 1 mM MET+VPA is inducing the same biological

pathways as at 2.5 mM and which are interacting with the AR signalling pathway, but is below the level of detection for a synergistic response in the current assay at 1 mM. Normal epithelial prostate cells (PrEC) were also studied here which do not exhibit AR expression (Sobel, Richard E et al. 2006). The absence of AR expression may have contributed to the lack of a significant inhibitory effect in response to MET+VPA. Another potential mechanism could involve a p53 - AR interaction which has recently been reported via AR cofactor WDR777 interacting with p53 to form the p53-WDR77-AR complex, thus enhancing the activity of AR (Kumari et al. 2016). However, it is not clear if MET+VPA has an effect on the p53-WDR77-AR complex in PCa cells. Therefore, further investigation on the protein-protein and protein-DNA interaction using co-immunoprecipitation (Co-IP) and chromatin immunoprecipitation (ChIP) could help to explore the interaction and the location of DNA-binding of these proteins.

5.3. MET+VPA synergistically inhibits proliferation of PCa cells regardless of p53 status

p53 activation can induce an anti-proliferative effect in response to MET+VPA via enhancing the expression of AMPK β1 and TSC2 which are mTOR inhibitors (Feng et al. 2007) (Figure 5-1). In the present *in vitro* and *in vivo* studies, MET+VPA synergistically inhibited PC-3 ($p53^-$) and LNCaP ($p53^+$) cell growth, which was supported by responses in *ex vivo* PCa explants. Additionally, MET+VPA significantly reduced the IC_{50} of proliferation in PCa cell lines LNCaP and PC-3. These findings suggest a p53-independent mechanism responsible for the antiproliferative effect of MET+VPA. MET is an mTOR inhibitor via AMPK activation (Bolster et al. 2002; Hardie 2003; Long et

al. 2006) and VPA can also target mTOR activity. The combination of RAD001, an mTOR inhibitor via Akt-p70S6k phosphorylation, and VPA further increased the expression of p21 and p27 targeting in the cell cycle. This combination also showed additive effects on migratory and invasive behaviour, but not on tumour endothelium and tumour matrix interaction (Wedel, Hudak, Seibel, Juengel, Tsaur, et al. 2011). Current evidence supports further investigation on the inhibitory effect of MET+VPA on mTOR in PCa cell lines and in other cancer cell types such as breast, colon, pancreas, and leukaemia.

5.4. MET+VPA selectively affects cancer cells and potentially protects from kidney and liver toxicity

In the present study, MET+VPA induced a synergistic anti-proliferation effect in PCa *in vitro*, *in vivo*, and *ex vivo*, however there was no significantly greater effect of MET+VPA compared to MET or VPA alone in PrEC cells. The major sites of MET and VPA metabolism are the kidney and liver, respectively, and hence MET has the potential to cause kidney damage and VPA has the potential to cause liver damage. However MET has been demonstrated to prevent alcohol-induced liver injury *in vivo* (Bergheim et al. 2006), while VPA can prevent the onset of kidney damage (glomerulosclerosis and proteinuria) (Van Beneden et al. 2011), suggesting that MET could reduce side effects of VPA and vice versa. No change in weight or histology of kidney and liver was observed in nude mice treated with MET, VPA, or MET+VPA in this study. However it is possible that any minor damage may have been counteracted by the combination.

5.5. Potential personalised application of MET+VPA as a cancer treatment based on present findings and current understanding

Personalised PCa treatment could be based on those molecules which are changed during the progression of PCa including p53, AR, PTEN, and ETS gene fusions.

PTEN loss ranges from 40% in primary PCa to 70% in metastatic PCa (El Sheikh et al. 2008; Reid et al. 2010; Taylor et al. 2010). PTEN controls the activation of the PI3k/Akt signalling pathway, which normally inhibits mTOR activation (Wu, X et al. 1998). The PCa cell lines, LNCaP and PC-3, used in this study, both lack PTEN, whereas normal prostate epithelial cells are $PTEN^{+}$. The expression of PTEN was not verified in the human prostate explants used here. MET+VPA inhibited cell proliferation in the $PTEN^{-}$ LNCaP and PC-3 cells, possibly due to MET+VPA co-targeting mTOR, suggesting that $PTEN^{-}$ patients may obtain benefit from MET+VPA. Further investigation of the role of *PTEN*, such as *PTEN* knock-down and insertion of *PTEN* into cancer cells, in the presence or absence of mTOR inhibitors, is needed to elucidate the role of PTEN in the response of PCa cells to MET+VPA.

ERG fusion positive PCa cells have altered metabolism, resulting in increased glucose uptake through neuropeptide Y expression (Massoner et al. 2013) and increased histone deacetylase activity (Björkman et al. 2008). Therefore, the combination of MET, a hypoglycaemic agent, and VPA, an HDACi, is a potential therapeutic candidate to counteract the effects of ERG over-expression. Understanding the interaction between PTEN loss, ERG over-expression, and MET+VPA response could provide useful information for clinical application as the combination of PTEN loss and TMPRSS2-ERG gene

fusion can increase the aggressiveness of disease with worse prognosis and early biochemical failure (Carver et al. 2009; Reid et al. 2010).

The combination of MET and VPA was shown to be more effective than either drug alone in the present study. Although the mechanism of MET+VPA is not fully elucidated, the combination of the drugs appears to be relatively non-toxic, and showing promising results in the presence and absence of p53 and AR and therefore may possibly be valuable in the range of stages of the disease. Based on the results presented here and the current understanding of the roles of p53, AR, and ETS gene fusions, clinical application of MET+VPA is projected to be useful in: **(1) Primary PCa and metastatic PCa where p53 and AR are still intact:** In PCa, p53 mutations occur in approximately 4% of primary PCa at local stage and approximately 23% at advanced stage (Bookstein et al. 1993), increasing to 53% in metastatic PCa (Robinson et al. 2015). Localised PCa rarely has abnormal AR status in the primary tumour (Marcelli et al. 2000), but AR mutations occur in 62.7% of metastatic PCa (Robinson et al. 2015). Therefore, patients with local stage PCa (≤ T2cNoMo or stage B) could benefit most from MET+VPA. For metastatic PCa, MET+VPA could also target more than two-thirds of the primary PCa and nearly half of the metastatic PCa which harbors normal p53. Although AR mutations are at high frequency in metastatic CRPC, MET+VPA could still be useful if the AR signalling is still intact such as in hypersensitive AR, promiscuous AR, and outlaw AR (Feldman et al. 2001). **(2) Advanced PCa with p53 and/or AR mutations**: Confirmation that MET+VPA therapy is indeed p53- and AR-dependent could provide a basis for individualised patient therapy in future clinical trials. MET+VPA reduced cell proliferation in PC-3 cells which has no

p53 nor AR expression, suggesting that MET+VPA can reduce cancer proliferation but not apoptosis independently of p53 and AR expression. Therefore, MET+VPA can still, potentially, provide a useful therapy in an advanced stage of PCa where p53 and AR mutations have occurred. **(3) Potentially useful in selective CRPC and ETS gene fusion**: The findings presented in this thesis suggest that the addition of ADT to MET+VPA would not increase apoptosis. However, this study tested MET+VPA and Enzalutamide, an AR inhibitor, in only 2 cell lines (LNCaP with AR^+ and PC-3 with AR^-) which is not sufficient to conclude the effectiveness of MET+VPA in CRPC. Also, ETS gene fusions (ERG overexpression), a poor prognostic factor, occurring in 56.7% of PCa (Robinson et al. 2015), are down-regulated by VPA and inhibit p53 activity via CBP/p300 inhibition which could be counteracted by MET+VPA, resulting in the potential of such cancers to respond to MET+VPA. Further investigation on the role of ERG overexpression, by knock down of ERG in ERG overexpressed PCa cell lines (VCaP and DuCaP) and insertion of ETS fusion (TMPRSS2-ERG fusion) in ERG^- PCa cell lines, may help to elucidate the potential role of ERG in response to MET+VPA.

As both MET and VPA are currently used for non-cancer indications with established toxicity profiles, repurposing of these drugs could be rapidly integrated into clinical use to potentially benefit treatment of various PCa stages after appropriately conducted clinical trials. MET+VPA could be trialled in active surveillance PCa, neo-adjuvant therapy in high-risk localised PCa, adjuvant therapy before or after ADT, and used alone or in combination with other chemotherapy in CRPC. Although current evidence does not support

MET+VPA with hormonal therapy, MET+VPA could be used before going to hormonal therapy or even after hormonal therapy, as it might delay the progression to CRPC (Figure 5-2). An early phase I clinical trial using the MET+VPA as neoadjuvant therapy prior to radical prostatectomy has recently been commenced based on the data presented in this thesis (ACTRN 12616001021460).

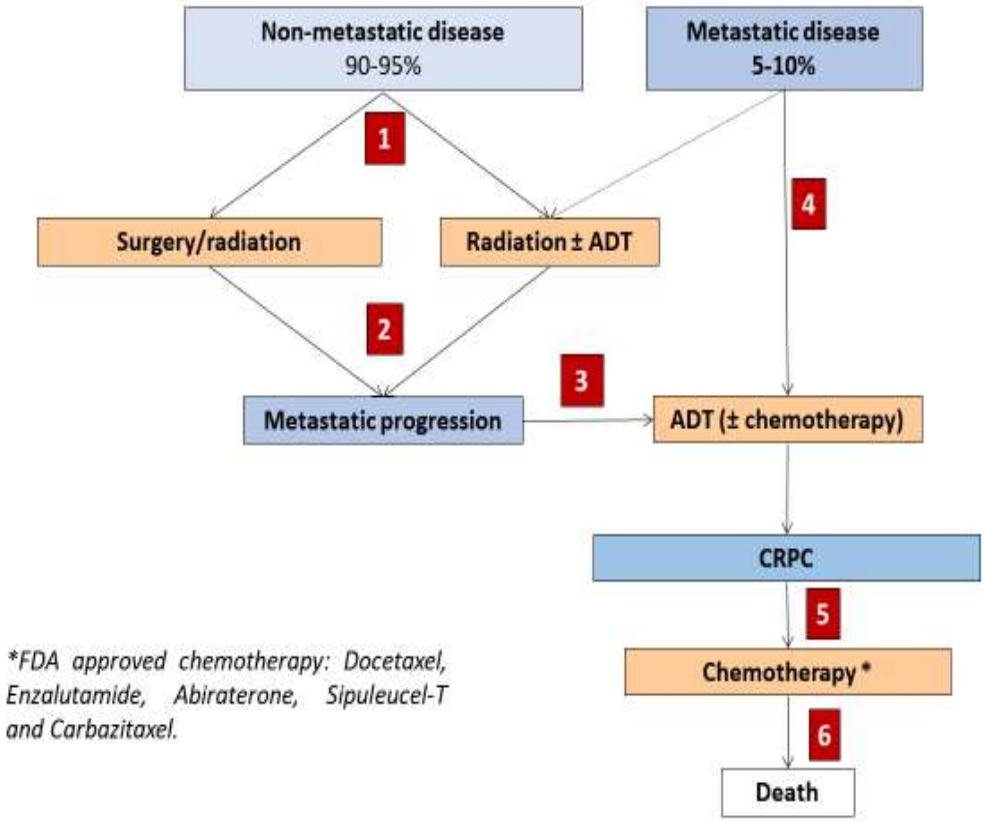

Figure 5-2. Potential clinical application of MET+VPA for PCa treatment according to the stage of disease.

(1) MET+VPA could be used before radical treatment for high risk localised PCa as a neoadjuvant therapy. (2) and (3) MET+VPA could be used after radical treatment or radiation ± ADT where there is evidence of high-risk disease. (4) MET+VPA could be used before ADT for metastatic PCa at the time of diagnosis. MET+VPA could be used before (5) or after (6) standard chemotherapy for CRPC which has developed after long-term ADT (ADT = androgen deprivation therapy).

In summary, the findings *in vitro*, *in vivo*, and *ex vivo* presented in this thesis indicate that the combination of MET and VPA may be a useful and relatively non-toxic systemic therapy for non-metastatic stage disease with greater efficacy in the presence of p53 and AR signalling. As both drugs are currently used for non-cancer indications, repurposing of these drugs could be rapidly integrated into clinical use to potentially benefit various stages of PCa. Future studies investigating the effect of MET+VPA in different cancer types such as kidney, breast, colon, brain, and the mechanism of their response is warranted. Future clinical trials could be conducted in high-risk localised PCa or in CRPC where the efficacy of current therapies is limited.

APPENDIX A: SOLUTIONS AND BUFFERS

All chemicals were reagent or analytical grade.

Metformin stock solution (100 mM)

Weigh 100 mg of metformin hydrochloride (Sigma)

Add 6.038 mL water

Vortex until complete solubilisation

Filter the solution into a sterile tube using a 0.22 µm filter membrane

Prepare 1 mL aliquots and store stock solution at -20°C.

Valproic acid stock solution (100 mM)

Weigh 100 mg of valproic acid sodium salt (Sigma)

Add 6.017 mL water

Vortex until complete solubilisation

Filter the solution into a sterile tube using a 0.22 µm filter membrane

Prepare 1 mL aliquots and store stock solution at -20°C.

Agarose gel electrophoresis

TAE buffer (50X)

Tris-base: 242 g

Acetate (100% acetic acid): 57.1 mL

EDTA: 100 mL 0.5M sodium EDTA

Add *Milli*-Q *water (*Milli-Q®*)* up to one litre

To make 1X TAE from 50X TAE stock, dilute 20 mL of stock into 980 mL of *Milli Q* water

Adjust pH to 8.3.

1% agarose gel

1% (w/v) of agarose (Scientifix, Australia) in 1 x TAE buffer.

Western blot

RIPA buffer recipe

(adapted from ThermoFisher)

25 mM Tris-HCl

150 mM NaCl

1% NP-40

1% sodium deoxycholate

0.1% SDS

Adjust pH to 7.6.

Running buffer (1X)

25 mM Tris

192 mM glycine

0.1% SDS.

Sample buffer (2X)

62.5 mM Tris-HCl

2% SDS

25% (v/v) glycerol

0.01% bromophenol blue

5% β-mercaptoethanol

Adjust pH to 6.8.

Sample buffer (4X)

250 mM Tris-HCl

4% SDS

40% (w/v) glycerol

0.02% bromophenol blue

15% beta-mercaptoethanol

Adjust pH to 6.8.

Transfer buffer (1X)

0.025 M Tris

0.192 M Glycine

20% Methanol

0.05% SDS

Tris buffered solution (TBS) (10X)

0.154 M Trizma HCl

1.37 M NaCl

Adjust pH to 7.6.

TBS-Tween (TBS-T) (1X)

1 x TBS solution

0.1% Tween-20

Phosphate buffer saline (PBS) (10X)

25.6 g $Na_2HPO_4 \cdot 7H_2O$

80 g NaCl

2 g KCl

2 g KH_2PO_4

Bring to 1 litre with *Milli*-Q water.

PBS-Tween (PBS-T) (1X)

1 x PBS solution

0.1% Tween-20.

Immunocytochemistry

Aqueous formaldehyde preparation

4 g paraformaldehyde

1 litre PBS

Heat the solution to 57°C while stirring with a magnetic stir bar until fully dissolved

Stock formaldehyde fixative (4%) was stored at 4°C.

Blocking solution

3% BSA in 1X PBS.

Plasmid transfection

Luria broth (LB) medium

To make 400 mL of LB

4 g NaCl

4 g Tryptone (Difco Laboratories, #0123-01-1)

2 g yeast extract (Oxoid, #X589B)

Add water to 400 mL

The solution was autoclaved and allowed to cool to room temperature.

LB agar plates

To make 500 mL of LB agar

5 g NaCl

5 g Tryptone (Difco Laboratories, #0123-01-1)

2.5 g Yeast extract (Oxoid, #X589B)

7.5 g Bacto-Agar (Difco, #0140-01)

Add water to 500 mL

The solution was autoclaved and allowed to cool to room temperature. To use, the solution was warmed to 55°C, then poured into a sterile agar plate.

Glycerol (50%) solution

Add 25 mL glycerol to 25 mL *Milli-Q* water

Autoclave

Store at room temperature.

Haematoxylin – eosin (H & E) staining

APES treatment of slides

2% (v/v) aminopropylethoxysilane (APES) was prepared in absolute ethanol. Glass slides were immersed and rinsed for 10 seconds in 100% ethanol, then immersed in APES for 5 mins. The slides were washed twice in distilled water, then allowed to dry and stored in a dust-free container.

Acid ethanol

160 mL 100% Ethanol

75 mL water

2.5 mL concentrated HCL (fume hood).

Ammonia water

Prepare in a fume hood

250 mL water

0.15 mL ammonia (fume hood).

APPENDIX B: GFP-P53 PLASMID

A

TAAAGATACCAGGCGTTTCCCCCTGGAAGCTCCCTCGTGCGCTCTCCTGTTCCGACCCTGCCGCTTACCGGATACCTGTCCGCCTTTCTCCCTTCGGGAAGCGTGGCGCTTTCTCATAGCTCACGCTGTAGGTATCTCAGTTCGGTGTA
GGTCGTTCGCTCCAAGCTGGGCTGTGTGCACGAACCCCCCGTTCAGCCCGACCGCTGCGCCTTATCCGGTAACTATCGTCTTGAGTCCAACCCGGTAAGACACGACTTATCGCCACTGGCAGCAGCCACTGGTAACAGGATTAGCAGA
GCGAGGTATGTAGGCGGTGCTACAGAGTTCTTGAAGTGGTGGCCTAACTACGGCTACACTAGAAGAACAGTATTTGGTATCTGCGCTCTGCTGAAGCCAGTTACCTTCGGAAAAAGAGTTGGTAGCTCTTGATCCGGCAAACAAACCAC
CGCTGGTAGCGGTGGTTTTTTTGTTTGCAAGCAGCAGATTACGCGCAGAAAAAAAGGATCTCAAGAAGATCCTTTGATCTTTTCTACGGGGTCTGACGCTCAGTGGAACGAAAACTCACGTTAAGGGATTTTGGTCATGAGATTATCAAAA
AGGATCTTCACCTAGATCCTTTTAAATTAAAAATGAAGTTTTAAATCAATCTAAAGTATATATGAGTAACCTGAGGCTATGGCAGGGCCTGCCGCCCCGACGTTGGCTGCGAGCCCTGGGCCTTCACCCGAACTTGGGGGGTGGGGTGG
GGAAAAGGAAGAAACGCGGGCGTATTGGCCCCAATGGGGTCTCGGTGGGGTATCGACAGAGTGCCAGCCCTGGGACCGAACCCCGCGTTTATGAACAAACGACCCAACACCGTGCGTTTTATTCTGTCTTTTTATTGCCGTCATAGCG
CGGGTTCCTTCCGGTATTGTCTCCTTCCGTGTTTCAGTTAGCCTCCCCCTAGGGTGGGCGAAGAACTCCAGCATGAGATCCCCGCGCTGGAGGATCATCCAGCCGGCGTCCCGGAAAACGATTCCGAAGCCCAACCTTTCATAGAAGG
CGGCGGTGGAATCGAAATCTCGTGATGGCAGGTTGGGCGTCGCTTGGTCGGTCATTTCGAACCCCAGAGTCCCGCTCAGAAGAACTCGTCAAGAAGGCGATAGAAGGCGATGCGCTGCGAATCGGGAGCGGCGATACCGTAAAGCA
CGAGGAAGCGGTCAGCCCATTCGCCGCCAAGCTCTTCAGCAATATCACGGGTAGCCAACGCTATGTCCTGATAGCGGTCCGCCACACCCAGCCGGCCACAGTCGATGAATCCAGAAAAGCGGCCATTTTCCACCATGATATTCGGCAA
GCAGGCATCGCCATGGGTCACGACGAGATCCTCGCCGTCGGGCATGCTCGCCTTGAGCCTGGCGAACAGTTCGGCTGGCGCGAGCCCCTGATGCTCTTCGTCCAGATCATCCTGATCGACAAGACCGGCTTCCATCCGAGTACGTGC
TCGCTCGATGCGATGTTTCGCTTGGTGGTCGAATGGGCAGGTAGCCGGATCAAGCGTATGCAGCCGCCGCATTGCATCAGCCATGATGGATACTTTCTCGGCAGGAGCAAGGTGAGATGACAGGAGATCCTGCCCCGGCACTTCGCC
CAATAGCAGCCAGTCCCTTCCCGCTTCAGTGACAACGTCGAGCACAGCTGCGCAAGGAACGCCCGTCGTGGCCAGCCACGATAGCCGCGCTGCCTCGTCTTGCAGTTCATTCAGGGCACCGGACAGGTCGGTCTTGACAAAAAGAAC
CGGGCGCCCCTGCGCTGACAGCCGGAACACGGCGGCATCAGAGCAGCCGATTGTCTGTTGTGCCCAGTCATAGCCGAATAGCCTCTCCACCCAAGCGGCCGGAGAACCTGCGTGCAATCCATCTTGTTCAATCATGCGAAACGATCC
TCATCCTGTCTCTTGATCGATCTTTGCAAAAGCCTAGGCCTCCAAAAAAGCCTCCTCACTACTTCTGGAATAGCTCAGAGGCCGAGGCGGCCTCGGCCTCTGCATAAATAAAAAAAATTAGTCAGCCATGGGGCGGAGAATGGGCGGAA
CTGGGCGGAGTTAGGGGCGGGATGGGCGGAGTTAGGGGCGGGACTATGGTTGCTGACTAAATTGAGATGCATGCTTTGCATACTTCTGCCTGCTGGGGAGCCTGGGGACTTTCCACACCTGGTTGCTGACTAATTGAGATGCATGCTT
TGCATACTTCTGCCTGCTGGGGAGCCTGGGGACTTTCCACACCCTAACTGACACACATTCCACAGCTGGTTCTTTCCGCCTCAGGACTCTTCCTTTTTCAATATTATTGAAGCATTTATCAGGGTTATTGTCTCATGAGCGGATACATATTT
GAATGTATTTAGAAAAATAAACAAATAGGGGTTCCGCGCACATTTCCCCGAAAAGTGCCACCTGACGCGCCCTGTAGCGGCGCATTAAGCGCGGCGGGTGTGGTGGTTACGCGCAGCGTGACCGCTACACTTGCCAGCGCCCTAGCG
CCCGCTCCTTTCGCTTTCTTCCCTTCCTTTCTCGCCACGTTCGCCGGCTTTCCCCGTCAAGCTCTAAATCGGGGGCTCCCTTTAGGGTTCCGATTTAGTGCTTTACGGCACCTCGACCCCAAAAAACTTGATTAGGGTGATGGTTCACGT
AGTGGGCCATCGCCCTGATAGACGGTTTTTCGCCCTTTGACGTTGGAGTCCACGTTCTTTAATAGTGGACTCTTGTTCCAAACTGGAACAACACTCAACCCTATCTCGGTCTATTCTTTTGATTTATAAGGGATTTTGCCGATTTCGGCCTA
TTGGTTAAAAAATGAGCTGATTTAACAAAAATTTAACGCGAATTTTAACAAAATATTAACGCTTACAATTTACGCCTTAAGATACATTGATGAGTTTGGACAAACCACAACTAGAATGCAGTGAAAAAAATGCTTTATTTGTGAAATTTGTGAT
GCTATTGCTTTATTTGTAACCATTATAAGCTGCAATAAACAAGTTAACAACAACAATTGCATTCATTTTATGTTTCAGGTTCAGGGGGAGGTGTGGGAGGTTTTTTAAAGCAAGTAAAACCTCTACAAATGTGGTATGGCTGATTATGATCTA
GAGTCGCGGCCGCTTTACTTGTACAGCTCGTCCATGCCGAGAGTGATCCCGGCGGCGGTCACGAACTCCAGCAGGACCATGTGATCGCGCTTCTCGTTGGGGTCTTTGCTCAGGGCGGACTGGGTGCTCAGGTAGTGGTTGTCGGGC
AGCAGCACGGGGCCGTCGCCGATGGGGGTGTTCTGCTGGTAGTGGTCGGCGAGCTGCACGCTGCCGTCCTCGATGTTGTGGCGGATCTTGAAGTTCACCTTGATGCCGTTCTTCTGCTTGTCGGCCATGATATAGACGTTGTGGCTG
TTGTAGTTGTACTCCAGCTTGTGCCCCAGGATGTTGCCGTCCTCCTTGAAGTCGATGCCCTTCAGCTCGATGCGGTTCACCAGGGTGTCGCCCTCGAACTTCACCTCGGCGCGGGTCTTGTAGTTGCCGTCGTCCTTGAAGAAGATGGT
GCGCTCCTGGACGTAGCCTTCGGGCATGGCGGACTTGAAGAAGTCGTGCTGCTTCATGTGGTCGGGGTAGCGGCTGAAGCACTGCACGCCGTAGGTCAGGGTGGTCACGAGGGTGGGCCAGGGCACGGGCAGCTTGCCGGTGGTG
CAGATGAACTTCAGGGTCAGCTTGCCGTAGGTGGCATCGCCCTCGCCCTCGCCGGACACGCTGAACTTGTGGCCGTTTACGTCGCCGTCCAGCTCGACCAGGATGGGCACCACCCCGGTGAACAGCTCCTCGCCCTTGCTCACCATG
GTGGCGACCGGTGGATCCCGGTCTGAGTCAGGCCCTTCTGTCTTGAACATGAGTTTTTTATGGCGGGAGGTAGACTGACCCTTTTTGGACTTCAGGTGGCTGGAGTGAGCCCTGCTCCCCCCTGGCTCCTTCCCAGCCTGGGCATCCT
TGAGTTCCAAGGCCTCATTCAGCTCTCGGAACATCTCGAAGCGCTCACGCCCACGGATCTGAAGGGTGAAATATTCTCCATCCAGTGGTTTCTTCTTTGGCTGGGGAGAGGAGCTGGTGTTGTTGGGCAGTGCTCGCTTAGTGCTCCCT
GGGGGCAGCTCGTGGTGAGGCTCCCCTTTCTTGCGGAGATTCTCTTCCTCTGTGCGCCGGTCTCTCCCAGGACAGGCACAAACACGCACCTCAAAGCTGTTCCGTCCCAGTAGATTACCACTGGAGTCTTCCAGTGTGATGATGGTGA
GGATGGGCCTCCGGTTCATGCCGCCCATGCAGGAACTGTTACACATGTAGTTGTAGTGGATGGTGGTACAGTCAGAGCCAACCTCAGGCGGCTCATAGGGCACCACCACACTATGTCGAAAAGTGTTTCTGTCATCCAAATACTCCACA
CGCAAATTTCCTTCCACTCGGATAAGATGCTGAGGAGGGGCCAGACCATCGCTATCTGAGCAGCGCTCATGGTGGGGGCAGCGCCTCACAACCTCCGTCATGTGCTGTGACTGCTTGTAGATGGCCATGGCGCGGACGCGGGTGCCG
GGCGGGGGTGTGGAATCAACCCACAGCTGCACAGGGCAGGTCTTGGCCAGTTGGCAAAACATCTTGTTGAGGGCAGGGGAGTACGTGCAAGTCACAGACTTGGCTGTCCCAGAATGCAAGAAGCCCAGACGGAAACCGTAGCTGCC
CTGGTAGGTTTTCTGGGAAGGGACAGAAGATGACAGGGGCCAGGAGGGGGCTGGTGCAGGGGCCGCCGGTGTAGGAGCTGCTGGTGCAGGGGCCACGCGGGGAGCAGCCTCTGGCATTCTGGGAGCTTCATCTGGACCTGGGTCT
TCAGTGAACCATTGTTCAATATCGTCCGGGGACAGCATCAAATCATCCATTGCTTGGGACGGCAAGGGGGACAGAACGTTGTTTTCAGGAAGTAGTTTCCATAGGTCTGAAAATGTTTCCTGACTCAGAGGGGGCTCGACGCTAGGATC
TGACTGCGGCTCCTCCATCTGCAGAATTCGAAGCTTGAGCTCGAGATCTGAGTCCGGTAGCGCTAGCGGATCTGACGGTTCACTAAACCAGCTCTGCTTATATAGACCTCCCACCGTACACGCCTACCGCCCATTTGCGTCAATGGGGC
GGAGTTGTTACGACATTTTGGAAAGTCCCGTTGATTTTGGTGCCAAAACAAACTCCCATTGACGTCAATGGGGTGGAGACTTGGAAATCCCCGTGAGTCAAACCGCTATCCACGCCCATTGATGTACTGCCAAAACCGCATCACCATGGT
AATAGCGATGACTAATACGTAGATGTACTGCCAAGTAGGAAAGTCCCATAAGGTCATGTACTGGGCATAATGCCAGGCGGGCCATTTACCGTCATTGACGTCAATAGGGGGCGTACTTGGCATATGATACACTTGATGTACTGCCAAGTG
GGCAGTTTACCGTAAATACTCCACCCATTGACGTCAATGGAAAGTCCCTATTGGCGTTACTATGGGAACATACGTCATTATTGACGTCAATGGGCGGGGGTCGTTGGGCGGTCAGCCAGGCGGGCCATTTACCGTAAGTTATGTAACGC
GGAACTCCATATATGGGCTATGAACTAATGACCCCGTAATTGATTACTATTAATAACTAATGCATGGCGGTAATACGGTTATCCACAGAATCAGGGGATAACGCAGGAAAGAACATGTGAGCAAAAGGCCAGCAAAAGGCCAGGAACCGT
AAAAAGGCCGCGTTGCTGGCGTTTTTCCATAGGCTCCGCCCCCCTGACGAGCATCACAAAAATCGACGCTCAAGTCAGAGGTGGCGAAACCCGACAGGACTA

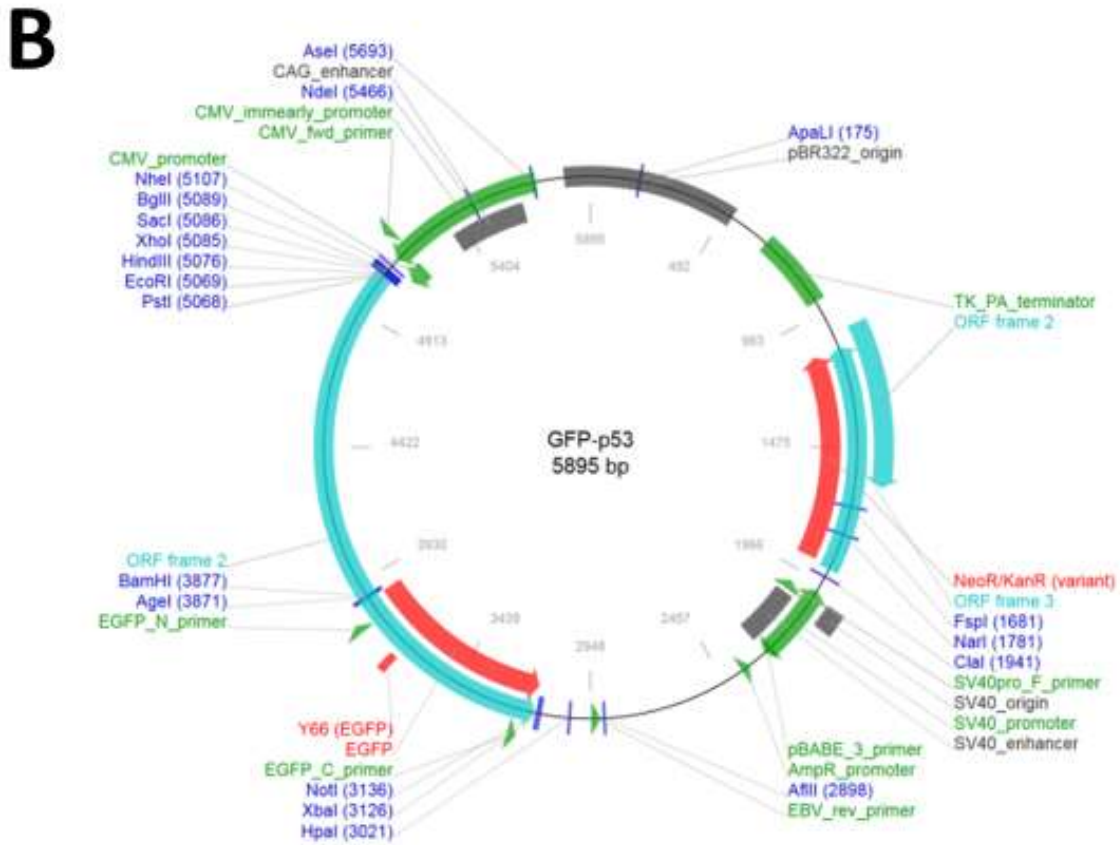

(A) *The sequence of GFP-p53 plasmid was confirmed by Addgene.* ***(B)*** *Structure of GFP-p53 plasmid and the location of digestion enzymes. (Adapted from* www.addgene.com*, accessed on 10/06/2016).*

APPENDIX C: HISTOLOGICAL SCORE FOR KIDNEY AND LIVER

Histological scoring for kidney

Score	Description
0	None or rather small foci of glomerular lesions.
1	Mild to moderate glomerular hypercellularity involving more than 50% of glomeruli.
2	Severe glomerular hypercellularity and hypertrophy involving almost all glomeruli.
3	Glomerular changes of 2 and cellular crescent formation involving more than 5% of glomeruli
4	Thrombotic changes of glomerular tufts with deposition of fibrinoid material involving more than 50% of glomeruli
5	Diffuse thrombotic changes of glomeruli and marked dilation of tubular lumina with epithelial flattening.

(taken from Chen, S-m et al. (2002)*)*

Histological scoring for liver

Score	Description
Portal fibrosis	
0	No Fibrosis.
1	Fibrous expansion of some portal areas, with or without short fibrous septa.
2	Fibrous expansion of most portal areas, with or without short fibrous septa.
3	Fibrous expansion of some portal areas, with occasional portal to portal (P-P) and/or portal to central (P-C) bridging.
4	Fibrous expansion of some portal areas with marked bridging (P-P as well as P-C).
5	Marked bridging (P-P and/or P-C) with occasional nodules (incomplete cirrhosis)
6	Cirrhosis, probable or definite.
Lobular Inflammation and Necrosis, Mallory Bodies, and Hepatocyte Ballooning (each scored individually 0-3)	
0	Absent.
1	Focal involvement of some globules.
2	Focal involvement of most globules.
4	Focal involvement of most or all globules, with diffuse involvement of some or most of the lobules.
Peri-sinusoidal Fibrosis	
0	Absent.
1	Perivenular and/or periportal involvement of some lobules.
2	Perivenular and/or periportal involvement of most lobules, without diffuse interstitial sinusoidal collagen deposition.
3	Perivenular and/or periportal involvement of most or all lobules, with diffuse interstitial fibrosis involving some or most of the lobules.
Fatty change	
1	< 5% liver cells involved
2	5-33% liver cells involved
3	34-66% liver cells involved
4	> 66% liver cells involved

(taken from Mendler et al. (2005)*)*

APPENDIX D: PUBLICATIONS ARISING DURING CANDIDATURE

Linh N.K. Tran, Ganessan Kichenadasse, Lisa M. Butler, Margaret M. Centenera, Katherine L. Morel, Rebecca J. Ormsby, Michael Z. Michael, Karen M. Lower, Pamela J. Sykes. The combination of metformin and valproic acid induces synergistic apoptosis in the presence of p53 and androgen signaling in PCa. Molecular Cancer Therapeutics, ISSN 1535-7163, 2017 *(in press, accepted for publication 11th July 2017)*.

Title:

The combination of metformin and valproic acid induces synergistic apoptosis in the presence of p53 and androgen signaling in prostate cancer.

Linh N.K. Tran[1], Ganessan Kichenadasse[1], Lisa M. Butler[3], Margaret M. Centenera[3], Katherine L. Morel[1], Rebecca J. Ormsby[1], Michael Z. Michael[1], Karen M. Lower[1,2], Pamela J. Sykes[1].

(1) Flinders Centre for Innovation in Cancer, Flinders University and Medical Centre, Bedford Park, Adelaide, South Australia.

(2) Molecular Medicine and Pathology, Flinders University and Medical Center, Bedford Park, Adelaide, South Australia.

(3) School of Medicine and Freemasons Foundation Centre for Men's Health, University of Adelaide, South Australian Health & Medical Research Institute (SAHMRI), Adelaide, South Australia.

Running title:

Metformin and valproic acid for prostate cancer treatment

Keywords: metformin, valproic acid, prostate cancer chemotherapy, androgen signaling pathway, enzalutamide, p53 protein, histone deacetylase inhibitor.

ABSTRACT

We investigated the potential of combining the hypoglycemic drug metformin (MET) and the anti-epileptic drug valproic acid (VPA), which act via different biochemical pathways, to provide enhanced anti-tumor responses in prostate cancer. Prostate cancer cell lines (LNCaP and PC-3), normal prostate epithelial cells (PrEC), and patient-derived prostate tumor explants were treated with MET and/or VPA. Proliferation and apoptosis were assessed. The role of p53 in response to MET+VPA was assessed in cell lines using RNA interference in LNCaP ($p53^+$) and ectopic expression of p53 in PC-3 ($p53^-$). The role of the androgen receptor (AR) was investigated using the AR antagonist, Enzalutamide. The combination of MET and VPA synergistically inhibited proliferation in LNCaP and PC-3, with no significant effect in PrEC. LNCaP, but not PC-3, demonstrated synergistic intrinsic apoptosis in response to MET+VPA. Knock-down of p53 in LNCaP ($p53^+$, AR^+) reduced the synergistic apoptotic response as did inhibition of AR. Ectopic expression of p53 in PC-3 ($p53^-$, AR^-) increased apoptosis in response to MET+VPA. In patient-derived prostate tumor explants, MET+VPA also induced a significant decrease in proliferation and an increase in apoptosis in tumor cells. In conclusion, we demonstrate that MET+VPA can synergistically kill more prostate cancer cells than either drug alone. The response is dependent on the presence of p53 and AR signaling which have critical roles in prostate carcinogenesis. Further *in vivo/ex vivo* pre-clinical studies are required to determine the relative efficacy of MET+VPA as a potential treatment for prostate cancer.

INTRODUCTION

Prostate cancer (PCa) is the most common cancer in men in the Western world (1, 2). Despite the curative potential of treatments such as radical prostatectomy and high dose radiotherapy, 20-30% of men will relapse after 5-10 years (3, 4). While reducing circulating hormone levels by androgen deprivation therapy (ADT) is the current standard treatment for metastatic disease, ADT inevitably fails with the emergence of castrate-resistant prostate cancer (CRPC), which is a lethal form of the disease. Mutations in *p53*, androgen receptor (*AR*), *PTEN*, and ETS gene fusions are commonly observed in CRPC (5). However, there is no durably effective targeted therapy for this stage of the disease. At present, FDA-approved treatments for CRPC consist of abiraterone acetate, enzalutamide, docetaxel, cabazitaxel, radium 223 and Sipuleucel-T, each of which only extend survival by a mean of 3-6 months (6-9).

Repurposing of commonly used drugs is an attractive approach for rapid development of new systemic cancer therapy options. Metformin and valproic acid have been trialed individually as anti-cancer drugs with varying success. The mechanisms of both drugs have been widely studied, and involve different molecular pathways suggesting that the combination of these drugs could have additive and possibly synergistic anti-cancer effects.

Metformin (MET; N', N-dimethylbiguanide) is widely used in diabetic patients as first-line therapy for control of blood glucose. Recent studies show pleiotropic beneficial effects of MET including reducing plasma lipid level and in cancer prevention (10). The anti-cancer mechanism of MET has been attributed to the inhibition of mammalian target of rapamycin (mTOR) activity via both direct (11) and indirect pathways (through adenosine monophosphate protein kinase (AMPK) activation) (12-14). One epidemiological study demonstrated that MET can reduce prostate cancer incidence by 37% after 7 years follow-up (15). A phase II clinical trial showed that MET also prolonged prostate-specific antigen (PSA) doubling time in progressive metastatic CRPC (16). However, the lack of a control arm, the use of a high dose of MET (1000 mg x 2 per day), and short treatment period (12 weeks) were limitations of this clinical study. On the contrary, in a case-control study, MET did not reduce the

incidence of PCa in the patients treated with MET for diabetes type II (17). This evidence suggests that MET alone is not effective in all subsets of PCa patients.

The antiepileptic drug, valproic acid (VPA) is a broad-range histone deacetylase inhibitor (HDACi) targeting HDAC class I (Ia, Ib) and class II (IIa) enzymes, and has been shown to have potential as an anti-cancer therapeutic. VPA has been shown to be responsible for a 20% overall change in the transcriptome in a tissue-dependent manner (18), having a marked effect on cellular activities which are important in cancer growth including cell cycle control, differentiation, DNA repair, and apoptosis (19-22). Besides its acetylation effect on histone proteins, VPA can also maintain the acetylation status of non-histone proteins such as Ku70 (23) and p53 (24), therefore further extending the time of protein activation. (25-27). A phase II clinical trial of 10 CRPC patients found that, although PSA levels in blood declined, no effect of the HDACi on disease progression was detected (28). This study had a small sample size and failed to achieve the optimal pharmacological level due to the toxicity of VPA which implies that VPA alone at an anti-cancer dose is not acceptable.

As both MET and VPA have limitations when used alone as anti-cancer agents, combinatorial therapy of MET and VPA could potentially be more effective than monotherapy as: (1) MET and VPA induce cell cycle arrest, and antiproliferative and proapoptotic effects via different mechanisms; (2) Lower doses of VPA and MET in combination could reduce the toxicity observed with higher doses of the single drugs; (3) Translation into the clinic would be rapid as MET and VPA are currently widely used drugs for non-cancer purposes.

There has been one report using MET and VPA in combination in clear cell renal cell carcinoma cell lines where synergistic antiproliferative and proapoptotic effects were observed but the mechanism of action was not reported (29). Here we demonstrate that the combination of MET and VPA induces at least an additive anti-tumor effect in prostate cancer cell lines and in human prostate tumor explants. Furthermore, we demonstrate that apoptosis induced by the combination of MET and VPA is dependent on the expression of p53 and AR, suggesting that the combination may be acting

through these pathways and could be particularly effective in tumors with functional p53 and AR.

MATERIALS AND METHODS

Cell lines and chemicals:

Authenticated human prostate cancer cell lines, LNCaP and PC-3, were newly obtained from the American Type Culture Collection (U.S.) in 2013 and Prostate Epithelial Cells (PrEC – CC2555) were newly obtained from Lonza (U.S.) in 2012, and cells were passaged for a maximum of 4 months. Metformin (PHR1084-500MG) and Valproic Acid (P4543-10G) were purchased from Sigma (U.S.) and stocks (100 mM) were made in distilled water and sterilized using a 0.22 µm filter. Enzalutamide (S1250) was purchased from Selleck Chemicals (U.S.), sterilized using a 0.22 µm filter and stored as a 5 mM stock in Dimethyl Sulfoxide (DMSO) (Sigma).

Cell culture:

Cancer cell lines were grown in RPMI 1640 medium supplemented with 100 Units/mL Penicillin, 100 µg/mL Streptomycin (ThermoFisher) and 5% Fetal Bovine Serum (FBS Lot No 1111A) from Bovogen (AU). When cells reached 90% confluence, they were passaged using 0.05% Trypsin/0.48 mM EDTA (ThermoFisher). PrEC were grown in Prostate Epithelial Cell Medium BulletKit® (Lonza - CC3166) containing Prostate Epithelial Cell Basal Medium and the following growth supplements for each 500 mL of media: 2 mL bovine pituitary extract; 0.5 mL hydrocortisone; 5 mL human epidermal growth factor; 0.5 mL epinephrine; 0.5 mL transferrin; 0.5 mL insulin; 0.5 mL retinoic acid; 0.5 mL triiodothyronine; 0.5 mL gentamicin-amphotericin B (GA-1000). PrEC were allowed to grow until 60-80% confluence and harvested using ReagentPack™ (Lonza-CC5034) following instructions from Lonza.

Cell proliferation and apoptosis in cell lines:

Cell proliferation was measured using an Incucyte® FLR imaging system (Essen BioScience) which analyzed the occupied area (% confluence) using live cell time-lapse imaging. Prostate cancer cell lines were seeded at 7000

cells/well (LNCaP) or 5000 cells/well (PC-3) in 96-well culture plates (Nunc 163320) in 100 µL/well RPMI 1640 with 5% FBS and allowed to grow overnight at 37^{o}C. The next day, fresh media containing a vehicle, MET alone, VPA alone, or MET and VPA in combination (1 mM or 2.5 mM of each drug) was added. The percentage of cell confluence was monitored every 2 hours for 3 days after treatment using the Incucyte® FLR – phase contrast mode.

The CellPlayer™ 96-well Kinetic Caspase 3/7 Apoptosis Assay Kit (Millennium Science, AU) containing NucView™ 488 fluorescence dye to identify activated caspase 3/7 in cells and the Incucyte® fluorescence mode was used to measure apoptosis every 2 hours for 3 days. At the end of day 3, the total number of cells was determined using Vybrant® DyeCycle™ Stain (ThermoFisher - V35004) and the percentage of apoptosis was calculated by dividing the number of cells undergoing apoptosis by the total cell number.

Cytochrome c analysis in mitochondrial and cytoplasmic cell fractions:

LNCaP and PC-3 cells were treated with either vehicle, MET, VPA or MET+VPA at 2.5 mM for 72 hours. Proteins from mitochondrial and cytoplasmic cell fractions were extracted using a Cell Fractionation Kit (Abcam Ab109719). Western blots were used to confirm the purity of cytoplasmic and mitochondrial fractions by measuring the presence of β-actin (Ab8227), pyruvate dehydrogenase subunit E1-α (PDH-E1-α), and ATP synthase subunit-α protein (CVα), as well as for detecting the release of cytochrome c from mitochondria to the cytoplasm (Ab110415). PDH-E1-α, CVα, and cytochrome c were probed simultaneously and β-actin was probed separately. Total protein expression in the stain-free gel (Biorad #4568124) was used as the loading control (30, 31). The level of cytochrome c expression was detected using a ChemiDoc™ MP system (BioRad) and normalized to total protein expression. The percentage of distribution of cytochrome c in the cytoplasm and mitochondria was calculated by dividing the expression of cytochrome c in the cytoplasm or mitochondria by the total expression of cytochrome c in the cytoplasmic and mitochondrial fractions.

TP53 RNA interference in LNCaP:

Small interference p53 siRNA (SignalSilence® #6231) and siRNA Control (SignalSilence® #6568) were transfected into the LNCaP cell line at a concentration of 25 nM using Lipofectamine® 2000 (ThermoFisher), according to the manufacturer's instructions. The transfection efficiency was validated by western blot using the Chemidoc™ MP system (Biorad) at 6 hours, 24 hours, 48 hours and 72 hours after transfection. Primary p53 antibody (Santa Cruz Biotechnology SC-126) binding was detected by horseradish peroxidase (HRP) secondary antibody using Clarity™ Western enhanced chemiluminescence (ECL) blotting substrate. β-actin primary antibody (Abcam ab8227) binding was detected by Alexa Fluor® 488 conjugated goat anti-rabbit IgG secondary antibody (ThermoFisher A-11008). Stain-free gel, 4X Laemmli Sample Buffer, Trans-Blot® Turbo™ RTA Mini PVDF Transfer kit (Biorad #1704247), and Precision Plus Protein™ Unstained Standards were purchased from Bio-Rad (AU). The EZQ® protein quantitation kit (Molecular Probes R33200) was used to quantitate protein concentration. The percentage of reduction in p53 expression was calculated using a ChemiDoc™ MP system (BioRad) and normalized to both β-actin and total protein.

Ectopic expression of p53 using plasmid transfection into PC-3:

PC-3 ($p53^{null}$) cells were grown in CellCarrier™ 96-microplates and allowed to reach 60-70% confluence before transfecting with 0.1 µg green fluorescence protein (GFP)-p53 plasmid (Addgene #12091) (32) or GFP-only plasmid transfection using Lipofectamine 3000® (ThermoFisher), according to the manufacturer's instructions. The GFP-only plasmid was made by relegation after removal of the p53 region from the GFP-p53 integrated plasmid using digestion enzymes BamHI and BglII (BioLab). Cell nuclei were then stained with *1,5-bis[[2-(dimethylamino)ethyl]amino]-4, 8-dihydroxyanthracene-9, 10-dione* (DRAQ5™) (Abcam ab108410) at 12 hours, 48 hours and 96 hours after transfection. Cells expressing p53/GFP were detected using green fluorescence (excitation band 460-490 nm and emission band 500-550 nm) on an Operetta® High Content Imaging System (PerkinElmer) and the total cell number was visualized using far-red fluorescence DRAQ5™ stain (excitation band 620-640 nm and emission band 650-760 nm). Transfection efficiency

was calculated by dividing the number of positive GFP cells by the number of total cells stained with DRAQ5™ (Harmony® High Content Imaging and Analysis Software, PerkinElmer).

Apoptosis of cells transfected with p53 plasmid:

Cells that were transfected with p53 plasmid were treated with vehicle, MET, VPA or MET+VPA (1 mM or 2.5 mM) 12 hours after transfection, and cultured for 3 days. Cells were first fixed with 4% formaldehyde and permeabilized with 0.5% Triton-X in phosphate-buffered saline (PBS), and then incubated with 3% Bovine Serum Albumin (Sigma) in PBS for 1 hour at room temperature. Cleaved-caspase 3 was labeled using anti-active caspase-3 primary antibody (Abcam – ab32042) and visualized with an Alexa Fluor 555 IgG (H+L) secondary antibody (Thermofisher – A21428). Cell nuclei were stained with DRAQ5™. The Operetta® and Harmony® Imaging systems were used to capture and analyze the images of cell cultures. Fluorescence intensity of cleaved caspase 3 was obtained using the Operetta® (excitation band 520-560 nm and emission band 560-630 nm). The emission and excitation bands of GFP and DRAQ5™ were the same as described above. Apoptosis was scored using mean fluorescent intensity of cleaved-caspase-3 (CC-3) in the nucleus. The cell apoptosis assay was optimized using PC-3 cells treated with 1 µM Paclitaxel (Abcam ab120143) for 72 hours in both the Operetta® High Content Imaging System (PerkinElmer) and the Incucyte® FLR imaging system (Essen BioScience) (Supplementary figure S1). Cell death was also investigated using Nuclear Fragmentation Index (NFI) which is the fluorescence intensity fluctuation of the nuclear stain (standard deviation/mean) (Supplementary figure S2A).

Treatment with Enzalutamide:

Androgen activation of the AR was chemically blocked in LNCaP (hormone sensitive) using Enzalutamide (S1250) (Selleckchem). AR inhibition efficiency was validated by determining the expression of prostate-specific antigen (PSA) on western blot using anti-PSA antigen (10679-1-AP - ProteinTech) at 24 hours, 72 hours and 96 hours. Cells were grown in 96-well culture plates and

treated with 1 μM Enzalutamide for 24 hours before treating with the vehicle, MET alone, VPA alone, or MET+VPA at 1 mM and 2.5 mM for 72 hours.

Combination Index (CI):

In order to validate the synergistic action of MET and VPA in combination, the drug combination index (CI) was calculated using at least 5 data points based on the Chou-Talalay method and CompuSyn software (33, 34). According to this method, a CI less than 0.9 indicates a synergistic effect of the combination, while a CI from 0.9 to 1.1 indicates an additive effect, and the combinatorial effect is antagonistic if the CI is more than 1.1 (34).

Explant culture of human prostate tumors.

Human ethics approval was obtained from the University of Adelaide Human Ethics Committee and the Southern Adelaide Clinical Human Research Ethics Committee. Fresh prostate cancer specimens were obtained with written informed consent from men undergoing robotic radical prostatectomy at St Andrew's Hospital, Adelaide, through the Australian Prostate Cancer BioResource. The prostatectomy specimens were sent for routine diagnostic pathology examination. Prior to fixing and paraffin embedding, small 6 mm cores of fresh tissue from regions of the prostatectomy specimen that exhibited gross tumor morphology were taken by a pathologist and made available for explant culture studies. Following explant culture, H&E staining for histological evaluation was performed on tissue from each treatment group, for every patient. A 6 mm core of tissue was dissected into 1 mm^3 pieces and cultured in triplicate on a pre-soaked gelatin sponge (Johnson and Johnson) in 24-well plates containing 500 μL RPMI 1640 with 10% FBS, antibiotic/antimycotic solution (Sigma), 0.01 mg/mL hydrocortisone, 0.01 mg/mL insulin (Sigma) (35). Tissues were treated by adding vehicle or MET (2.5 mM or 5 mM) and VPA (2.5 mM or 5 mM) to the culture medium. Tissues were cultured at 37°C for 48 hours and then formalin-fixed and paraffin embedded before being analyzed by immunohistochemistry for the proliferative marker Ki67 and apoptosis marker cleaved caspase-3 (CC-3).

Immunohistochemistry.

Paraffin-embedded explant tissue sections (2 μm) on SuperFrost-plus slides were de-paraffinized, rehydrated and blocked for endogenous peroxidase before being subjected to heat-induced epitope retrieval. Sections were blocked in 5% goat serum and incubated with Ki67 (DAKO) (1:200), cleaved caspase-3 (Abcam) (1:1000), and AR (1:1000) (Santacruz SC-816) primary antibodies followed by the appropriate secondary antibody (1:400), then developed using 3-3'-diaminobenzidine chromogen and counterstained with hematoxylin. Positive and negative controls were included in all runs. Images were captured with a Nanozoomer scanner (Hamamatsu, Japan). The proportion of Ki67 positive cells was calculated using the ImmunoRatio plugin in ImageJ (36). The proportion of CC-3 positive cells was counted using the Cell Counter plugin in ImageJ.

Statistical tests

Triplicate to quadruplicate samples were used in each *in vitro* experiment and experiments were repeated 2-3 times. Data are presented as mean ± SEM. The difference in the mean at single time points was calculated using an independent Student t-test or ANOVA test and for multiple time points was calculated using repeated measures ANOVA (RM-ANOVA) in IBM SPSS 23.0. Differences were considered significant when $p < 0.05$.

RESULTS

The combination of metformin and valproic acid synergistically inhibits proliferation of prostate cancer cells but not normal prostate epithelial cells.

The proliferation of normal and prostate cancer cell lines in response to MET and/or VPA was examined. Treatment with MET or VPA alone reduced proliferation of LNCaP ($p=0.018$ and 0.0001, respectively) and PC-3 ($p=0.047$ and 0.003, respectively) prostate cancer cell lines over 72 hours of treatment (Figure 1A & 1B), but not the proliferation of normal PrEC cell line ($p=0.687$ and 0.077, respectively) (Figure 1C) (RM-ANOVA) compared to vehicle. In LNCaP and PC-3, the combination of MET and VPA significantly reduced cell proliferation ($p<0.001$) compared to vehicle, MET alone, and VPA alone, but

not in PrEC ($p>0.05$). The CI for combination treatment with MET and VPA indicated a synergistic decrease for both LNCaP (CI=0.42) and PC-3 (CI=0.51) cells at 72 hours, and an antagonistic effect in PrEC (CI=1.35) (Figure 1D). The IC_{50} of MET alone, VPA alone, and MET+VPA were 2.9 mM, 2.7 mM, and 0.5 mM respectively in LNCaP (Figure 1E), 16.5 mM, 6.5 mM, and 2.9 mM respectively in PC-3 (Figure 1F), and 3.4 mM, 2.4 mM, and 2.8 mM respectively in PrEC (Figure 1G). The IC_{50} for MET+VPA was significantly reduced compared to using MET and VPA alone in LNCaP (5.8 and 5.4-fold decrease respectively; $p<0.001$) and PC-3 (5.6 and 2.2-fold decrease respectively; $p<0.001$), but not in PrEC ($p = 0.16$).

The combination of MET and VPA induces synergistic apoptosis in LNCaP, but was antagonistic in PC-3 and PrEC cells.

In order to investigate the role of apoptosis in the anti-proliferative effect of MET and VPA in combination, cell apoptosis was analyzed by calculating the proportion of cleaved caspase 3/7 positive cells exposed to two concentrations of MET and VPA (1 mM and 2.5 mM). Each cell line demonstrated different baseline levels of apoptosis, with PrEC (10-15%) and PC-3 (5-10%) being higher than LNCaP (2-4%) (Figure 2A, B, C). In comparison with vehicle control, LNCaP was the only cell line to exhibit a significant increase in apoptosis when treated with either drug alone or in combination at 1 mM doses. At 2.5 mM MET+VPA, LNCaP exhibited significantly higher apoptosis in comparison with VPA alone (260% increase, $p < 0.001$), MET alone (470% increase, $p < 0.001$), or vehicle control (1010% increase, $p < 0.001$) (Figure 2A). In PrEC and PC-3, although the combination of MET and VPA at 2.5 mM induced significantly higher apoptosis ($p = 0.007$ and 0.011, respectively) in comparison with the vehicle, there was no significant difference compared with MET alone or VPA alone ($p>0.05$) (Figure 2B, C). The CI of apoptosis at 72 hours indicated that the apoptotic increase was strongly synergistic (CI = 0.03) in LNCaP, whereas the apoptotic response was antagonistic in PrEC and PC-3 (CI = 1.46 and 2.62, respectively) (Figure 2D). The release of cytochrome c from the mitochondria to the cytoplasm was compared for LNCaP and PC-3. The percentage of cytochrome c in the cytoplasm was significantly increased up to 12-fold ($p<0.05$) in LNCaP, but not in PC-3, in response to 2.5 mM

MET+VPA compared to vehicle, 2.5 mM MET alone, and 2.5 mM VPA alone (Figure 2E, F).

The apoptotic effect of MET and VPA combination treatment is p53-dependent.

Knock-down of p53 expression in LNCaP cells reduces apoptosis response to MET and VPA combination treatment.

We next investigated whether the apoptotic response to combined MET and VPA in LNCaP cells was dependent on p53 expression. LNCaP cells ($p53^{+}$) were transfected with p53 siRNA and then treated with MET and/or VPA at 1 mM or 2.5 mM. Knock down of p53 after 72 hours post-transfection was confirmed by the relative expression of p53 to both β-actin (81.1%) and total protein (82.5%) in western blots (Figure 3A and Supplementary figure S3). This removal of p53 was associated with a significant reduction in apoptosis in response to the combination of MET and VPA at both 1 mM (47% decrease, $p < 0.001$) and 2.5 mM (58% decrease, $p = 0.001$) doses (Figure 3B), suggesting that the apoptotic effect of these drugs occurs in a p53-dependent manner.

Ectopic expression of p53 in PC-3 cells induces apoptosis in response to MET and VPA combination treatment.

To further confirm the role of p53 in response to MET and VPA combination treatment, GFP-p53 plasmid was transfected into PC-3 ($p53^{null}$) cells (Figure 4A). The control was GFP-only plasmid. Transfection efficiency was approximately 50% at 12 hours, 60 hours and 84 hours (Supplementary figure S4). Transfected cells were treated with MET and/or VPA and apoptosis was evaluated by measuring nuclear cleaved-caspase 3 (CC-3) intensity using the Operetta® High-Content Imaging System. In the absence of p53 transfection in PC-3, an antagonistic effect was observed in the presence of MET+VPA as previously shown (Figure 4B). In the presence of p53 transfection in PC-3, MET+VPA induced a significant increase in apoptosis compared to MET+VPA in the absence of p53 transfection (13.2% increase, $p=0.009$ at 1 mM and 24.5% increase, $p= 0.002$ at 2.5 mM). Ectopic expression of p53 in PC-3 cells resulted in a significantly higher apoptosis in response to MET+VPA

combination than in both MET alone (10.3% increase, p=0.009 at 1 mM and 18.9% increase, p<0.001 at 2.5 mM) and VPA alone (6.9% increase, p = 0.046 at 1 mM and 14.1% increase, p = 0.002 at 2.5 mM) (Figure 4B). The nuclear fragmentation index showed the same general pattern of response where the combination of MET and VPA induced a significantly higher NFI in comparison with the vehicle, MET, or VPA (Supplementary figure S2B). Furthermore, the combination index of apoptosis at 0.07 in GFP-p53 transfected cells and >10 in GFP-only transfected cells indicated that, in the presence of p53, MET+VPA induced synergistic apoptosis, whereas this response was antagonistic in the absence of p53.

The androgen signaling pathway contributes to the apoptotic response to MET+VPA

In order to determine if the AR signaling pathway plays a role in the apoptotic response to MET and VPA combination treatment, the AR antagonist Enzalutamide (1 μM) was used in the AR-positive prostate cancer cell line LNCaP. As expected, treatment of LNCaP cells with Enzalutamide inhibited PSA expression at 24 hours, 72 hours and 96 hours (Figure 5A) and also induced a significant dose-dependent increase in apoptosis (Figure 5B) (53.7% increase at 1 μM and 90% increase at 2 μM, p< 0.05). In the presence of Enzalutamide, the apoptotic response to 2.5 mM MET+VPA was significantly reduced (28.5% decrease, p = 0.029) compared to MET+VPA treated cells in the absence of Enzalutamide (Figure 5C). There was no change in the apoptotic response of PC-3, an androgen-resistant prostate cancer cell line, to MET and/or VPA alone or in combination in the presence of absence of Enzalutamide (Supplementary figure S5).

The combination of MET and VPA reduces tumor cell proliferation and induces apoptosis in human prostate tumor explants

Eight human prostate tumor explants were available for this study. The clinicopathological features of the PCa patients who had undergone radical prostatectomy are given in Table 1. The mean age was 64.6 years. The pathological stage ranged from pT2C to pT3A with Gleason score of 7 or 9. All prostate tumor explants expressed normal AR. The prostate tumor explants

from these patients were exposed to vehicle or combined MET and VPA treatment at doses of either 2.5 mM or 5 mM. The individual patient responses are shown for proliferation (Figure 6A i) and apoptosis (Figure 6B i) 48 hours after treatment. Compared to vehicle control, 2.5 mM MET+VPA significantly decreased (90% decrease, $p < 0.001$) the proportion of Ki-67 positive cells (Figure 6A ii, iii, and iv) and increased the percentage of positive cleaved-caspase 3 cells (300% increase, $p < 0.001$) (Figure 6B ii, iii, and iv). When the dose was increased to 5 mM, the inhibitory effect of MET+VPA on proliferation was not significantly changed compared to 2.5 mM MET+VPA, while apoptosis increased by a further 200% ($p<0.05$) compared to 2.5 mM MET+VPA (Figure 6A ii, 6B ii). The vast majority of the explant tissue exhibited tumor morphology, with only four patient samples exhibiting any normal tissue. Only ten normal prostatic glands were identified in a total of six images out of 757 images analyzed. No positive staining for Ki67 or cleaved-caspase 3 was identified in these glands.

DISCUSSION

There are currently no curative therapies for CRPC and new therapeutic approaches are urgently needed. Here, we investigated whether two drugs commonly used for non-cancer indications could be repurposed for treatment of prostate cancer. We investigated the potential of MET+VPA as a cancer therapy based on the hypothesis that their different mechanisms of action could combine to give a synergistic anti-cancer effect.

Although VPA shows promise as an anti-cancer monotherapy, the doses tested so far in humans have demonstrated unacceptable toxicity. We hypothesized that a lower drug concentration of VPA could be achievable if additive or synergistic anti-cancer effects were obtained in combination with another drug, such as MET. Monotherapy doses of MET or VPA ranging from 1 mM to 10 mM have been used in previous *in vitro* studies (37, 38) with up to 40 mM in the one study where MET and VPA were combined (29). In the present study, we investigated MET and VPA either alone or in combination at doses of 1 mM and 2.5 mM. Doses of VPA in our study are lower than the toxic threshold level of VPA in human plasma at 3.1 mM (39). Doses of MET used prior *in vitro* and *in vivo* studies were higher than the toxic threshold in human

plasma (at 0.31 mM) (40, 41). Here doses of MET were in the low range of previous *in vitro* studies.

We have demonstrated that the combination of MET and VPA synergistically inhibits cell proliferation in two prostate cancer cell lines (PC-3 and LNCaP) derived from metastatic prostate cancer patients (42, 43), while being antagonistic in normal prostatic epithelial cells (PrEC). Also, MET+VPA significantly lowered the IC_{50} for proliferation compared to MET or VPA alone in both LNCaP and PC-3, but not in PrEC, suggesting that the concentration of MET and VPA could be reduced in combination treatment for prostate cancer, potentially reducing the toxicity caused by higher doses of MET and/or VPA. This differential antiproliferative response in cancer and normal cells may be explained by the selective inhibition of metformin on glucose metabolism in cancer cells, which is more effective than in normal epithelial cells (44). Cancer cells, in general, have a higher rate of glycolysis even under aerobic conditions and are less adaptive to glucose starvation compared to normal cells (45, 46). Furthermore, Zhuang et al (2014) also confirmed that lower glucose concentration in the culture medium preferentially sensitized breast and ovarian cancer cell lines to MET compared to normal cells (47). VPA, a histone deacetylation inhibitor, can cause DNA double strand breaks (DSBs) in cells and preferentially targets cancer cells due to their low ability to repair the DSBs compared to normal cells (48).

Although the combination of MET and VPA synergistically inhibited the proliferation of both LNCaP and PC-3 cells, synergistic apoptosis was only observed in LNCaP in our study. Furthermore, apoptosis was found to be antagonistic in both PC-3 cells and the normal prostatic epithelial cell line PrEC. In the one previous report using MET+VPA in combination, Zhang et al (2015) observed a similar synergistic decrease in proliferation and increase in apoptosis in 2 renal cell carcinoma cell lines (786-0 and Caki-2 cells) compared to the single drug alone (29). However, responses in normal renal cell lines were not reported.

The reason for a differential response to MET+VPA treatment between LNCaP and PC-3 cells is unclear but is likely to be due to the underlying genetic differences between these cell lines. LNCaP cells have intact p53 and

AR signaling, while PC-3 cells do not express p53 (due to a premature stop codon) or AR (42, 43, 49). Both LNCaP and PC-3 have mutations in *PTEN*. Therefore, p53 and AR are potential candidates for mediating the synergistic apoptotic response observed in LNCaP in response to MET+VPA treatment. In support of this hypothesis, when p53 was substantially depleted in LNCaP cells, the synergistic apoptotic response was reduced by approximately 50%. Likewise, a synergistic apoptotic response could be established in PC-3 cells which expressed ectopic p53. Taken together, these results suggest that p53 is required for the apoptotic response of prostate cancer cell lines to the combination of MET and VPA. Prior evidence supports this finding, as MET has been shown to inhibit cell growth and induce cell apoptosis to a greater extent in p53 (+) cells compared with p53 (-) cells (50-52). It has been shown that MET targets prostate cancer cell metabolism by inhibiting mitochondrial respiration and glycolysis (37). The inhibition of mitochondrial complex 1 alters the AMP/ATP ratio, which in turn activates AMPK, resulting in phosphorylation of p53 at Ser15 and leading to p53-dependent cell death (53-56). In a study similar to the present one, Sahra et al (2010) found that ectopic expression of p53 in PC-3 cells significantly enhanced cleaved-caspase 3 activity in response to MET and 2-deoxyglucose in combination (50). In addition, VPA has also been shown to cause acetylation of p53 at lysine residues 373 and 382, resulting in its activation (24). Therefore, the combination of MET and VPA may result in increased p53 protein activation, driving p53-dependent cell death via intrinsic or extrinsic pathways. We demonstrated a significant increase in cytochrome c released from the mitochondria to the cytoplasm in LNCaP (p53+) cells indicating that intrinsic apoptosis was induced in response to MET+VPA. The two renal cancer cell lines that responded to MET and VPA combination treatment in the study by Zhang et al (29) also expressed wild-type p53 (57, 58). These results suggest that combining MET and VPA may provide a useful therapeutic option in a variety of cancer types, particularly those expressing p53.

The androgen signaling pathway plays a vital role in prostate cancer development in which the mutation rate of AR increases from a low frequency in localized prostate cancer to a higher frequency in CRPC (59). Previous reports showed that the second generation AR antagonist Enzalutamide

increased apoptosis in a dose-dependent manner in androgen-sensitive LNCaP cells (60, 61). We found the same response in our study with Enzalutamide increasing apoptosis in LNCaP. Apoptosis was also increased by Enzalutamide in the presence of MET alone. Previous studies found that the androgen signaling pathway stimulates aerobic glycolysis (62, 63) and anabolism in prostate cancer cells (64). Consequently, blocking the AR signaling pathway impairs the effectiveness of aerobic glucose metabolism in prostate cancer cells, causing them to be more susceptible to MET as the result of interrupting the ATP/AMP ratio as well as preventing glucose recruitment into oxidative phosphorylation processes. MET has also been shown to inhibit mTOR which can further inhibit cell anabolism in the absence of the AR signaling pathway (65).

Using VPA in the presence of Enzalutamide induced more apoptosis than VPA alone in our study. Gaughan et al. showed that direct or indirect acetylation (through Tip60) of AR increases AR transcriptional activity, and histone deacetylase 1 (HDAC1) down-regulates AR activity (66). In this way, the HDACi activity of VPA enhances the transcriptional activity of AR (67), which may recover androgen responsiveness in CRPC (68).

In response to MET and VPA combination treatment, although there was no significant difference in the apoptosis frequency in LNCaP at the lower dose of 1 mM, the apoptotic response was significantly reduced in the presence of Enzalutamide at the higher dose of 2.5 mM compared to in the absence of Enzalutamide, suggesting that the AR signalling pathway is important in the synergistic apoptosis response. As expected, there was no significant effect of Enzalutamide in the presence of MET+VPA on the apoptotic response of PC-3 cells which have no AR expression. PrEC cells also do not exhibit AR expression (69), which may contribute to the lack of the significant inhibitory response in response to MET+VPA in our study. Although an interaction between p53 and AR in prostate cancer is not well defined, the AR cofactor WDR777 may interact with p53 to form the p53-WDR77-AR complex and enhance the activity of AR (70). However, it is not clear if MET+VPA has an effect on the p53-WDR77-AR complex in prostate cancer

cells. Further investigation is needed to explore the interaction between AR and p53 in response to MET+VPA.

The efficacy of combining MET and VPA to inhibit proliferation and increase apoptosis in prostate cancer was further confirmed in clinical specimens using human prostate tumor explants. MET+VPA reduced the proliferation and increased apoptosis in all 8 prostatic explants as almost all prostate cancer patients with localized disease express both AR and p53 (71-73). Due to the nature of the collection of prostate tumor explants, very little normal tissue was present. It was therefore not possible to determine the effect of MET+VPA on normal tissue in the explants. Our group has recently commenced an early Phase I clinical trial with the combination of MET+VPA as neoadjuvant therapy prior to radical prostatectomy (ACTRN 12616001021460), which will directly inform the issue of normal tissue toxicity.

Recent next-generation sequencing efforts have revealed that the most frequent aberrations in CRPC include mutations in p53 (53.3%), AR (62.7%) and PTEN (40.7%), as well as ETS gene fusions (56.7%) (5). Confirming that MET and VPA combination therapy is indeed p53- and AR-dependent could provide a basis for individualized patient therapy in future clinical trials. Our observation that MET+VPA reduced cell proliferation in PC-3 which lacks p53 and AR expression, suggests that the combination of MET+VPA can reduce cancer cell proliferation, but not apoptosis, independently of p53 and AR expression. Therefore, MET+VPA can still potentially provide an anti-proliferative effect in an advanced stage of PCa where mutations in these genes have occurred.

In summary, our *in vitro* and *ex vivo* results suggest that the combination of MET and VPA may be a useful, relatively non-toxic, systemic cancer therapy for non-metastatic stage disease with greater efficacy in the presence of p53 and AR signaling. The combination may also be useful in hormone sensitive prostate cancer prior to initiation of anti-androgens or those CRPC with wild-type p53. However, further *in vivo* pre-clinical studies are required to determine the relative efficacy of MET+VPA *ex vivo*.

As both drugs are currently used for non-cancer indications with established toxicity profiles, there is the potential for them to be rapidly repurposed for integration into clinical trials to benefit treatment in at least a proportion of prostate cancer patients.

REFERENCES

1. Grönberg H. Prostate cancer epidemiology. The Lancet. 2003;361(9360):859-64.
2. Torre LA, Bray F, Siegel RL, Ferlay J, Lortet-Tieulent J, Jemal A. Global cancer statistics, 2012. CA: a cancer journal for clinicians. 2015;65(2):87-108.
3. Luo Q, Yu XQ, Smith DP, O'Connell DL. A population-based study of progression to metastatic prostate cancer in Australia. Cancer epidemiology. 2015.
4. Hirst C, Cabrera C, Kirby M. Epidemiology of castration resistant prostate cancer: A longitudinal analysis using a UK primary care database. Cancer epidemiology. 2012;36(6):e349-e53.
5. Robinson D, Van Allen EM, Wu Y-M, Schultz N, Lonigro RJ, Mosquera J-M, et al. Integrative Clinical Genomics of Advanced Prostate Cancer. Cell. 2015;161(5):1215-28.
6. Ryan CJ, Smith MR, Fizazi K, Saad F, Mulders PF, Sternberg CN, et al. Abiraterone acetate plus prednisone versus placebo plus prednisone in chemotherapy-naive men with metastatic castration-resistant prostate cancer (COU-AA-302): final overall survival analysis of a randomised, double-blind, placebo-controlled phase 3 study. The Lancet Oncology. 2015;16(2):152-60.
7. Beer TM, Armstrong AJ, Rathkopf DE, Loriot Y, Sternberg CN, Higano CS, et al. Enzalutamide in metastatic prostate cancer before chemotherapy. New England Journal of Medicine. 2014;371(5):424-33.
8. Tannock IF, de Wit R, Berry WR, Horti J, Pluzanska A, Chi KN, et al. Docetaxel plus prednisone or mitoxantrone plus prednisone for advanced prostate cancer. New England Journal of Medicine. 2004;351(15):1502-12.
9. Kantoff PW, Higano CS, Shore ND, Berger ER, Small EJ, Penson DF, et al. Sipuleucel-T immunotherapy for castration-resistant prostate cancer. New England Journal of Medicine. 2010;363(5):411-22.
10. Zhou G, Myers R, Li Y, Chen Y, Shen X, Fenyk-Melody J, et al. Role of AMP-activated protein kinase in mechanism of metformin action. Journal of Clinical Investigation. 2001;108(8):1167-74.
11. Sahra IB, Laurent K, Loubat A, Giorgetti-Peraldi S, Colosetti P, Auberger P, et al. The antidiabetic drug metformin exerts an antitumoral effect in vitro and in vivo through a decrease of cyclin D1 level. Oncogene. 2008;27(25):3576-86.
12. Bolster DR, Crozier SJ, Kimball SR, Jefferson LS. AMP-activated protein kinase suppresses protein synthesis in rat skeletal muscle through down-regulated mammalian target of rapamycin (mTOR) signaling. Journal of Biological Chemistry. 2002;277(27):23977-80.
13. Long YC, Zierath JR. AMP-activated protein kinase signaling in metabolic regulation. Journal of Clinical Investigation. 2006;116(7):1776-83.
14. Hardie DG. Minireview: the AMP-activated protein kinase cascade: the key sensor of cellular energy status. Endocrinology. 2003;144(12):5179-83.
15. Murtola TJ, Tammela TL, Lahtela J, Auvinen A. Antidiabetic medication and prostate cancer risk: a population-based case-control study. American journal of epidemiology. 2008;168(8):925-31.
16. Rothermundt C, Hayoz S, Templeton AJ, Winterhalder R, Strebel RT, Bärtschi D, et al. Metformin in chemotherapy-naive castration-resistant prostate cancer: a multicenter phase 2 trial (SAKK 08/09). European urology. 2014.
17. Azoulay L, Dell'Aniello S, Gagnon B, Pollak M, Suissa S. Metformin and the incidence of prostate cancer in patients with type 2 diabetes. Cancer Epidemiology Biomarkers & Prevention. 2011;20(2):337-44.
18. Chateauvieux S, Dicato M, Diederich M, Morceau F. Molecular and therapeutic potential and toxicity of valproic acid. Journal of Biomedicine and Biotechnology. 2010.
19. Rosato RR, Almenara JA, Grant S. The histone deacetylase inhibitor MS-275 promotes differentiation or apoptosis in human leukemia cells through a process regulated by generation of reactive oxygen species and induction of p21CIP1/WAF1. Cancer research. 2003;63(13):3637-45.
20. Savickiene J, Borutinskaite V-V, Treigyte G, Magnusson K-E, Navakauskiene R. The novel histone deacetylase inhibitor BML-210 exerts growth inhibitory, proapoptotic and differentiation stimulating effects on the human leukemia cell lines. European journal of pharmacology. 2006;549(1):9-18.
21. Martirosyan A, Leonard S, Shi X, Griffith B, Gannett P, Strobl J. Actions of a histone deacetylase inhibitor NSC3852 (5-nitroso-8-quinolinol) link reactive oxygen species to cell differentiation and apoptosis in MCF-7 human mammary tumor cells. Journal of Pharmacology and Experimental Therapeutics. 2006;317(2):546-52.
22. Chen Y, Pan RL, Zhang XL, Shao JZ, Xiang LX, Dong XJ, et al. Induction of hepatic differentiation of mouse bone marrow stromal stem cells by the histone deacetylase inhibitor VPA. Journal of cellular and molecular medicine. 2009;13(8b):2582-92.
23. Cohen HY, Lavu S, Bitterman KJ, Hekking B, Imahiyerobo TA, Miller C, et al. Acetylation of the C terminus of Ku70 by CBP and PCAF controls Bax-mediated apoptosis. Molecular cell. 2004;13(5):627-38.
24. Condorelli F, Gnemmi I, Vallario A, Genazzani A, Canonico P. Inhibitors of histone deacetylase (HDAC) restore the p53 pathway in neuroblastoma cells. British journal of pharmacology. 2008;153(4):657-68.
25. Gurvich N, Tsygankova OM, Meinkoth JL, Klein PS. Histone deacetylase is a target of valproic acid-mediated cellular differentiation. Cancer research. 2004;64(3):1079-86.
26. Duenas-Gonzalez A, Candelaria M, Perez-Plascencia C, Perez-Cardenas E, de la Cruz-Hernandez E, Herrera LA. Valproic acid as epigenetic cancer drug: preclinical, clinical and transcriptional effects on solid tumors. Cancer treatment reviews. 2008;34(3):206-22.
27. Göttlicher M, Minucci S, Zhu P, Krämer OH, Schimpf A, Giavara S, et al. Valproic acid defines a novel class of HDAC inhibitors inducing differentiation of transformed cells. The EMBO journal. 2001;20(24):6969-78.

28. Sharma S, Symanowski J, Wong B, Dino P, Manno P, Vogelzang N. A phase II clinical trial of oral valproic acid in patients with castration-resistant prostate cancers using an intensive biomarker sampling strategy. Translational oncology. 2008;1(3):141.
29. Zhang X, Zhang X, Huang T, Geng J, Liu M, Zheng J. Combination of metformin and valproic acid synergistically induces cell cycle arrest and apoptosis in clear cell renal cell carcinoma. Int J Clin Exp Pathol. 2015;8(3):2823-8.
30. Colella AD, Chegenii N, Tea MN, Gibbins IL, Williams KA, Chataway TK. Comparison of stain-free gels with traditional immunoblot loading control methodology. Analytical biochemistry. 2012;430(2):108-10.
31. Eaton SL, Roche SL, Hurtado ML, Oldknow KJ, Farquharson C, Gillingwater TH, et al. Total protein analysis as a reliable loading control for quantitative fluorescent Western blotting. PloS one. 2013;8(8):e72457.
32. Boyd SD, Tsai KY, Jacks T. An intact HDM2 RING-finger domain is required for nuclear exclusion of p53. Nature cell biology. 2000;2(9):563-8.
33. Chou T-C, Talalay P. Quantitative analysis of dose-effect relationships: the combined effects of multiple drugs or enzyme inhibitors. Advances in enzyme regulation. 1984;22:27-55.
34. Chou T-C. Drug combination studies and their synergy quantification using the Chou-Talalay method. Cancer research. 2010;70(2):440-6.
35. Centenera MM, Gillis JL, Hanson AR, Jindal S, Taylor RA, Risbridger GP, et al. Evidence for efficacy of new Hsp90 inhibitors revealed by ex vivo culture of human prostate tumors. Clinical Cancer Research. 2012;18(13):3562-70.
36. Tuominen VJ, Ruotoistenmaki S, Viitanen A, Jumppanen M, Isola J. ImmunoRatio: a publicly available web application for quantitative image analysis of estrogen receptor (ER), progesterone receptor (PR), and Ki-67. Breast Cancer Res. 2010;12(4):R56.
37. Fendt S-M, Bell EL, Keibler MA, Davidson SM, Wirth GJ, Fiske B, et al. Metformin decreases glucose oxidation and increases the dependency of prostate cancer cells on reductive glutamine metabolism. Cancer research. 2013;73(14):4429-38.
38. Sahra IB, Regazzetti C, Robert G, Laurent K, Le Marchand-Brustel Y, Auberger P, et al. Metformin, independent of AMPK, induces mTOR inhibition and cell-cycle arrest through REDD1. Cancer research. 2011;71(13):4366-72.
39. Spiller HA, Krenzelok EP, Klein-Schwartz W, Winter ML, Weber JA, Sollee DR, et al. Multicenter case series of valproic acid ingestion: serum concentrations and toxicity. Clinical Toxicology. 2000;38(7):755-60.
40. Vecchio S, Giampreti A, Petrolini V, Lonati D, Protti A, Papa P, et al. Metformin accumulation: Lactic acidosis and high plasmatic metformin levels in a retrospective case series of 66 patients on chronic therapy*. Clinical Toxicology. 2014;52(2):129-35.
41. Dowling RJ, Niraula S, Stambolic V, Goodwin PJ. Metformin in cancer: translational challenges. Journal of molecular endocrinology. 2012;48(3):R31-R43.
42. Kaighn M, Narayan KS, Ohnuki Y, Lechner J, Jones L. Establishment and characterization of a human prostatic carcinoma cell line (PC-3). Investigative urology. 1979;17(1):16-23.
43. Horoszewicz JS, Leong SS, Kawinski E, Karr JP, Rosenthal H, Chu TM, et al. LNCaP model of human prostatic carcinoma. Cancer research. 1983;43(4):1809-18.
44. Tsai C-C, Chuang T-W, Chen L-J, Niu H-S, Chung K-M, Cheng J-T, et al. Increase in apoptosis by combination of metformin with silibinin in human colorectal cancer cells. World journal of gastroenterology: WJG. 2015;21(14):4169.
45. Warburg O. On the origin of cancer cells. Science. 1956;123(3191):309-14.
46. Menendez JA, Oliveras-Ferraros C, Cufí S, Corominas-Faja B, Joven J, Martin-Castillo B, et al. Metformin is synthetically lethal with glucose withdrawal in cancer cells. Cell cycle. 2012;11(15):2782-92.
47. Zhuang Y, Chan DK, Haugrud AB, Miskimins WK. Mechanisms by which low glucose enhances the cytotoxicity of metformin to cancer cells both in vitro and in vivo. PloS one. 2014;9(9):e108444.
48. Lee J-H, Choy M, Ngo L, Foster S, Marks PA. Histone deacetylase inhibitor induces DNA damage, which normal but not transformed cells can repair. Proceedings of the National Academy of Sciences. 2010;107(33):14639-44.
49. Carroll AG, Voeller HJ, Sugars L, Gelmann EP. p53 oncogene mutations in three human prostate cancer cell lines. The Prostate. 1993;23(2):123-34.
50. Sahra IB, Laurent K, Giuliano S, Larbret F, Ponzio G, Gounon P, et al. Targeting cancer cell metabolism: the combination of metformin and 2-deoxyglucose induces p53-dependent apoptosis in prostate cancer cells. Cancer research. 2010;70(6):2465-75.
51. Zakikhani M, Dowling R, Fantus IG, Sonenberg N, Pollak M. Metformin is an AMP kinase–dependent growth inhibitor for breast cancer cells. Cancer research. 2006;66(21):10269-73.
52. Gotlieb WH, Saumet J, Beauchamp M-C, Gu J, Lau S, Pollak MN, et al. In vitro metformin anti-neoplastic activity in epithelial ovarian cancer. Gynecologic oncology. 2008;110(2):246-50.
53. Jones RG, Plas DR, Kubek S, Buzzai M, Mu J, Xu Y, et al. AMP-activated protein kinase induces a p53-dependent metabolic checkpoint. Molecular cell. 2005;18(3):283-93.
54. Okoshi R, Ozaki T, Yamamoto H, Ando K, Koida N, Ono S, et al. Activation of AMP-activated protein kinase induces p53-dependent apoptotic cell death in response to energetic stress. Journal of biological chemistry. 2008;283(7):3979-87.
55. Feng Z, Levine AJ. The regulation of energy metabolism and the IGF-1/mTOR pathways by the p53 protein. Trends in cell biology. 2010;20(7):427-34.
56. Bensaad K, Vousden KH. p53: new roles in metabolism. Trends in cell biology. 2007;17(6):286-91.

57. Stickle NH, Cheng LS, Watson IR, Alon N, Malkin D, Irwin MS, et al. Expression of p53 in renal carcinoma cells is independent of pVHL. Mutation Research/Fundamental and Molecular Mechanisms of Mutagenesis. 2005;578(1):23-32.
58. Warburton HE, Brady M, Vlatković N, Linehan WM, Parsons K, Boyd MT. p53 regulation and function in renal cell carcinoma. Cancer research. 2005;65(15):6498-503.
59. Marcelli M, Ittmann M, Mariani S, Sutherland R, Nigam R, Murthy L, et al. Androgen receptor mutations in prostate cancer. Cancer research. 2000;60(4):944-9.
60. Tran C, Ouk S, Clegg NJ, Chen Y, Watson PA, Arora V, et al. Development of a second-generation antiandrogen for treatment of advanced prostate cancer. Science. 2009;324(5928):787-90.
61. Li Y, Chan SC, Brand LJ, Hwang TH, Silverstein KA, Dehm SM. Androgen receptor splice variants mediate enzalutamide resistance in castration-resistant prostate cancer cell lines. Cancer research. 2013;73(2):483-9.
62. Christofk HR, Vander Heiden MG, Harris MH, Ramanathan A, Gerszten RE, Wei R, et al. The M2 splice isoform of pyruvate kinase is important for cancer metabolism and tumour growth. Nature. 2008;452(7184):230-3.
63. Vander Heiden MG, Cantley LC, Thompson CB. Understanding the Warburg effect: the metabolic requirements of cell proliferation. science. 2009;324(5930):1029-33.
64. Massie CE, Lynch A, Ramos-Montoya A, Boren J, Stark R, Fazli L, et al. The androgen receptor fuels prostate cancer by regulating central metabolism and biosynthesis. The EMBO journal. 2011;30(13):2719-33.
65. Xu Y, Chen S-Y, Ross KN, Balk SP. Androgens induce prostate cancer cell proliferation through mammalian target of rapamycin activation and post-transcriptional increases in cyclin D proteins. Cancer research. 2006;66(15):7783-92.
66. Gaughan L, Logan IR, Cook S, Neal DE, Robson CN. Tip60 and histone deacetylase 1 regulate androgen receptor activity through changes to the acetylation status of the receptor. Journal of Biological Chemistry. 2002;277(29):25904-13.
67. Xia Q, Sung J, Chowdhury W, Chen C-l, Höti N, Shabbeer S, et al. Chronic administration of valproic acid inhibits prostate cancer cell growth in vitro and in vivo. Cancer research. 2006;66(14):7237-44.
68. Iacopino F, Urbano R, Graziani G, Muzi A, Navarra P, Sica G. Valproic acid activity in androgen-sensitive and-insensitive human prostate cancer cells. International journal of oncology. 2008;32(6):1293-303.
69. Sobel RE, Wang Y, Sadar MD. Molecular analysis and characterization of PrEC, commercially available prostate epithelial cells. In Vitro Cellular & Developmental Biology-Animal. 2006;42(1-2):33-9.
70. Kumari S, Schlanger S, Wang D, Liu S, Heemers H. OR43-2: Defining Coregulator Contribution to AR-Dependent Transcription Uncovers a Novel AR-WDR77-p53-Dependent Transcriptional Code. Endocrine Society's 98th Annual Meeting and Expo; Boston: Endocrine Society; 2016.
71. Taplin M-E, Bubley GJ, Shuster TD, Frantz ME, Spooner AE, Ogata GK, et al. Mutation of the androgen-receptor gene in metastatic androgen-independent prostate cancer. New England Journal of Medicine. 1995;332(21):1393-8.
72. Feldman BJ, Feldman D. The development of androgen-independent prostate cancer. Nature Reviews Cancer. 2001;1(1):34-45.
73. Bookstein R, MacGrogan D, Hilsenbeck SG, Sharkey F, Allred DC. p53 is mutated in a subset of advanced-stage prostate cancers. Cancer research. 1993;53(14):3369-73.
74. Edge SB, Compton CC. The American Joint Committee on Cancer: the 7th edition of the AJCC cancer staging manual and the future of TNM. Annals of surgical oncology. 2010;17(6):1471-4.

Table 1. Clinicopathological features of patient explants

Patient No.	Patient age (years)	PSA (ng/mL)	Gleason grade [a]	Pathological stage [a]	AR status
1	67.2	14.1	3+4=7	pT3a	+
2	58.9	8.3	3+4=7	pT3a	+
3	57.4	7.8	3+4=7	pT3a	+
4	69	8.3	4+3=7	pT3a	+
5	71.5	10.4	4+3=7	pT3a	+
6	66.5	5.7	3+4=7	pT2c	+
7	70.6	6.5	3+4=7	pT2c	+
8	55.8	12	5+4=9	pT3b	+

[a] All tumors are adenocarcinoma of acinar type. Pathological stage as per AJCC TNM 7th Edition (74).

FIGURE LEGENDS

Figure 1. MET and VPA in combination synergistically reduces proliferation of prostate cancer cell lines, but not of normal prostatic epithelial cells. **A,** LNCaP, **B,** PC-3, and **C,** PrEC were grown in 96 well plates and treated for 72 hours with vehicle control, 2.5 mM MET alone, 2.5 mM VPA alone or 2.5 mM (MET +VPA). Cell proliferation was monitored by measuring the confluence (mean ± SE) using Incucyte real-time imaging. **D,** Combination index (CI) of anti-proliferative effect of MET and VPA at 72 hours using Chou-Talalay method (CompuSyn) based on at least 2 different doses. Dose-response curves for proliferation at 72 hours of LNCaP **(E)**, PC-3 **(F)**, and PrEC **(G)** cells. $p < 0.05$ in comparison with (*) vehicle ($3 \leq n \leq 4$) and (**) vehicle, MET alone, and VPA alone ($3 \leq n \leq 4$).

Figure 2. MET and VPA in combination induces synergistic apoptosis in LNCaP but not in PC-3 and PrEC. Cells were treated with MET and VPA at 1 mM or 2.5 mM, either alone or in combination. The percentage of apoptosis (mean ± SE) per total cells was measured at 72 hours after treatment. A, LNCaP cells. B, PC-3 cells. C, PrEC cells. D, Combination index (CI) of the percentage of apoptosis at 72 hours using Chou-Talalay method (CompuSyn). Percentage of cytochrome C (mean ± SE) in (E) LNCaP and (F) PC-3 in the cytoplasm (C) and mitochondria (M) in response to vehicle, 2.5 mM MET, 2.5 mM VPA, and 2.5 mM MET+VPA. Pyruvate dehydrogenase subunit E1-α (PDH-E1-α) and ATP synthase subunit-α protein (CV α) are mitochondrial markers. β-actin is a cytoplasmic marker. $p < 0.05$ in Student T-Test in comparison with (*) vehicle control and (**) vehicle control, MET alone, and VPA alone, ($3 \leq n \leq 4$).

Figure 3. siRNA knock-down of p53 in LNCaP cells reduces apoptosis in response to MET and VPA combination treatment. LNCaP cells were grown in 24 well plates, transfected with p53 siRNA or control siRNA and treated with MET and/or VPA at 1 mM or 2.5 mM. Apoptosis was investigated using a CellPlayer™ Kinetic Caspase 3/7 Apoptosis Assay Kit. The percentage of apoptosis was measured at 72 hours. **A,** Western blot showing siRNA knock-down of p53 in LNCaP. Positive control: PrEC cell line. Negative control: PC-

3 cell line. **B,** The percentage of apoptosis (mean ± SE) in LNCaP cells with control siRNA or p53 siRNA. *****, $p < 0.05$ in Student T-test in comparison with the same dose of MET+VPA in siRNA groups ($3 \leq n \leq 4$).

Figure 4. Ectopic expression of p53 in PC-3 ($p53^{null}$) cells induces apoptosis in response to MET and VPA combination treatment. PC-3 cells were grown in 96 well plates, transfected with a GFP-p53 plasmid or GFP-only plasmid transfected and treated with MET and/or VPA at 1 mM or 2.5 mM for 3 days. Apoptosis was evaluated by mean fluorescence intensity of nuclear cleaved caspase 3 (CC-3). **A**, 40X images were taken using an Operetta® High Content Imaging System. The cell nucleus and cytosol were stained using DRAQ5™, Cleaved Caspase 3 was detected using Alexa 555® dye and p53-transfected cells were detected using green fluorescence protein (GFP). **B,** Mean fluorescence intensity of nuclear CC-3 (mean ± SE) in GFP-p53 transfected and GFP-only transfected PC-3. ***** $p < 0.05$ in Student T-test in comparison with the vehicle, MET alone, and VPA alone ($3 \leq n \leq 4$)**.**

Figure 5. Inhibition of AR activity with the antagonist enzalutamide reduced the synergistic apoptosis in LNCaP cells in response to MET+VPA. LNCaP cells were grown in 96 well plates, exposed to 1 μM Enzalutamide (ENZA) for 24 hours before treating with MET and/or VPA at 1 mM or 2.5 mM. The percentage of cleaved caspase 3/7 positive cells was measured at 96 hours. **A**, Enzalutamide (1 μM) inhibited PSA expression in LNCaP at 24 hours, 72 hours and 96 hours. (-) control: PC-3, (+) control: LNCaP. ENZA: Enzalutamide. Vehicle: DMSO. **B,** Percentage apoptosis (mean ± SE) with increasing doses of Enzalutamide at 1 μM and 2 μM at 96 hours. **C**, Percentage apoptosis (mean ± SE) in LNCaP cells with and without Enzalutamide in response to MET and/or VPA alone, and in combination, at 1 mM or 2.5 mM. * $p < 0.05$ in Student T-test in comparison with the vehicle and with the same dose of MET alone and VPA alone in the presence and absence of Enzalutamide. ** $p < 0.05$ in Student T-test in comparison with the same dose of MET+VPA in the presence and absence of Enzalutamide ($3 \leq n \leq 4$).

Figure 6. MET+VPA reduced cell proliferation and increased apoptosis in patient-derived human prostatic *ex vivo* tumor explants. Tissues were treated with 2.5 mM or 5 mM MET+VPA for 48 hours, and then sections were fixed in

formalin and paraffin embedded. Ki67 and cleaved-caspase 3 (CC3) immunochemistry staining were performed. **A, (i)** Percentage of Ki67 positive cells in individual patients (n=8), **(ii)** Percentage (mean ± SE) of Ki67 positive cells in all patients, and representative Ki67 stained sections (scale bar = 50 µm) in patient No.1 of **(iii)** vehicle treated and **(iv)** MET+VPA (2.5 mM) treated explants at 48 hours. **B, (i)** Percentage of CC3 positive cells in individual patients (n=8), **(ii)** Percentage (mean ± SE) of CC3 positive cells in all patients, and representative CC3 stained sections in the patient No.1 of **(iii)** vehicle treated and **(iv)** MET+VPA (2.5 mM) treated explants at 48 hours. * $p < 0.05$ in Student T-test in comparison with the vehicle. ** $p < 0.05$ in Student T-test in comparison with MET+VPA (2.5 mM) and vehicle (n=8).

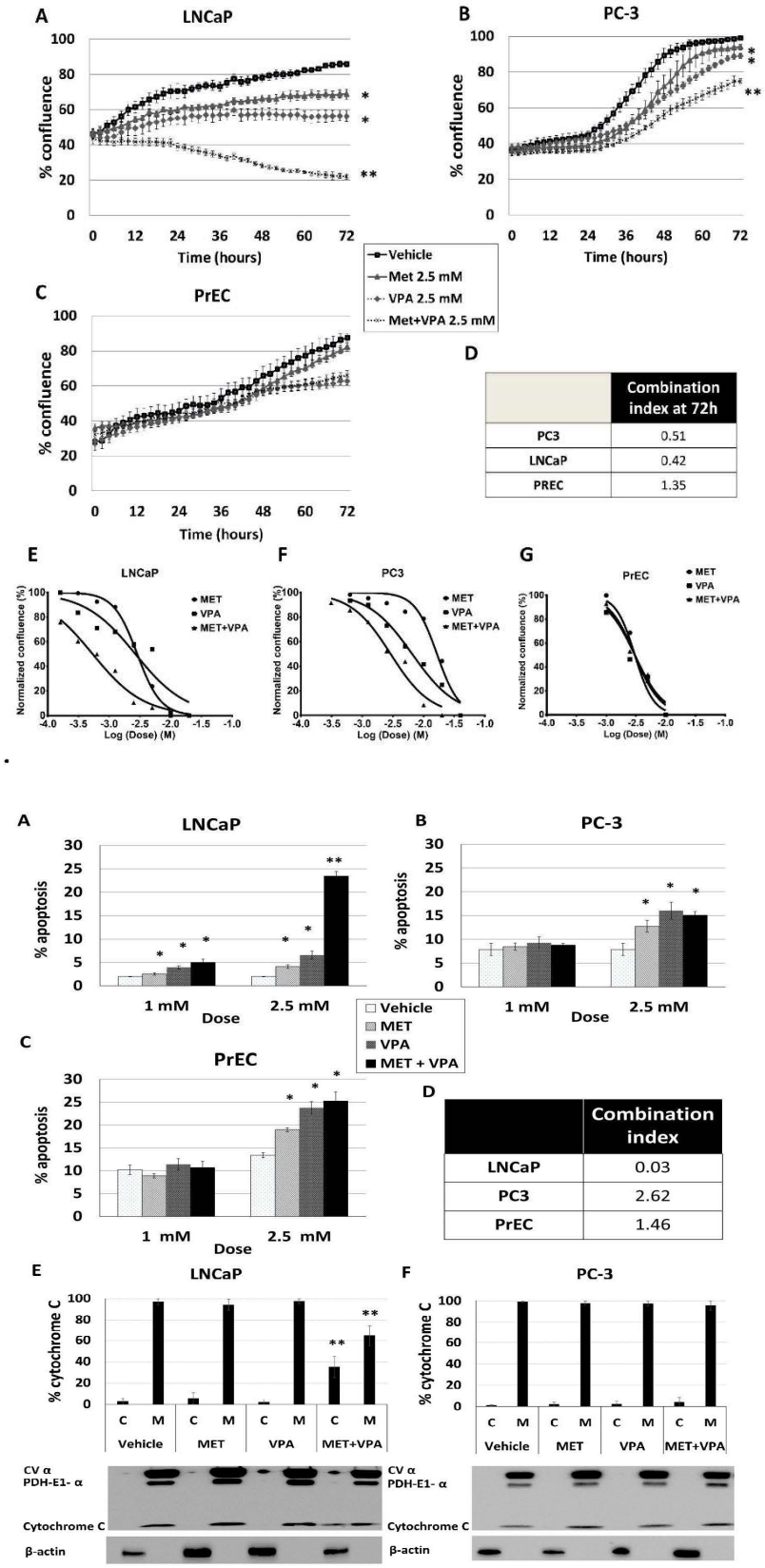
A
LNCaP
% confluence
Time (hours)
B
PC-3
% confluence
Time (hours)
Vehicle
Met 2.5 mM
VPA 2.5 mM
Met+VPA 2.5 mM
C
PrEC
% confluence
Time (hours)
D
Combination index at 72h
PC3 0.51
LNCaP 0.42
PREC 1.35
E
LNCaP
F
PC3
G
PrEC
MET
VPA
MET+VPA
Normalized confluence (%)
Log (Dose) (M)
A
LNCaP
% apoptosis
1 mM
2.5 mM
Dose
B
PC-3
Vehicle
MET
VPA
MET + VPA
C
PrEC
D
Combination index
LNCaP 0.03
PC3 2.62
PrEC 1.46
E
LNCaP
% cytochrome C
C M
Vehicle
MET
VPA
MET+VPA
F
PC-3
CV α
PDH-E1- α
Cytochrome C
β-actin

Figure 2.

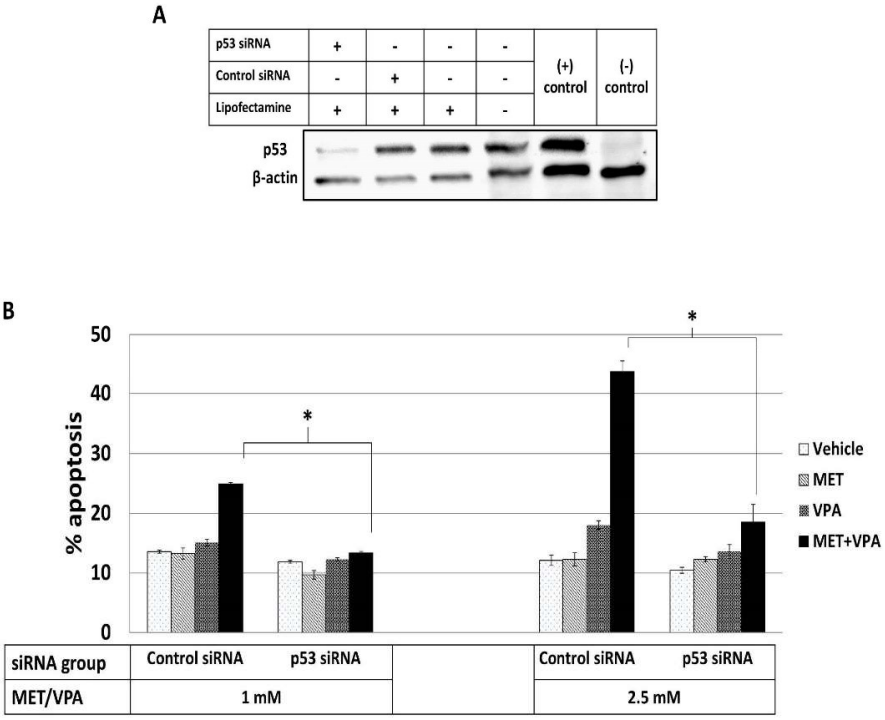

Figure 3.

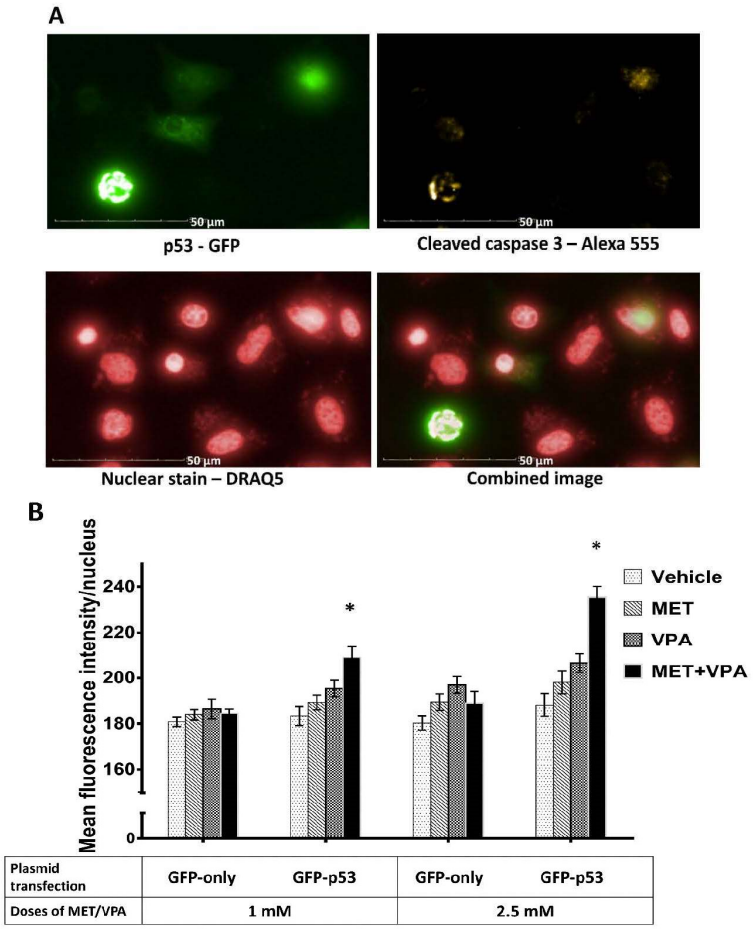

Figure 4.

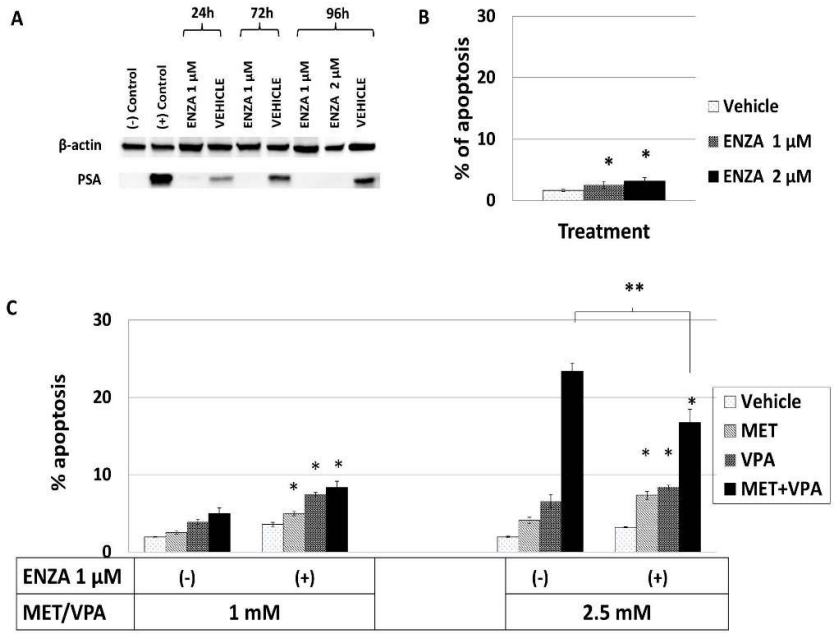

Figure 5.

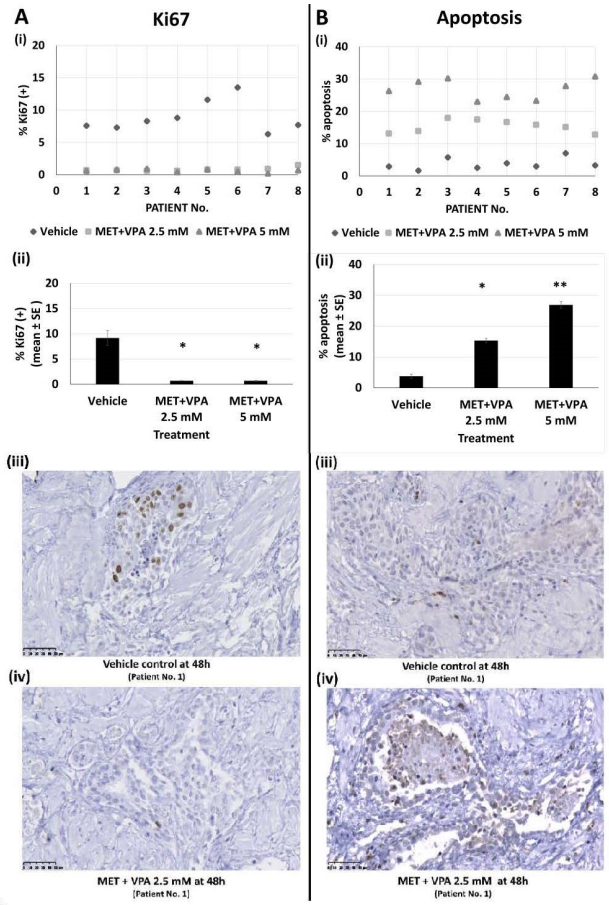

Figure 6.

REFERENCES

AIHW & AACR 2012, *Cancer in Australia: an overview 2012*, AIHW, Canberra.

Aimola, P, Carmignani, M, Volpe, AR, Di Benedetto, A, Claudio, L, Waalkes, MP, Van Bokhoven, A, Tokar, EJ & Claudio, PP 2012, 'Cadmium induces p53-dependent apoptosis in human prostate epithelial cells', *PLoS One*, vol. 7, no. 3, p. e33647.

Al-Hendy, A, Diamond, MP, Boyer, TG & Halder, SK 2016, 'Vitamin D3 inhibits Wnt/β-catenin and mTOR signaling pathways in human uterine fibroid cells', *The Journal of Clinical Endocrinology & Metabolism*, vol. 101, no. 4, pp. 1542-51.

Andriole, GL, Crawford, ED, Grubb III, RL, Buys, SS, Chia, D, Church, TR, Fouad, MN, Gelmann, EP, Kvale, PA & Reding, DJ 2009, 'Mortality results from a randomized prostate-cancer screening trial', *New England Journal of Medicine*, vol. 360, no. 13, pp. 1310-9.

Annicotte, JS, Iankova, I, Miard, S, Fritz, V, Sarruf, D, Abella, A, Berthe, ML, Noel, D, Pillon, A, Iborra, F, Dubus, P, Maudelonde, T, Culine, S & Fajas, L 2006, 'Peroxisome proliferator-activated receptor gamma regulates E-cadherin expression and inhibits growth and invasion of prostate cancer', *Mol Cell Biol*, vol. 26, no. 20, pp. 7561-74.

Attard, G, Swennenhuis, JF, Olmos, D, Reid, AH, Vickers, E, A'Hern, R, Levink, R, Coumans, F, Moreira, J & Riisnaes, R 2009, 'Characterization of ERG, AR and PTEN gene status in circulating tumor cells from patients with castration-resistant prostate cancer', *Cancer Res*, vol. 69, no. 7, pp. 2912-8.

Azoulay, L, Dell'Aniello, S, Gagnon, B, Pollak, M & Suissa, S 2011, 'Metformin and the incidence of prostate cancer in patients with type 2 diabetes', *Cancer Epidemiology Biomarkers & Prevention*, vol. 20, no. 2, pp. 337-44.

Babcook, MA, Shukla, S, Fu, P, Vazquez, EJ, Puchowicz, MA, Molter, JP, Oak, CZ, MacLennan, GT, Flask, CA & Lindner, DJ 2014, 'Synergistic Simvastatin and Metformin Combination Chemotherapy for Osseous Metastatic Castration-Resistant Prostate Cancer', *Mol Cancer Ther*, vol. 13, no. 10, pp. 2288-302.

Babcook, MA, Sramkoski, RM, Fujioka, H, Daneshgari, F, Almasan, A, Shukla, S, Nanavaty, RR & Gupta, S 2014, 'Combination simvastatin and metformin induces G1-phase cell cycle arrest and Ripk1- and Ripk3-dependent necrosis in C4-2B osseous metastatic castration-resistant prostate cancer cells', *Cell Death Dis*, vol. 5, p. e1536.

Bardin, CW, Brown, T, Isomaa, VV & Jänne, OA 1983, 'Progestins can mimic, inhibit and potentiate the actions of androgens', *Pharmacology & therapeutics*, vol. 23, no. 3, pp. 443-59.

Beer, TM, Armstrong, AJ, Rathkopf, DE, Loriot, Y, Sternberg, CN, Higano, CS, Iversen, P, Bhattacharya, S, Carles, J & Chowdhury, S 2014, 'Enzalutamide in metastatic prostate cancer before chemotherapy', *New England Journal of Medicine*, vol. 371, no. 5, pp. 424-33.

Ben-Sahra, I, Laurent, K, Giuliano, S, Larbret, F, Ponzio, G, Gounon, P, Le Marchand-Brustel, Y, Giorgetti-Peraldi, S, Cormont, M & Bertolotto, C 2010, 'Targeting cancer cell metabolism: the combination of metformin and 2-deoxyglucose induces p53-dependent apoptosis in prostate cancer cells', *Cancer Res*, vol. 70, no. 6, pp. 2465-75.

Ben-Sahra, I, Laurent, K, Loubat, A, Giorgetti-Peraldi, S, Colosetti, P, Auberger, P, Tanti, J-F, Le Marchand-Brustel, Y & Bost, F 2008, 'The antidiabetic drug metformin exerts an antitumoral effect in vitro and in vivo through a decrease of cyclin D1 level', *Oncogene*, vol. 27, no. 25, pp. 3576-86.

Ben-Sahra, I, Le Marchand-Brustel, Y, Tanti, J-F & Bost, F 2010, 'Metformin in cancer therapy: a new perspective for an old antidiabetic drug?', *Mol Cancer Ther*, vol. 9, no. 5, pp. 1092-9.

Ben-Sahra, I, Regazzetti, C, Robert, G, Laurent, K, Le Marchand-Brustel, Y, Auberger, P, Tanti, J-F, Giorgetti-Peraldi, S & Bost, F 2011, 'Metformin, independent of AMPK, induces mTOR inhibition and cell-cycle arrest through REDD1', *Cancer Res*, vol. 71, no. 13, pp. 4366-72.

Ben-Sahra, I, Tanti, JF & Bost, F 2010, 'The combination of metformin and 2 deoxyglucose inhibits autophagy and induces AMPK-dependent apoptosis in prostate cancer cells', *Autophagy*, vol. 6, no. 5, pp. 670-1.

Bennett, M, Macdonald, K, Chan, S-W, Luzio, JP, Simari, R & Weissberg, P 1998, 'Cell surface trafficking of Fas: a rapid mechanism of p53-mediated apoptosis', *Science*, vol. 282, no. 5387, pp. 290-3.

Bensaad, K & Vousden, KH 2007, 'p53: new roles in metabolism', *Trends in cell biology*, vol. 17, no. 6, pp. 286-91.

Bergheim, I, Guo, L, Davis, MA, Lambert, JC, Beier, JI, Duveau, I, Luyendyk, JP, Roth, RA & Arteel, GE 2006, 'Metformin prevents alcohol-induced liver injury in the mouse: critical role of plasminogen activator inhibitor-1', *Gastroenterology*, vol. 130, no. 7, pp. 2099-112.

Bertolini, F, Sukhatme, VP & Bouche, G 2015, 'Drug repurposing in oncology patient and health systems opportunities', *Nature Reviews Clinical Oncology*, vol. 12, no. 12, pp. 732-42.

Bhattacharya, SK, Ramchandani, S, Cervoni, N & Szyf, M 1999, 'A mammalian protein with specific demethylase activity for mCpG DNA', *Nature*, vol. 397, no. 6720, pp. 579-83.

Bilen, MA, Lin, SH, Tang, DG, Parikh, K, Lee, MH, Yeung, SC & Tu, SM 2015, 'Maintenance Therapy Containing Metformin and/or Zyflamend for Advanced Prostate Cancer: A Case Series', *Case Rep Oncol Med*, vol. 2015, p. 471861.

Bill-Axelson, A, Holmberg, L, Ruutu, M, Häggman, M, Andersson, S-O, Bratell, S, Spångberg, A, Busch, C, Nordling, S & Garmo, H 2005, 'Radical prostatectomy versus watchful waiting in early prostate cancer', *New England Journal of Medicine*, vol. 352, no. 19, pp. 1977-84.

Birsoy, K, Possemato, R, Lorbeer, FK, Bayraktar, EC, Thiru, P, Yucel, B, Wang, T, Chen, WW, Clish, CB & Sabatini, DM 2014, 'Metabolic determinants of cancer cell sensitivity to glucose limitation and biguanides', *Nature*, vol. 508, no. 7494, pp. 108-12.

Björkman, M, Iljin, K, Halonen, P, Sara, H, Kaivanto, E, Nees, M & Kallioniemi, OP 2008, 'Defining the molecular action of HDAC inhibitors and synergism with androgen deprivation in ERG-positive prostate cancer', *International Journal of Cancer*, vol. 123, no. 12, pp. 2774-81.

Blondal, J & Benchimol, S 1994, 'The role of p53 in tumor progression', in *Seminars in cancer biology*, vol. 5, pp. 177-86.

Bode, AM & Dong, Z 2004, 'Post-translational modification of p53 in tumorigenesis', *Nature Reviews Cancer*, vol. 4, no. 10, pp. 793-805.

Bolster, DR, Crozier, SJ, Kimball, SR & Jefferson, LS 2002, 'AMP-activated protein kinase suppresses protein synthesis in rat skeletal muscle through down-regulated mammalian target of rapamycin (mTOR) signaling', *Journal of Biological Chemistry*, vol. 277, no. 27, pp. 23977-80.

Bookstein, R, MacGrogan, D, Hilsenbeck, SG, Sharkey, F & Allred, DC 1993, 'p53 is mutated in a subset of advanced-stage prostate cancers', *Cancer Res*, vol. 53, no. 14, pp. 3369-73.

Bouzar, AB, Boxus, M, Defoiche, J, Berchem, G, Macallan, D, Pettengell, R, Willis, F, Burny, A, Lagneaux, L & Bron, D 2009, 'Valproate synergizes with purine nucleoside analogues to induce apoptosis of B-chronic lymphocytic leukaemia cells', *British journal of haematology*, vol. 144, no. 1, pp. 41-52.

Boyd, SD, Tsai, KY & Jacks, T 2000, 'An intact HDM2 RING-finger domain is required for nuclear exclusion of p53', *Nature cell biology*, vol. 2, no. 9, pp. 563-8.

Bradbury, C, Khanim, F, Hayden, R, Bunce, C, White, D, Drayson, M, Craddock, C & Turner, B 2005, 'Histone deacetylases in acute myeloid leukaemia show a distinctive pattern of expression that changes selectively in response to deacetylase inhibitors', *Leukemia*, vol. 19, no. 10, pp. 1751-9.

Briganti, A, Karnes, JR, Da Pozzo, LF, Cozzarini, C, Gallina, A, Suardi, N, Bianchi, M, Freschi, M, Doglioni, C & Fazio, F 2009, 'Two positive nodes represent a significant cut-off value for cancer specific survival in patients with node positive prostate cancer. A new proposal based on a two-institution experience on 703 consecutive N+ patients treated with radical prostatectomy, extended pelvic lymph node dissection and adjuvant therapy', *Eur Urol*, vol. 55, no. 2, pp. 261-70.

Burke, J & Thenot, J 1985, 'Determination of antiepileptic drugs', *Journal of Chromatography B: Biomedical Sciences and Applications*, vol. 340, pp. 199-241.

Burton, B 1882, 'On the propyl derivatives and decomposition products of ethylacetoacetate', *Am Chem J*, vol. 3, pp. 385-95.

Cai, J, Kandagatla, P, Singareddy, R, Kropinski, A, Sheng, S, Cher, ML & Chinni, SR 2010, 'Androgens induce functional CXCR4 through ERG factor expression in TMPRSS2-ERG fusion-positive prostate cancer cells', *Translational oncology*, vol. 3, no. 3, pp. 195-IN1.

Calabrese, JR & Delucchi, GA 1989, 'Phenomenology of rapid cycling manic depression and its treatment with valproate', *Journal of Clinical Psychiatry*.

Calleja, S, Salas-Puig, J, Ribacoba, R & Lahoz, C 2001, 'Evolution of juvenile myoclonic epilepsy treated from the outset with sodium valproate', *Seizure*, vol. 10, no. 6, pp. 424-7.

Carroll, AG, Voeller, HJ, Sugars, L & Gelmann, EP 1993, 'p53 oncogene mutations in three human prostate cancer cell lines', *Prostate*, vol. 23, no. 2, pp. 123-34.

Carver, BS, Tran, J, Gopalan, A, Chen, Z, Shaikh, S, Carracedo, A, Alimonti, A, Nardella, C, Varmeh, S & Scardino, PT 2009, 'Aberrant ERG expression cooperates with loss of PTEN to promote cancer progression in the prostate', *Nature genetics*, vol. 41, no. 5, pp. 619-24.

Centenera, MM, Gillis, JL, Hanson, AR, Jindal, S, Taylor, RA, Risbridger, GP, Sutherland, PD, Scher, HI, Raj, GV & Knudsen, KE 2012, 'Evidence for efficacy of new Hsp90 inhibitors revealed by ex vivo culture of human prostate tumors', *Clinical cancer research*, vol. 18, no. 13, pp. 3562-70.

Centenera, MM, Raj, GV, Knudsen, KE, Tilley, WD & Butler, LM 2013, 'Ex vivo culture of human prostate tissue and drug development', *Nature Reviews Urology*.

Cerezo, M, Tichet, M, Abbe, P, Ohanna, M, Lehraiki, A, Rouaud, F, Allegra, M, Giacchero, D, Bahadoran, P & Bertolotto, C 2013, 'Metformin blocks melanoma invasion and metastasis development in AMPK/p53-dependent manner', *Mol Cancer Ther*, vol. 12, no. 8, pp. 1605-15.

Cervoni, N, Detich, N, Seo, S-B, Chakravarti, D & Szyf, M 2002, 'The oncoprotein Set/TAF-1β, an inhibitor of histone acetyltransferase, inhibits active demethylation of DNA, integrating DNA methylation and transcriptional silencing', *Journal of Biological Chemistry*, vol. 277, no. 28, pp. 25026-31.

Cervoni, N & Szyf, M 2001, 'Demethylase activity is directed by histone acetylation', *Journal of Biological Chemistry*, vol. 276, no. 44, pp. 40778-87.

Chateauvieux, S, Dicato, M, Diederich, M & Morceau, F 2010, 'Molecular and therapeutic potential and toxicity of valproic acid', *Journal of Biomedicine and Biotechnology*.

Chen-Pin, W, Javier, H, Lorenzo, C, Downs, JR, Thompson, IM, Pollock, B & Lehman, D 2014, 'Statins and Finasteride Use Differentially Modify the Impact of Metformin on Prostate Cancer Incidence in Men with Type 2 Diabetes', *Ann Transl Med Epidemiol*, vol. 1, no. 1.

Chen, H, Dzitoyeva, S & Manev, H 2012, 'Effect of valproic acid on mitochondrial epigenetics', *European journal of pharmacology*, vol. 690, no. 1, pp. 51-9.

Chen, L, Ahmad, N & Liu, X 2016, 'Combining p53 stabilizers with metformin induces synergistic apoptosis through regulation of energy metabolism in castration-resistant prostate cancer', *Cell Cycle*, vol. 15, no. 6, pp. 840-9.

Chen, S-m, Mukoyama, T, Sato, N, Yamagata, S-I, Arai, Y, Satoh, N & Ueda, S 2002, 'Induction of nephrotoxic serum nephritis in inbred mice and suppressive effect of colchicine on the development of this nephritis', *Pharmacological Research*, vol. 45, no. 4, pp. 319-24.

Chen, X, Wong, JY, Wong, P & Radany, EH 2011, 'Low-dose valproic acid enhances radiosensitivity of prostate cancer through acetylated p53-dependent modulation of mitochondrial membrane potential and apoptosis', *Molecular Cancer Research*.

Chen, Y, Pan, RL, Zhang, XL, Shao, JZ, Xiang, LX, Dong, XJ & Zhang, GR 2009, 'Induction of hepatic differentiation of mouse bone marrow stromal stem cells by the histone deacetylase inhibitor VPA', *Journal of cellular and molecular medicine*, vol. 13, no. 8b, pp. 2582-92.

Chipuk, JE, Kuwana, T, Bouchier-Hayes, L, Droin, NM, Newmeyer, DD, Schuler, M & Green, DR 2004, 'Direct activation of Bax by p53 mediates mitochondrial membrane permeabilization and apoptosis', *Science*, vol. 303, no. 5660, pp. 1010-4.

Chou, T-C 2010, 'Drug combination studies and their synergy quantification using the Chou-Talalay method', *Cancer Res*, vol. 70, no. 2, pp. 440-6.

Chou, T-C & Talalay, P 1984, 'Quantitative analysis of dose-effect relationships: the combined effects of multiple drugs or enzyme inhibitors', *Advances in enzyme regulation*, vol. 22, pp. 27-55.

Chou, Y-W, Chaturvedi, NK, Ouyang, S, Lin, F-F, Kaushik, D, Wang, J, Kim, I & Lin, M-F 2011, 'Histone deacetylase inhibitor valproic acid suppresses the growth and increases the androgen responsiveness of prostate cancer cells', *Cancer letters*, vol. 311, no. 2, pp. 177-86.

Christofk, HR, Vander Heiden, MG, Harris, MH, Ramanathan, A, Gerszten, RE, Wei, R, Fleming, MD, Schreiber, SL & Cantley, LC 2008, 'The M2 splice isoform of pyruvate kinase is important for cancer metabolism and tumour growth', *Nature*, vol. 452, no. 7184, pp. 230-3.

Cifuentes, FF, Valenzuela, RH, Contreras, HR & Castellón, EA 2015, 'Development of an orthotopic model of human metastatic prostate cancer in the NOD-SCIDγ mouse (Mus musculus) anterior prostate', *Oncol Lett*, vol. 10, no. 4, pp. 2142-8.

Cohen, HY, Lavu, S, Bitterman, KJ, Hekking, B, Imahiyerobo, TA, Miller, C, Frye, R, Ploegh, H, Kessler, BM & Sinclair, DA 2004, 'Acetylation of the C terminus of Ku70 by CBP and PCAF controls Bax-mediated apoptosis', *Molecular cell*, vol. 13, no. 5, pp. 627-38.

Colella, AD, Chegenii, N, Tea, MN, Gibbins, IL, Williams, KA & Chataway, TK 2012, 'Comparison of stain-free gels with traditional immunoblot loading control methodology', *Analytical biochemistry*, vol. 430, no. 2, pp. 108-10.

Colquhoun, A, Venier, N, Vandersluis, A, Besla, R, Sugar, L, Kiss, A, Fleshner, N, Pollak, M, Klotz, L & Venkateswaran, V 2012, 'Metformin enhances the antiproliferative and apoptotic effect of bicalutamide in prostate cancer', *Prostate Cancer Prostatic Dis*, vol. 15, no. 4, pp. 346-52.

Condorelli, F, Gnemmi, I, Vallario, A, Genazzani, A & Canonico, P 2008, 'Inhibitors of histone deacetylase (HDAC) restore the p53 pathway in neuroblastoma cells', *British journal of pharmacology*, vol. 153, no. 4, pp. 657-68.

Coppola, G, Auricchio, G, Federico, R, Carotenuto, M & Pascotto, A 2004, 'Lamotrigine versus Valproic Acid as First-line Monotherapy in Newly Diagnosed Typical Absence Seizures: An Open-label, Randomized, Parallel-group Study', *Epilepsia*, vol. 45, no. 9, pp. 1049-53.

Currie, C, Poole, C & Gale, E 2009, 'The influence of glucose-lowering therapies on cancer risk in type 2 diabetes', *Diabetologia*, vol. 52, no. 9, pp. 1766-77.

D'Amico, AV, Moul, J, Carroll, PR, Sun, L, Lubeck, D & Chen, M-H 2003, 'Cancer-specific mortality after surgery or radiation for patients with clinically localized prostate cancer managed during the prostate-specific antigen era', *Journal of Clinical Oncology*, vol. 21, no. 11, pp. 2163-72.

Danzig, MR, Kotamarti, S, Ghandour, RA, Rothberg, MB, Dubow, BP, Benson, MC, Badani, KK & McKiernan, JM 2015, 'Synergism between metformin and statins in modifying the risk of biochemical recurrence following radical prostatectomy in men with diabetes', *Prostate Cancer Prostatic Dis*, vol. 18, no. 1, pp. 63-8.

David, KA, Mongan, NP, Smith, C, Gudas, LJ & Nanus, DM 2010, 'Phase I trial of ATRA-IV and Depakote in patients with advanced solid tumor malignancies', *Cancer Biol Ther*, vol. 9, no. 9, pp. 678-84.

Davoodpour, P, Landström, M & Welsh, M 2007, 'Reduced tumor growth in vivo and increased c-Abl activity in PC3 prostate cancer cells overexpressing the Shb adapter protein', *BMC Cancer*, vol. 7, no. 1, p. 161.

Dean, JC & Penry, JK 1988, 'Valproate monotherapy in 30 patients with partial seizures', *Epilepsia*, vol. 29, no. 2, pp. 140-4.

Dienstmann, R, Jang, IS, Bot, B, Friend, S & Guinney, J 2015, 'Database of genomic biomarkers for cancer drugs and clinical targetability in solid tumors', *Cancer discovery*, vol. 5, no. 2, pp. 118-23.

Doran, E & Halestrap, AP 2000, 'Evidence that metformin exerts its anti-diabetic effects through inhibition of complex 1 of the mitochondrial respiratory chain', *Biochemical Journal*, vol. 348, no. 3, pp. 607-14.

Dowling, RJ, Niraula, S, Stambolic, V & Goodwin, PJ 2012, 'Metformin in cancer: translational challenges', *Journal of molecular endocrinology*, vol. 48, no. 3, pp. R31-R43.

Duenas-Gonzalez, A, Candelaria, M, Perez-Plascencia, C, Perez-Cardenas, E, de la Cruz-Hernandez, E & Herrera, LA 2008, 'Valproic acid as epigenetic cancer drug: preclinical, clinical and transcriptional effects on solid tumors', *Cancer treatment reviews*, vol. 34, no. 3, pp. 206-22.

Eaton, SL, Roche, SL, Hurtado, ML, Oldknow, KJ, Farquharson, C, Gillingwater, TH & Wishart, TM 2013, 'Total protein analysis as a reliable loading control for quantitative fluorescent Western blotting', *PLoS One*, vol. 8, no. 8, p. e72457.

Ecke, TH, Schlechte, HH, Hübsch, A, Lenk, SV, Schiemenz, K, Rudolph, BD & Miller, K 2007, 'TP53 mutation in prostate needle biopsies-comparison with patients follow-up', *Anticancer Res*, vol. 27, no. 6B, pp. 4143-8.

Ecke, TH, Schlechte, HH, Schiemenz, K, Sachs, MD, Lenk, SV, Rudolph, BD & Loening, SA 2010, 'TP53 gene mutations in prostate cancer progression', *Anticancer Res*, vol. 30, no. 5, pp. 1579-86.

Edge, SB & Compton, CC 2010, 'The American Joint Committee on Cancer: the 7th edition of the AJCC cancer staging manual and the future of TNM', *Annals of surgical oncology*, vol. 17, no. 6, pp. 1471-4.

eHealthMe 2016, 'eHealthMe study from FDA and social media reports', *eHealthMe report*.

El Sheikh, SS, Romanska, HM, Abel, P, Domin, J & Lalani, E-N 2008, 'Predictive value of PTEN and AR coexpression of sustained responsiveness to hormonal therapy in prostate cancer—a pilot study', *Neoplasia*, vol. 10, no. 9, pp. 949-53.

Engel, J, Bastian, PJ, Baur, H, Beer, V, Chaussy, C, Gschwend, JE, Oberneder, R, Rothenberger, KH, Stief, CG & Hölzel, D 2010, 'Survival benefit of radical prostatectomy in lymph node–positive patients with prostate cancer', *Eur Urol*, vol. 57, no. 5, pp. 754-61.

Erenberg, G & Rothner, AD 1982, 'Valproic acid in the treatment of intractable absence seizures in children: a single-blind clinical and quantitative EEG study', *Archives of Pediatrics & Adolescent Medicine*, vol. 136, no. 6, p. 526.

FDA 2015, *Dockets Management of Metformin tablet*, U.S Food and Drug Administration, viewed May 2016, <http://www.fda.gov/ohrms/dockets/dailys/02/May02/053102/800471e6.pdf>.

Feldman, BJ & Feldman, D 2001, 'The development of androgen-independent prostate cancer', *Nature Reviews Cancer*, vol. 1, no. 1, pp. 34-45.

Fendt, S-M, Bell, EL, Keibler, MA, Davidson, SM, Wirth, GJ, Fiske, B, Mayers, JR, Schwab, M, Bellinger, G & Csibi, A 2013, 'Metformin decreases glucose oxidation and increases the dependency of prostate cancer cells on reductive glutamine metabolism', *Cancer Res*, vol. 73, no. 14, pp. 4429-38.

Feng, Z, Hu, W, De Stanchina, E, Teresky, AK, Jin, S, Lowe, S & Levine, AJ 2007, 'The regulation of AMPK β1, TSC2, and PTEN expression by p53: stress, cell and tissue specificity, and the role of these gene products in modulating the IGF-1-AKT-mTOR pathways', *Cancer Res*, vol. 67, no. 7, pp. 3043-53.

Feng, Z & Levine, AJ 2010, 'The regulation of energy metabolism and the IGF-1/mTOR pathways by the p53 protein', *Trends in cell biology*, vol. 20, no. 7, pp. 427-34.

Ferlay, J, Shin, HR, Bray, F, Forman, D, Mathers, C & Parkin, DM 2010, 'Estimates of worldwide burden of cancer in 2008: GLOBOCAN 2008', *International Journal of Cancer*, vol. 127, no. 12, pp. 2893-917.

Fogh, J, Tiso, J, Orfeo, T, Fogh, J, Daniels, W & Sharkey, F 1982, 'Analysis of human tumor growth in nude mice', in *Proceedings of the third international workshop on nude mice*, vol. 2, pp. 447-56.

Fortson, WS, Kayarthodi, S, Fujimura, Y, Xu, H, Matthews, R, Grizzle, WE, Rao, VN, Bhat, GK & Reddy, ESP 2011, 'Histone deacetylase inhibitors, valproic acid and trichostatin-A induce apoptosis and affect acetylation status of p53 in ERG-positive prostate cancer cells', *Int J Oncol*, vol. 39, no. 1, p. 111.

Frank, GR 2003, 'Role of estrogen and androgen in pubertal skeletal physiology', *Pediatric Blood & Cancer*, vol. 41, no. 3, pp. 217-21.

Friis, M 1998, 'Valproate in the treatment of epilepsy in people with intellectual disability', *Journal of intellectual disability research: JIDR*, vol. 42, pp. 32-5.

Gaughan, L, Logan, IR, Cook, S, Neal, DE & Robson, CN 2002, 'Tip60 and histone deacetylase 1 regulate androgen receptor activity through changes to the acetylation status of the receptor', *Journal of Biological Chemistry*, vol. 277, no. 29, pp. 25904-13.

Gavrilov, V, Leibovich, Y, Ariad, S, Lavrenkov, K & Shany, S 2010, 'A combined pretreatment of 1,25-dihydroxyvitamin D3 and sodium valproate enhances the damaging effect of ionizing radiation on prostate cancer cells', *J Steroid Biochem Mol Biol*, vol. 121, no. 1-2, pp. 391-4.

Gerlinger, M, Rowan, AJ, Horswell, S, Larkin, J, Endesfelder, D, Gronroos, E, Martinez, P, Matthews, N, Stewart, A & Tarpey, P 2012, 'Intratumor heterogeneity and branched evolution revealed by multiregion sequencing', *N Engl j Med*, vol. 2012, no. 366, pp. 883-92.

Ghavamian, R, Bergstralh, EJ, Blute, ML, Slezak, J & Zincke, H 1999, 'Radical retropubic prostatectomy plus orchiectomy versus orchiectomy alone for pTxN+ prostate cancer: a matched comparison', *J Urol*, vol. 161, no. 4, pp. 1223-8.

Gonnissen, A, Isebaert, S, McKee, CM, Muschel, RJ & Haustermans, K 2017, 'The Effect of Metformin and GANT61 Combinations on the Radiosensitivity of Prostate Cancer Cells', *Int J Mol Sci*, vol. 18, no. 2.

Gonzalgo, ML & Isaacs, WB 2003, 'Molecular pathways to prostate cancer', *J Urol*, vol. 170, no. 6, pp. 2444-52.

Gotlieb, WH, Saumet, J, Beauchamp, M-C, Gu, J, Lau, S, Pollak, MN & Bruchim, I 2008, 'In vitro metformin anti-neoplastic activity in epithelial ovarian cancer', *Gynecologic oncology*, vol. 110, no. 2, pp. 246-50.

Göttlicher, M, Minucci, S, Zhu, P, Krämer, OH, Schimpf, A, Giavara, S, Sleeman, JP, Coco, FL, Nervi, C & Pelicci, PG 2001, 'Valproic acid defines a novel class of HDAC

inhibitors inducing differentiation of transformed cells', *The EMBO journal*, vol. 20, no. 24, pp. 6969-78.

Gottlieb, B, Lehvaslaiho, H, Beitel, LK, Lumbroso, R, Pinsky, L & Trifiro, M 1998, 'The androgen receptor gene mutations database', *Nucleic Acids Research*, vol. 26, no. 1, pp. 234-8.

Gou, S, Cui, P, Li, X, Shi, P, Liu, T & Wang, C 2013, 'Low concentrations of metformin selectively inhibit CD133+ cell proliferation in pancreatic cancer and have anticancer action', *PLoS One*, vol. 8, no. 5, p. e63969.

Gravis, G, Fizazi, K, Joly, F, Oudard, S, Priou, F, Esterni, B, Latorzeff, I, Delva, R, Krakowski, I & Laguerre, B 2013, 'Androgen-deprivation therapy alone or with docetaxel in non-castrate metastatic prostate cancer (GETUG-AFU 15): a randomised, open-label, phase 3 trial', *The Lancet Oncology*, vol. 14, no. 2, pp. 149-58.

Graziani, G, Tentori, L, Portarena, I, Vergati, M & Navarra, P 2003, 'Valproic acid increases the stimulatory effect of estrogens on proliferation of human endometrial adenocarcinoma cells', *Endocrinology*, vol. 144, no. 7, pp. 2822-8.

Grönberg, H 2003, 'Prostate cancer epidemiology', *The Lancet*, vol. 361, no. 9360, pp. 859-64.

Gu, W & Roeder, RG 1997, 'Activation of p53 sequence-specific DNA binding by acetylation of the p53 C-terminal domain', *Cell*, vol. 90, no. 4, pp. 595-606.

Guerrero, J, Alfaro, IE, Gómez, F, Protter, AA & Bernales, S 2013, 'Enzalutamide, an androgen receptor signaling inhibitor, induces tumor regression in a mouse model of castration-resistant prostate cancer', *Prostate*, vol. 73, no. 12, pp. 1291-305.

Gurvich, N, Tsygankova, OM, Meinkoth, JL & Klein, PS 2004, 'Histone deacetylase is a target of valproic acid-mediated cellular differentiation', *Cancer Res*, vol. 64, no. 3, pp. 1079-86.

Gustavsson, H, Tešan, T, Jennbacken, K, Kuno, K, Damber, J-E & Welén, K 2010, 'ADAMTS1 alters blood vessel morphology and TSP1 levels in LNCaP and LNCaP-19 prostate tumors', *BMC Cancer*, vol. 10, no. 1, p. 288.

Gwinn, DM, Shackelford, DB, Egan, DF, Mihaylova, MM, Mery, A, Vasquez, DS, Turk, BE & Shaw, RJ 2008, 'AMPK phosphorylation of raptor mediates a metabolic checkpoint', *Molecular cell*, vol. 30, no. 2, pp. 214-26.

Hardie, DG 2003, 'Minireview: the AMP-activated protein kinase cascade: the key sensor of cellular energy status', *Endocrinology*, vol. 144, no. 12, pp. 5179-83.

Hardie, DG 2007, 'AMP-activated/SNF1 protein kinases: conserved guardians of cellular energy', *Nature Reviews Molecular Cell Biology*, vol. 8, no. 10, pp. 774-85.

Hardy, JR, Rees, EA, Gwilliam, B, Ling, J, Broadley, K & A'Hern, R 2001, 'A phase II study to establish the efficacy and toxicity of sodium valproate in patients with cancer-related neuropathic pain', *Journal of pain and symptom management*, vol. 21, no. 3, pp. 204-9.

Harikrishnan, K, Karagiannis, TC, Chow, MZ & El-Osta, A 2008, 'Effect of valproic acid on radiation-induced DNA damage in euchromatic and heterochromatic compartments', *Cell Cycle-Landes Bioscience*, vol. 7, no. 4, p. 468.

Harris, WP, Mostaghel, EA, Nelson, PS & Montgomery, B 2009, 'Androgen deprivation therapy: progress in understanding mechanisms of resistance and optimizing androgen depletion', *Nature clinical practice Urology*, vol. 6, no. 2, pp. 76-85.

Hayakawa, S, Tochigi, M, Chishima, F, Shiraishi, H, Takahashi, N, Watanabe, K, Fujii, KT & Satoh, K 1996, 'Expression of the recombinase-activating gene (RAG-1) in murine early embryogenesis', *Immunol Cell Biol*, vol. 74, no. 1, pp. 52-6.

Heidenreich, A, Bastian, PJ, Bellmunt, J, Bolla, M, Joniau, S, van der Kwast, T, Mason, M, Matveev, V, Wiegel, T & Zattoni, F 2014a, 'EAU guidelines on prostate cancer. Part 1: screening, diagnosis, and local treatment with curative intent—update 2013', *Eur Urol*, vol. 65, no. 1, pp. 124-37.

Heidenreich, A, Bastian, PJ, Bellmunt, J, Bolla, M, Joniau, S, van der Kwast, T, Mason, M, Matveev, V, Wiegel, T & Zattoni, F 2014b, 'EAU guidelines on prostate cancer. Part II: treatment of advanced, relapsing, and castration-resistant prostate cancer', *Eur Urol*, vol. 65, no. 2, pp. 467-79.

Heidenreich, A, Bellmunt, J, Bolla, M, Joniau, S, Mason, M, Matveev, V, Mottet, N, Schmid, H-P, van der Kwast, T & Wiegel, T 2011, 'EAU guidelines on prostate cancer. Part 1: screening, diagnosis, and treatment of clinically localised disease', *Eur Urol*, vol. 59, no. 1, pp. 61-71.

Heinlein, CA & Chang, C 2004, 'Androgen receptor in prostate cancer', *Endocrine reviews*, vol. 25, no. 2, pp. 276-308.

Hermans, KG, van der Korput, HA, van Marion, R, van de Wijngaart, DJ, Ziel-van der Made, A, Dits, NF, Boormans, JL, van der Kwast, TH, van Dekken, H & Bangma, CH 2008, 'Truncated ETV1, fused to novel tissue-specific genes, and full-length ETV1 in prostate cancer', *Cancer Res*, vol. 68, no. 18, pp. 7541-9.

Hirsch, HA, Iliopoulos, D, Tsichlis, PN & Struhl, K 2009, 'Metformin selectively targets cancer stem cells, and acts together with chemotherapy to block tumor growth and prolong remission', *Cancer Res*, vol. 69, no. 19, pp. 7507-11.

Honjo, S, Ajani, JA, Scott, AW, Chen, Q, Skinner, HD, Stroehlein, J, Johnson, RL & Song, S 2014, 'Metformin sensitizes chemotherapy by targeting cancer stem cells and the mTOR pathway in esophageal cancer', *Int J Oncol*, vol. 45, no. 2, pp. 567-74.

Hooper, JD, Clements, JA, Quigley, JP & Antalis, TM 2001, 'Type II transmembrane serine proteases - insights into an emerging class of cell surface proteolytic enzymes', *Journal of Biological Chemistry*, vol. 276, no. 2, pp. 857-60.

Horoszewicz, JS, Leong, SS, Kawinski, E, Karr, JP, Rosenthal, H, Chu, TM, Mirand, EA & Murphy, GP 1983, 'LNCaP model of human prostatic carcinoma', *Cancer Res*, vol. 43, no. 4, pp. 1809-18.

Hsing, AW, Gao, Y-T, Wu, G, Wang, X, Deng, J, Chen, Y-L, Sesterhenn, IA, Mostofi, FK, Benichou, J & Chang, C 2000, 'Polymorphic CAG and GGN repeat lengths in the androgen receptor gene and prostate cancer risk: a population-based case-control study in China', *Cancer Res*, vol. 60, no. 18, pp. 5111-6.

Hudak, L, Tezeeh, P, Wedel, S, Makarevic, J, Juengel, E, Tsaur, I, Bartsch, G, Wiesner, C, Haferkamp, A & Blaheta, RA 2012, 'Low dosed interferon alpha augments the anti-tumor potential of histone deacetylase inhibition on prostate cancer cell growth and invasion', *Prostate*, vol. 72, no. 16, pp. 1719-35.

Huggins, C & Hodges, CV 1941, 'Studies on prostatic cancer. I. The effect of castration, of estrogen and of androgen injection on serum phosphatases in metastatic carcinoma of the prostate', *Cancer Res*, vol. 1, no. 4, pp. 293-7.

Iacopino, F, Urbano, R, Graziani, G, Muzi, A, Navarra, P & Sica, G 2008, 'Valproic acid activity in androgen-sensitive and-insensitive human prostate cancer cells', *Int J Oncol*, vol. 32, no. 6, pp. 1293-303.

Iliopoulos, D, Hirsch, HA & Struhl, K 2011, 'Metformin decreases the dose of chemotherapy for prolonging tumor remission in mouse xenografts involving multiple cancer cell types', *Cancer Res*, vol. 71, no. 9, pp. 3196-201.

James, ND, Sydes, MR, Clarke, NW, Mason, MD, Dearnaley, DP, Spears, MR, Ritchie, AW, Parker, CC, Russell, JM & Attard, G 2016, 'Addition of docetaxel, zoledronic acid, or both to first-line long-term hormone therapy in prostate cancer (STAMPEDE): survival results from an adaptive, multiarm, multistage, platform randomised controlled trial', *The Lancet*, vol. 387, no. 10024, pp. 1163-77.

Joerger, M, van Schaik, R, Becker, M, Hayoz, S, Pollak, M, Cathomas, R, Winterhalder, R, Gillessen, S & Rothermundt, C 2015, 'Multidrug and toxin extrusion 1 and human organic cation transporter 1 polymorphisms in patients with castration-resistant prostate cancer receiving metformin (SAKK 08/09)', *Prostate Cancer Prostatic Dis*, vol. 18, no. 2, pp. 167-72.

John, JS, Powell, K, Conley-LaComb, MK & Chinni, SR 2012, 'TMPRSS2-ERG fusion gene expression in prostate tumor cells and its clinical and biological significance in prostate cancer progression', *Journal of cancer science & therapy*, vol. 4, no. 4, p. 94.

Jones, RG, Plas, DR, Kubek, S, Buzzai, M, Mu, J, Xu, Y, Birnbaum, MJ & Thompson, CB 2005, 'AMP-activated protein kinase induces a p53-dependent metabolic checkpoint', *Molecular cell*, vol. 18, no. 3, pp. 283-93.

Kaighn, M, Narayan, KS, Ohnuki, Y, Lechner, J & Jones, L 1979, 'Establishment and characterization of a human prostatic carcinoma cell line (PC-3)', *Investigative urology*, vol. 17, no. 1, pp. 16-23.

Kantoff, PW, Higano, CS, Shore, ND, Berger, ER, Small, EJ, Penson, DF, Redfern, CH, Ferrari, AC, Dreicer, R & Sims, RB 2010, 'Sipuleucel-T immunotherapy for castration-resistant prostate cancer', *New England Journal of Medicine*, vol. 363, no. 5, pp. 411-22.

Kimura, N, Okuda, M & Inui, K-i 2005, 'Metformin transport by renal basolateral organic cation transporter hOCT2', *Pharmaceutical research*, vol. 22, no. 2, pp. 255-9.

Kleinman, HK & Martin, GR 2005, 'Matrigel: basement membrane matrix with biological activity', in *Seminars in cancer biology*, vol. 15, pp. 378-86.

Ko, LJ & Prives, C 1996, 'p53: puzzle and paradigm', *Genes & development*, vol. 10, no. 9, pp. 1054-72.

Kohler, BA, Ward, E, McCarthy, BJ, Schymura, MJ, Ries, LA, Eheman, C, Jemal, A, Anderson, RN, Ajani, UA & Edwards, BK 2011, 'Annual report to the nation on the status of cancer, 1975–2007, featuring tumors of the brain and other nervous system', *J Natl Cancer Inst*, vol. 103, no. 9, pp. 714-36.

Kozka, I, Clark, A, Reckless, J, Cushman, S, Gould, G & Holman, G 1995, 'The effects of insulin on the level and activity of the GLUT4 present in human adipose cells', *Diabetologia*, vol. 38, no. 6, pp. 661-6.

Kuczyk, M, Serth, J, Bokemeyer, C, Machtens, S, Minssen, A, Bathke, W, Hartmann, J & Jonas, U 1998, 'The prognostic value of p53 for long-term and recurrence-free survival following radical prostatectomy', *European Journal of Cancer*, vol. 34, no. 5, pp. 679-86.

Kumar-Sinha, C, Tomlins, SA & Chinnaiyan, AM 2008, 'Recurrent gene fusions in prostate cancer', *Nature Reviews Cancer*, vol. 8, no. 7, pp. 497-511.

Kumari, S, Schlanger, S, Wang, D, Liu, S & Heemers, H 2016, 'OR43-2: Defining Coregulator Contribution to AR-Dependent Transcription Uncovers a Novel AR-

WDR77-p53-Dependent Transcriptional Code', paper presented to Endocrine Society's 98th Annual Meeting and Expo, Boston.

Lane, D & Benchimol, S 1990, 'p53: oncogene or anti-oncogene', *Genes Dev*, vol. 4, no. 1, pp. 1-8.

Lee, J-H, Choy, M, Ngo, L, Foster, S & Marks, PA 2010, 'Histone deacetylase inhibitor induces DNA damage, which normal but not transformed cells can repair', *Proceedings of the National Academy of Sciences*, vol. 107, no. 33, pp. 14639-44.

Lehman, DM, Lorenzo, C, Hernandez, J & Wang, CP 2012, 'Statin use as a moderator of metformin effect on risk for prostate cancer among type 2 diabetic patients', *Diabetes care*, vol. 35, no. 5, pp. 1002-7.

Levine, AJ 1997, 'p53, the cellular gatekeeper for growth and division', *Cell*, vol. 88, no. 3, pp. 323-31.

Li, HX, Gao, JM, Liang, JQ, Xi, JM, Fu, M & Wu, YJ 2015, 'Vitamin D3 potentiates the growth inhibitory effects of metformin in DU145 human prostate cancer cells mediated by AMPK/mTOR signalling pathway', *Clin Exp Pharmacol Physiol*, vol. 42, no. 6, pp. 711-7.

Li, J, Yen, C, Liaw, D, Podsypanina, K, Bose, S, Wang, SI, Puc, J, Miliaresis, C, Rodgers, L & McCombie, R 1997, 'PTEN, a putative protein tyrosine phosphatase gene mutated in human brain, breast, and prostate cancer', *Science*, vol. 275, no. 5308, pp. 1943-7.

Li, Y, Chan, SC, Brand, LJ, Hwang, TH, Silverstein, KA & Dehm, SM 2013, 'Androgen receptor splice variants mediate enzalutamide resistance in castration-resistant prostate cancer cell lines', *Cancer Res*, vol. 73, no. 2, pp. 483-9.

Lilienfeld, AM 1983, 'Practical limitations of epidemiologic methods', *Environmental health perspectives*, vol. 52, p. 3.

Liu, Q-Y, Rubin, MA, Omene, C, Lederman, S & Stein, C 1998, 'Fas ligand is constitutively secreted by prostate cancer cells in vitro', *Clinical cancer research*, vol. 4, no. 7, pp. 1803-11.

Long, YC & Zierath, JR 2006, 'AMP-activated protein kinase signaling in metabolic regulation', *Journal of Clinical Investigation*, vol. 116, no. 7, pp. 1776-83.

Lowsley, OS 1912, 'The development of the human prostate gland with reference to the development of other structures at the neck of the urinary bladder', *American Journal of Anatomy*, vol. 13, no. 3, pp. 299-349.

Marcelli, M, Ittmann, M, Mariani, S, Sutherland, R, Nigam, R, Murthy, L, Zhao, Y, DiConcini, D, Puxeddu, E & Esen, A 2000, 'Androgen receptor mutations in prostate cancer', *Cancer Res*, vol. 60, no. 4, pp. 944-9.

Marchion, DC, Bicaku, E, Daud, AI, Sullivan, DM & Munster, PN 2005, 'Valproic acid alters chromatin structure by regulation of chromatin modulation proteins', *Cancer Res*, vol. 65, no. 9, pp. 3815-22.

Martirosyan, A, Leonard, S, Shi, X, Griffith, B, Gannett, P & Strobl, J 2006, 'Actions of a histone deacetylase inhibitor NSC3852 (5-nitroso-8-quinolinol) link reactive oxygen species to cell differentiation and apoptosis in MCF-7 human mammary tumor cells', *Journal of Pharmacology and Experimental Therapeutics*, vol. 317, no. 2, pp. 546-52.

Massie, CE, Lynch, A, Ramos-Montoya, A, Boren, J, Stark, R, Fazli, L, Warren, A, Scott, H, Madhu, B & Sharma, N 2011, 'The androgen receptor fuels prostate cancer by regulating central metabolism and biosynthesis', *The EMBO journal*, vol. 30, no. 13, pp. 2719-33.

Massoner, P, Kugler, KG, Unterberger, K, Kuner, R, Mueller, LA, Fälth, M, Schäfer, G, Seifarth, C, Ecker, S & Verdorfer, I 2013, 'Characterization of transcriptional changes in ERG rearrangement-positive prostate cancer identifies the regulation of metabolic sensors such as neuropeptide Y', *PLoS One*, vol. 8, no. 2, p. e55207.

Mayer, MJ, Klotz, LH & Venkateswaran, V 2017, 'The Effect of Metformin Use during Docetaxel Chemotherapy on Prostate Cancer Specific and Overall Survival of Diabetic Patients with Castration Resistant Prostate Cancer', *J Urol*, vol. 197, no. 4, pp. 1068-75.

McDougal, WS, Wein, AJ, Kavoussi, LR, Novick, AC, Partin, AW, Peters, CA & Ramchandani, P 2011, *Campbell-Walsh Urology 10th Edition Review*, Elsevier Health Sciences.

McMenamin, ME, Soung, P, Perera, S, Kaplan, I, Loda, M & Sellers, WR 1999, 'Loss of PTEN expression in paraffin-embedded primary prostate cancer correlates with high Gleason score and advanced stage', *Cancer Res*, vol. 59, no. 17, pp. 4291-6.

McNeal, JE 1981, 'The zonal anatomy of the prostate', *Prostate*, vol. 2, no. 1, pp. 35-49.

McNeal, JE 1988, 'Normal histology of the prostate', *The American journal of surgical pathology*, vol. 12, no. 8, pp. 619-33.

Mendler, MH, Kanel, G & Govindarajan, S 2005, 'Proposal for a histological scoring and grading system for non-alcoholic fatty liver disease', *Liver International*, vol. 25, no. 2, pp. 294-304.

Menendez, JA, Oliveras-Ferraros, C, Cufí, S, Corominas-Faja, B, Joven, J, Martin-Castillo, B & Vazquez-Martin, A 2012, 'Metformin is synthetically lethal with glucose withdrawal in cancer cells', *Cell Cycle*, vol. 11, no. 15, pp. 2782-92.

Mesdjian, E, Ciesielski, L, Valli, M, Bruguerolle, B, Jadot, G, Bouyard, P & Mandel, P 1982, 'Sodium valproate: kinetic profile and effects on GABA levels in various brain areas of the rat', *Progress in Neuro-Psychopharmacology and Biological Psychiatry*, vol. 6, no. 3, pp. 223-33.

Meunier, H, Carraz, G, Neunier, Y, Eymard, P & Aimard, M 1962, 'Pharmacodynamic properties of N-dipropylacetic acid', *Therapie*, vol. 18, pp. 435-8.

Minucci, S & Pelicci, PG 2006, 'Histone deacetylase inhibitors and the promise of epigenetic (and more) treatments for cancer', *Nature Reviews Cancer*, vol. 6, no. 1, pp. 38-51.

Monteagudo, S, Perez-Martinez, FC, Perez-Carrion, MD, Guerra, J, Merino, S, Sanchez-Verdu, MP & Cena, V 2012, 'Inhibition of p42 MAPK using a nonviral vector-delivered siRNA potentiates the anti-tumor effect of metformin in prostate cancer cells', *Nanomedicine (Lond)*, vol. 7, no. 4, pp. 493-506.

Müller, M, Wilder, S, Bannasch, D, Israeli, D, Lehlbach, K, Li-Weber, M, Friedman, SL, Galle, PR, Stremmel, W & Oren, M 1998, 'p53 activates the CD95 (APO-1/Fas) gene in response to DNA damage by anticancer drugs', *The Journal of experimental medicine*, vol. 188, no. 11, pp. 2033-45.

Murakami, K, Mavrothalassitis, G, Bhat, N, Fisher, R & Papas, T 1993, 'Human ERG-2 protein is a phosphorylated DNA-binding protein--a distinct member of the ets family', *Oncogene*, vol. 8, no. 6, pp. 1559-66.

Murtola, TJ, Tammela, TL, Lahtela, J & Auvinen, A 2008, 'Antidiabetic medication and prostate cancer risk: a population-based case-control study', *American journal of epidemiology*, vol. 168, no. 8, pp. 925-31.

Nagata, S & Golstein, P 1995, 'The Fas death factor', *Science*, vol. 267, no. 5203, pp. 1449-56.

Nightingale, KP, Gendreizig, S, White, DA, Bradbury, C, Hollfelder, F & Turner, BM 2007, 'Cross-talk between Histone Modifications in Response to Histone Deacetylase Inhibitors MLL4 LINKS HISTONE H3 ACETYLATION AND HISTONE H3K4 METHYLATION', *Journal of Biological Chemistry*, vol. 282, no. 7, pp. 4408-16.

Nobes, JP, Langley, SE, Klopper, T, Russell-Jones, D & Laing, RW 2012, 'A prospective, randomized pilot study evaluating the effects of metformin and lifestyle intervention on patients with prostate cancer receiving androgen deprivation therapy', *BJU Int*, vol. 109, no. 10, pp. 1495-502.

Okoshi, R, Ozaki, T, Yamamoto, H, Ando, K, Koida, N, Ono, S, Koda, T, Kamijo, T, Nakagawara, A & Kizaki, H 2008, 'Activation of AMP-activated protein kinase induces p53-dependent apoptotic cell death in response to energetic stress', *Journal of Biological Chemistry*, vol. 283, no. 7, pp. 3979-87.

Ouyang, D-y, Ji, Y-h, Saltis, M, Xu, L-h, Zhang, Y-t, Zha, Q-b, Cai, J-y & He, X-h 2011, 'Valproic acid synergistically enhances the cytotoxicity of gossypol in DU145 prostate cancer cells: An iTRTAQ-based quantitative proteomic analysis', *J Proteomics*, vol. 74, no. 10, pp. 2180-93.

Owen-Schaub, LB, Zhang, W, Cusack, JC, Angelo, LS, Santee, SM, Fujiwara, T, Roth, JA, Deisseroth, AB, Zhang, W-W & Kruzel, E 1995, 'Wild-type human p53 and a temperature-sensitive mutant induce Fas/APO-1 expression', *Mol Cell Biol*, vol. 15, no. 6, pp. 3032-40.

Paller, CJ, Wissing, MD, Mendonca, J, Sharma, A, Kim, E, Kim, HS, Kortenhorst, MS, Gerber, S, Rosen, M, Shaikh, F, Zahurak, ML, Rudek, MA, Hammers, H, Rudin, CM, Carducci, MA & Kachhap, SK 2014, 'Combining the pan-aurora kinase inhibitor AMG 900 with histone deacetylase inhibitors enhances antitumor activity in prostate cancer', *Cancer Med*, vol. 3, no. 5, pp. 1322-35.

Pennanen, P, Syvala, H, Blauer, M, Savinainen, K, Ylikomi, T, Tammela, TL & Murtola, TJ 2016, 'The effects of metformin and simvastatin on the growth of LNCaP and RWPE-1 prostate epithelial cell lines', *Eur J Pharmacol*, vol. 788, pp. 160-7.

Pettaway, CA, Pathak, S, Greene, G, Ramirez, E, Wilson, MR, Killion, JJ & Fidler, IJ 1996, 'Selection of highly metastatic variants of different human prostatic carcinomas using orthotopic implantation in nude mice', *Clinical cancer research*, vol. 2, no. 9, pp. 1627-36.

Pflueger, D, Rickman, DS, Sboner, A, Perner, S, LaFargue, CJ, Svensson, MA, Moss, BJ, Kitabayashi, N, Pan, Y & de la Taille, A 2009, 'N-myc downstream regulated gene 1 (NDRG1) is fused to ERG in prostate cancer', *Neoplasia (New York, NY)*, vol. 11, no. 8, p. 804.

Qian, DZ, Wang, X, Kachhap, SK, Kato, Y, Wei, Y, Zhang, L, Atadja, P & Pili, R 2004, 'The histone deacetylase inhibitor NVP-LAQ824 inhibits angiogenesis and has a greater antitumor effect in combination with the vascular endothelial growth factor receptor tyrosine kinase inhibitor PTK787/ZK222584', *Cancer Res*, vol. 64, no. 18, pp. 6626-34.

Reagan-Shaw, S, Nihal, M & Ahmad, N 2008, 'Dose translation from animal to human studies revisited', *The FASEB Journal*, vol. 22, no. 3, pp. 659-61.

Reddy, E, Rao, VN & Papas, TS 1987, 'The erg gene: a human gene related to the ets oncogene', *Proceedings of the National Academy of Sciences*, vol. 84, no. 17, pp. 6131-5.

Reid, A, Attard, G, Ambroisine, L, Fisher, G, Kovacs, G, Brewer, D, Clark, J, Flohr, P, Edwards, S & Berney, D 2010, 'Molecular characterisation of ERG, ETV1 and PTEN gene loci identifies patients at low and high risk of death from prostate cancer', *Br J Cancer*, vol. 102, no. 4, pp. 678-84.

Rickman, DS, Pflueger, D, Moss, B, VanDoren, VE, Chen, CX, de la Taille, A, Kuefer, R, Tewari, AK, Setlur, SR & Demichelis, F 2009, 'SLC45A3-ELK4 is a novel and frequent erythroblast transformation–specific fusion transcript in prostate cancer', *Cancer Res*, vol. 69, no. 7, pp. 2734-8.

Rider, JR, Sandin, F, Andrén, O, Wiklund, P, Hugosson, J & Stattin, P 2013, 'Long-term outcomes among noncuratively treated men according to prostate cancer risk category in a nationwide, population-based study', *Eur Urol*, vol. 63, no. 1, pp. 88-96.

Robinson, D, Van Allen, EM, Wu, Y-M, Schultz, N, Lonigro, RJ, Mosquera, J-M, Montgomery, B, Taplin, M-E, Pritchard, CC & Attard, G 2015, 'Integrative Clinical Genomics of Advanced Prostate Cancer', *Cell*, vol. 161, no. 5, pp. 1215-28.

Rodd, AL, Ververis, K & Karagiannis, TC 2012, 'Current and Emerging Therapeutics for Cutaneous T-Cell Lymphoma: Histone Deacetylase Inhibitors', *Lymphoma*, vol. 2012.

Rosato, RR, Almenara, JA & Grant, S 2003, 'The histone deacetylase inhibitor MS-275 promotes differentiation or apoptosis in human leukemia cells through a process regulated by generation of reactive oxygen species and induction of p21CIP1/WAF1', *Cancer Res*, vol. 63, no. 13, pp. 3637-45.

Rosner, B 2015, *Fundamentals of biostatistics*, Nelson Education.

Rothermundt, C, Hayoz, S, Templeton, AJ, Winterhalder, R, Strebel, RT, Bärtschi, D, Pollak, M, Lui, L, Endt, K & Schiess, R 2014, 'Metformin in chemotherapy-naive castration-resistant prostate cancer: a multicenter phase 2 trial (SAKK 08/09)', *Eur Urol*.

Rubin, MA, Maher, CA & Chinnaiyan, AM 2011, 'Common gene rearrangements in prostate cancer', *Journal of Clinical Oncology*, vol. 29, no. 27, pp. 3659-68.

Ryan, CJ, Smith, MR, Fizazi, K, Saad, F, Mulders, PF, Sternberg, CN, Miller, K, Logothetis, CJ, Shore, ND & Small, EJ 2015, 'Abiraterone acetate plus prednisone versus placebo plus prednisone in chemotherapy-naive men with metastatic castration-resistant prostate cancer (COU-AA-302): final overall survival analysis of a randomised, double-blind, placebo-controlled phase 3 study', *The Lancet Oncology*, vol. 16, no. 2, pp. 152-60.

Ryu, B, Jones, J, Blades, NJ, Parmigiani, G, Hollingsworth, MA, Hruban, RH & Kern, SE 2002, 'Relationships and differentially expressed genes among pancreatic cancers examined by large-scale serial analysis of gene expression', *Cancer Res*, vol. 62, no. 3, pp. 819-26.

Saha, A, Blando, J, Tremmel, L & DiGiovanni, J 2015, 'Effect of Metformin, Rapamycin, and Their Combination on Growth and Progression of Prostate Tumors in HiMyc Mice', *Cancer Prev Res (Phila)*, vol. 8, no. 7, pp. 597-606.

Sakr, W, Haas, G, Cassin, B, Pontes, J & Crissman, J 1993, 'The frequency of carcinoma and intraepithelial neoplasia of the prostate in young male patients', *J Urol*, vol. 150, no. 2, pp. 379-85.

Savickiene, J, Borutinskaite, V-V, Treigyte, G, Magnusson, K-E & Navakauskiene, R 2006, 'The novel histone deacetylase inhibitor BML-210 exerts growth inhibitory, proapoptotic and differentiation stimulating effects on the human leukemia cell lines', *European journal of pharmacology*, vol. 549, no. 1, pp. 9-18.

Schobben, F, van der Kleijn, E & Vree, TB 1980, 'Therapeutic monitoring of valproic acid', *Therapeutic drug monitoring*, vol. 2, no. 1, pp. 61-72.

Schröder, FH, Hugosson, J, Roobol, MJ, Tammela, TL, Ciatto, S, Nelen, V, Kwiatkowski, M, Lujan, M, Lilja, H & Zappa, M 2009, 'Screening and prostate-cancer mortality in a randomized European study', *New England Journal of Medicine*, vol. 360, no. 13, pp. 1320-8.

Shabbeer, S, SQ Kortenhorst, M, Kachhap, S, Galloway, N, Rodriguez, R & Carducci, MA 2007, 'Multiple Molecular pathways explain the anti-proliferative effect of valproic acid on prostate cancer cells in vitro and in vivo', *Prostate*, vol. 67, no. 10, pp. 1099-110.

Shah, ET, Upadhyaya, A, Philp, LK, Tang, T, Skalamera, D, Gunter, J, Nelson, CC, Williams, ED & Hollier, BG 2016, 'Repositioning "old" drugs for new causes: identifying new inhibitors of prostate cancer cell migration and invasion', *Clin Exp Metastasis*, vol. 33, no. 4, pp. 385-99.

Sharkey, FE & Fogh, J 1979, 'Metastasis of human tumors in athymic nude mice', *International Journal of Cancer*, vol. 24, no. 6, pp. 733-8.

Sharma, S, Symanowski, J, Wong, B, Dino, P, Manno, P & Vogelzang, N 2008, 'A phase II clinical trial of oral valproic acid in patients with castration-resistant prostate cancers using an intensive biomarker sampling strategy', *Translational oncology*, vol. 1, no. 3, p. 141.

Sharma, VK, Nautiyal, V, Goel, KK & Sharma, A 2010, 'Assessment of thermal stability of metformin hydrochloride', *Asian J Chem*, vol. 22, pp. 3561-6.

Shaw, RJ, Lamia, KA, Vasquez, D, Koo, S-H, Bardeesy, N, DePinho, RA, Montminy, M & Cantley, LC 2005, 'The kinase LKB1 mediates glucose homeostasis in liver and therapeutic effects of metformin', *Science*, vol. 310, no. 5754, pp. 1642-6.

Shi, W, Xiao, D, Wang, L, Dong, L, Yan, Z, Shen, Z, Chen, S, Chen, Y & Zhao, W 2012, 'Therapeutic metformin/AMPK activation blocked lymphoma cell growth via inhibition of mTOR pathway and induction of autophagy', *Cell Death Dis*, vol. 3, no. 3, p. e275.

Smith, AD 2007, *Smith's textbook of endourology*, PMPH-USA.

So, A, Gleave, M, Hurtado-Col, A & Nelson, C 2005, 'Mechanisms of the development of androgen independence in prostate cancer', *World J Urol*, vol. 23, no. 1, pp. 1-9.

Sobel, RE & Sadar, MD 2005, 'Cell lines used in prostate cancer research: a compendium of old and new lines - part 1', *J Urol*, vol. 173, no. 2, pp. 342-59.

Sobel, RE, Wang, Y & Sadar, MD 2006, 'Molecular analysis and characterization of PrEC, commercially available prostate epithelial cells', *In Vitro Cellular & Developmental Biology-Animal*, vol. 42, no. 1-2, pp. 33-9.

Spiller, HA, Krenzelok, EP, Klein-Schwartz, W, Winter, ML, Weber, JA, Sollee, DR & Bangh, SA 2000, 'Multicenter case series of valproic acid ingestion: serum concentrations and toxicity', *Clinical Toxicology*, vol. 38, no. 7, pp. 755-60.

Spratt, DE, Zhang, C, Zumsteg, ZS, Pei, X, Zhang, Z & Zelefsky, MJ 2013, 'Metformin and prostate cancer: reduced development of castration-resistant disease and prostate cancer mortality', *Eur Urol*, vol. 63, no. 4, pp. 709-16.

Stickle, NH, Cheng, LS, Watson, IR, Alon, N, Malkin, D, Irwin, MS & Ohh, M 2005, 'Expression of p53 in renal carcinoma cells is independent of pVHL', *Mutation Research/Fundamental and Molecular Mechanisms of Mutagenesis*, vol. 578, no. 1, pp. 23-32.

Sweeney, CJ, Chen, Y-H, Carducci, M, Liu, G, Jarrard, DF, Eisenberger, M, Wong, Y-N, Hahn, N, Kohli, M & Cooney, MM 2015, 'Chemohormonal therapy in metastatic hormone-sensitive prostate cancer', *New England Journal of Medicine*, vol. 373, no. 8, pp. 737-46.

Tai, S, Sun, Y, Squires, JM, Zhang, H, Oh, WK, Liang, CZ & Huang, J 2011, 'PC3 is a cell line characteristic of prostatic small cell carcinoma', *Prostate*, vol. 71, no. 15, pp. 1668-79.

Takai, N, Desmond, JC, Kumagai, T, Gui, D, Said, JW, Whittaker, S, Miyakawa, I & Koeffler, HP 2004, 'Histone deacetylase inhibitors have a profound antigrowth activity in endometrial cancer cells', *Clinical cancer research*, vol. 10, no. 3, pp. 1141-9.

Tan, ME, Li, J, Xu, HE, Melcher, K & Yong, E-l 2015, 'Androgen receptor: structure, role in prostate cancer and drug discovery', *Acta Pharmacologica Sinica*, vol. 36, no. 1, pp. 3-23.

Tannock, IF, de Wit, R, Berry, WR, Horti, J, Pluzanska, A, Chi, KN, Oudard, S, Théodore, C, James, ND & Turesson, I 2004, 'Docetaxel plus prednisone or mitoxantrone plus prednisone for advanced prostate cancer', *New England Journal of Medicine*, vol. 351, no. 15, pp. 1502-12.

Taplin, M-E, Bubley, GJ, Shuster, TD, Frantz, ME, Spooner, AE, Ogata, GK, Keer, HN & Balk, SP 1995, 'Mutation of the androgen-receptor gene in metastatic androgen-independent prostate cancer', *New England Journal of Medicine*, vol. 332, no. 21, pp. 1393-8.

Taylor, BS, Schultz, N, Hieronymus, H, Gopalan, A, Xiao, Y, Carver, BS, Arora, VK, Kaushik, P, Cerami, E & Reva, B 2010, 'Integrative genomic profiling of human prostate cancer', *Cancer Cell*, vol. 18, no. 1, pp. 11-22.

Thelen, P, Schweyer, S, Hemmerlein, B, Wuttke, W, Seseke, F & Ringert, R-H 2004, 'Expressional changes after histone deacetylase inhibition by valproic acid in LNCaP human prostate cancer cells', *Int J Oncol*, vol. 24, no. 1, p. 25.

Tomlins, SA, Laxman, B, Varambally, S, Cao, X, Yu, J, Helgeson, BE, Cao, Q, Prensner, JR, Rubin, MA & Shah, RB 2008, 'Role of the TMPRSS2-ERG gene fusion in prostate cancer', *Neoplasia (New York, NY)*, vol. 10, no. 2, p. 177.

Tomlins, SA, Rhodes, DR, Perner, S, Dhanasekaran, SM, Mehra, R, Sun, X-W, Varambally, S, Cao, X, Tchinda, J, Kuefer, R, Lee, C, Montie, JE, Shah, RB, Pienta, KJ, Rubin, MA & Chinnaiyan, AM 2005, 'Recurrent Fusion of TMPRSS2 and ETS Transcription Factor Genes in Prostate Cancer', *Science*, vol. 310, no. 5748, pp. 644-8.

Torre, LA, Bray, F, Siegel, RL, Ferlay, J, Lortet-Tieulent, J & Jemal, A 2015, 'Global cancer statistics, 2012', *CA: a cancer journal for clinicians*, vol. 65, no. 2, pp. 87-108.

Tran, C, Ouk, S, Clegg, NJ, Chen, Y, Watson, PA, Arora, V, Wongvipat, J, Smith-Jones, PM, Yoo, D & Kwon, A 2009, 'Development of a second-generation antiandrogen for treatment of advanced prostate cancer', *Science*, vol. 324, no. 5928, pp. 787-90.

Tsai, C-C, Chuang, T-W, Chen, L-J, Niu, H-S, Chung, K-M, Cheng, J-T & Lin, K-C 2015, 'Increase in apoptosis by combination of metformin with silibinin in human colorectal cancer cells', *World journal of gastroenterology: WJG*, vol. 21, no. 14, p. 4169.

Tuominen, VJ, Ruotoistenmaki, S, Viitanen, A, Jumppanen, M & Isola, J 2010, 'ImmunoRatio: a publicly available web application for quantitative image analysis of estrogen receptor (ER), progesterone receptor (PR), and Ki-67', *Breast Cancer Res*, vol. 12, no. 4, p. R56.

Turnbull, D, Rawlins, M, Weightman, D & Chadwick, D 1983, 'Plasma concentrations of sodium valproate: their clinical value', *Annals of neurology*, vol. 14, no. 1, pp. 38-42.

Universal Protein Resource (UniProt) 2013, *P11308 (ERG_HUMAN)*, viewed 06 2014, <http://www.uniprot.org/uniprot/P11308#P11308>.

Untae Kim, S, NY (US); Stefan A. Cohen, Tierra Verde, FL (US), 2011, *Method of separating tumor cells with and without lymphotropic metastatic potential in a human carcinoma*, patent, 10/939,974, US 7,989,001 B2, USA.

Van Beneden, K, Geers, C, Pauwels, M, Mannaerts, I, Verbeelen, D, van Grunsven, LA & Van den Branden, C 2011, 'Valproic acid attenuates proteinuria and kidney injury', *Journal of the American Society of Nephrology*, vol. 22, no. 10, pp. 1863-75.

Van Bokhoven, A, Varella-Garcia, M, Korch, C, Johannes, WU, Smith, EE, Miller, HL, Nordeen, SK, Miller, GJ & Lucia, MS 2003, 'Molecular characterization of human prostate carcinoma cell lines', *Prostate*, vol. 57, no. 3, pp. 205-25.

Van Kuppeveld, F, Van der Logt, J, Angulo, A, Van Zoest, M, Quint, W, Niesters, H, Galama, J & Melchers, W 1992, 'Genus-and species-specific identification of mycoplasmas by 16S rRNA amplification', *Applied and environmental microbiology*, vol. 58, no. 8, pp. 2606-15.

Vander Heiden, MG, Cantley, LC & Thompson, CB 2009, 'Understanding the Warburg effect: the metabolic requirements of cell proliferation', *Science*, vol. 324, no. 5930, pp. 1029-33.

Vecchio, S, Giampreti, A, Petrolini, V, Lonati, D, Protti, A, Papa, P, Rognoni, C, Valli, A, Rocchi, L & Rolandi, L 2014, 'Metformin accumulation: Lactic acidosis and high plasmatic metformin levels in a retrospective case series of 66 patients on chronic therapy*', *Clinical Toxicology*, vol. 52, no. 2, pp. 129-35.

Ververis, K, Rodd, AL, Tang, MM, El-Osta, A & Karagiannis, TC 2011, 'Histone deacetylase inhibitors augment doxorubicin-induced DNA damage in cardiomyocytes', *Cell Mol Life Sci*, vol. 68, no. 24, pp. 4101-14.

Vogelstein, B, Papadopoulos, N, Velculescu, VE, Zhou, S, Diaz, LA & Kinzler, KW 2013, 'Cancer genome landscapes', *Science*, vol. 339, no. 6127, pp. 1546-58.

Vu Le, C, Dao, OQ & Khac Tran, LN 2010, 'Mass screening of prostate cancer in Vietnam: Current status and our opinions', in *Urologic Oncology: Seminars and Original Investigations*, vol. 28, pp. 673-6.

Wang, D-S, Jonker, JW, Kato, Y, Kusuhara, H, Schinkel, AH & Sugiyama, Y 2002, 'Involvement of organic cation transporter 1 in hepatic and intestinal distribution of

metformin', *Journal of Pharmacology and Experimental Therapeutics*, vol. 302, no. 2, pp. 510-5.

Wang, J, Cai, Y, Yu, W, Ren, C, Spencer, DM & Ittmann, M 2008, 'Pleiotropic biological activities of alternatively spliced TMPRSS2/ERG fusion gene transcripts', *Cancer Res*, vol. 68, no. 20, pp. 8516-24.

Wang, Y, Liu, G, Tong, D, Parmar, H, Hasenmayer, D, Yuan, W, Zhang, D & Jiang, J 2015, 'Metformin represses androgen-dependent and androgen-independent prostate cancers by targeting androgen receptor', *Prostate*, vol. 75, no. 11, pp. 1187-96.

Warburg, O 1956, 'On the origin of cancer cells', *Science*, vol. 123, no. 3191, pp. 309-14.

Warburton, HE, Brady, M, Vlatković, N, Linehan, WM, Parsons, K & Boyd, MT 2005, 'p53 regulation and function in renal cell carcinoma', *Cancer Res*, vol. 65, no. 15, pp. 6498-503.

Waring, P & Müllbacher, A 1999, 'Cell death induced by the Fas/Fas ligand pathway and its role in pathology', *Immunology and cell biology*, vol. 77, no. 4, pp. 312-7.

Wedel, S, Hudak, L, Seibel, JM, Juengel, E, Oppermann, E, Haferkamp, A & Blaheta, RA 2011, 'Critical analysis of simultaneous blockage of histone deacetylase and multiple receptor tyrosine kinase in the treatment of prostate cancer', *Prostate*, vol. 71, no. 7, pp. 722-35.

Wedel, S, Hudak, L, Seibel, JM, Juengel, E, Tsaur, I, Wiesner, C, Haferkamp, A & Blaheta, RA 2011, 'Inhibitory effects of the HDAC inhibitor valproic acid on prostate cancer growth are enhanced by simultaneous application of the mTOR inhibitor RAD001', *Life Sci*, vol. 88, no. 9-10, pp. 418-24.

Wedel, S, Hudak, L, Seibel, JM, Makarevic, J, Juengel, E, Tsaur, I, Waaga-Gasser, A, Haferkamp, A & Blaheta, RA 2011, 'Molecular targeting of prostate cancer cells by a triple drug combination down-regulates integrin driven adhesion processes, delays cell cycle progression and interferes with the cdk-cyclin axis', *BMC Cancer*, vol. 11, p. 375.

Wedel, S, Hudak, L, Seibel, JM, Makarevic, J, Juengel, E, Tsaur, I, Wiesner, C, Haferkamp, A & Blaheta, RA 2011, 'Impact of combined HDAC and mTOR inhibition on adhesion, migration and invasion of prostate cancer cells', *Clin Exp Metastasis*, vol. 28, no. 5, pp. 479-91.

Wheaton, WW, Weinberg, SE, Hamanaka, RB, Soberanes, S, Sullivan, LB, Anso, E, Glasauer, A, Dufour, E, Mutlu, GM & Budigner, GS 2014, 'Metformin inhibits mitochondrial complex I of cancer cells to reduce tumorigenesis', *Elife*, vol. 3, p. e02242.

Wheler, JJ, Janku, F, Falchook, GS, Jackson, TL, Fu, S, Naing, A, Tsimberidou, AM, Moulder, SL, Hong, DS, Yang, H, Piha-Paul, SA, Atkins, JT, Garcia-Manero, G & Kurzrock, R 2014, 'Phase I study of anti-VEGF monoclonal antibody bevacizumab and histone deacetylase inhibitor valproic acid in patients with advanced cancers', *Cancer Chemother Pharmacol*, vol. 73, no. 3, pp. 495-501.

Whibley, C, Pharoah, PD & Hollstein, M 2009, 'p53 polymorphisms: cancer implications', *Nature Reviews Cancer*, vol. 9, no. 2, pp. 95-107.

White-Al Habeeb, NM, Garcia, J, Fleshner, N & Bapat, B 2016, 'Metformin Elicits Antitumor Effects and Downregulates the Histone Methyltransferase Multiple Myeloma SET Domain (MMSET) in Prostate Cancer Cells', *Prostate*, vol. 76, no. 16, pp. 1507-18.

Wilt, TJ, Brawer, MK, Jones, KM, Barry, MJ, Aronson, WJ, Fox, S, Gingrich, JR, Wei, JT, Gilhooly, P & Grob, BM 2012, 'Radical prostatectomy versus observation for localized prostate cancer', *New England Journal of Medicine*, vol. 367, no. 3, pp. 203-13.

Wissing, MD, Mendonca, J, Kortenhorst, MS, Kaelber, NS, Gonzalez, M, Kim, E, Hammers, H, van Diest, PJ, Carducci, MA & Kachhap, SK 2013, 'Targeting prostate cancer cell lines with polo-like kinase 1 inhibitors as a single agent and in combination with histone deacetylase inhibitors', *Faseb j*, vol. 27, no. 10, pp. 4279-93.

Wright, JL & Stanford, JL 2009, 'Metformin use and prostate cancer in Caucasian men: results from a population-based case–control study', *Cancer Causes & Control*, vol. 20, no. 9, pp. 1617-22.

Wu, TT, Sikes, RA, Cui, Q, Thalmann, GN, Kao, C, Murphy, CF, Yang, H, Zhau, HE, Balian, G & Chung, LW 1998, 'Establishing human prostate cancer cell xenografts in bone: induction of osteoblastic reaction by prostate-specific antigen-producing tumors in athymic and SCID/bg mice using LNCaP and lineage-derived metastatic sublines', *International Journal of Cancer*, vol. 77, no. 6, pp. 887-94.

Wu, X, Senechal, K, Neshat, MS, Whang, YE & Sawyers, CL 1998, 'The PTEN/MMAC1 tumor suppressor phosphatase functions as a negative regulator of the phosphoinositide 3-kinase/Akt pathway', *Proceedings of the National Academy of Sciences*, vol. 95, no. 26, pp. 15587-91.

Xia, Q, Sung, J, Chowdhury, W, Chen, C-l, Höti, N, Shabbeer, S, Carducci, M & Rodriguez, R 2006, 'Chronic administration of valproic acid inhibits prostate cancer cell growth in vitro and in vivo', *Cancer Res*, vol. 66, no. 14, pp. 7237-44.

Xie, Z, Dong, Y, Scholz, R, Neumann, D & Zou, M-H 2008, 'Phosphorylation of LKB1 at serine 428 by protein kinase C-ζ is required for metformin-enhanced activation of the AMP-activated protein kinase in endothelial cells', *Circulation*, vol. 117, no. 7, pp. 952-62.

Xu, W, Parmigiani, R & Marks, P 2007, 'Histone deacetylase inhibitors: molecular mechanisms of action', *Oncogene*, vol. 26, no. 37, pp. 5541-52.

Xu, Y, Chen, S-Y, Ross, KN & Balk, SP 2006, 'Androgens induce prostate cancer cell proliferation through mammalian target of rapamycin activation and post-transcriptional increases in cyclin D proteins', *Cancer Res*, vol. 66, no. 15, pp. 7783-92.

Zakikhani, M, Dowling, R, Fantus, IG, Sonenberg, N & Pollak, M 2006, 'Metformin is an AMP kinase–dependent growth inhibitor for breast cancer cells', *Cancer Res*, vol. 66, no. 21, pp. 10269-73.

Zhang, X, Zhang, X, Huang, T, Geng, J, Liu, M & Zheng, J 2015, 'Combination of metformin and valproic acid synergistically induces cell cycle arrest and apoptosis in clear cell renal cell carcinoma', *Int J Clin Exp Pathol*, vol. 8, no. 3, pp. 2823-8.

Zhou, G, Myers, R, Li, Y, Chen, Y, Shen, X, Fenyk-Melody, J, Wu, M, Ventre, J, Doebber, T & Fujii, N 2001, 'Role of AMP-activated protein kinase in mechanism of metformin action', *Journal of Clinical Investigation*, vol. 108, no. 8, pp. 1167-74.

Zhuang, Y, Chan, DK, Haugrud, AB & Miskimins, WK 2014, 'Mechanisms by which low glucose enhances the cytotoxicity of metformin to cancer cells both in vitro and in vivo', *PLoS One*, vol. 9, no. 9, p. e108444.

Zhuang, Y & Miskimins, WK 2008, 'Cell cycle arrest in Metformin treated breast cancer cells involves activation of AMPK, downregulation of cyclin D1, and requires p27Kip1 or p21Cip1', *J Mol Signal*, vol. 3, no. 18, p. 0.